AN ABSTRACT OF THE DISSERTATION OF

Cristina Isabel Coelho Dias Lopes for the degree of Doctor of Philosophy in Oceanography presented on July 25, 2006.
Title: Late Quaternary Paleoceanography of the Northeast Pacific and Atlantic Oceans Based on Diatom Transfer Functions

Abstract approved:_____
Alan C. Mix

Modern upwelling conditions and corresponding oceanographic properties are investigated and reconstructed for the Late Quaternary. The oceanographic conditions considered influence diatom ecology and the record of fossil diatom frustules in the sediments.

Diatoms from modern sediments are evaluated as paleoceanographic proxies and transfer functions (TFs) are calibrated using the Imbrie and Kipp (I&K) method and Weighted Averaging (WA) from Canonical Correspondence Analysis (CCA). CCA is used to define the most appropriate environmental variables to model.

TFs for productivity, sea-surface temperature, salinity and PO_4 are developed from both methods (I&K and WA) for the northeast Pacific. WA is more efficient and robust than I&K, specially regarding extrapolations and weak no-analogs.

Downcore studies for the northeast Pacific revealed the presence of no-analogs related to late Pleistocene mega-floods that emanated from the Columbia River and reduced regional sea-surface salinities by as much as 10 PSU. Two methods were applied to address the no-analog problem: method 1 reflects the combination of all samples (downcore and modern) and method 2 reflects the removal of the species/groups that comprises the no-analogs. Some of the TFs had to be re-calibrated in order to apply them to the particular cores selected for the past reconstructions. For the northeast Pacific, the reconstructions go back 60,000 years (B.P.) and method 2 resulted in significant reconstructions for productivity and sea-surface temperature.

For the northeast Atlantic upwelling area, the TFs development is limited by the quality of the datasets (floral and environmental). The modern sample dataset characteristics precluded the use of the environmental datasets analogous to those from the northeast Pacific. Nevertheless, both I&K and WA resulted in significant TFs for the modern calibration, regarding “in situ” data for sea-surface temperature and chlorophyll. The downcore reconstructions have low resolution and only a realistic evaluation can be done between modern conditions and Oxygen Isotope Stage 2.

This dissertation reflects the necessary studies to develop paleoceanographic proxies and transfer functions for past oceanic reconstructions that can be linked to climate changes. Although this study contemplates only two geographic upwelling areas, the tools used here can be applied to other upwelling regions.

Late Quaternary Paleoceanography of the Northeast Pacific and Atlantic Oceans Based on Diatom Transfer Functions

by
Cristina Isabel Coelho Dias Lopes

A DISSERTATION

submitted to

Oregon State University

in partial fulfillment of
the requirements for the
degree of

Doctor of Philosophy

Presented July 25, 2006
Commencement June 2007

Doctor of Philosophy dissertation of Cristina Isabel Coelho Dias Lopes presented on July 25, 2006.

APPROVED:

Major Professor, representing Oceanography

Dean of the College of Oceanic and Atmospheric Sciences

Dean of the Graduate School

I understand that my dissertation will become part of the permanent collection of Oregon State University libraries. My signature bellow authorizes release of my dissertation to any reader upon request.

Cristina Isabel Coelho Dias Lopes, Author

ACKNOWLEDGEMENTS

I would like to thank my advisors: Alan Mix and Fátima Abrantes. I have no words that can express how thankful I am. Your knowledge and wisdom will always be present in my life. Your devotion and passion for science has influenced me in many ways, not only as a student but also has a person.

Thanks are also due to my committee members Nicklas Pisias, Ricardo Letelier, Peter Clark and Stephen Giovannoni and to Jim McManus, David Cristie and Gary Klinkhammer that were present in previous exams and committee meetings. All of your comments and advices are precious to me and made me think about new aspects of my research.

These past five years were not easy, especially for my family, the core of my life. All this time we were separated by one ocean and one continent. I would like to thank my beloved husband for his endurance, patience and trust. For believing in me, for believing that it would be worth to wait all this time for my return home and for his daily phone calls. Thank you for your unconditional love and respect. My parents were always used to my insane adventures and always tolerate my decisions. The work presented in this dissertation could not have been accomplished without their love and support.

Friends are also in order of gratitude. Thanking all of them by writing all their names would require more paper than the one used to print this dissertation. That is how fortunate I am. I am sorry if I neglected your friendship in the past six months. Nevertheless, I really appreciated your phone calls checking if I was still alive.

I would like to acknowledge the funding involved in this project: grant SFRH/BD/7232/2001 from Portugal-Fundação para a Ciência e Tecnologia and grant 0319016 from United States-National Science Foundation.

Finally, thank you all for the memories…

CONTRIBUTION OF AUTHORS

Dr. Alan C. Mix was involved in all aspects of data analysis and publication of every chapter in this dissertation. Dr. Fátima Abrantes assisted in the development of the diatom datasets and publications of Chapters 2 and 3.

TABLE OF CONTENTS

TABLE OF CONTENTS (Continued)

TABLE OF CONTENTS (Continued)

LIST OF FIGURES

LIST OF FIGURES (Continued)

LIST OF FIGURES (Continued)

LIST OF TABLES

LIST OF TABLES (Continued)

LIST OF APPENDICES

LIST OF APPENDIX TABLES

LIST OF APPENDIX TABLES (Continued)

Late Quaternary Paleoceanography of the Northeast Pacific and Atlantic Oceans Based on Diatom Transfer Functions

1. INTRODUCTION

Climate variability is a consequence of changes internal to the Earth's atmospheric-ocean system, as well as those forced externally, such as by rhythmic changes in Earth's orbit. These changes are reflected in the patterns of ocean circulation that can be recorded in ocean sediments.

The accumulation of biogenic particles in the sediments is mainly a function of the ocean's biological productivity by phytoplankton. Primary production is light dependant and therefore is restricted to the photic zone (upper ≈100m of the ocean). The second major control of primary production is nutrient availability (phosphate, nitrate, and micronutrients such as iron). Because of these controls, phytoplankton production is sensitive to oceanic and atmospheric conditions and therefore climate change.

Primary productivity is higher in areas of the oceans where upwelling is present. Upwelling brings nutrients from deeper waters to the surface. These areas are important not only because they represent possible atmospheric CO_2 sources (due to warming and degassing of CO_2-rich waters) and sinks (due to rain of organic matter to the deep sea), but also because they support approximately 50% of the world's fisheries, even though these areas only comprise 0.1% of the global oceans (Barber and Smith, 1981).

The amount of phytoplankton remains (shells or frustules) reaching the sediments is not only a function of the amount of living organisms that the ocean surface conditions allow, but also the physical and chemical conditions that are present in the water column and in the sediment-water interface. These conditions can produce dissolution of the remains or can transport them to areas far from those where the organisms lived.

Diatom remains (silica frustules) are one of the most common indicators of primary production preserved in the ocean sediments (Schrader and Schuette, 1981).

Diatom species diversity and abundance in sediments can trace processes such as upwelling events or river runoff. The upwelling areas of the northeast Pacific and Atlantic Oceans were chosen for detailed study because no quantitative reconstructions of oceanographic properties from upwelling nature was done before using diatoms as environmental indicators.

A fundamental goal of this research is to develop a geologic proxy for past oceanic conditions in these upwelling regions. A proxy is defined as a variable that can be measured in ancient samples and that can be used through equations, called transfer functions (TFs), to estimate an environmental property that per se cannot be directly measured (Wefer et al., 1999). The development of these proxies depends on a modern calibration. In this dissertation, diatom remains from sediments serves as a proxy for the reconstruction of several past oceanic properties. The application of proxies is based on a simple assumption: the relationship between the microorganisms and the environmental conditions remain constant in time (Hutson, 1977). Failure of this assumption results in no-analog situations. No-analog situations are also created when the species assemblages and/or abundances fall outside the modern calibration range (Hutson, 1977).

Thus, the major contribution of this research is to transform studies of micropaleontology of diatom species from a traditional qualitative approach, toward quantitative reconstructions of past oceanic conditions. Although several studies indicate that diatoms can be used as paleoceanographic indicators, no study has yet investigated in detail which and how many environmental variables the diatoms can reconstruct. The ultimate goal is to use the methods developed in this work in future multi-proxy approaches, where comparisons and better refinement of paleoceanographic reconstructions can be obtained combining several proxies.

This dissertation reports the necessary steps for a proxy and TF development in order to study the paleoceanography derived from upwelling areas: from obtaining samples from modern sediments to calibrate modern transfer functions (TFs, equations relating oceanographic conditions and diatom assemblages). Finally, application of the proxy to ancient samples in order to reconstruct past oceanic properties that can be

linked to past climate variability. More than a final project completion, the work presented here represents the opening of many more doors with a question and an hypothesis behind each one of them.

This first chapter introduces the major themes of this dissertation, which is presented as a series of publishable papers.

The second chapter reports the development of the diatom dataset from modern sediments for the northeast Pacific. The core-top samples were all collected from cores stored in the Oregon State University Marine Geology Repository. Overall, 54 core-tops were used for investigation of diatom abundances (#valves/g of sediment). However, due to different sedimentation rates in the study area, diatom assemblages were preferred for the quantitative study of oceanographic conditions. For diatom assemblage analysis, 30 core-tops were chosen. The raw diatom dataset (containing 47 species and/or groups) could be represented in terms of five statistical end-members (factors) defined by Q-Mode Factor Analysis (each one with its particular species or species groups), that are significantly correlated with the different oceanographic conditions present in our highly dynamic study area. The study presented in chapter 2 also provides a new insight about the type of upwelling and associated productivity in this region. Here, it was found that percentages of *Chaetoceros spores* (commonly associated with strong coastal upwelling and high productivity) are not able to differentiate between coastal and wind-stress curl induced upwelling.

Chapter 3 describes the next step in TF development. After understanding how the diatom assemblages from modern sediments are recording the oceanographic conditions, it is necessary to quantify that relationship by calibrating the modern floral and environment variables dataset. For this calibration two methods were used: the Imbrie and Kipp, 1971 (I&K) and the Weighted Averaging (WA) from Canonical Correspondence Analysis (CCA). CCA is used to evaluate which environmental variables are more appropriate to develop TFs. The details of these two approaches are reported and discussed in chapter 3. I&K is an unconstrained technique because it only uses the diatom dataset and the correlations with the environmental variables is done a posteriori. The CCA uses both the floral and environmental datasets and applies

correlations to extract variance in species that is related to a certain environmental variable. In addition, this method also allows investigation of correlations among environmental variables that cause problems in TF development. After selecting the best environmental variables, CCA uses WA to calculate the "weight" of the environmental variables in the floral dataset. The results from chapter 3 indicate that for 30 environmental variables, both methods yield similar results for certain environmental results. However, CCA is more efficient in extracting variance from the floral dataset that can be related to a particular environmental variable. The modern calibration produced significant TFs for winter and spring productivity, summer sea-surface temperature, annual and winter salinity and spring PO_4. No independent TF could be developed for SIO_2 or NO_3 because these two variables are correlated with almost all other environmental variables.

In Chapter 4, the study of diatom assemblages in ancient samples for cores ODP 1019D and MD02-2499 indicate the presence of no-analogs. Some diatom species and/or groups relative abundances were three times higher than the ones present in the modern calibration. One particular case is the freshwater diatom group. After further studies, the no-analog created by this group was associated with the presence of late Pleistocene massive floods in the northeast Pacific. The freshwater diatom records were combined with $\delta^{18}O$ records from planktonic and benthic foraminifera and the timing of flood events compared with terrestrial flood deposits and turbidites on the ocean floor. The episodic floods happened frequently from 16,000 to 31,000 calendar years BP and decreased the salinity off Northern California by 5 to 10 PSU.

Although a possible explanation was found for the presence of one of the no-analogs in one of the oceanographic properties, the remaining properties still needed to be investigated. The work presented in Chapter 5 addresses the no-analogs in past oceanographic reconstructions. Two approaches were used to investigate the implications of the no-analogs. In one method the diatom factors dataset included all species present in both the modern and ancient samples combined, in order to overcome low communalities. In the second approach the no-analog species were

removed from the datasets. The diatom dataset reorganizations led to new calibrations in some cases. The second approach provided more conservative paleoceanographic reconstructions (within the range of modern calibration values). However, the origin of the no-analogs (except the one addressed in the previous chapter) remains controversial. Significant paleoceanographic reconstructions extending the past 60,000 calendar years BP for winter productivity and summer sea-surface temperature indicate a small decrease in productivity and in sea-surface temperature at 8,000 calendar years BP. During the Last Glacial Maximum the coastal upwelling decreased. However, the productivity was high, suggesting that the oceanographic conditions shifted towards a system dominated by wind-stress curl induced upwelling that was not efficient in exporting organic matter, similar to the one present today in the Alaska Gyre. Although there is no evidence of millennial-scale climate changes during deglaciation, the oscillations present in the paleoceanographic reconstruction for Oxygen Isotope Stage 3 may indicate regional millennial-scale climate variability.

Chapter 6 of this dissertation reflects the application of all the tools developed in the previous chapters to another upwelling area: the northeast Atlantic Portuguese margin. For this area, only sea-surface temperature and chlorophyll (an indirect measure of productivity) were available as oceanographic environmental variables. Nevertheless, the same calibration methods were applied (I&K and WA/CCA) and no no-analogs conditions were found. The modern and ancient diatom datasets are the main focus in this chapter. The modern calibration resulted in promising TFs for this study area.

So far, only reconstructions for Oxygen Isotope Stage 2 are understood because of the low sampling resolution for the rest of the record. In this stage, coastal upwelling was almost double of the modern conditions and wind-stress curl induced upwelling was virtually absent. However, the chlorophyll only doubled at 20,000 calendar years BP coincident with a peak in productivity reported from previous studies. This peak matches a peak in river influence suggesting that although during Oxygen Isotope Stage 2 coastal upwelling was stronger than today, the biological

system was not efficient in using the available nutrients. The river influence reflects the input of micronutrients such as iron, probably indicating that at this point the oceanographic conditions changed from high nutrient low chlorophyll towards a productive system efficient in exporting organic matter to the sediments. The sea-surface temperature reconstructions based on the I&K method agree with other studies. However, because the modern calibration underestimates this variable by almost 2^{o}C, these reconstructions need to be better constrained.

2. DIATOMS IN NORTHEAST PACIFIC SURFACE SEDIMENTS AS PALEOCEANOGRAPHIC PROXIES

Cristina Lopes, Alan C. Mix and Fátima Abrantes

Marine Micropaleontology
www.elsevier.com/locate/marmicro
Volume 60 (2006), 45-65

Abstract

Fossil diatom total abundances (# valves/g) in 54 surface-sediment samples from the northeast (NE) Pacific Ocean reflect the position of high primary production associated with coastal upwelling, and that possible biases associated with dilution or dissolution are small. Diatom species assemblages, defined by Q-mode Factor Analysis in 30 samples with abundant diatoms, are related to modern oceanographic properties. Five statistical assemblages, given by five specific diatom species and/or groups, are related to upwelling (*Chaetoceros spores*), subtropical (*Thalassionema nitzschioides*), subarctic (*Rhizosolenia hebetata*), transitional (*Neodenticula seminae*) and freshwater (freshwater diatoms) ecological environments. These factors are significantly correlated with primary productivity, temperature, nutrient concentrations and salinity, although the strongest relationship is that between diatom assemblages and productivity. However, it is not possible to distinguish between coastal and open-ocean (curl driven) upwelling based on *Chaetoceros spores* relative percentages by themselves or on the floral factors.

2.1 Introduction

Marine export productivity plays an important role in natural CO_2 variations through the mechanism of the "biological pump" (Berger et al., 1991). The processes that drive CO_2 sequestration are focused in specific regions. For example, about 5% of the total annual North Pacific uptake of atmospheric CO_2 (and as much as 100% of the summer uptake) occurs in the upwelling region off Oregon and California, even though this region comprises < 2% of the total North Pacific, likely because the coastal upwelling system contains preformed nutrients (relative to its CO_2 content) and is efficient at exporting carbon to the deep sea (Hales et al., 2005). To understand the component of natural variations in atmospheric CO_2 that is driven by this biological pumping, we must understand the long-term history of these regional upwelling systems.

Primary production is higher in upwelling areas where nutrients such as phosphate and nitrate are brought to the surface. As more nutrients (including

micronutrients such as iron, and other limiting compounds such as silica) are available in the photic zone, phytoplankton activity, and especially that of diatoms, increases drastically (Margalef, 1978; Blasco et al., 1980). Because of this sensitivity to wind-driven upwelling and nutrients, long-term variations in diatom production are sensitive to climate change. However, diatom remains preserved in the geologic record reflect not only production of living organisms near the sea-surface, but also physical and chemical conditions in the water column and in near-surface sediments. These conditions can produce dissolution or can transport diatoms to areas far from those in which they lived.

Here we compare the spatial distribution of diatoms in NE Pacific surface sediments to the modern upper-ocean conditions, as a step toward calibrating relationships between the flora preserved in sediments and the environment of the upper ocean. Diatoms have already shown promise as a tool for assessing past ocean conditions (Sancetta and Silvestri, 1986; Abrantes, 1988, Barron et al, 2003). These previous studies reveal that diatoms are useful large-scale indicators for paleoecological reconstructions. We add much more detail from the NE Pacific upwelling system. Although this region was included in a previous study of the entire Pacific (Sancetta and Silvestri, 1986), it was represented by only four sites, which is not sufficient to discern regional oceanographic gradients that constrain interpretation of oceanographic processes.

We focus here on the relative impact of coastal and open-ocean upwelling and major river inputs on diatom assemblages preserved in the region from southern British Columbia to Northern California – a region of high production that spans the transition from subtropical to subpolar climate regimes (figure 2.1).

2.2 Regional setting

Coastal upwelling is driven by along-shore winds. Major coastal upwelling regions are located along the eastern boundaries of the oceans where predominantly equatorward winds track the eastern edge of large atmospheric high-pressure systems (figure 2.2a). In contrast to coastal upwelling, open-ocean upwelling is driven by the

curl of the wind-stress (Bakun and Nelson, 1991). This phenomenon is commonly associated with wind jets or gradients over the ocean, especially in the subpolar oceans such as in the NE Pacific off Washington and British Columbia (throughout the year) and off Oregon and California (in winter). The regional and seasonal separation of coastal (mostly south of 46^0N and west of 127^0W, figure 2.2b) and open-ocean (mostly north of 46^0N and west of 127^0W, figure 2.2b) upwelling processes in the Northeast Pacific make this a good region to examine the relative importance of these two different upwelling processes on diatom floras. With our sign convention, positive curl implies divergence and open-ocean upwelling. Although both kinds of upwelling systems are characterized by high productivity, coastal upwelling favors intermittent blooms of larger phytoplankton that yield high export flux to the sediments, whereas open-ocean upwelling is often associated with the presence of small phytoplankton and low export productivity flux to the sediments, perhaps due to constant recycling of nutrients associated with high grazing activity (Miller et al., 1991) or limitation of micronutrients such as iron (Hutchins and Bruland, 1998).

Even though coastal upwelling systems are normally confined to within 50 km from shoreline (Huyer, 1983), it is common for giant cold-water plumes and eddies to extend into the open ocean (e.g. Traganza et al., 1983; Hood et al., 1990 and Hickey, 1998). These offshore filaments or plumes meander in the jet that separates the coastal and open ocean systems (Brink and Cowles, 1991), and transport cold nutrient-rich water from the coastal area to the open ocean, thus extending coastal upwelling's effects well offshore (Haidvogel et al., 1991). In the California Current, strong filaments and eddies persist off Cape Mendocino and Point Arena and transport coastal upwelling influence several hundred km offshore (Mooers and Robinson, 1984).

Off Oregon, coastal upwelling typically occurs intermittently between April and August (Smith, 1983). The wind system can change within a few days, and downwelling events may occur (driven by southerly winds) even during an upwelling season (Smith, 1983). The position of the North Pacific high-pressure cell relative to the Aleutian low-pressure cell influences the seasonal features of coastal upwelling

associated with the California Current. In summer, the low-pressure cell moves northward and high-pressure replace it, driving northerly winds (Huyer, 1983). Farther south (off California), coastal upwelling conditions are more persistent (figure 2.2a) and can even be present year-round (Huyer, 1983). The strongest coastal upwelling on an annual average occurs between 36^{o} N and 42^{o} N (Hostetler et al., 1999).

The source waters that upwell into the California Current are a blend of two distinct water masses: the Pacific Subarctic and the Equatorial Pacific (Tibby, 1941; Sverdrup et al., 1942 and Pickard, 1964). The Subarctic water mass is colder, less salty and richer in nutrients than Equatorial waters (Lynn and Simpson, 1987) and its extreme intrusions into the California Current can cause increases in productivity, especially off Oregon (Wheeler et al., 2003). Water that supplies the California Current coastal upwelling system includes the North Pacific Intermediate Water (NPIW), which comes from depths between 100 and 200 m (Barber and Smith, 1981). This source water is characterized by higher oxygen and lower salinity than the surrounding water masses (Talley, 1993). The California Undercurrent or Countercurrent transports Equatorial water at depths of 200 to 500 m from south to north. This water is warmer (9.5 ^{o}C to 7.0 ^{o}C), saltier (34.6 to 33.9 PSU) and has lower dissolved oxygen content than the Subarctic water (Lynn and Simpson, 1987; Hickey, 1979). The poleward-flowing Davidson Current surfaces during winter and enhances the reach of the Equatorial waters to the north. The region is sensitive to changes in source waters, which can result in intermittent disoxia, with significant ecologic and economic impacts (Grantham et al., 2004).

A local source of nutrients for the Northeast Pacific is the Columbia River (figure 2.3), which empties into the ocean near 46^{0}N. This river is important not only because the discharge of nutrients can cause diatom blooms, but also because its freshwater forms a highly stratified surface plume. This plume (Anderson, 1964) can sometimes extend as far as 650 km offshore and can reach California during the fall season, while during winter it tracks to the north along the Washington coast (figure 2.3). The river plume also transports freshwater diatoms into the ocean (Anderson,

1964). In the geologic record, presence of these species may help to track intensity of river flow or direction of currents that divert the river plume in the marine realm.

Other coastal rivers, such as the Eel River (figure 2.3) do not have as large and geographically distinct plume as the Columbia. Nevertheless, the Eel is known for a large input of sediment eroded from steep coastal mountains, and this influence of Eel River transport into the ocean can be assessed from its sediment deposition, which can reach 50 Km north and to the 100 m isobath (Ogston et al., 2004). The Eel River Canyon located to the southwest of the river mouth, near 40.6^0N, is a pathway for transporting river sediments (and freshwater diatoms) to deeper offshore areas of the ocean (Mullenbach and Nittrouer, 2000).

2.3 Materials and Methods

2.3.1 Diatom abundances

Fifty-four core-top samples (figure 2.4a and appendix B) were obtained from the Oregon State University Marine Geology Repository (corelab-www.coas.oregonstate.edu). The core-tops (0 to 0.5 cm) are assumed to represent modern conditions. Core sites were chosen based on geographic distribution, to approximate spacing 1^0 by 1^0 latitude-longitude grid (to the extent possible), type of sampling device (multicores or gravity cores favored over piston cores), date of collection (as recent as possible) and sediment preservation conditions. During the selection process more that 100 cores were open and examined. Data regarding local sedimentation rates were not available in most cases, but regional sedimentation rates are known to range from 10's to 100's of cm per kyr (Mix et al., 1999a), so the assumption of modern conditions for core-tops is reasonable. After the preparation of smear slides for a initial microscopic examination, 39 samples were processed by addition of 35% hydrogen peroxide and 10% hydrochloric acid and boiling the samples on a hot plate (after Fenner, 1982) and the remaining eighteen samples were processed using the same chemicals (but 30% hydrogen peroxide) after adding 0.33% calgon for sediment disaggregation. These methods give compatible results

(Abrantes, et al., 2004). After processing, all slides were prepared according to the settling method of Battarbee (1973).

Diatoms were identified and counted by transmitted light microscope with 1000X magnification under phase contrast. When counting total diatom abundance, we observed 100 fields of view distributed along the entire slide and covering both central and marginal zones of the cover slip (Abrantes et al., 2004). Only diatoms that were essentially whole were counted for purposes of calculating total diatom abundances. Diatom fragments and other siliceous microfossils (radiolarians and silicoflagelates) were also counted and recorded separately. Centric diatoms were counted as whole specimens if more than half of a valve was present (including the central area), and pennate diatoms were counted as half if only a single apex was found on a valve (Schrader and Gersonde, 1978).

To improve the statistical value of absolute abundances, we counted three slides of each sample and accepted the median value for each of the categories under evaluation. This treatment was most effective at removing obvious outliers associated with slide preparation. Absolute diatom abundances were calculated based on the weight of dry sediment processed, the fraction of solution poured into the evaporation trays and the slide area observed in the microscope:

$$\text{Absolute Abundance (\#valves/g sediment)} = (J*Q)/W$$

J = the median value times F (conversion factor given by the relation between the total objective area divided by the area counted and the evaporation tray area);

Q = volume of solution (ml) poured into the evaporation tray divided by 250 ml (the dilution used for the solution);

W = the dry weight of the sample.

2.3.2 Diatom relative species percentages

Thirty of the fifty-four core-top (figure 2.4b and appendix B) samples had sufficient diatoms (>11 valves/300 fields of vision) to warrant quantitative analysis. This cut-off allows us to produce the species identifications for each sample in a

reasonable amount of time (one sample/day minimum). For each of these samples, between 200 and 300 frustules were identified to the species level (appendix B). Only species with more than 2% relative abundance in at least one sample were included in further statistical analyses. Freshwater and benthic diatoms were formed into two groups, according to their common ecological meanings.

2.4 Results and Discussion

2.4.1 Comparison of relative species percentages in core-tops and sediment Traps

We compared the diatoms from our southern samples with a previous three-year sediment trap study in an offshore transect near 42^0N (Sancetta, 1992), to test whether the species deposited at the sea floor are representative of the living community at the sea-surface. Only species that are relatively resistant to dissolution are preserved in the sediments (Schrader, 1972). We evaluate whether these species are representative of the seasonality and geographic patterns of upwelling areas in our study area.

The most abundant taxa in our core-top samples include those that Sancetta (1992) found reaching the sediments under the sediment traps: *Chaetoceros spores*, *Thalassionema nitzschioides*, and *Fragilariopsis doliolus*. Sancetta (1992) was not able to compare core-top and trap fluxes quantitatively, because her three sediment samples were prepared on non-quantitative smear slides, but found similar assemblages of robust species in the traps and sediments. We add to this analysis with a larger and more quantitative dataset on surface sediments. We convert Sancetta's fluxes of these species from the sediment traps to annual-average percentage values, and compare these results with our core-top data (calculated with the same data closure, where all species considered add to a fixed total of 100%) from sites nearest the sediment trap locations. The Nearshore sediment trap (figure 2.4b) (42.086^0N, 125.771^0W, at 2829 m depth) is the most appropriate for comparison to the sediment cores because it has the longest temporal record (from September, 1987 to July, 1990). Our nearest core top, W8909A-24GC (42.082^0N, 125.302^0W, at 2790 m depth), has diatom abundance of 4.8×10^7 valves/g of dry sediment. This value is similar to that

reported for the Peru region (5 x 10^7; Schuette and Schrader, 1981a), and higher than values of 1 x 10^5 found for the Canary (Abrantes, 1988) and 1.5 x 10^5 found for the Southwest Africa upwelling regions (Schuette and Schrader, 1981b). To compare the diatom fluxes between the sediment trap and core-top sediments we used the sedimentation rate of 0.004 cm/y reported for nearby core W8709-13PC (42.070^{0}N, 125.450^{0}W, at 2712 m depth; Gardner et al., 1997) (figure 2.4) and converted the diatom abundance in #valves/cm^3 (3 x 10 ^{6} valves/cm^3) to flux units, corresponding to a flux of 3.3 x 10 ^{6} valves/m^2/d. This value represents 4% of the total diatom flux reaching the sea floor (7.7 x 10 ^{7} valves/m^2/d) and 8% of the resistant diatom flux (4 x 10 ^{7} valves/m^2/d). This preservation rate is generally higher than rates reported for other upwelling regimes (Table I in Abrantes, 2000): from 0.05% in the Benguela system to 5% in Station PAPA, North Pacific.

The difference in the methodology used in this study and in the sediment trap study of Sancetta (1992) prevents a comparison of all species. Three resistant species groups appear in both studies: *Chaetoceros spores, Thalassiossira* spp. and *Thalassionema nitzschioides*. We used two different data closures: assuming closure (i.e., 100%) around the three species counted in common, and assuming closure around all the species in each data set by clustering the rest of the species as "others" (figure 2.5). When closure is around three species, *Chaetoceros spores, Thalassiossira* spp. and *Thalassionema nitzschioides* have relative abundances in the sediment trap similar to those in nearby core-top sediments. When closure is around all species, about half of the other species are not preserved in the sediment, and as a result the percentages of *Chaetoceros spores* and *Thalassiossira* spp. are double their value in the sediment traps.

Our finding of a good relation between the sediment trap and our core-top data for the three-species closure shows that sedimentary samples record integrated diatom production and export in the water column without major preservation bias for these resistant taxa, but that preservation induces a bias in the percentages when all the species are considered. Other upwelling areas yield similar results, suggesting that the relative abundance of robust diatom taxa is sufficiently well preserved to represent

upper-ocean gradients around upwelling centers (Sancetta, 1979; Abrantes, 1988). The presence of fragile species (e.g. *Chaetoceros* vegetative cells and bristles) in our sediment samples shows that preservation is generally good in this region (Schuette and Schrader, 1981a).

Seasonal sediment trap records (Sancetta, 1992) show that species abundances can change dramatically from season to season and geographically. The nearshore location comprises the longest available trap record, with three years of information that include both high and low productivity years. *Chaetoceros spores* in the traps are generally present during productive episodes of fall and early winter (Sancetta, 1992). This finding is consistent with known biological responses by this species, which produces spores as nutrients are depleted following upwelling events (Margalef, 1978). The total number of preserved spores likely reflects production of vegetative cells during active upwelling. *Thalassionema nitzschioides* in the traps is more closely linked to spring production conditions (Sancetta et al., 1992). Standing stocks of this species are also known to be associated with upwelling fronts (Margalef, 1978). *Thalassiossira* spp. is not as abundant in the sediment traps as other species, but can be present throughout the year (Sancetta 1992).

In this comparison of sediment trap and nearby sediment data, we find, as did Sancetta (1992), that the relative abundance among robust species in surface sediments is consistent with that of a nearby sediment trap. The species preserved in the sediments may reflect different patterns of seasonal production. Sancetta (1992) suggested that sediments from the Nearshore area, preferentially record late fall conditions (i.e., the termination of seasonal upwelling and the time of peak production of *Chaetoceros spores*). This finding may be an artifact of the short three-year time series recorded by the sediment trap, in which fall conditions were relatively consistent but other seasons were different in each of the three years. Sancetta (1992) considerated *Chaetoceros spores* to be transported from nearby shelves. The particular sample she studied also contained significant numbers of benthic diatoms. The sediment sample considered in our study also has abundant *Chaetoceros spores*, however it does not contain significant benthic diatom abundances. Therefore, we

consider *Chaetoceros spores* to reflect overlying production rather than downslope transport, and include this sample in our analysis. Similarly, Sancetta (1992) concluded that the "Gyre" (offshore, subtropical) location (where *Chaetoceros* is rare or absent) records spring/summer conditions. We examine this issue of seasonal bias further by comparison of spatial patterns of species abundance with seasonal spatial pattern of oceanographic properties.

2.4.2 Comparison of diatoms and regional productivity

To investigate whether the geographic pattern of diatom abundances and species composition in sediments mimics modern sea-surface conditions, we obtained, for our core-top locations, in-situ chlorophyll measurements (gridded at 1^0 latitude-longitude intervals; World Ocean Atlas, 1998), and productivity estimates based on satellite color measurements (CZCS, gridded at 0.5^0 latitude-longitude intervals; Antoine and Morel, 1996). We exclude more recent satellite productivity estimates based on SeaWIFS data, because the few years now available for SeaWIFS estimates are considered anomalous due to the El Niño/Southern Oscillation influence (Behrenfeld, personal communication). Satellite productivity estimates are problematic for high latitudes and more coastal areas, in part due to issues of cloud cover, especially in the coastal zone during summer, and throughout the region during winter (Antoine and Morel, 1996). The in-situ data coverage for chlorophyll is relatively poor in winter, because of hostile weather and sea states. Nevertheless, significant correlation between satellite and in-situ datasets (Table 2.1, sigificance tests from Devore and Peck, 1986) is encouraging and (except for the winter season) this supports the viability of using either in-situ chlorophyll or satellite productivity data for comparison with regional diatom abundances.

In addition to considering the full study region, we divided our samples in four sub-areas that reflect different oceanic environments: north of 46^0N and west of 127^0W (little or no coastal upwelling, but strong open-ocean upwelling), south of 46^0N and east of 127^0W (strong coastal upwelling area), west of 127^0W (open ocean)

and east of 127^0W (coastal ocean). Five temporal periods (annual, winter, spring, summer and fall) are considered for all correlations.

Although on an annual average, chlorophyll and productivity are significantly correlated in all regions (Table 2.1), this pattern breaks down within regions and seasons. In winter, satellite productivity and in-situ chlorophyll are not significantly correlated for all areas considered. The regions north of 46^0N and west of 127^0W have significant correlations between chlorophyll and production during spring – suggesting the dominance of a spring bloom in this region. In the southern and eastern regions, the significant correlation between chlorophyll and production is in the summer, consistent with the importance of summer coastal upwelling.

Following the same approach, we calculated regional correlations of both productivity and chlorophyll with core-top diatom abundances (#valves/g sediment), with absolute abundances of *Chaetoceros spores* (#valves/g sediment), and with percentages of *Chaetoceros spores* (relative to total diatoms) (Table 2.2). Diatom abundances and *Chaetoceros spores* percentages have been used in previous works as upwelling/productivity indicators (Margalef, 1978; Schuette and Schrader, 1981a; Abrantes and Sancetta, 1985; Abrantes, 1988). Absolute abundances (diatom and *Chaetoceros spores*) increases to the south, reflecting the effect of coastal upwelling (figure 2.6). The diatom absolute abundances include the effect of dilution with terrigenous sediment close to the coast (Jousé et al., 1971). Relative percentages are independent of this effect.

The most significant correlations for these diatom indices over the full region are between the percentage of *Chaetoceros spores* and fall productivity or chlorophyll, or between absolute *Chaetoceros spores* abundance and summer chlorophyll. When we investigate these relationships for the four sub areas, the same association is found in the sub area south of 46^0N, were the coastal upwelling is strong (figure 2.2a). For the region north of 46^0N, the only significant correlation is between diatom abundances and winter chlorophyll (but note uncertainties in winter data), consistent with the importance of winter curl-driven upwelling in this area (figure 2.2b).

In the open-ocean region west of 127^0W, some of the significant correlations (Table 2.2) are between absolute diatom abundance and annual chlorophyll, or absolute *Chaetoceros spores* abundance and annual chlorophyll or productivity. This is not surprising. This subtropical area lacks strong seasonal events, and low levels of productivity occur continuously, associated with the constant recycling of nutrients (Dugdale and Goering, 1967). However, there are also significant correlations between diatom and *Chaetoceros spores* abundances and spring, summer and fall productivity suggesting that some of the coastal waters reach the area (Mooers and Robinson, 1984). The region east of 127^0N has significant correlations between *Chaetoceros spores* and summer chlorophyll or annual productivity, although in this region the satellite productivity dataset is less reliable due to heavy cloud cover.

Absolute abundance of total diatoms or *Chaetoceros spores*, and the relative percentages of *Chaetoceros spores*, provide useful semi-quantitative geologic proxies for biological production, especially for summer and fall conditions in which production reflects coastal upwelling *Chaetoceros spore* percentages provide a better semi-quantitative index of paleoproductivity than absolute abundance, which is compromised by dilution with terrigenous sediment near the coast (figure 2.6 and 2.7). *Chaetoceros spores* are also abundant under both regions of coastal upwelling and open-ocean curl-driven upwelling, so with this index alone it is not possible to distinguish between these two different upwelling processes.

2.4.3 Benthic and freshwater diatoms

The benthic and freshwater diatoms comprise two minor groups with different regional patterns. The benthic diatom species are anomalously abundant in a single sample (Y7409-15-24) off the Columbia River at a water depth ≈ 200 m (figure 2.8). Because benthic diatoms are limited to the euphotic zone (i.e., shallow shelf), high percentages of this group at sites deeper than light penetration may indicate down-slope transport of sediment. Finding abundant benthic diatoms in a sample would suggest caution regarding use of other diatom data in the sample as a reflection of local conditions (Blasco et al., 1980). In our data set, only one sample is compromised

in this way. Although there is some downslope transport of benthic diatoms in the Columbia River area, reworking does not appear to be significant in the rest of the samples.

The percentage of freshwater species is relatively high near the mouth of the Columbia River and off Northern California (figure 2.9a and b). This likely reflects the presence of the Columbia River plume in the north, where freshwater diatoms are transported into more offshore areas, and perhaps to a lesser extent the Eel River plume and other coastal rivers to the south. In both areas, some downslope transport of freshwater diatoms may occur at the sea floor, via the Astoria Canyon in the north, and the Eel River Canyon in the south. The low correlation between abundance of freshwater diatoms and shallow-water benthic diatoms (r=0.24 when the Columbia River site Y7409-15-24 is excluded, 0.71 when this site is included) suggests that downslope transport is a minor issue for most of the sites examined here. Wind may also bring freshwater diatoms to the ocean (Pokras and Mix, 1985; Nave et. al, 2001). However, in the modern NE Pacific region, easterly winds are relatively rare, so wind transport is unlikely important in explaining the core-top data (although this may have changed in the past under different climate regimes; Sancetta et al., 1992). We conclude that the distribution of freshwater diatoms in our core-top dataset primarily reflects transport in freshwater plumes from major rivers, with additional minor contributions from down-slope transport.

2.4.4 Floral assemblages based on Q-mode factor analysis

Q-mode Factor Analysis is commonly used to confirm and simplify regional patterns of species abundances (e.g., Imbrie and Kipp, 1971) by expressing the primary orthogonal patterns in multivariate data. Factor scores quantify the relative importance of each species in each factor, and factor loadings (which can be plotted geographically) help to give insight into the distributions and ecological controls of each factor.

Species with less than 2% abundance in all samples were removed from the dataset (Imbrie and Kipp, 1971). Experiments with data pre-treatment revealed no

significant differences between using raw data and log-transformed data (a common treatment to amplify the importance of rare species). Therefore results shown here are based on factor analysis of untreated data. A varimax rotation transforms the factor loadings into mostly positive parameter space to approximate a more physical mixing model between orthogonal end members (e.g., Davis, 2002).

Communalities document the fraction of original sample information captured by the factor model for each sample (Davis, 2002) and may vary between zero and one; zero indicates that the factors do not represent any of the sample data, and one indicates complete representation of the original data without loss of information. The number of factors is chosen based on their description of a significant amount of the total information (Davis, 2002), and also based on ecologically reasonable distributions of factors (i.e., factor loadings with coherent geographic patterns).

Q-mode analysis returned five factors (Table 2.3), which explained 97% of the data. All communalities were higher than 0.75 (appendix B).

- Factor 1 (figure 2.10a) accounts for 56% of the total data and is dominated by *Chaetoceros spores*. The spatial distribution shows some confinement to the area east of 127^0W where coastal upwelling dominates, but with high percentages spreading westward in the northern area, where curl-driven upwelling dominates. This band is interrupted near the Columbia River mouth, showing the influence of the river plume. Because the geographic distribution of this factor fails to separate between the two different upwelling processes, we will simply designate this factor as the "Upwelling Factor".
- Factor 2 (figure 2.10b) accounts for 17% of the data and is dominated by *Thalassionema nitzschioides* with a smaller contribution of *Fragilariopsis doliolus*. Factor loadings are highest in the open ocean south of 46^0N and west of 127^0W, under the influence of the Central Pacific Gyre. We refer to this factor as the "Subtropical Factor".
- Factor 3 (figure 2.10c), in which *Rhizosolenia hebetata (forma hebetata)* is the major species, accounts for 10% of the data. Geographically, this factor is

confined to a northern open-ocean region, under the influence of the Subarctic Front. We name this factor the "Subarctic Front Factor".

- Factor 4 (figure 2.10d) accounts for 9% of the total data, and has *Neodenticula seminae* as its main species. It is located on the northern part of our study area, in both open-ocean and coastal regions. It has low factor scores in most areas (appendix B). Due to its location, we think that "Mixture Factor" is a suitable designation.
- Factor 5 (figure 2.10e) accounts for 5% of the data. It is dominated by the freshwater group (with a high contribution from *Thalassiossira eccentrica*), and is associated with a sample near the mouth of the Columbia River. This factor is named the "Freshwater Factor".

The Q-Mode factor loadings suggest that each assemblage is associated with specific geographic locations with different physical and chemical characteristics. In addition to considering the distribution of the factors (figure 2.10) relative to water masses and currents (figure 2.1) and ecology, we also investigated the linear correlations between the factors and several oceanic properties.

- *Chaetoceros spores*, which dominate Factor 1, have been extensively reported as associated with coastal upwelling and are known to bloom quickly in response to nutrient injections into surface waters, producing spores as a survival mechanism when nutrients are depleted (Margalef, 1978). These factor scores are positively correlated with summer productivity and fall chlorophyll (Table 2.4). The negative correlations of this factor with nutrients, such as spring phosphate and nitrate (Table 2.4), is consistent with observations that living *Chaetoceros* form spores at the termination of upwelling events. Given these associations, it is not surprising to find this factor associated with productivity/chlorophyll off Oregon and northern California. What is surprising is that this factor extends west off 46^0N, where coastal upwelling is not strong. However, wind-stress curl drives open-ocean upwelling here (Bakun and Nelson, 1991). Both upwelling processes appear to yield *Chaetoceros spores*. To separately consider these two possible causes for

the spatial distribution of this factor, we divided the area into the four regions discussed before and calculated the same type of correlations (appendix B). The resulting correlations show significant positive values for fall productivity south of 46^0N, and for summer wind-stress curl north of this latitude (figure 2.11 appendix B).

- The Subtropical Factor 2 has a significant negative correlation with silica concentrations in surface waters and with wind-stress curl during spring (figure 2.12a and Table 2.4). This factor is positively correlated with temperature and salinity, which in our data are highest under subtropical waters. The dominant species, *Thalassionema nitzschioides* is a cosmopolitan species, commonly found in low latitudes (Jousé et al., 1971, Sancetta and Silvestri, 1986) and in eastern boundary systems during times of weak upwelling (Margalef, 1978). Barron et al. (2003) suggested that this species could be an indicator of open ocean upwelling, but we find this not to be the case because of the significant negative correlations to wind-stress curl. The geographic distribution of this factor marks a boundary between subtropical waters and the more open-ocean displacement of the coastal upwelling filament. The high relative abundance of *Thalassionema nitzschioides* in offshore areas may indicate that it is better able to survive in areas of low productivity than other diatoms species, while in the strong upwelling regions it is effectively diluted by species that bloom more rapidly (*e.g.*, *Chaetoceros*) in response to nutrient input. Factor 2 is also the only one that yields a significant correlation with temperature in this region (Table 2.4), although this may be a regional coincidence of this species' ability to survive in oligotrophic subtropical waters to a greater extent than other diatom species, and the fact that in the NE Pacific region, oligotrophic waters are relatively warm. When we separate the correlations for the sub areas, the significance of the correlations for this factor increase dramatically, and become clearer (appendix B). Since this factor is strongest in the southern open-ocean area, the correlations show not only the same pattern as the ones for the entire region, but also indicate a stronger positive correlation with

spring salinity and temperature (figure 2.12c and d and appendix B). The correlations from the open-ocean region (west of 127^0W) and coastal-ocean region (east of 127^0W) show that this factor is positively correlated with winter and fall productivity and negatively correlated with spring and summer productivity (figure 2.12b and appendix B).

- Factor 3, the Subarctic Front Factor, is dominated by *Rhizosolenia hebetata* (*forma hebetata*). This species has been associated with the Alaskan Gyre and with the Subarctic Front (e. g. Jousé et al., 1971; Sancetta 1979; Sancetta and Silvestri, 1986) and has been characterized as a winter and northern cold-water organism (Cupp, 1943; Tomas, 1996). Its loadings are positively correlated with phosphate and spring nitrate concentrations in surface waters and negatively correlated with chlorophyll and productivity (figure 2.13 and Table 2.4). In the NE Pacific, the Subarctic water mass that upwells has relatively high nutrients and dissolved oxygen, low temperatures and low salinity (Bograd and Lynn, 2003). The significant negative correlations with chlorophyll and productivity (Table 2.4 and appendix B also indicate relation of this factor with more open oligotrophic waters.
- Although there is no significant correlation of the "Mixture" Factor 4 to any of the oceanic properties considered here (Table 2.4 and appendix B), its primary species, *Neodenticula seminae*, is known to be associated with the cold Subarctic waters of the North Pacific (Hasle, 1977; Semina and Tarkhova, 1972, Jousé et al., 1971). Intrusion of this water into more coastal areas of the California Current system can induce higher productivity than normally observed for this area (Wheeler et. al, 2003). If *Denticula seminae* is tracking Subarctic water intrusions that reach the coast, by using this factor in a reconstruction we might be able to separate past production caused by Subarctic water displacement into the California Current system from that associated with coastal upwelling.
- Factor 5, the "Freshwater" factor, clearly shows the influence of freshwater species in our study. This factor has a strong negative correlation with salinity

in all seasons and has significant positive correlations with silicate concentrations (Table 2.4) and provides an opportunity to understand the role that rivers play in marine diatom ecology and productivity. River plumes bring dissolved silica needed by marine diatoms, as well as turbidity that changes light levels needed by primary producers, and also stratify the water column which influences ecosystems (Anderson, 1964; Margalef, 1978).

2.5 Conclusions

Comparison of core-tops and the sediment traps show that diatom remains reaching the sea floor generally reflect the export of robust diatom species from the upper ocean. Although there are differences between the methodologies used for sediment and sediment trap studies, we infer that about 50% of the diatoms species exported from surface waters are not preserved in the sediments. Nevertheless, the relative abundance among resistant species in our surface sediments is representative of the relative abundances recorded in a sediment trap. Although not representing the most productive season of summer (coastal upwelling), *Chaetoceros spores* are indicative of late summer/fall conditions when nutrients became scarce, a phenomenon that is also recorded in the sediment trap study.

Diatom absolute abundances, *Chaetoceros spores* absolute abundances and *Chaetoceros spores* percentages (relative to total diatoms) are correlated with regional atlas data on seasonal productivity and/or chlorophyll concentrations. The relative abundance of *Chaetoceros* appears to respond to both coastal upwelling and to open ocean (curl-driven) upwelling in the NE Pacific. In open-ocean settings, *Chaetoceros* spp. tracks annual average conditions, whereas in the coastal region, *Chaetoceros* spp. are associated with summer/fall production.

Samples from areas under the influence of coastal and open ocean (curl-driven) upwelling have similar percentages of *Chaetoceros spores,* although total diatom concentration is higher under the coastal regime. Nevertheless, small dilution and/or dissolution biases might affect these diatom concentrations.

Freshwater diatoms track large river plumes and are important in understanding climate changes on land. The location and intensity of the freshwater plume in the open ocean areas likely varied in the past. It may be possible to track such changes in the geologic record by the presence/absence of freshwater diatoms.

The presence of benthic diatom species at significant percentages in samples from water depths deeper than the euphotic zone likely indicate downslope transport. This information is useful for understanding transport events, and for culling samples in which the other diatom species assemblages may be biased by transport and not representative of overlying oceanic conditions. In the core-top samples examined here, benthic diatom species are relatively rare, rising above 2% in just one sample (which also contained abundant freshwater diatoms) suggesting that lateral bottom transport is a secondary process in the study area.

Q-mode Factor Analysis defines five different assemblages (each dominated by just a few diatom species) that are associated with different oceanic conditions, including high productivity associated with upwelling (Factor 1, *Chaetoceros spores*), warmer subtropical waters (Factor 2, *Thalassionema nitzschioides*), the subpolar front in the open ocean (Factor 3, *Rhizosolenia hebetata*), intrusions of Subarctic watermasses into the upwelling system (Factor 4, *Neodenticula seminae*), and the influence of freshwater from the continents (Factor 5, freshwater diatoms). These clearly defined factors will facilitate the future development of transfer functions for estimating past oceanic properties in the Northeast Pacific. However, Q-mode Factor Analysis failed to produce a factor that would distinguish between coastal and open-ocean (curl driven) upwelling. This problem will be address in future work using different statistical approaches.

Table 2.1 - Correlation coefficient between productivity and chlorophyll (gray boxes indicate significant correlations for p=0.05).

		Productivity				
		annual	winter	spring	summer	fall
Chlorophyll	annual	0.85				
	winter		-0.34			
	spring			0.78		
	summer				0.65	
	fall					0.85
Chlorophyll south of 46^{0}N	annual	0.94				
	winter		0.48			
	spring			0.88		
	summer				0.95	
	fall					0.93
Chlorophyll north of 46^{0}N	annual	0.80				
	winter		**0.19**			
	spring			0.90		
	summer				**-0.18**	
	fall					0.66
Chlorophyll west of 127^{0}W	annual	0.71				
	winter		-0.64			
	spring			0.80		
	summer				**0.08**	
	fall					0.76
Chlorophyll east of 127^{0}W	annual	0.63				
	winter		**-0.42**			
	spring			0.53		
	summer				0.75	
	fall					0.71

Table 2.2 - Correlation coefficient for productivity and chlorophyll, and diatom abundances, *Chaetoceros spores* abundances and percentages (gray boxes indicate significant correlations for p=0.05).

	Productivity					Chlorophyll				
Full area	annual	winter	spring	summer	fall	annual	winter	spring	summer	fall
Diatom abundances	0.36	0.34	0.23	0.30	0.34	0.39	0.16	0.16	0.45	0.41
Chaetoceros spores abundances	0.51	0.32	0.31	0.45	0.38	0.40	0.05	0.03	0.52	0.47
Chaetoceros spores (%)	0.48	0.51	0.00	0.25	0.58	0.43	-0.09	0.10	0.47	0.52
south of 46^{0}N										
Diatom abundances	0.38	0.39	0.29	0.37	0.42	0.40	0.19	0.15	0.50	0.45
Chaetoceros spores abundances	0.51	0.40	0.44	0.52	0.43	0.51	0.30	0.21	0.61	0.56
Chaetoceros spores (%)	0.45	0.24	0.24	0.49	0.68	0.34	0.32	0.39	0.28	0.34
north of 46^{0}N										
Diatom abundances	0.22	0.14	0.36	0.07	0.04	0.31	0.47	0.36	0.22	0.26
Chaetoceros spores abundances	-0.26	-0.27	-0.10	0.09	-0.39	-0.22	0.24	-0.18	-0.28	-0.24
Chaetoceros spores (%)	0.29	0.28	0.47	-0.18	0.03	0.37	0.33	0.44	0.28	0.31
West of 127^{0}W										
Diatom abundances	0.44	-0.05	0.31	0.34	0.11	0.64	0.45	0.46	0.49	0.47
Chaetoceros spores abundances	0.54	-0.25	0.48	0.51	-0.05	0.60	0.53	0.51	0.36	0.30
Chaetoceros spores (%)	-0.22	0.33	-0.29	-0.34	0.27	0.50	0.24	0.22	0.41	0.61
East of 127^{0}W										
Diatom abundances	0.20	0.27	0.02	0.15	0.22	0.17	-0.29	-0.32	0.40	0.32
Chaetoceros spores abundances	0.50	0.41	0.21	0.36	0.36	0.33	-0.25	-0.33	0.56	0.51
Chaetoceros spores (%)	0.23	0.33	-0.22	0.18	0.41	-0.32	-0.50	-0.41	-0.10	-0.14

Table 2.3 - Factor scores from Q-mode analysis (gray boxes indicate highest score for each factor).

Species	Factor 1	Factor 2	Factor 3	Factor 4	Factor 5
Freshwater	0.001	-0.163	0.104	-0.023	0.597
Benthics	-0.014	-0.037	-0.016	-0.012	0.246
Actinocyclus curvatulus	0.010	-0.030	0.059	0.000	0.035
Actinocyclus normanii	-0.018	-0.009	-0.017	0.041	0.153
Actinoptychus senarius	0.037	-0.057	-0.029	0.030	0.161
Stephanodiscus rotula (f minutula)	-0.012	-0.014	0.008	-0.010	0.157
Bacteriastrum spp.	-0.007	-0.045	0.007	-0.017	0.202
Chaetoceros spores	0.980	0.025	0.058	0.122	0.015
Coscinodiscus decrescens	-0.030	-0.010	0.136	0.014	-0.003
Coscinodiscus marginatus	0.022	-0.064	0.182	-0.025	-0.014
Coscinodiscus radiatus	-0.002	0.033	0.070	0.159	0.016
Cyclotella litoralis	0.012	-0.004	0.016	0.010	-0.005
Cyclotella spp	0.028	-0.030	0.016	0.020	0.048
Cyclotella striata	0.014	-0.010	-0.010	0.005	0.039
Hemidiscus cuneiformis	0.001	0.015	0.020	-0.003	-0.010
Leptocylindrus spores	0.047	-0.048	-0.015	0.038	0.036
Odontella aurita	0.009	-0.027	-0.005	0.030	0.035
Paralia sulcata	0.052	-0.099	-0.007	0.086	0.168
Rhizosolenia setigera	-0.001	0.010	-0.002	-0.003	-0.003
Rhizosolenia cf hebetata (f. hebetata)	-0.013	-0.088	0.805	-0.166	-0.134
Rhizosolenia styliformis	0.013	-0.005	-0.004	-0.003	-0.005
Roperia tesselata	-0.003	0.040	-0.010	0.002	-0.014
Thalassiossira allenii	0.001	0.005	-0.003	0.005	0.000
Thalassiossira anguste-lineata	0.003	0.010	-0.010	0.021	-0.012
Thalassiossira angulata	-0.004	0.009	-0.009	0.030	-0.004
Thalassiossira eccentrica	-0.066	-0.093	0.086	0.055	0.557
Thalassiossira leptotus	-0.014	-0.017	0.065	-0.015	0.113
Thalassiossira lineata	0.002	-0.011	-0.009	0.034	-0.004
Thalassiossira nanolineata	0.001	0.002	-0.001	-0.002	0.002
Thalassiossira oestrupii	-0.073	0.000	0.303	0.124	-0.025
Thalassiossira cf poroseriata	-0.007	0.021	-0.002	-0.001	-0.002
Thalassiossira cf trifulta	-0.012	-0.007	0.045	0.009	0.001

(continued on next page)

Table 2.3 (continued)

Species	Factor 1	Factor 2	Factor 3	Factor 4	Factor 5
Thalassiossira sp1	-0.025	-0.033	0.157	0.051	-0.013
Thalassiossira sp2	0.017	-0.046	0.191	-0.108	-0.020
Thalassiossira sp6	-0.011	-0.006	0.039	0.008	0.001
Thalassiossira spp.	-0.008	0.003	0.137	-0.016	-0.023
Delphineis surillela	-0.005	-0.005	-0.007	-0.006	0.078
Fragilariopsis doliolus	-0.078	0.277	0.000	0.124	-0.079
Gomphonema constrictum	-0.009	-0.022	-0.006	-0.006	0.120
Lioloma elongatum	0.001	-0.010	0.078	-0.005	-0.015
Lioloma pacificum	-0.002	0.022	0.059	-0.003	-0.020
Lioloma spp.	-0.004	-0.013	0.216	-0.049	-0.030
Neodenticula seminae	-0.109	-0.175	0.096	0.921	-0.086
Nitzschia gp bicapitata	0.001	0.029	0.003	-0.005	0.020
Raphoneis amphiceros	0.010	-0.006	-0.005	-0.016	0.060
Thalassionema bacillare	-0.003	0.022	-0.002	0.000	-0.003
Thalassionema nitzschioides	-0.020	0.902	0.153	0.125	0.221

Table 2.4- Correlation coefficient for Q-mode factors and oceanic properties (gray boxes indicate significant correlations for p=0.05).

Full Region		Factor 1	Factor 2	Factor 3	Factor 4	Factor 5
	annual	0.37	-0.12	-0.46	-0.11	-0.14
	winter	0.36	0.43	-0.46	-0.30	-0.18
Productivity	spring	0.05	-0.46	0.01	0.18	0.11
	summer	0.41	0.22	-0.47	-0.24	-0.23
	fall	0.20	-0.50	-0.10	0.07	-0.10
	annual	0.09	0.38	-0.28	-0.22	-0.05
	winter	0.17	0.45	-0.35	-0.26	-0.05
Temperature	spring	0.21	0.34	-0.46	-0.24	0.08
	summer	-0.09	0.20	-0.06	-0.11	-0.12
	fall	0.01	0.41	-0.16	-0.21	-0.13
	annual	0.05	0.43	0.23	-0.01	-0.71
	winter	0.12	0.39	0.18	0.05	-0.79
Salinity	spring	0.03	0.43	0.25	0.00	-0.70
	summer	-0.05	0.43	0.32	-0.03	-0.57
	fall	0.09	0.46	0.12	-0.05	-0.67
	annual	0.38	-0.21	-0.58	-0.06	0.27
	winter	0.10	-0.32	-0.02	0.12	0.27
Chlorophyll	spring	0.17	-0.48	-0.27	0.11	0.44
	summer	0.37	-0.01	-0.57	-0.12	0.09
	fall	0.41	0.01	-0.64	-0.14	0.13
	annual	-0.20	-0.40	0.34	0.23	0.11
	winter	-0.19	-0.48	0.31	0.26	0.12
Nitrate	spring	-0.40	-0.33	0.58	0.21	-0.07
	summer	-0.15	-0.30	0.26	0.17	0.19
	fall	0.00	-0.22	0.11	0.18	0.19
	annual	-0.01	-0.39	-0.03	0.13	0.44
	winter	-0.01	-0.34	-0.07	0.12	0.46
Silicate	spring	-0.32	-0.65	0.14	0.13	0.56
	summer	0.08	-0.35	-0.05	0.15	0.34
	fall	0.14	-0.17	-0.08	0.10	0.30
	annual	-0.39	-0.32	0.56	0.18	0.11
	winter	-0.28	-0.49	0.42	0.25	0.15
Phosphate	spring	-0.63	-0.29	0.78	0.15	-0.06
	summer	-0.45	0.02	0.57	0.02	0.01
	fall	0.01	-0.03	0.11	0.05	0.19

(continued on next page)

Table 2.4 (continued)

Full Region		Factor 1	Factor 2	Factor 3	Factor 4	Factor 5
	annual	0.08	-0.45	0.11	0.27	0.21
	winter	-0.03	-0.29	0.20	0.24	0.40
Wind-stress	spring	-0.05	-0.58	0.25	0.27	0.10
curl	summer	0.37	-0.36	-0.25	0.15	0.06
	fall	-0.01	-0.38	0.19	0.27	0.19

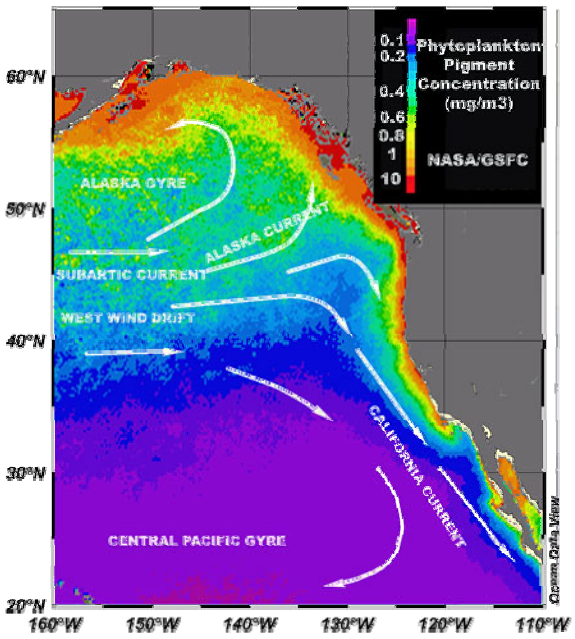

Figure 2.1 – Map of the Western North America and NE Pacific System. Background picture shows phytoplankton pigments concentrations (annual composite 1997-2000) measured by satellite (from http://meer.org/M13.htm; October 2002).

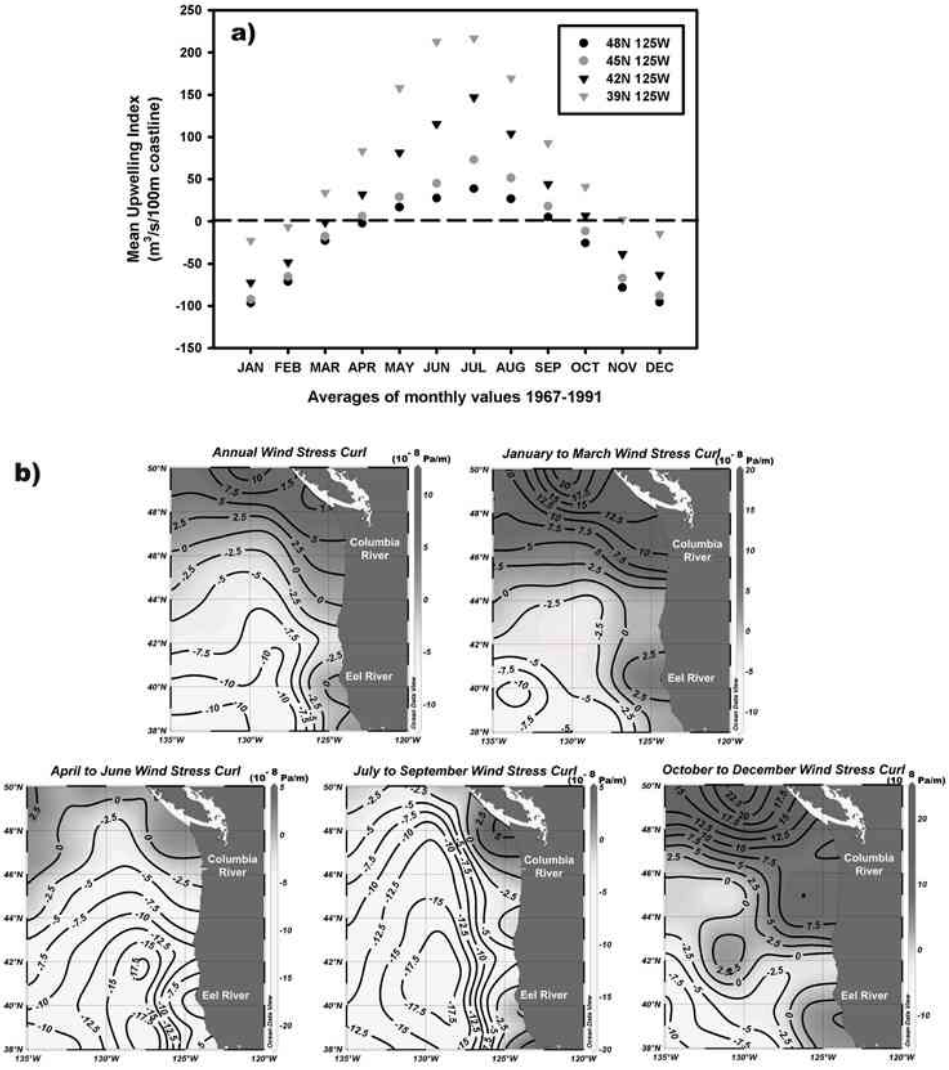

Figure 2.2 - a) Coastal upwelling indexes from monthly values averaged from 1967 to 1991 for four locations along the NE Pacific coast (from www.pfel.noaa.gov/javamenu.html: July 2005); and b) Maps of Wind-stress Curl (from January 2000 to September 2004) for our study area (contours are 10^{-8} Pa m^{-1}). Positive values (dark shading) are associated with open-ocean upwelling and negative values (light shading) with downwelling (from QuickScat monthly mean wind field data in http://las.pfel.noaa.gov/OceanWatch.html; July 2005).

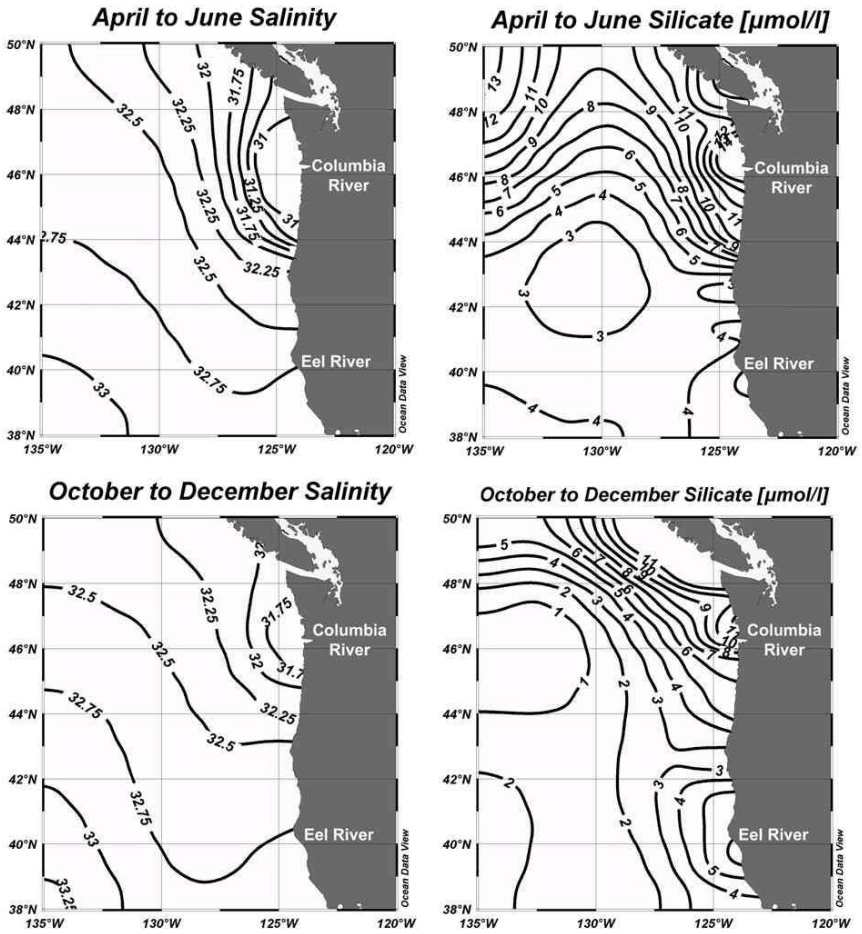

Figure 2.3 – Surface ocean salinity (PSU) and dissolved silicate (µmol/l) for April to June (top panel) and October to December (bottom panel) (from World Ocean Atlas 1998). Note low salinity and high silicate plume near Columbia River.

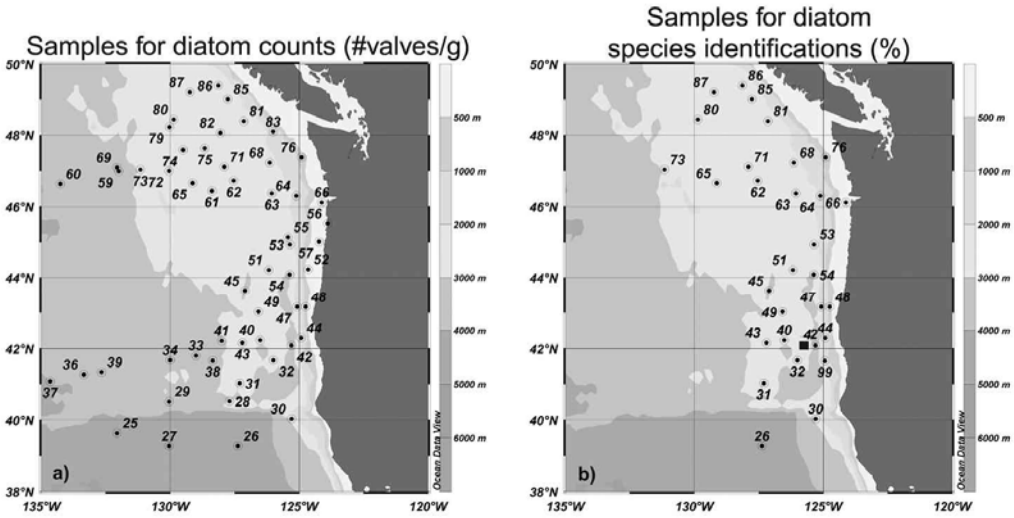

Figure 2.4 – Core-top locations for a) diatom counts (#valves/g of sediment) and b) diatom species identifications (species relative percentages). Black square shows sediment trap location and location for W8709A-13PC (these two positions are too close to distinct them at the level of the map scale). Numbers refer to core ID # in the electronic data supplement.

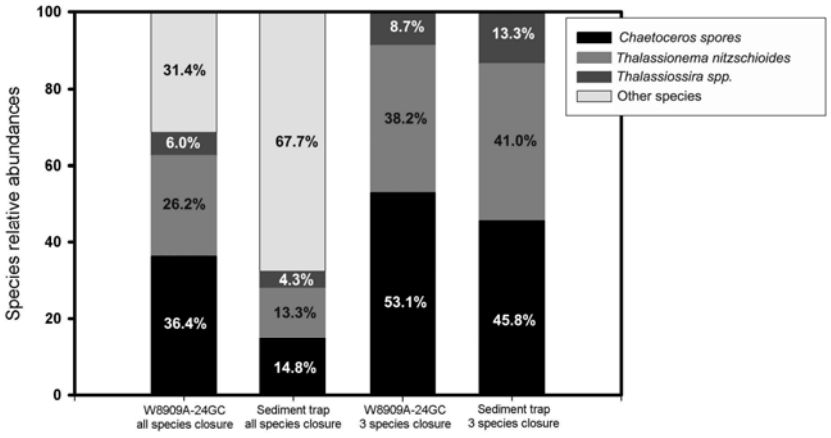

Figure 2.5 – Histogram of relative percentages (closure around all species on left and around three species on right) for species in common between core W8909-24GC and the Nearshore sediment trap (Sancetta, 1992).

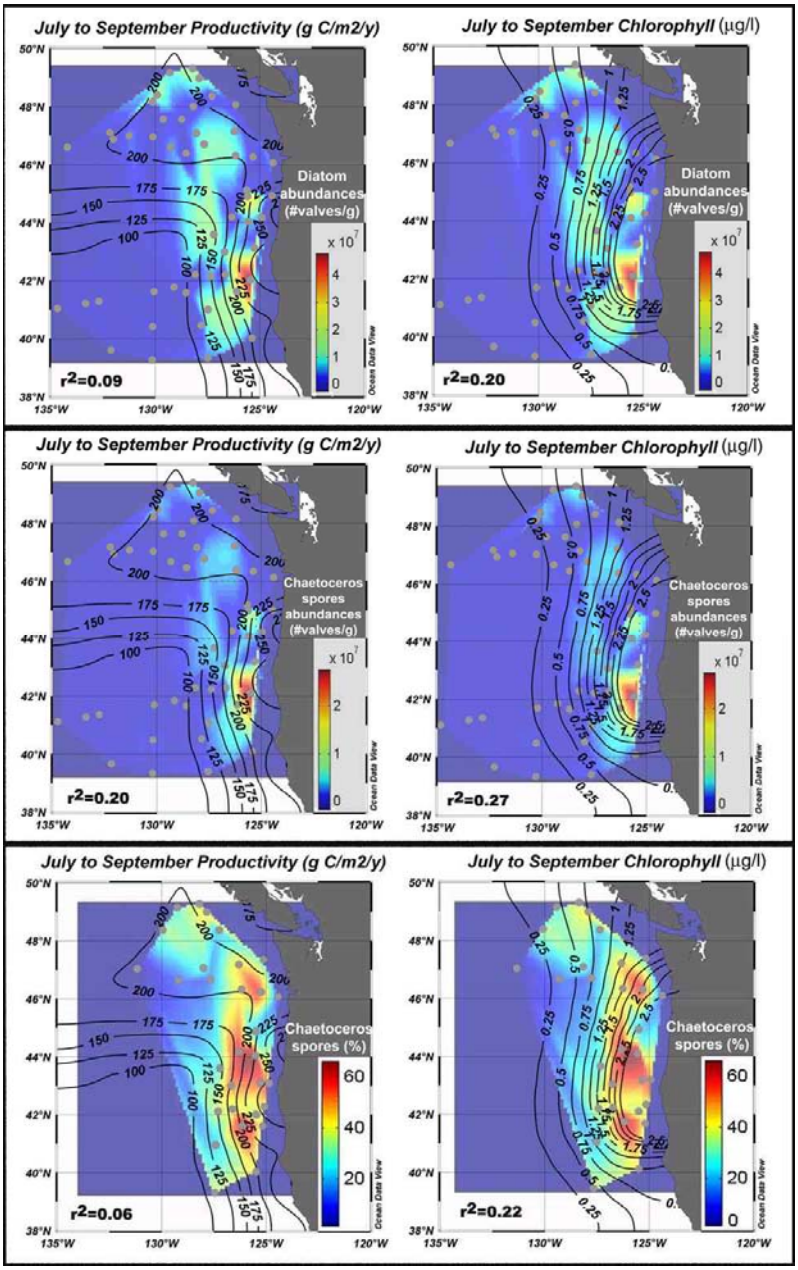

Figure 2.6 – Spatial distribution of satellite productivity (contours $gC/m^2/y$) and in-situ chlorophyll (contours in µg/l) and diatom abundances (color bar, upper panel), *Chaetoceros spores* abundances (color bar, middle panel) and *Chaetoceros spores* percentages (color bar, lower panel). Grey dots are sample locations.

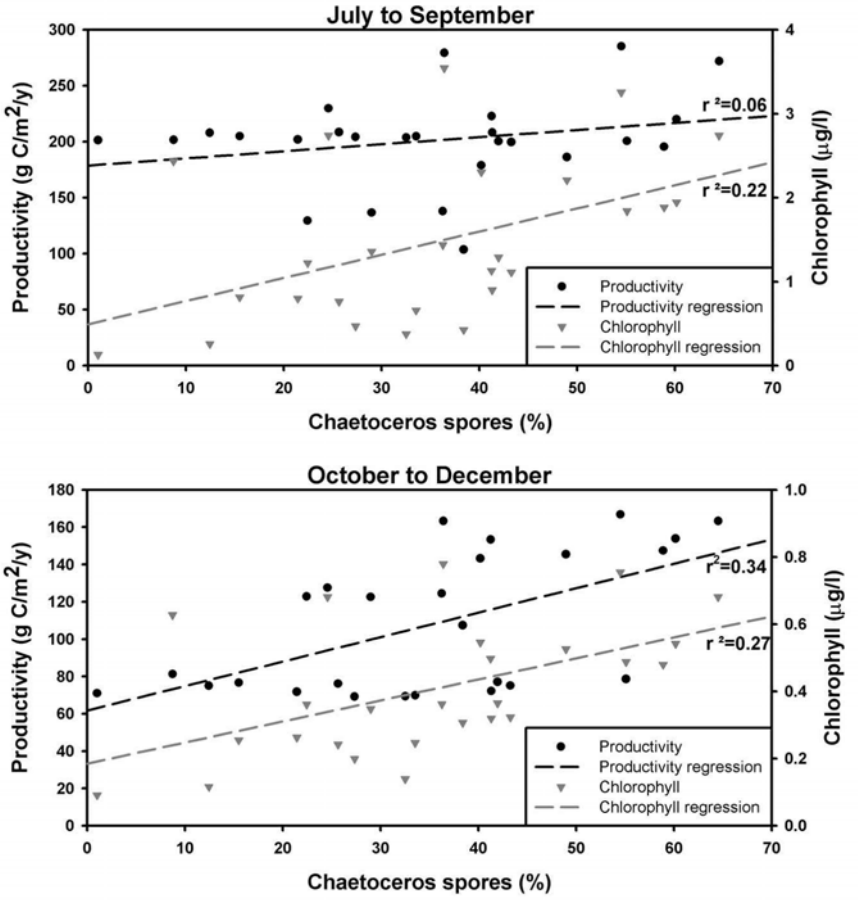

Figure 2.7 – Scatter plots for *Chaetoceros spores* (%) versus productivity (g C/m^2/y) and chlorophyll (µg/l). Top panel refers to summer (July to September) and bottom panel refers to fall (October to December).

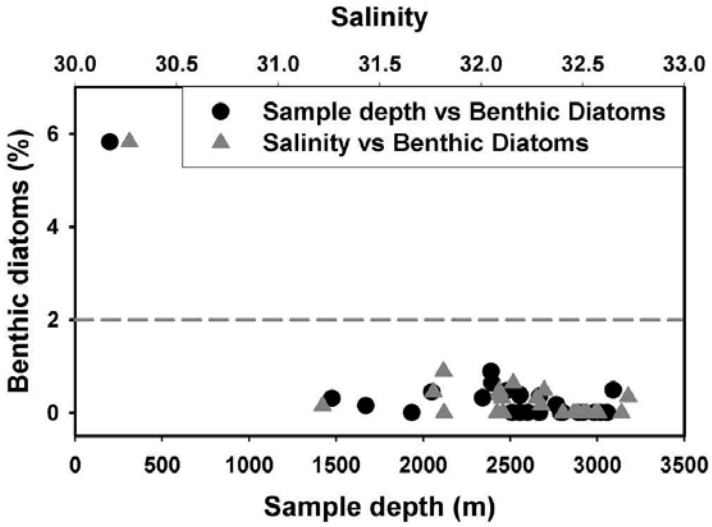

Figure 2.8 – Benthic diatom abundance plotted versus annual average salinity (PSU) and sample depth (m). The dashed line marks 2 %.

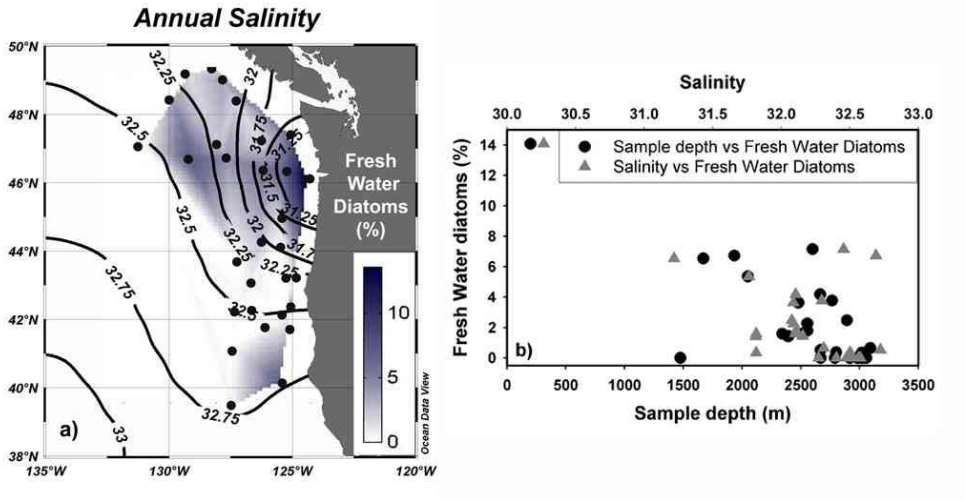

Figure 2.9 – a) Spatial distribution of freshwater diatoms (%) and annual average salinity (contours in PSU; from World Ocean Atlas 1998; black dots are sample locations), and b) freshwater diatoms (%) plotted versus annual average salinity (PSU) and sample depth (m).

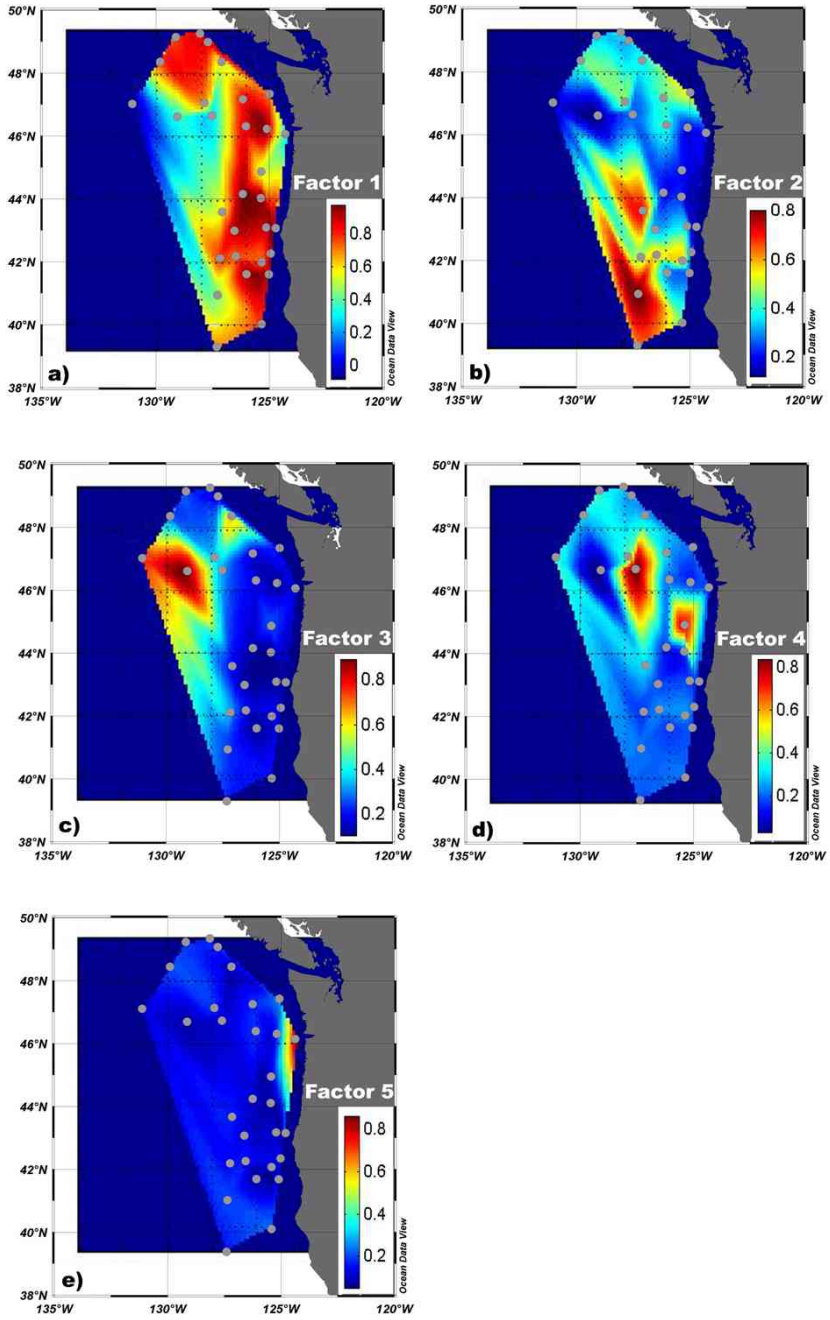

Figure 2.10 – Spatial distribution of factor loadings for the five factors (gray dots are the samples locations).

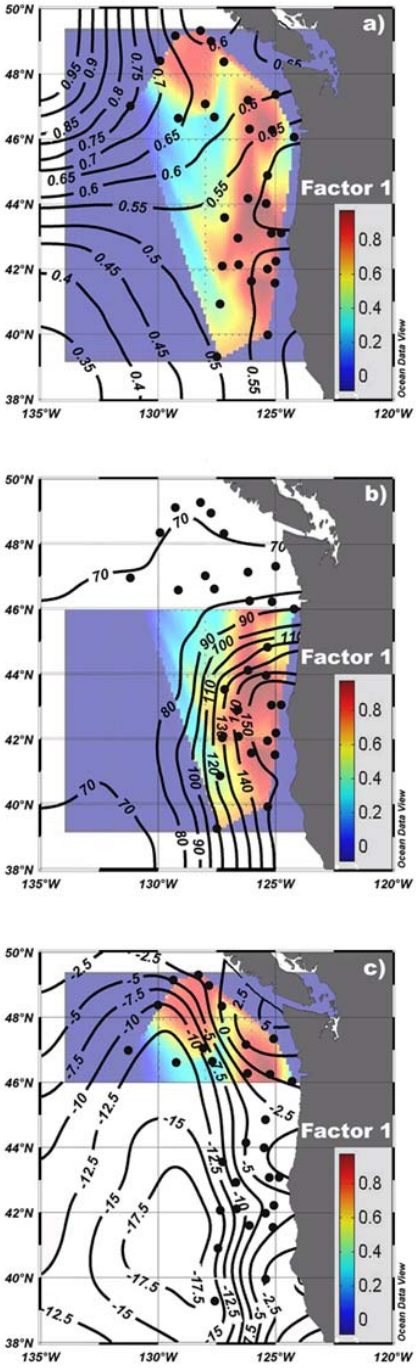

Figure 2.11 – Spatial relations between loadings of Factor 1 (color) and a) spring phosphate (contours in µM/l), b) fall productivity (contours in $gC/m^2/y$) for south of 46^0N and c) summer wind-stress curl (contours in 10^{-8} Pa/m) for north of 46^0N. Black dots are sample locations.

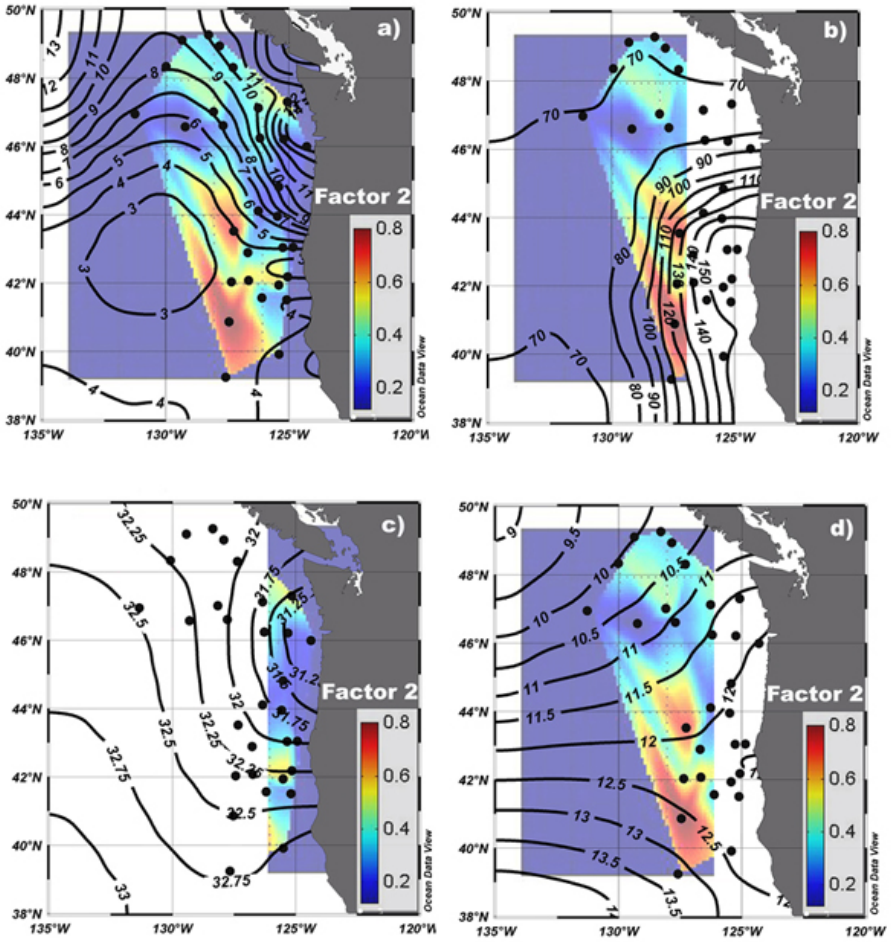

Figure 2.12 - Spatial relations between loadings of Factor 2 and a) spring silicate (contours in µmol/l), b) fall productivity (contours in $gC/m^2/y$) west of 127^0W, c) summer salinity (contours in PSU) east of 127^0W and d) spring temperature (contours in ^{0}C) west of 127^0W. Black dots are sample locations.

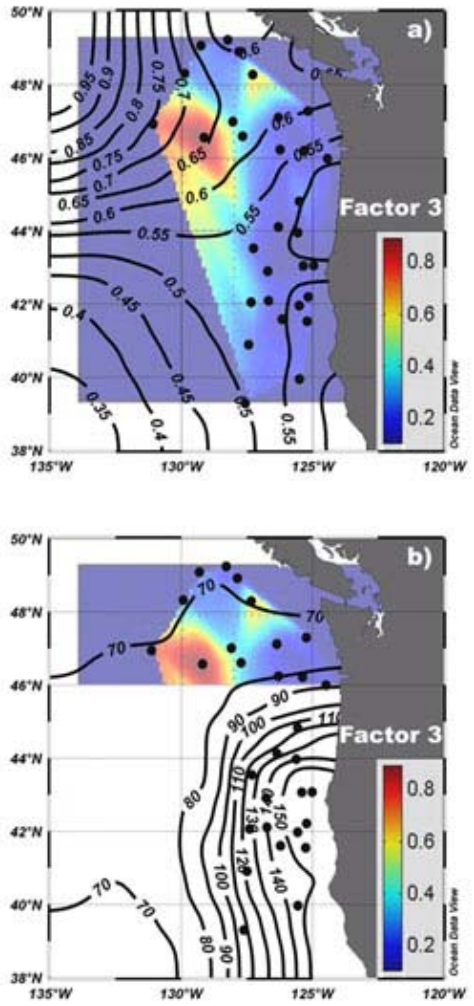

Figure 2.13 - Spatial relations between loadings of Factor 3 and a) spring phosphate (contours in µM/l) and b) fall productivity (contours in $gC/m^2/y$) north of 46^0N. Black dots are sample locations.

3. NORTHEAST PACIFIC DIATOM-BASED TRANSFER FUNCTIONS: IMBRIE AND KIPP VERSUS CANONICAL CORRESPONDENCE ANALYSIS

Cristina Lopes, Alan C. Mix and Fátima Abrantes

Submitted to Quaternary Science Reviews in May 2006
http://ees.elsevier.com/quascirev/

Abstract

We develop transfer functions (TFs) to estimate environmental properties in the northeast Pacific from diatom species based on two common approaches: the Imbrie and Kipp (I&K) and the Canonical Correspondence Analysis (CCA) methods. The I&K method is an unconstrained technique (the resulting ordination only contains information from the species dataset) based on the multiple regressions of orthogonal Q-mode factor loadings on user-selected environmental variables. CCA is a constrained technique that allows two datasets (the floral and the environmental) to interrelate together, seeking objective best-fit relationships (the ordination is therefore constrained by the environmental dataset). We also employ a constrained discriminant analysis (Canonical Variate Analysis) to better understand which diatom species are more suitable to differentiate between specific environments present in our study area. The TFs were developed using a modern dataset of 30 core-top samples, 51 diatom species and 30 environmental variables (oceanic properties). The I&K method resulted in significant TFs with modern calibrations for winter primary productivity, annual and winter salinity and spring PO_4. The CCA method produced TFs for winter and spring productivity, summer sea-surface temperature, winter salinity and spring PO_4. We found that both methods can yield similar results for certain environmental variables.

3.1 Introduction:

Diatoms are the most common primary producers in the oceans that are preserved in marine sediments (Schuette and Schrader, 1981). As rapidly blooming organisms, they are sensitive to oceanic and atmospheric conditions. For example, diatom species diversity and abundance in sediments can qualitatively track well-known processes such as upwelling or river runoff (Lopes et al., 2006).

Although general insight may come from qualitative studies, relationships became clearer with the early application of the quantitative transfer function (TF) methods. For example, Sancetta (1979) applied the Imbrie and Kipp (1971) method (hereafter, I&K) to diatoms from the North Pacific, and estimated winter, summer and range (summer minus winter) sea-surface temperatures. At that time, data for

calibration of other sea-surface properties was not readily available. Today, with the availability of global atlases of many environmental properties (e.g., World Ocean Atlas), satellite data, and better instrumental technologies, more information is available. Furthermore, modern computer technology and power enable us to apply stronger and faster statistical tools and models. For paleoceanographic applications it is important to understand what is really controlling different species presence, and which statistical approaches provide robust quantitative information on past environmental conditions.

Although the I&K approach is still one of the most used methods to develop TFs, other methods (e.g. Modern Analog Technique, Artificial Neural Networks) have also been applied to paleoceanography (Kucera et al., 2005). Here we focus on two methods, I&K and Canonical Correspondence Analysis (CCA) (ter Braak, 1986). We include all diatom species in our analysis, and we consider possible biases due to intercorrelations between oceanic properties. We have two goals. The first is to objectively discover which of the environmental variables that are available for our study area are most suitable for TF development using our floral database. This will avoid any tendency to force the development of a biased TF. The second goal is to compare TFs for those environmental variables using the CCA results and the I&K method, which have very different basic assumptions and thus serve as a check on the robustness of quantitative estimates.

3.2 Regional setting

Our study region (figure 3.1) includes a broad range of oceanic surface properties. Maps (on a 1^0 by 1^0 grid, from Antoine and Morel, 1996 and from the World Ocean Atlas, 1998) show annual averages and seasonal (winter, spring, summer and fall) standard deviations (STDs) for some of the oceanic properties considered in this study (figure 3.2). This annual average versus seasonal STD allow us to identify the position of constant more or less year round processes (low STD) with seasonal events (high STD).

Figure 3.1 shows how the West Wind Drift Current separates near the northwest margin of the United States to form the Alaska and the California Currents. The Alaska Current flows north and forms the eastern edge of the Alaska Gyre, while the California Current flows south as the eastern edge of the North Pacific Subtropical Gyre. The Subarctic Front occurs seasonally between ~40^0 and 50^0 N, while and the Subtropical Front is found between 28 and 35^0 N (Roden, 1975). The wind fields, controlled by the positions of the North Pacific atmospheric high-pressure cell and the Aleutian low-pressure cell, affect the position of these fronts (Roden, 1975).

The position of atmospheric pressure cells also controls the seasonal distribution of coastal upwelling associated with the California Current. Off Oregon, coastal upwelling occurs intermittently between April and August (Smith, 1983). Farther south (off California), coastal upwelling conditions are more persistent (figure 3.3) and can even be present year-round (Huyer, 1983). The strongest coastal upwelling on an annual average occurs between 36^o N and 42^o N (Hostetler et al., 1999). Figure 3.2e shows geographically, the positions of year-round coastal upwelling (strong annual average for primary productivity) and where the seasonal coastal upwelling is more common (high annual average and high STD in primary productivity).

Another type of upwelling is also present in our study area: open-ocean upwelling driven by the curl of the wind-stress (Bakun and Nelson, 1991). This type of upwelling is associated with wind jets or gradients over the ocean, especially in the Subarctic area off Washington and British Columbia (throughout the year) and off Oregon and California (in winter). Figure 3.2f shows the annual position and the STD associated with this type of upwelling (positive curl indicated by the shaded area, is divergence and upwelling). Although both coastal and open-ocean upwelling systems can be characterized by high productivity, coastal upwelling favors intermittent blooms of larger phytoplankton that yield high export flux to the sediments, whereas open-ocean upwelling is often associated with the presence of small phytoplankton and low export productivity flux to the sediments, perhaps due to constant recycling of

nutrients associated with high grazing activity (Miller et al., 1991) or limitation of micronutrients such as iron (Hutchins and Bruland, 1998).

We consider four sub-areas based on dominant character of upwelling systems (figure 3.4). An approximate western boundary for coastal upwelling occurs near 127^0 W. Coastal upwelling systems are normally confined to within 50 km from shoreline (Huyer, 1983). Nevertheless, it is common for giant cold-water plumes and eddies to extend into the open ocean (e.g. Hood et al., 1990 and Hickey, 1998). In the southern part of our region, to the west of the strong coastal upwelling system is the oligotrophic subtropical gyre. An approximate southern boundary of strong open-ocean upwelling is 46^0 N (figure 3.4). The boundary locations also provide us to keep the same number of samples on each side. This geographic separation defines four sub-areas that have different physical and chemical oceanic gradients of productivity, sea-surface temperature, salinity and nutrients (figures 3.2, 3.4):

- Sub-area 1 (NW): north of 46^0 N and west of 127^0 W. This area is under the influence of the Subarctic Front and the Subarctic water mass that is relative cold, less salty and rich in nutrients (Lynn and Simpson, 1987). Upwelling in this sub-area is driven primarily by the curl of the wind-stress (figure 3.2f);
- Sub-area 2 (NE): north of 46^0 N and east of 127^0 W. This area is under the same influences as sub-area 1, with the addition of river run-off (reflected by the annual mean and seasonal STD of salinity shown in figure 3.2b). The curl of the wind-stress is also strong in this sub-area.
- Sub-area 3 (SW): south of 46^0 N and west of 127^0 W. This southern open-ocean area is characterized by oligotrophic waters (low productivity (figure 3.2e) and low nutrient content (figures 3.2c, 3.2d)), and is relatively warm and salty (figure 3.2b), and in the subsurface has a lower dissolved oxygen content than the Subarctic water (Lynn and Simpson, 1987; Hickey, 1979). This sub-area is also under the influence of the Subtropical Front (figure 3.1).
- Sub-area 4 (SE): south of 46^0 N and east of 127^0 W. This area is under the influence of coastal upwelling (figure 3.2e), driven by northerly winds in summer, which brings cold, nutrient-rich water to the surface and fuels high

productivity including diatom blooms. In this sub-area, some curl of the wind-stress can also occur (figure 3.2f).

3.3 Methods

We focus on two ordination techniques, i.e., statistical methods that represent the variance contained in a raw dataset with a smaller set of orthogonal components (McGarigal et al., 2000). The goal is to select end members that will express the essential information contained in a multivariate dataset through the creation of eigenvectors (axes, dimensions, gradients), while minimizing the contributions of analytical noise.

Ordination techniques can be constrained (direct gradient analysis) or unconstrained (indirect gradient analysis) depending on the existence or not of a second dataset such as ecological information (McGarigal et al., 2000). In unconstrained methods, the eigenvectors are independent of the environment, and are later compared with the environmental variables. The constrained methods are able to use two sets of information (species and environmental variables) at the same time, allowing objective optimization of relationships between species and environmental variables.

3.3.1 The Imbrie and Kipp method

The I&K approach is an unconstrained method based on the Q-mode Factor Analysis (Imbrie and Kipp, 1971). This analysis extracts factors or gradients that combine variables (species) based on sample information. It operates on a matrix of sample similarities (cosine theta) and solves for eigenvectors that contain variation information. The eigenvectors are then converted into factor scores for each species, and the scores are then used as a set of weights that to produce the factor loadings for each sample. The sample factor loadings represent the position of each sample in the newly defined gradients and show how important each end member (that create those gradients) is within a sample. The factor loading can also be plotted in maps to show the geographic importance of the end members or factors defined by the species. For

each sample loading, a communality documents the fraction of original sample variance captured by the factor model for each sample (Davis, 2002) and may vary between zero and one; zero indicates that the factors do not represent any of the sample data, and one indicates complete representation of the original data without loss of information. The number of factors is chosen based on their description of a significant amount of the total information (Davis, 2002), and also based on ecologically reasonable distributions of factors (i.e., factor loadings with coherent geographic patterns).

The sample factor loadings from core tops are the input for calibration of the TFs. Multiple stepwise regressions are performed to get the best weighing of factors loadings to estimate a particular environmental variable. The resulting set of coefficients for the equations that estimate the environmental variable is the modern calibration. Sample factor loadings for downcore samples are obtained from applying the species factor scores from the modern calibration to the downcore raw species dataset. The calibrated TF is then applied to the downcore sample factors loadings in order to estimate past variations in the environment. There is not a strict requirement that factor analysis must be performed on the core-top samples used for calibration. For example, Mix et al. (1999b) develop a method that reverses the process by performing factor analysis on ancient (downcore) samples and applying them to core-tops, for purpose of environmental calibration, and then applying the calibrated transfer function equations onto the ancient samples. This flexibility of the method helps to avoid problems with so-called "no-analog" effects (Hutson, 1977), in which past sample variability is outside the range of modern samples.

3.3.2 Canonical Correspondence approach

Canonical Correspondence Analysis (CCA) was performed using CANOCO (version 4.2) software (ter Braak and Smilauer, 1998). A general discussion of the application of this method to marine microfossils is given by Morey et al. (2005). This is a constrained ordination technique, which allows for interaction between species and environmental variables. The canonical ordination can use two different

approaches: one that includes regressions between the environmental variables and samples (that result in the new axes or dimensions) and another based on weighting average (WA) techniques (ter Braak and Smilauer, 1998). The axes that have environmental information (i.e. resulting from linear combinations of environmental variables) are called the canonical axes (CCA axes) and their eigenvalues reflect the amount of canonical variance between the species and the environmental variables datasets. The amount of variance that remains after the variance explained by the constrained analysis is removed (CCA axes) is the variance that is still contained in the species dataset only (Lepŝ and Ŝmilauer, 2003).

CCA is a unimodal technique because it is based on the concept that species have a maximum abundance value for a certain "optima" of environmental variables (ter Braak, 1986). This method also produces factor loadings and factor scores, but the information contained in the factor scores reflects the species "optima" relative to each environmental variable. In Q-mode, the sample loadings are calculated from the species scores in a very straightforward way. CCA species and sample scores are calculated in a more complicated way through an algorithm that applies multiple regressions and weighted average techniques (ter Braak, 1986):

- S1) Start with arbitrary, but unequal, initial site scores.
- S2) Calculate species scores by weighted averaging of the site scores.
- S3) Calculate new site scores by weighting averaging of the species scores.
- S4) Obtain regression coefficients by weighted multiple regression of the site scores (from S3) on the environmental variables. The weights are the site totals.
- S5) Calculate new site scores. The new site scores are in fact the fitted values of the regression of the previous step.
- S6) Center and standardize the site scores (mean = 0 and variance = 1).
- S7) Stop on convergence, i.e. when the new site scores are sufficiently close to the site scores of the previous iteration; otherwise go to S2.

When going from S7 to S2, the new site scores are used. Site scores are what we refer to as sample scores. Species scores depend on the sample scores. The sample

scores depend on the species scores and on the regression coefficients from fitting the environmental variables information.

The algorithm produces two types of sample scores and this has been cause for debate regarding the CCA ordination plots and which type of sample scores should be plotted (McCune and Grace, 2002). Palmer (1993) labeled the sample scores resulting from step S3 the WA scores (scores determined by weighting averaging) and the ones from S5 the LC scores (scores determined from linear combinations of explanatory variables or environmental variables). In CANOCO, ter Braak and Smilauer (1998) label the sample scores as "sample scores that are derived from the environment" (corresponding to Palmer's, 1993, designation of LC) and sample scores "which are derived from the species" (corresponding to Palmer's, 1993, designation of WA). McCune and Grace (2002) note that plots of LC scores are in "environmental space" in which the axes are linear combinations of the environmental variables, whereas the plots of WA scores are in "species space" in which the axes are linear combinations of species. In other words, if one chooses to plot WA scores, the axes of that plot are not constrained (i.e., do not carry environmental information) (McCune and Grace, 2002). In CANOCO, ter Braak and Smilauer (1998) consider that each axis in the ordination has two variables: one designated "SPEC AX" and another designated "ENVI AX". The two variables are the reflection of the two types of sample scores ("SPEC AX" from WA scores and "ENVI AX" from LC scores). However, the two types of axes are correlated between them through the species-environment correlations. These correlations result from S4 in the algorithm and they are a "measure of how well the extracted variation in community composition can be explained by the environmental variables and is equal to the correlation between the site scores, which are weighted mean species scores, and the sites scores, which are a linear combination of the environmental variables" (ter Braak, 1986). Therefore, the mentioned correlations are the link to obtain a CCA plot that is composed of constrained axes and where the WA scores (samples and species) can be plotted. In addition, because the algorithm is iterative, the axes of CCA plots are defined from LC scores, which were in turn actually derived from WA scores.

The CCA ordination plots shown here use WA scores in constrained axes. The species scores position the species "optima" relative to linear combinations of the environmental variables. The sample score positions reflect the importance of each sample for the species "optima's" definition into the axes. In addition, the plots show axes that were standardized to zero weighted mean and unit weighted variance (ter Braak and Verdonschot, 1995). In this case the vector lengths represent the correlation between the environmental variables and the canonical axes (ter Braak and Verdonschot, 1995). The projection of a species onto the environmental vector shows approximately the species "optima" regarding that particular environmental variable. The projection of a sample position into the environmental vector shows the ordering of samples with respect to that particular environmental variable (Lepŝ and Ŝmilauer, 2003).

In TFs develop from CCA methods, the ancient (downcore) species are considered "supplementary" and the scores are calculated based upon the algorithm application of the samples that have environmental information (i.e. that resulted from our modern calibration). The species and samples scores for downcore samples are regressed into the existing ordination axes (ter Braak and Smilauer, 1998).

By default, CANOCO is programmed to extract four ordination axes (ter Braak and Smilauer, 1998). If the number of environmental variables is less than four, the axes that contain environmental information (the constrained axes) are less than the ones containing species information (unconstrained axes) (ter Braak and Smilauer, 1998). This means that for example if we have only two environmental variables, the first two axes have both "SPEC" and "ENVI" variables and the last two axes only have the "SPEC" variable and no correlations between species and environment exist within the dataset. However, the information from the last two axes is still important and should not be discarded because it provides information from species variance that is not related with the selected environmental variables.

If the species dataset violates the assumption of unimodal behavior, an "arch effect" will occur when plotting the sample scores against the CCA axes (ter Braak and Smilauer, 1998). The "arch effect" problem is removed by performing a

Detrended Canonical Analysis (DCA), and by verifying the unimodal behavior of the species data by checking the length of the gradients (ter Braak and Smilauer, 1998).

We used two criteria to choose the best environmental variables: their statistical significance and the variance inflation factor (VIF). CCA allows checking the statistical significance of the environmental variables and it also checks the statistical significance of the analysis final results, using Monte Carlo permutation tests (ter Braak and Smilauer, 1998). The Monte Carlo test of significance basically shows that under each permutation of the original data, the samples in the species dataset can be randomly linked with samples from the environmental dataset (ter Braak and Smilauer, 1998). We set the number of permutations of our analysis to 999 because we noticed that with only 199 permutations we would get contradictory significances if we tested the same environmental variable more than once before including it or not in the analysis. The increase of the number of permutations solved this problem. The VIF value shows how an environmental variable is correlated to (i.e., dependent on) the others (ter Braak and Smilauer, 1998). Our CCA was set for a significance level of $p \leq 0.05$.

Because we have a large number of environmental variables with some degree of intercorrelation (appendix C), we follow ter Braak and Smilauer (1998) in using CANOCO's "automatic selection" option in order to retain the most significant variables (starting with the ten best variables). From these ten variables, we then used the VIF to reduce environmental variables based on their significant correlations with other environmental variables.

Many CCA studies allow variables into the analysis if the VIF is <10 (e.g. Jiang, et al., 1998; Morey et al., 2005). The VIF is calculated from the multiple correlations (r) between one environmental variable and the others (ter Braak and Smilauer, 1998) through the equation $VIF = 1/(1-r^2)$. A VIF of 20 retains variables with an r^2 of 0.95 between environmental variables, a VIF of 10 results in an r^2 of 0.9. However, because significant correlations depend on the number of samples used in the analysis (Devore and Peck, 1986), one should estimate a VIF cut off for a

particular analysis. The critical value to accept significance of a correlation can be used (Devore and Peck, 1986), as the r^2 for the above equation, allowing researchers to estimate the critical VIF that retains only independent environmental variables. In our study, critical VIF value has to be in close to one. The correlation matrix guides which environmental variable should be removed from the analysis. It is often not clear which of two environmental variables should be removed if they have similar VIFs, and in this case we performed the analysis iteratively by choosing first one, and then the other, environmental variable for removal, seeking a final solution that maximizes the variance explained.

The CCA method was also used to perform a discriminant analysis (Canonical Variate Analysis) in order to investigate if we were able to extract patterns given by species or combinations of species that would reflect the division of our sub-areas (figure 3.4). We followed the approached made by Ŝtech (1998), as reported by Lepŝ and Ŝmilauer (2003). This approach was also made to investigate if we could find a solution for the issue raised by Lopes et al. (2006) that Q-mode Factor Analysis did not discriminate between floras associated with coastal upwelling and those associated with open-ocean upwelling induced by wind-stress curl.

3.3.3 Data

Our species dataset is comprised of 51 diatom species/groups and 30 samples (figures 3.1, 3.4, Table 3.1 and appendix C). The dataset is comprised of species relative abundance (%), with only species that have relative abundances of at least 1% in at least one sample. This dataset differs from the one documented by Lopes et al., (2006) because we discovered based on ^{14}C data that one of the core tops in that study (MD02-2499 PC; 41.653^0 N, 124.940^0 W, 904 m depth) was not of modern age. This core top was replaced with one nearby that is of modern age (ODP 1019D; 41.683^0 N, 124.933^0 W, 978 m depth). Also, Lopes et al. (2006) only include species that are present in some samples at >2% abundance. Here, we allow species present at > 1% abundance in core tops, to include species that are rare at present but abundant in Pleistocene samples.

The environmental variables dataset (appendix C) includes the following sea-surface properties: primary productivity (PP) (Antoine and Morel, 1996), sea-surface temperature (SST), salinity (SSS) and nutrients (NO_3, PO_4 and SiO_2) (World Ocean Atlas 98). The environmental variables at each site were divided into five temporal averages: annual mean, winter (January to March), spring (April to June), summer (July to September) and fall (October to December).

Because diatoms are the major primary producers in our study area (Hood et al., 1990), we separated productivity from the other properties and perform two CCAs. This makes sense because SST, salinity, and nutrients control the diatom ecology. PP is therefore a consequence of how well the diatoms respond to the ecological conditions. In other words, diatoms are not dependent on PP like other microorganisms used to develop TFs (e.g. foraminifera and radiolarian). We called the CCA for the PP dataset the "CCA_PP" and the CCA for the other environmental variables (the TSN dataset, only with temperature, salinity and nutrients) the "CCA_TSN". Because we used different sources to obtain our environmental variables, the dataset used for "CCA_PP" has information for all the 30 sample locations. The dataset used to obtain the other environmental variables does not have information for four of our sample locations (appendix C).

3.4 Results

3.4.1 R-mode factor analysis

We followed the approach made by Morey et al. (2005) and performed an R-Mode Factor Analysis in our environmental and species datasets to investigate how many significant dimensions exist. The number of dimensions resulting from the R-mode analysis should be about the same as the number of environmental variables gradients resulting from the CCA. Also, because R-mode was set to calculate its eigenvalues from the correlation matrix, it also indicates the important correlations present between the variables. We evaluate the R-mode results using the scree-plot (Cattel and Vogelman, 1977) and the broken-stick (Frontier, 1976, as reported by Jackson, 1993) methods. The scree-plot method retains eigenvalues to the left of a line

regressed through eigenvalues of higher rank, plus one additional eigenvalue. The broken-stick method retains eigenvalues higher that the broken-stick values (i.e., the variance explained by random data). R-mode analyses were performed using the PC-Ord program (McCune and Mefford, 1999), which calculates the broken-stick values automatically.

While the broken-stick method shows that as many as 10 species dimensions may be retained, the scree-plot method retains six species dimensions (figure 3.5). The R-mode results show that for the TSN environmental properties dataset, three to five dimensions are retained, while in the PP environmental properties dataset two to three dimensions are retained (figure 3.5).

3.4.2 Imbrie and Kipp approach

Q-mode Factor Analysis was performed in Lopes et al. (2006). However, due to the differences in the species dataset used in this study, values are recalculated here. Q-mode returned five factors (Table 3.2) that explained 97% of the total variance. All communalities were higher than 0.7. The description of the factors follows Lopes et al. (2006):

- Factor 1 (figure 3.6a), the "Upwelling Factor" accounts for 56% of the total data and is dominated by *Chaetoceros spores*. The geographic position of this factor covers sub-areas 1, 2 and 4; indicating both coastal and wind-stress curl induced upwelling. This factor has significant positive correlations with summer productivity and negative correlations with spring phosphate and nitrate (Lopes, et al., 2006).
- Factor 2 (figure 3.6b) is called the "Subtropical Factor" because of the high species loadings of *Thalassionema nitzschioides* and its confinement to sub-area 3. This factor was also the only one that showed significant positive correlations with SST and salinity (Lopes, et al., 2006). This factor accounts for 16% of the total variance explained.
- Factor 3 (figure 3.6c) is the "Subarctic Front Factor", which accounts for 10% of the total variance explained. Lopes et al. (2006) show the relation of this

factor (which has the highest species loadings for *Rhizosolenia hebetata* (*forma hebetata*)) to the nutrient rich waters from the Subarctic water mass. This factor has significant positive correlations with phosphate and it is located in sub-area 1.

- Factor 4 (figure 3.6d) was named by Lopes et al. (2006) as the "Mixture Factor". Although it accounts for 10% of the total variance, its dominant species, *Neodenticula seminae* spreads between sub-area 1 and 2. This species is associated with Subarctic waters and its extension into more coastal waters can be used to track intrusions of this water mass into the California current.
- Factor 5 (figure 3.6e) is controlled by the freshwater diatom group. This "Freshwater Factor" accounts for 5% of the variance and its geographic distribution shows the obvious confinement to sub-area 2 and to the Columbia River region. This factor has significant negative correlation with salinity.

The next step in the I&K TF development method is to apply a multiple stepwise regression relating the sample scores and the environmental variables for each sample. This results in 30 equations because we have 30 environmental variables and a first selection of the best equations is made based on the r^2 and the residual mean standard error (RMSE). A compilation of the best TFs (winter productivity, annual and winter salinity and spring PO_4), including r^2 and RMSE, is shown in Table 3.3 and figure 3.7.

3.4.3 Canonical Correspondence Analysis (CCA)

None of the CCAs performed in this study was contaminated by "arch effects". Therefore there was no need to perform DCA or to check the gradient lengths for non-unimodal behavior.

In the "CCA_TSN" run (figure 3.8), the environmental variables that meet our criteria (statistical significance and VIF) are summer SST, winter salinity, and spring PO_4. These environmental variables are expressed in three CCA axes that are able to explain 100% of the canonical variance between species and environmental variables. The same number of axes explains only 33% of the total variance contained in the

species dataset. This means that 33% of the species community variance is explained by the environmental variables considered in the analysis. The remaining 67% of the community variance is caused either by noise, competition among species, other environmental variables or a combination of all. Because the number of environmental variables is less than the number of CCA axes that CANOCO produces by default, the fourth axes only has species variance information. This run has a p level = 0.001. CCA Axis 1 has a correlation of 0.8 with spring PO_4, CCA Axis 2 has a correlation of 0.8 with winter salinity and CCA Axis 3 has a correlation of 0.8 with summer SST. The gradients from the CCA axes are expressed geographically by plotting the sample scores in maps (figure 3.8c). Table 3.4 shows the amount of variability and percent fit for each species, regarding the three canonical axes. A species' percent fit for each CCA axes expresses how that species "fit" in the ordination diagram (ter Braak and Smilauer, 1998) and the cumulative fit (i.e. from all CCA axes) is expressed as the % variance explained. In a TF context, if we compare the % variance explained from the table to the value of species variance that the CCA axes explain (33% in the "CCA_TSN" run), one can infer about the species capacity as an environmental indicator (Morey et al., 2005). Species with high percent fit values should be included in the next-generation transfer functions, whereas species with low percent-fit values could be excluded without substantial loss of information (Morey et al., 2005).

In the "CCA_PP" run (figure 3.9), environmental variables retained are winter and spring PP. These environmental variables are expressed through two CCA axes that explain 100% of the canonical variance between species and environmental variables. The same number of axes explains only 13% of the total variance contained only in the species dataset. This means that 13% of the species community variance is related with winter and spring PP. In this case the third and fourth axes only has species variance information. The p level of this run is < 0.05 (0.006 for the first CCA axis and 0.002 for all CCA axes). CCA Axis 1 has a correlation of 0.7 with winter PP and CCA Axis 2 has a correlation of 0.7 with spring PP. figure 3.9c shows the

geographic maps for this run and Table 3.5 shows the species fit. figure 3.10 and Table 3.6 show the TFs developed from the CCA runs.

3.4.4 Canonical Variate Analysis (CVA)

As it can be seen from figure 3.6a and from Lopes et al. (2006), Q-mode Factor Analysis does not discriminate between the effects of coastal upwelling (south of 46^0 N) and the effects of open-ocean upwelling (north of 46^0 N). Because the "upwelling" factor (Factor 1) is dominated only by one species (*Chaetoceros spores*) we want to investigate if a combination of species or if any other species would be able to give us a geographic separation. Canonical methods allow us to work with two datasets at the same time, imposing an environmental condition that better explains the species variation. For the CVA we classified the environmental information by giving the sample locations a geographic value regarding the sub-division of our study area (Table 3.1). This sample geographic location classification follows a simple approach: we give a sample a value of one if it belongs to a particular sub-region and a value of zero if it does not belong to that particular sub-region (Lepŝ and Ŝmilauer, 2003). For example a sample that is located north of 46^0 N and west of 127^0 W will have ones for north of 46^0 N and west of 127^0 W, and zeros for south of 46^0 N and east of 127^0 W.

This classification will create a homogeneous gradient (presence versus absence) reflecting the samples location and therefore, the results of the analysis are qualitative: they do not express increases in the magnitude of the physical processes present in each sub-area. We reversed the approach of normal CCA: we used the species dataset to examine which species or linear combination of species would best explain the variation in the sample locations (Lepŝ and Ŝmilauer, 2003). This means that the species dataset in CVA plays the environmental variables dataset role in CCA (i.e. the explanatory variables). In addition, we also remove the freshwater and benthic diatoms from the analysis in order to eliminate the effect of river runoff.

Five species (*Actinoptychus senarius*, *Chaetoceros spores*, *Nitzschia group bicapita*, *Thalassionema nitzschioides* and *Paralia sulcata)* distinguish the four sub-

regions (figure 3.11). The northern (curl-driven upwelling) and southern (coastal upwelling) sub-regions positioned east of 127^0 W can be distinguished by *Actinoptychus senarius*, *Chaetoceros spores* and *Nitzschia group bicapita*. The southern samples have higher ranks of *Actinoptychus senarius* and *Chaetoceros spores* and lower ranks of *Nitzschia group bicapita*. The northern samples have the opposite ranks for the same species and also have high ranks for *Paralia sulcata*. In addition, the samples south of 46^0 N show a clear separation between west and east of 127^0 W given by *Thalassionema nitzschioides*, which have higher ranks for the samples west of 127^0 W.

The species retained within the CVA have VIFs close to one, demonstrating that these species are independent of each other. The final results show a significance level of p=0.005 and that the first two canonical axes explain 100% of the canonical variance between the species and the geographic locations and explain 74% of the variance contain in our geographic dataset. This means that 74% of the variance in our geographic dataset can be explained by two CCA axes that are linear combinations of the five species mentioned above. The projection of our samples into the environmental variables in figure 3.11 now expresses the "optima" of that sample regarding the species (remember that in CVA the species play the role of the environmental variables in CCA and the samples play the role of species).

3.4.5 Sensitivity tests

Since the results of the I&K are not subjected to the Monte Carlo permutation test (section 3.2), we performed another sensitivity test based on bootstrapping techniques (Jöckel et al., 1992). We randomly formed 6 groups of 5 samples (Table 3.7). None of the samples would be removed more than once in order to ensure that all the samples would fall into one of the groups. This type of approach serves not only to check if our results depend on our sampling decisions, but also to check if our samples are similar (and therefore some autocorrelation exists within the dataset).

The CCA runs were evaluated by comparing the final p level achieved by the new runs in which the groups were removed. If the p level stayed the same, no

difference would be found between the original runs and the ones from the sensitivity tests. For the I&K method new Q-mode Factor Analyses were performed and the new sample factors used in new regression equations. The final evaluation is based on the r^2 and RMSE of the new equations.

The sensitivity runs showed that the results from sections 4.2 and 4.4 were not reproduced by any of the sample group removal and that the removal of the samples yielded worse final results (p levels, r^2 and RMSE).

3.5 Discussion

The results from R-mode analysis (section 4.1) agree with the number of dimensions retained from CCA runs: three dimension for "CCA_TSN" (summer SST, winter salinity and spring PO_4), two dimensions for the "CCA_PP" run (winter and spring PP).

Some authors do not encourage the use of CCA methods because it does not take in consideration the full species or community variance (e.g. McCune and Grace, 2002). However, the same authors state that if the goal of the analysis is to investigate the amount of species variance that can be related to particular environmental variables, the CCA can be an adequate tool (McCune and Grace, 2002). Since this is part of our goal, we think that, in our case, CCA can be used.

One problem that his intrinsic to the TF development using CCA is the potential for circularity of applying a multiple stepwise regression to a method which results already derive from correlations with environmental variables. However, we can compare and maybe assess how this circularity can affect the TF results. The major concern is that the circularity of regressions can amplify and exaggerate the relations in our CCA TFs. If correct, then our CCA TFs would show much better results than our I&K TFs.

Comparing all the TF results (figures 3.7, 3.10, Tables 3.3 and 3.6), three TFs are common to both CCA and I&K: winter PP, winter salinity and spring PO_4. For winter salinity and spring PO_4 no difference is found between CCA or I&K. The r^2 are similar and the residuals show the same problem: the TFs overestimate higher

environmental variable values and underestimate lower ones. The geographic patterns of the Q-mode and CCA analysis reveal that CCA Axis 1 (figure 3.8c) and Q-mode Factor 3 (figure 3.6c) are very similar. CCA Axis 1 is correlated with spring PO_4 and Factor 3 is significantly correlated with annual, winter, spring and summer PO_4 (Lopes et al., 2006). CCA Axis 2 and Q-mode Factor 5 are also similar geographically (figures 3.8c, 3.6e). CCA Axis 2 is correlated with winter salinity and Factor 5 is negatively correlated (because its given by freshwater species) with salinity for all seasons (Lopes et al., 2006). Therefore, in the case of winter salinity and spring PO_4, both methods agree and no exaggeration is show from the CCA TFs. Both methods detected a strong environmental gradient and were able to express it in the same way through the TFs. Finally, the I&K method resulted in one TF for annual salinity that did not show in the CCA method. Within our dataset all seasons are correlated for salinity (appendix C). The CCA criteria for choosing the environmental variables discarded the annual average and considered only winter salinity. Therefore, we will not consider the annual salinity I&K TF in this discussion section.

The other comparable environmental variables between the two methods are winter PP. In this case, we have a strong regression for the CCA TF (r^2=0.97) and a modest regression for the I&K TF (r^2=0.6). The residuals from the CCA TF are random (figure 3.10a) as opposed to the residuals from the I&K TF (figure 3.7a). Factor 1 (the one that explains more than half of the species variance in Q-mode) has been related with PP (Lopes et al., 2006), although unable to separate PP caused by wind-stress curl induced upwelling and coastal upwelling. The geographic pattern of CCA Axis 1 (from "CCA_PP" run) looks very similar to the south pattern of Q-mode Factor 1 (figures 3.9c, 3.6a). In addition, the CCA Axis 1 geographic pattern is given by a sharp gradient between north and south (figures 3.9b, 3.11a). Factor 1 is significantly correlated with fall PP south of 46^{o}N when the same physical separation was artificially forced in Lopes et al. (2006). In addition, PP values for winter (figures 3.7a, 3.10a) have a clear distinction in which northern samples have lower PP values and southern samples have higher PP values. Although the TFs from both methods pick this gradient, the CCA seems to be more sensitive than the I&K. Is this a

reflection of the circularity in CCA TFs? We do not think so. The correlation of CCA Axis 1 with winter PP (0.7) is lower than for example the correlations between the axis from the "CCA_TSN" run and its respective environmental variables (0.8). If there was an amplifying effect caused by the TF regression, the TFs of "CCA_TSN" run should be stronger than they are, or at least stronger than winter PP TF. If there is no amplification of the TF regression for winter PP in CCA TF, the high (almost perfect) regression (r^2=0.97) most likely reflects CCA's ability to extract variance from the species that is directly related with PP winter. The low regression (r^2=0.6) from the I&K TF could be caused by the fact that the variance expressed by Q-mode Factor Analysis does not fully extract this north south gradient present in PP during winter.

The other two remaining TFs only result from CCA: spring PP and summer SST. The geographic pattern of the CCA axis that is correlated (r=0.7) with spring PP (figure 3.9c) is very similar to the geographic pattern expressed by the STD of PP (figure 3.2e). This pattern reflects the position of coastal upwelling. During spring, coastal upwelling starts to develop at north and is active in the south (figure 3.3). However, the TF regression for spring PP is lower than the one for winter PP (figures 3.10a, b), even though the correlation from the CCA axes and the environmental variables are the same (0.7). Once more, if the regression step intrinsic to TF development would amplify the signal from the CCA correlations, then probably it would affect the TFs for the same CCA run in the same way, which is not the case. We think that I&K TF does not pick the spring PP signal because it might be mixed with the winter PP signal. CCA on the other hand can extract the variance related to each season and separate them in different TFs.

Finally, we have a TF from CCA for summer SST (figure 3.10c) but not from I&K. Factor 2 was the only one that Lopes et al. (2006) found to be correlated with SST and salinity. The geographic patterns from the CCA axis correlated with summer SST (figure 3.8c) and Factor 2 (figure 3.6b) are very different. The pattern in figure 3.8c seems to indicate (with high positive values) the presence of colder waters in the north and in the south (next to the coast, probably related to strong coastal upwelling).

Factor 2 pattern (figure 3.6b) indicates southern open ocean conditions. Therefore, it can be that when we regress the factors in the TF from I&K, the variance from this factor is not only caused by SST (as suggested by the correlations in Lopes et al., 2006) and therefore do not result in a TF. However, CCA was able to extract the variance that was related with this environmental variable and therefore a TF was developed. Finally, both spring PP and summer SST residuals from the TFs have non-random residuals (figure 3.10a,c).

Another relation between I&K and CCA methods can be investigated by calculating how much of the total species variance from Q-mode is being captured in CCA (Morey et al., 2005). The species (not canonical) variance expressed by the "CCA_TSN" constrained axes is 33%, while 13% is expressed by the constrained axes from the "CCA_PP" run. This means that 46% of the species variance (assuming no possible overlapping between the two runs) can be explained by the environmental variables considered in the CCA runs. Q-mode was able to extract five factors that explained 97% of the total variance contained in the species dataset. Dividing 46% by 97% we found that almost half of the total species variance from Q-mode can be related to winter and spring PP, summer SST, winter salinity and spring PO_4. The remaining half can be a result of noise, other environmental variables, competition or a combination of these effects.

Our CVA differs from most discriminate analysis because it was done with CCA techniques, resulting in a constrained discriminant analysis (the constraining nature comes from the inclusion of geographic information in the analysis). Lopes et al. (2006) showed that, for the northeast Pacific region, although *Chaetoceros spores* indicate PP, they are common to both types of upwelling (coastal and wind-stress curl induced) and are not able to separate them. This has serious implications in previous studies of modern conditions and past upwelling reconstructions, because only variations in coastal upwelling are considered (Sancetta et al., 1992; Barron et al. 2003). If there was a shift in the past from coastal upwelling to wind-stress curl induced upwelling (e.g., Ortiz et al, 1997), would the relative abundances of *Chaetoceros spores* show it? CVA shows that five species can be used (section 4.5), in

the present, to separate our four sub-areas. Since we can translate this information to downcore studies, more information on past upwelling/PP conditions can be achieved. However, these results are derived from the application of a qualitative analysis, and no magnitude in the physical processes mentioned above can be estimated.

CCA results showed that it is possible to overcome the problem of intercorrelated environmental variables when developing TFs. With CANOCO one can verify the correlations between environmental variables during the CCA run. Even if a chosen environmental variable yields significant correlations with any other environmental variables, if those environmental variables did not show up as the best environmental variables in the beginning of the CCA run (as statistical significant), then in spite of the correlation they are not suitable to explain the species variation.

Sensitivity tests showed that our final results depend on the use of all our samples, and this is worrisome given the small size of our dataset. Nevertheless, our results seem not be affected by the problem noted by Telford et al. (2004) regarding autocorrelated samples and consequent decreases in RSME in methods such as the I&K. However, CCA seems to be more affected by the sensitivity tests than I&K, a consequence of the constrained nature of CCA (Telford et al., 2004).

3.6 Conclusions

Q-mode Factor Analysis resulted in five significant diatom species assemblages in northeast Pacific core tops. These factors are dominated by different species and represent different ecological environments. Factor 1, which is dominated by *Chaetoceros spores,* is not able to produce differences between coastal and wind-stress curl induced upwelling.

The application of a constrained discriminate analysis (CVA) showed that the qualitative differences between the upwelling processes can be achieved through linear combinations of five different species: *Chaetoceros spores*, *Thalassionema nitzschioides*, *Paralia sulcata*, *Actinopthycus senarius* and *Nitzschia group bicapita*.

These species and their linear combinations can be reproduced for downcore studies in order to investigate the processes affecting a particular site in the past.

The I&K method to develop TFs returned significant regressions for winter PP, annual and winter salinity and spring PO_4. However, the high number of significant correlations between NO_3 and SiO_2 prevents us from considering these environmental variables as independent. In addition, we question the TF independency for annual and winter salinity as the seasons in question are also correlated with the other environmental variables. The residuals for these TFs show that our equations overestimate higher observed values and underestimate lower ones.

Using CCA , winter and spring PP, summer SST, winter salinity and spring PO_4 are the best correlated environmental variables to our floral dataset. The results show that 46% of the species variance can be explained by these environmental variables. The TFs for the modern calibration have significant r^2 and low RMSE, although the resulting residuals show, except for winter PP, that the regression underestimates lower values and overestimates higher values in all TFs.

Two TFs result from both the I&K and CCA methods: winter Salinity and spring PO_4. The TFs from both methods yield similar r^2 and RMSE, showing that the I&K and CCA methods are extracting the variance in the species that is related to this environmental variables in the same manner (although using different assumptions). The TFs for winter PP seem to be better expressed by the TF resulting from CCA than from I&K. We conclude that this is the result of the ability of CCA to extract the variance that is directly related to this environmental variable and not the result of the circularity from the method and the TF development. The same reason applies to the TFs that CCA produced and that were not reproduced in I&K results: spring PP and summer SST. We infer that the signals for these last two environmental variables might not be fully expressed by Q-mode and therefore are not “strong” enough to generate a TF with the existing dataset.

There is little difference between using TFs derived from I&K or CCA for the comparable environmental variables. However, CCA resolved TFs that I&K did not. If

the variance for I&K is a mixture of several signals (e.g. environmental variables) the TFs are not able to fully express that relation, and CCA TFs will yield better results.

Table 3.1 – Core-top locations, depths and diatom abundances (GC - Gravity, PC-Piston , MG -Multicorer, AC - Trigger).

Core ID #	Core ID	latitude (N)	longitude (W)	water depth (m)	Sub-area
C1	W8809-11 GC	41.672	-126.003	3020	4 (SE)
C2	W8909-24 GC	42.082	-125.302	2790	4 (SE)
C3	TT39-15 AC	49.210	-129.243	2396	1 (NW)
C4	TT39-5 AC	46.720	-127.542	2665	1 (NW)
C5	W8306A-1 GC	44.938	-125.362	2511	2 (NE)
C6	L6-85-NC 3 GC	41.028	-127.308	2983	3 (SW)
C7	W8508-9 GC	43.030	-126.578	3092	4 (SE)
C8	W7905-160 GC	43.165	-125.087	1476	4 (SE)
C9	W9205-1 GC	44.085	-125.373	3020	4 (SE)
C10	7407 Y-1 GC	43.628	-127.100	2918	3 (SW)
C11	TT39-18 AC	48.437	-129.870	2765	1 (NW)
C12	TT29-22 AC	47.113	-127.907	2555	1 (NW)
C13	TT39-11 AC	49.013	-127.767	2480	1 (NW)
C14	TT31-11 GC	47.033	-131.158	3056	1 (NW)
C15	Y73-10 100 GC	40.032	-125.298	1935	4 (SE)
C16	W8209B-19 GC	39.272	-127.380	4355	3 (SW)
C17	TT68-18 AC	47.383	-124.913	1240	2 (NE)
C18	TT39-19 PC	48.390	-127.153	2555	1 (NW)
C19	TT68-27 PC	46.372	-126.063	2050	2 (NE)
C20	Y7409-15 24 GC	46.118	-124.125	200	2 (NE)
C21	W7905A-163 GC	43.167	-124.752	308	4 (SE)
C22	W7905A-109 GC	46.300	-125.115	1670	2 (NE)
C23	W8809A-19 GC	42.230	-126.517	2669	4 (SE)
C24	Y6908-5A GC	46.652	-129.133	2600	1 (NW)
C25	W8909A-31 GC	42.155	-127.208	2800	3 (SW)
C26	AT8408-17 GC	47.228	-126.145	2390	2 (NE)
C27	W7610B-7 MG	44.213	-126.177	2893	4 (SE)
C28	W8909A-7 GC	42.295	-124.930	1100	4 (SE)
C29	TT39-12 AC	49.397	-128.140	2341	1 (NW)
C30	ODP1019D	41.683	-124.933	978	4 (SE)

Table 3.2 - Factor scores from Q-mode analysis (gray boxes indicate highest score for each factor).

Species/Groups	Factor 1	Factor 2	Factor 3	Factor 4	Factor 5
Freshwater group (sp1)	0.017	-0.180	0.129	0.001	0.582
Benthic group (sp2)	-0.013	-0.040	-0.009	-0.022	0.249
Actinocyclus curvatulus (sp3)	0.010	-0.031	0.058	-0.001	0.038
Actinocyclus normanii (sp4)	-0.018	-0.011	-0.018	0.037	0.156
Actinoptychus senarius (sp5)	0.030	-0.053	-0.030	0.028	0.163
Stephanodiscus rotula (forma minutula) (sp6)	-0.012	-0.016	0.017	-0.018	0.154
Bacteriastrum spp. (sp7)	-0.009	-0.046	0.006	-0.020	0.203
Chaetoceros resting spores (sp8)	0.981	0.014	0.059	0.124	0.007
Coscinodiscus decrescens (sp9)	-0.032	-0.004	0.133	0.015	-0.006
Coscinodiscus oculus iridis (sp10)	-0.001	0.005	0.000	-0.001	0.002
Coscinodiscus marginatus (sp11)	0.010	-0.063	0.248	-0.059	-0.022
Coscinodiscus radiatus (sp12)	-0.012	0.040	0.068	0.159	0.029
Cyclotella litoralis (sp13)	0.017	-0.006	0.014	0.007	-0.003
Cyclotella spp. (sp14)	0.005	-0.012	0.012	0.026	0.058
Cyclotella striata (sp15)	0.014	-0.012	-0.009	0.004	0.038
Hemidiscus cuneiformis (sp16)	0.000	0.016	0.019	-0.002	-0.011
Leptocylindrus resting spores (sp17)	0.035	-0.032	-0.020	0.040	0.032
Melosira westi (sp18)	0.003	-0.005	0.000	0.005	0.004
Odontella aurita (sp19)	0.009	-0.025	-0.006	0.029	0.032
Paralia sulcata (sp20)	0.048	-0.107	-0.007	0.079	0.189
Rhizosolenia setigera (sp21)	0.000	0.010	-0.002	-0.002	-0.003
Rhizosolenia hebetata (forma hebetatata) (sp22)	-0.016	-0.083	0.791	-0.151	-0.142
Rhizosolenia styliformis (sp23)	0.010	-0.015	-0.006	-0.006	0.038
Roperia tesselata (sp24)	0.001	0.041	-0.011	0.001	-0.015
Stephanopyxis turris (sp25)	0.004	-0.005	0.006	-0.001	0.000
Thalassiossira allenii (sp26)	0.001	0.005	-0.003	0.006	0.000
Thalassiossira anguste-lineata (sp27)	0.004	0.010	-0.010	0.021	-0.014
Thalassiossira eccentrica (sp28)	-0.072	-0.088	0.081	0.043	0.565
Thalassiossira leptotus (sp29)	-0.005	0.006	0.070	-0.009	-0.008
Thalassiossira lineata (sp30)	0.002	-0.009	-0.009	0.034	-0.004
Thalassiossira nanolineata (sp31)	0.002	0.002	-0.001	-0.002	0.001
Thalassiossira oestrupii (sp32)	-0.078	0.007	0.295	0.124	-0.013

(continued on next page)

Table 3.2 (continued)

Species/Groups	Factor 1	Factor 2	Factor 3	Factor 4	Factor 5
Thalassiossira cf poroseriata (sp33)	-0.006	0.020	-0.002	-0.002	0.000
Thalassiossira angulata/pacifica (sp34)	-0.004	0.008	-0.009	0.030	-0.004
Thalassiossira cf trifulta (sp35)	-0.013	-0.005	0.044	0.009	0.001
Thalassiossira sp1 (sp36)	-0.026	-0.029	0.153	0.052	-0.016
Thalassiossira sp2 (sp37)	0.017	-0.048	0.188	-0.104	-0.023
Thalassiossira sp6 (sp38)	-0.012	-0.005	0.038	0.008	0.001
Thalassiossira spp. (sp39)	-0.012	0.010	0.135	-0.012	-0.028
Delphineis surilella (sp40)	-0.005	-0.005	-0.006	-0.007	0.076
Delphineis karstenii (sp41)	0.001	0.003	-0.006	-0.006	0.045
Fragilariopsis doliolus (sp42)	-0.073	0.280	-0.001	0.125	-0.081
Gomphonema constrictum (sp43)	-0.010	-0.021	-0.007	-0.009	0.120
Lioloma elongatum (sp44)	0.000	-0.006	0.076	-0.003	-0.018
Lioloma pacificum (sp45)	-0.004	0.027	0.056	-0.002	-0.021
Lioloma spp. (sp46)	-0.004	-0.012	0.212	-0.046	-0.030
Neodenticula seminae (sp47)	-0.110	-0.175	0.088	0.923	-0.093
Nitzschia gp bicapitata (sp48)	0.002	0.024	0.005	-0.005	0.023
Raphoneis amphiceros (sp49)	0.011	-0.005	-0.006	-0.018	0.060
Thalassionema bacillare (sp50)	-0.003	0.022	-0.001	0.000	-0.002
Thalassionema nitzschioides (sp51)	-0.009	0.899	0.150	0.125	0.228

Table 3.3 - Compilation of the TF equations from the I&K method (F represents the factors from Q-Mode Analysis).

	r^2	Error (RMSE)	Equation (TF)
PP winter	0.6	29.0 ($gC/m^2/y$)	estimated=352.5-250.5(F2)-202.9(F5)-157.5(F4)-127.5(F1)
Salinity annual	0.7	0.3 (PSU)	estimated=31.8-2.2(F5)+1.5(F3)+0.7(F2)
Salinity winter	0.7	0.3 (PSU)	estimated=32.3-3.1(F5)+1.3(F3)
PO_4 spring	0.8	0.04 (µM)	estimated=0.4+0.5(F2)-0.5(F1*F2)+0.8(F1*F5)-0.2(F5^2)

Table 3.4 - Cumulative species fit as % of environmental variance explained by each species for "CCA_TSN" constrained axes (CCA). Species are listed in decreasing order of variance explained.

Species #	CCA Axis1	CCA Axis 2	CCA Axis3	species variability	% variance explained
sp2	0.1100	0.6477	0.6499	6.67	64.99
sp43	0.1226	0.6277	0.6421	26.97	64.21
sp32	0.6088	0.6236	0.6327	1.65	63.27
sp6	0.0793	0.5702	0.5947	3.11	59.47
sp1	0.0121	0.5857	0.5929	1.24	59.29
sp7	0.0892	0.5589	0.5598	8.71	55.98
sp36	0.4889	0.5215	0.5511	1.90	55.11
sp28	0.0005	0.5033	0.5078	2.27	50.78
sp5	0.3919	0.4689	0.4857	0.80	48.57
sp46	0.4429	0.4430	0.4807	1.13	48.07
sp35	0.4198	0.4441	0.4471	24.87	44.71
sp38	0.4198	0.4441	0.4471	24.87	44.71
sp41	0.1753	0.4061	0.4354	1.36	43.54
sp8	0.2889	0.4153	0.4172	0.20	41.72
sp22	0.3961	0.3971	0.4016	1.68	40.16
sp9	0.3378	0.3421	0.3857	8.22	38.57
sp29	0.3638	0.3750	0.3794	2.56	37.94
sp4	0.1196	0.3443	0.3581	1.78	35.81
sp44	0.2585	0.2619	0.3431	0.95	34.31
sp20	0.0513	0.1031	0.3302	1.25	33.02
sp51	0.0497	0.3061	0.3295	0.13	32.95
sp40	0.1680	0.3106	0.3264	3.20	32.64
sp49	0.1429	0.2567	0.3256	1.84	32.56
sp11	0.3180	0.3206	0.3229	3.23	32.29
sp45	0.1236	0.2084	0.3022	0.63	30.22
sp15	0.2093	0.2225	0.2656	1.55	26.56
sp3	0.1094	0.1586	0.2510	0.78	25.10
sp18	0.0000	0.0003	0.2508	13.67	25.08
sp26	0.0163	0.0603	0.2390	4.82	23.90
sp24	0.0173	0.1553	0.2295	2.53	22.95
sp42	0.0022	0.1544	0.2186	0.89	21.86
sp39	0.1363	0.1490	0.2074	4.00	20.74
sp19	0.1007	0.1829	0.1961	3.08	19.61

(continued on next page)

Table 3.4 (continued)

Species #	CCA Axis1	CCA Axis 2	CCA Axis3	species variability	% variance explained
sp37	0.1462	0.1478	0.1804	11.92	18.04
sp27	0.0544	0.1669	0.1684	3.15	16.84
sp17	0.1484	0.1496	0.1498	1.04	14.98
sp48	0.0047	0.1275	0.1336	1.92	13.36
sp31	0.0005	0.0376	0.1335	17.92	13.35
sp50	0.0063	0.0523	0.1315	2.95	13.15
sp12	0.0828	0.1211	0.1311	0.37	13.11
sp34	0.0000	0.0142	0.1230	3.56	12.30
sp30	0.0851	0.0911	0.1099	9.37	10.99
sp16	0.0630	0.0953	0.1022	1.82	10.22
sp14	0.0001	0.1004	0.1005	0.91	10.05
sp25	0.0370	0.0431	0.0829	7.00	8.29
sp13	0.0328	0.0382	0.0822	1.74	8.22
sp47	0.0506	0.0609	0.0633	2.05	6.33
sp10	0.0488	0.0488	0.0525	15.83	5.25
sp23	0.0246	0.0281	0.0452	16.45	4.52
sp21	0.0053	0.0315	0.0427	10.26	4.27
sp33	0.0006	0.0263	0.0310	14.73	3.10

Table 3.5 - Cumulative species fit as % of environmental variance explained by each species for "CCA_PP" constrained axes (CCA). Species are listed in decreasing order of variance explained.

Species #	CCA Axis1	CCA Axis 2	species variability	% variance explained
sp51	0.1564	0.3963	0.13	39.63
sp24	0.3266	0.3273	2.06	32.73
sp1	0.2917	0.3235	1.31	32.35
sp8	0.2543	0.2818	0.17	28.18
sp17	0.0928	0.2614	1.02	26.14
sp19	0.0230	0.2502	2.76	25.02
sp36	0.2176	0.2181	2.34	21.81
sp42	0.1218	0.2084	0.82	20.84
sp45	0.0080	0.2059	0.58	20.59
sp27	0.1347	0.1928	2.97	19.28
sp14	0.1480	0.1902	0.97	19.02
sp47	0.1832	0.1845	2.39	18.45
sp5	0.0585	0.1821	0.77	18.21
sp31	0.0408	0.1644	20.83	16.44
sp32	0.1270	0.1615	1.80	16.15
sp3	0.0293	0.1523	0.72	15.23
sp48	0.1342	0.1354	4.53	13.54
sp21	0.0665	0.1349	11.99	13.49
sp22	0.1140	0.1337	1.84	13.37
sp25	0.0236	0.1282	7.11	12.82
sp16	0.0941	0.1245	1.37	12.45
sp20	0.0826	0.1164	1.15	11.64
sp39	0.1104	0.1104	3.35	11.04
sp13	0.0007	0.1057	1.91	10.57
sp11	0.1004	0.1004	2.72	10.04
sp33	0.0152	0.0914	17.15	9.14
sp6	0.0887	0.0897	2.84	8.97
sp18	0.0884	0.0884	15.93	8.84
sp4	0.0699	0.0762	1.79	7.62
sp44	0.0750	0.0752	1.05	7.52
sp2	0.0668	0.0710	5.26	7.10
sp23	0.0137	0.0633	19.14	6.33
sp7	0.0205	0.0628	6.79	6.28

(continued on next page)

Table 3.5 (continued)

Species #	CCA Axis1	CCA Axis 2	species variability	% variance explained
sp46	0.0515	0.0627	1.26	6.27
sp41	0.0573	0.0615	1.68	6.15
sp28	0.0588	0.0609	2.07	6.09
sp49	0.0342	0.0497	1.42	4.97
sp15	0.0008	0.0486	1.52	4.86
sp35	0.0449	0.0474	28.85	4.74
sp38	0.0449	0.0474	28.85	4.74
sp37	0.0410	0.0455	13.91	4.55
sp9	0.0234	0.0438	9.63	4.38
sp30	0.0173	0.0320	8.34	3.20
sp34	0.0298	0.0307	3.80	3.07
sp43	0.0219	0.0238	31.27	2.38
sp29	0.0200	0.0215	1.92	2.15
sp10	0.0066	0.0098	12.90	0.98
sp40	0.0032	0.0033	3.85	0.33
sp26	0.0000	0.0024	5.71	0.24
sp12	0.0002	0.0006	0.33	0.06
sp50	0.0003	0.0003	3.04	0.03

Table 3.6 - Compilation of the TF equations from the CCA method (A represents the canonical axes from CCA).

	r^2	Error (RMSE)	Equation (TF)
PP winter	0.97	8.0 ($gC/m^2/y$)	estimated=112.7+36.2(A1)+31.7(A3)+7.9(A2)+25.6(A4)+ 10.3(A1*A2)+9.1(A1^2)+9.4(A1*A3)
PP spring	0.7	24.0 ($gC/m^2/y$)	estimated=202.1+30.2(A2)+19.3(A3)
SST summer	0.7	0.4 (^oC)	estimated=15.6-0.5(A3)-0.2(A2)-0.2(A2*A4)
Salinity winter	0.8	0.2 (PSU)	estimated=32.2-0.6(A2)+0.3(A1)+0.1(A2^2)
PO_4 spring	0.8	0.04 (µM)	estimated=0.6+0.1(A1)+0.02(A2)

Table 3.7 - Random division of samples into groups for the sensitivity tests.

	Samples removed
Group 1	CL4
	CL24
	CL25
	CL26
	CL28
Group 2	CL2
	CL10
	CL17
	CL20
	CL27
Group 3	CL8
	CL13
	CL15
	CL16
	CL29
Group 4	CL9
	CL11
	CL14
	CL18
	CL30
Group 5	CL1
	CL5
	CL12
	CL19
	CL21
Group 6	CL30
	CL6
	CL7
	CL22
	CL23

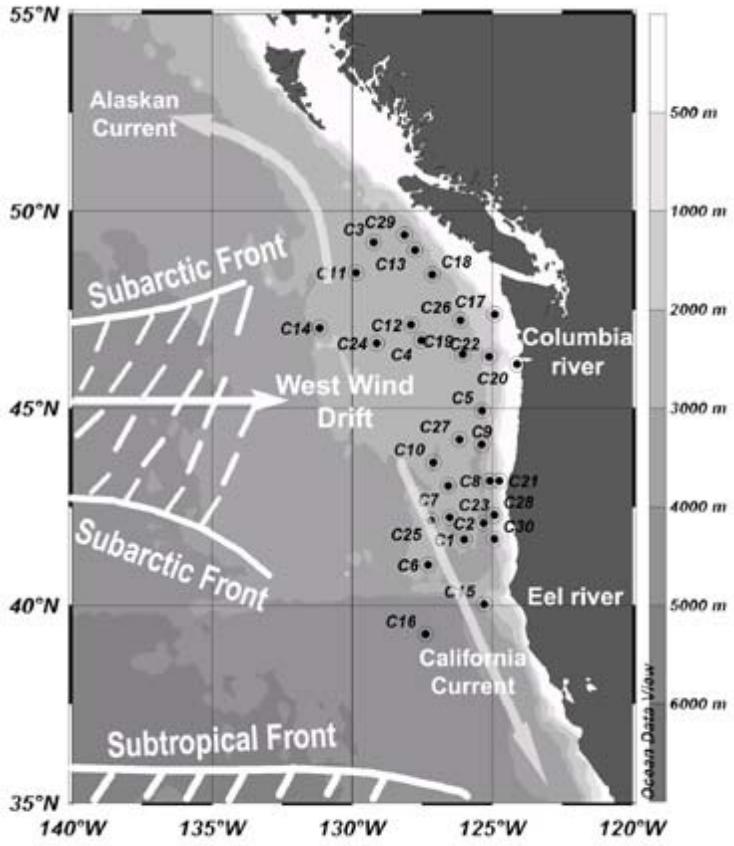

Figure 3.1 – Schematic of major oceanic currents and fronts in the NE Pacific system. Black dots are core-top sample locations. The range of positions for the Subarctic Front reflects summer (northern) and winter (southern) extremes. Shading reflects bathymetry.

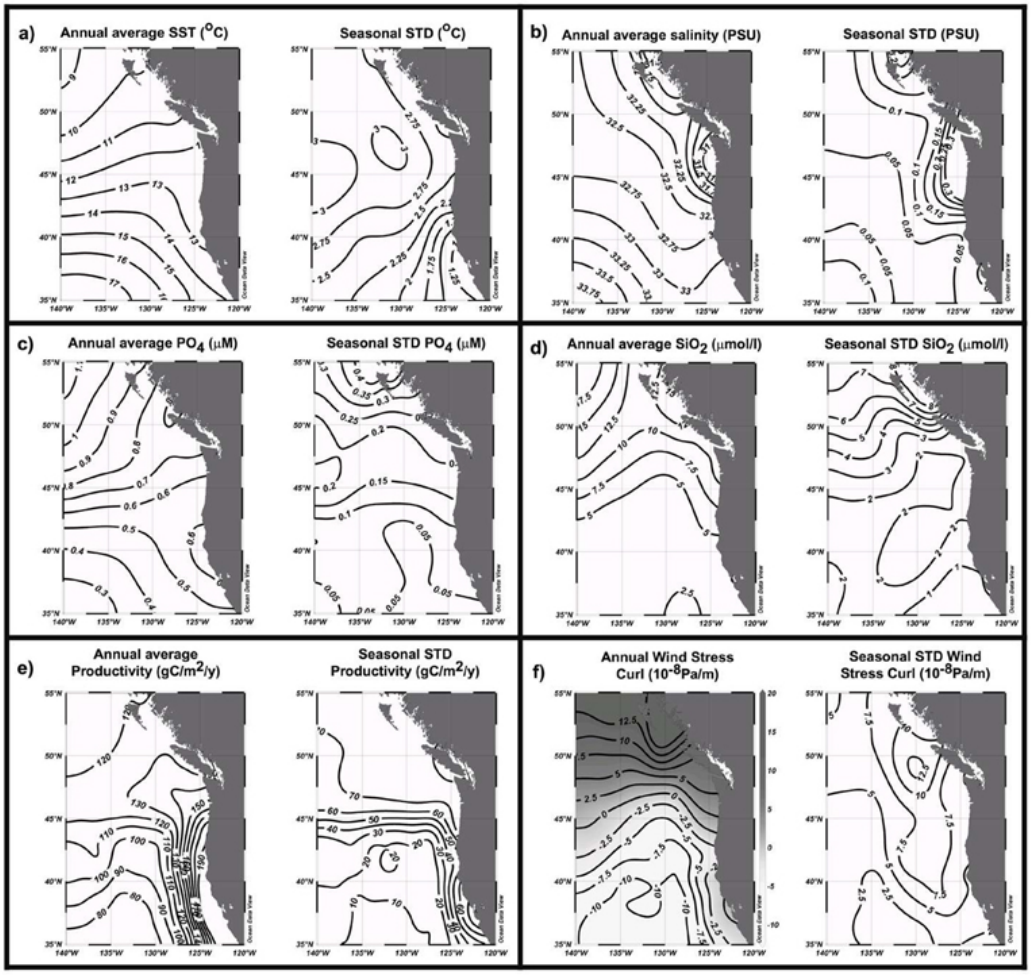

Figure 3.2 – Maps of annual averages and seasonal standard deviations (STD) for a) sea-surface temperature (contours are in ^{o}C) from WOA98, b) salinity (contours are in PSU) from WOA98, c) PO_4 (contours are in µM) from WOA98, d) SiO_2 (contours are in µmol/l) from WOA98, e) productivity (contours are in gC/m^2/y) from Antoine and Morel, 1996 and f) wind-stress curl (contours are in 10^{-8} Pa/m; positive values (dark shading) are associated with upwelling) from QuickScat monthly mean wind field data in http://las.pfel.noaa.gov/OceanWatch.html; July 2005.

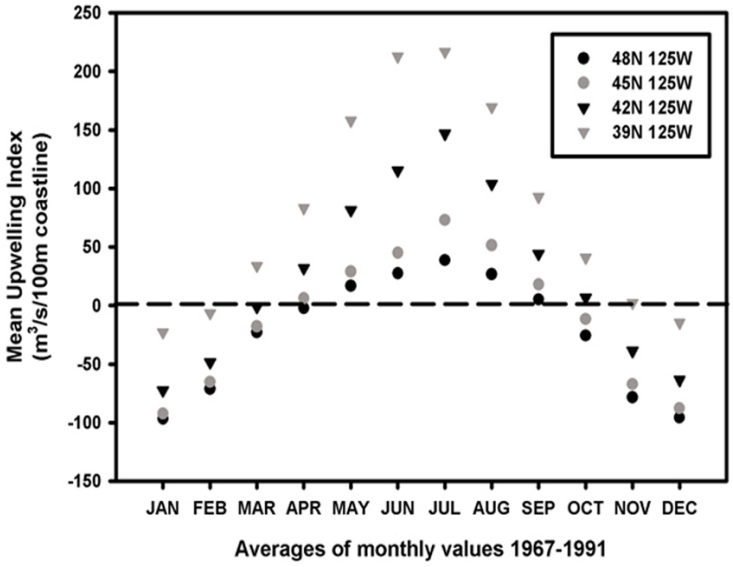

Figure 3.3 - Coastal upwelling indexes from monthly values averaged from 1967 to 1991 for four locations along the NE Pacific coast (from www.pfel.noaa.gov/javamenu.html; July 2005).

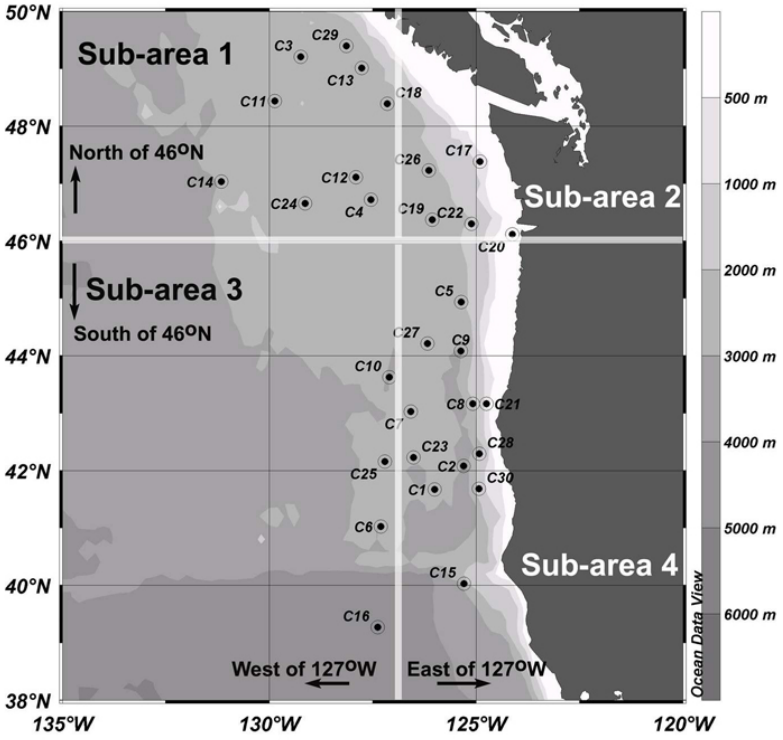

Figure 3.4 – Map showing the geographic separation of the study region in four sub-areas. Black dots are sample locations. Shading reflects bathymetry.

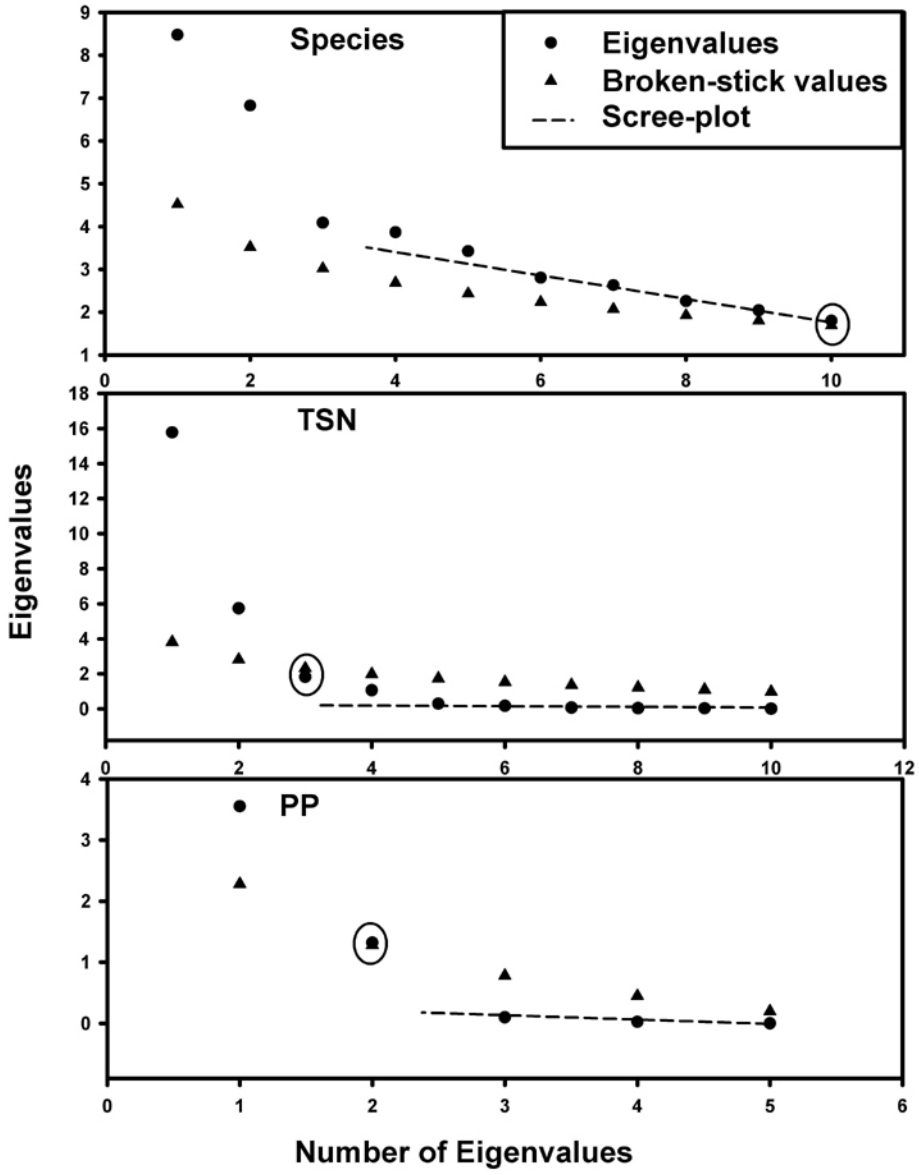

Figure 3.5 – Scatter plots for the R-mode Factor Analysis resulting eigenvalues and the stopping criteria used for the species dataset (upper panel), the TSN environmental properties dataset (middle panel) and the PP environmental properties dataset (lower panel). Dashed line is the "scree-plot" stopping criteria and the open circles are the "broken-stick" stopping criteria.

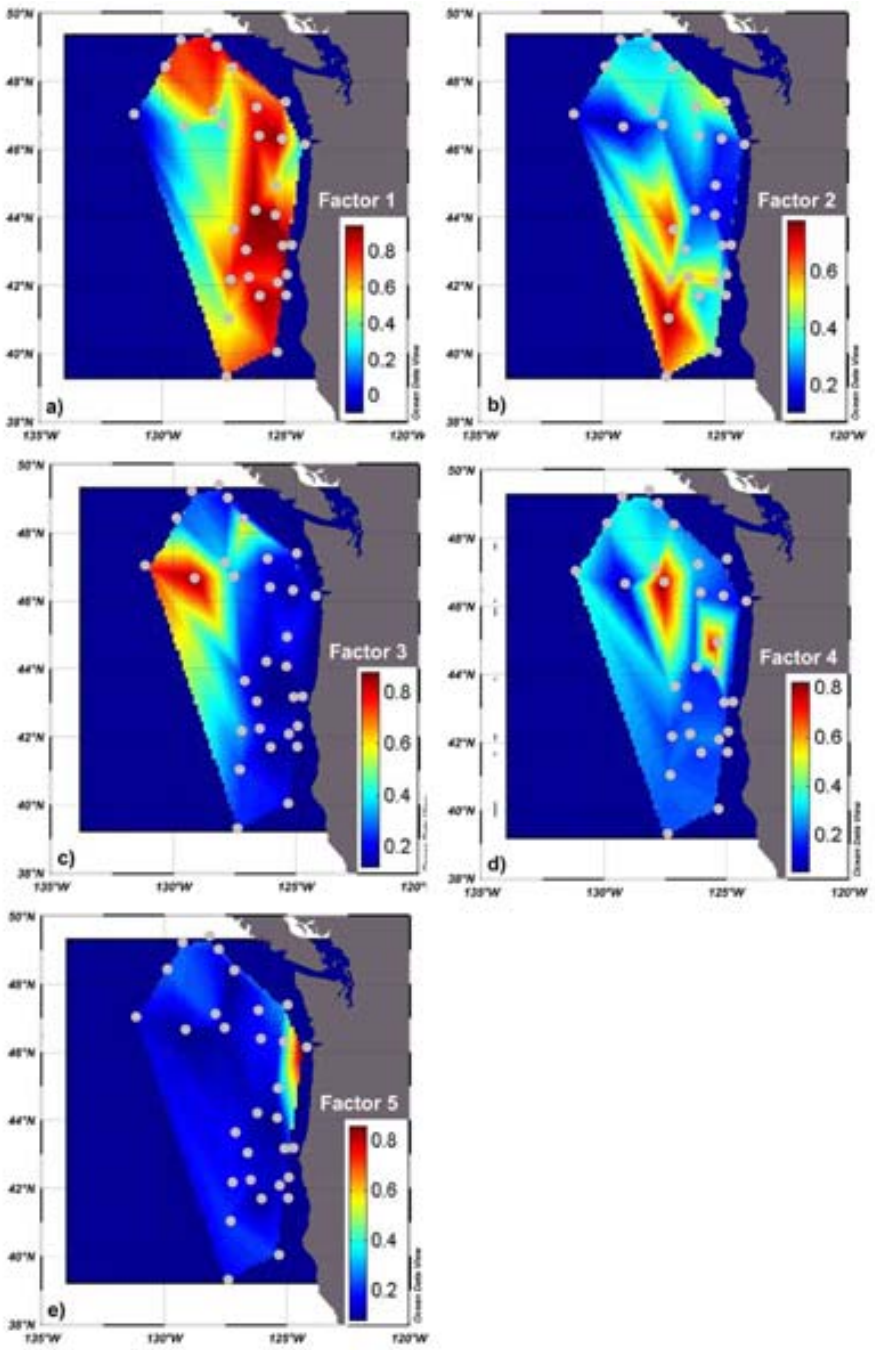

Figure 3.6 - Spatial distribution of factor loadings for the five factors (gray dots are the samples locations).

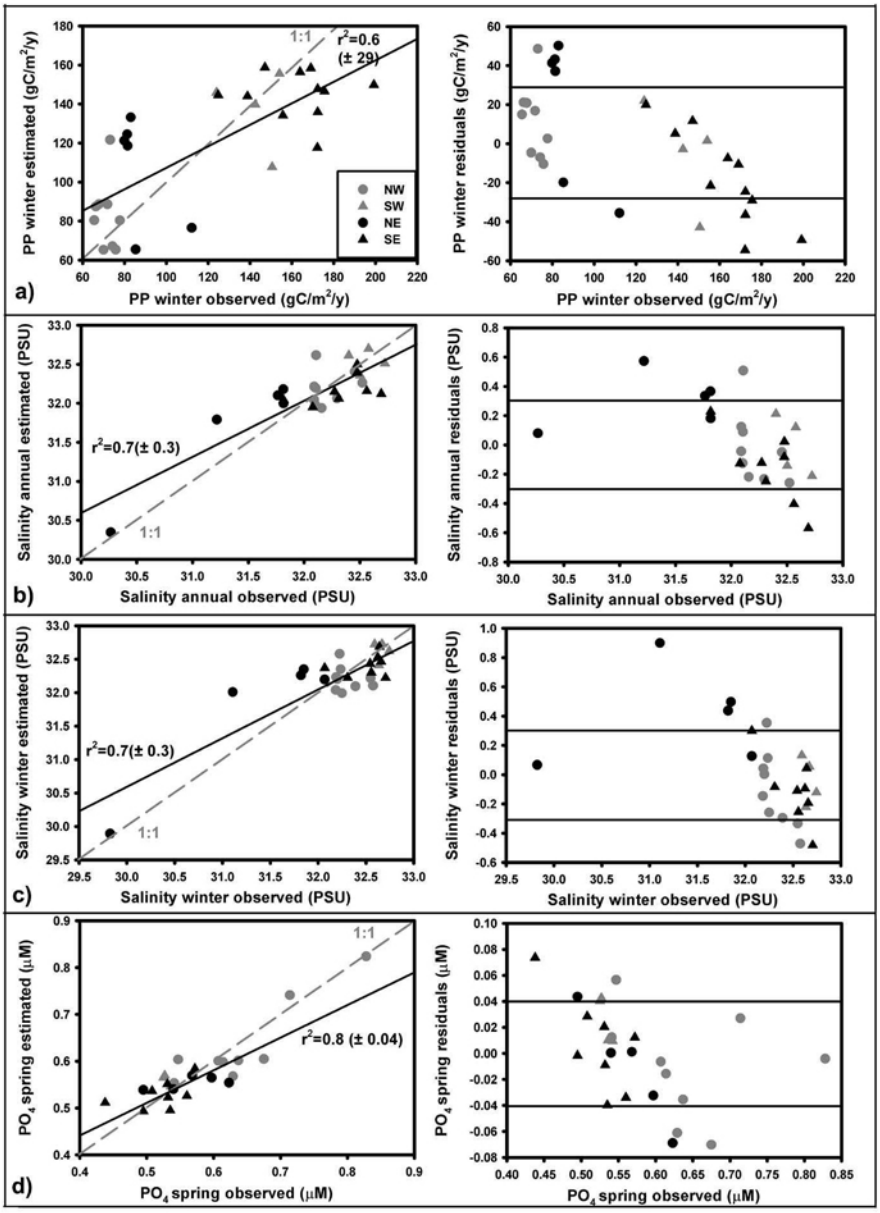

Figure 3.7 - Scatter plots for regression equations (gray line represents the 1:1 line) and residuals from modern transfer functions calibrations from Imbrie and Kipp method: a) winter productivity, b) annual salinity, c) winter salinity and d) spring PO_4. Sample symbols follow the division in figure 3.4.

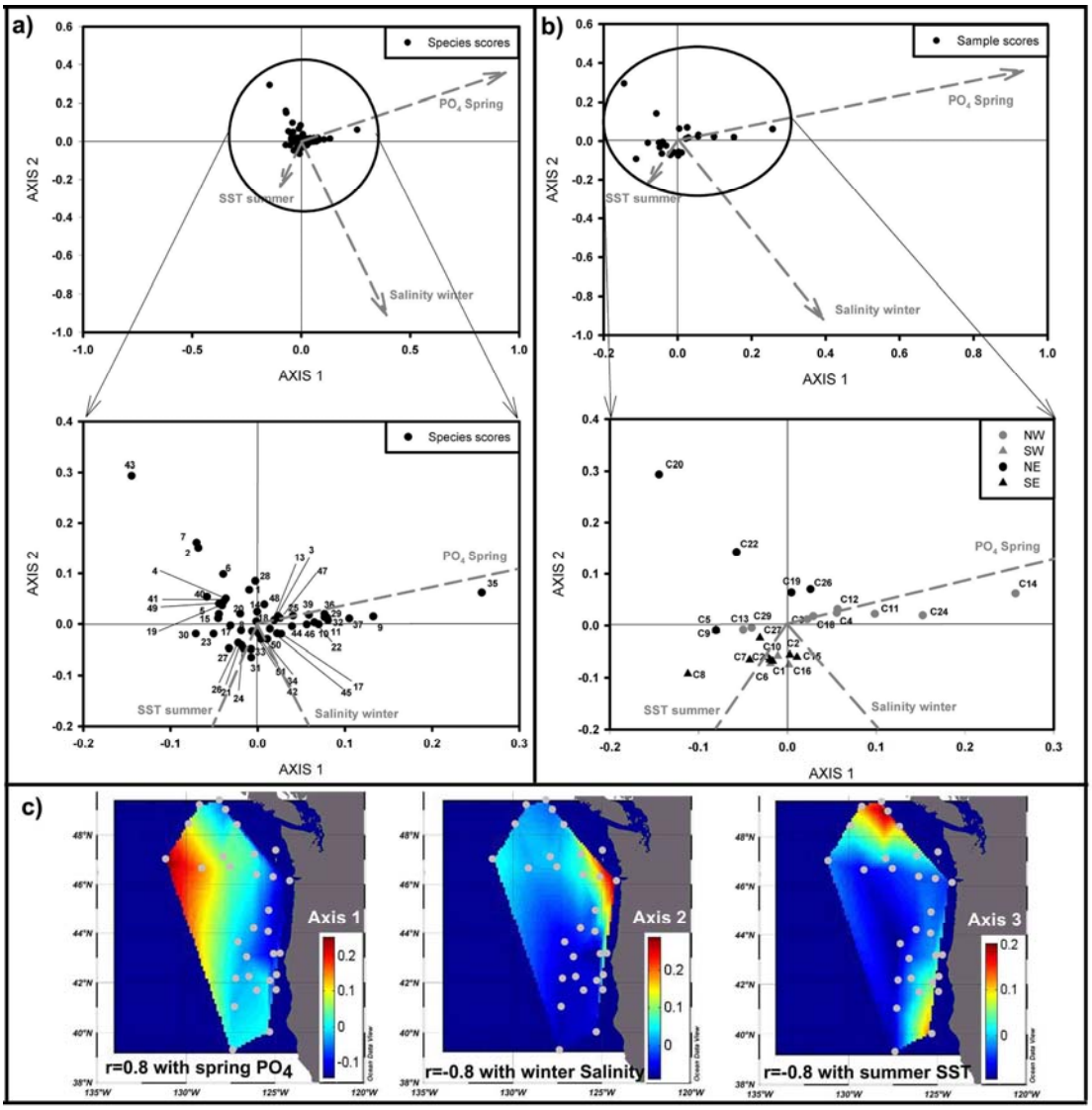

Figure 3.8 – Results for the "CCA_TSN": a) standardized Canonical plot for species scores (see table 3.2 for a list of corresponding species number and names); b) standardized Canonical plot for sample scores and c) geographic distribution of sample scores and correlations between environmental variables and Canonical axes.

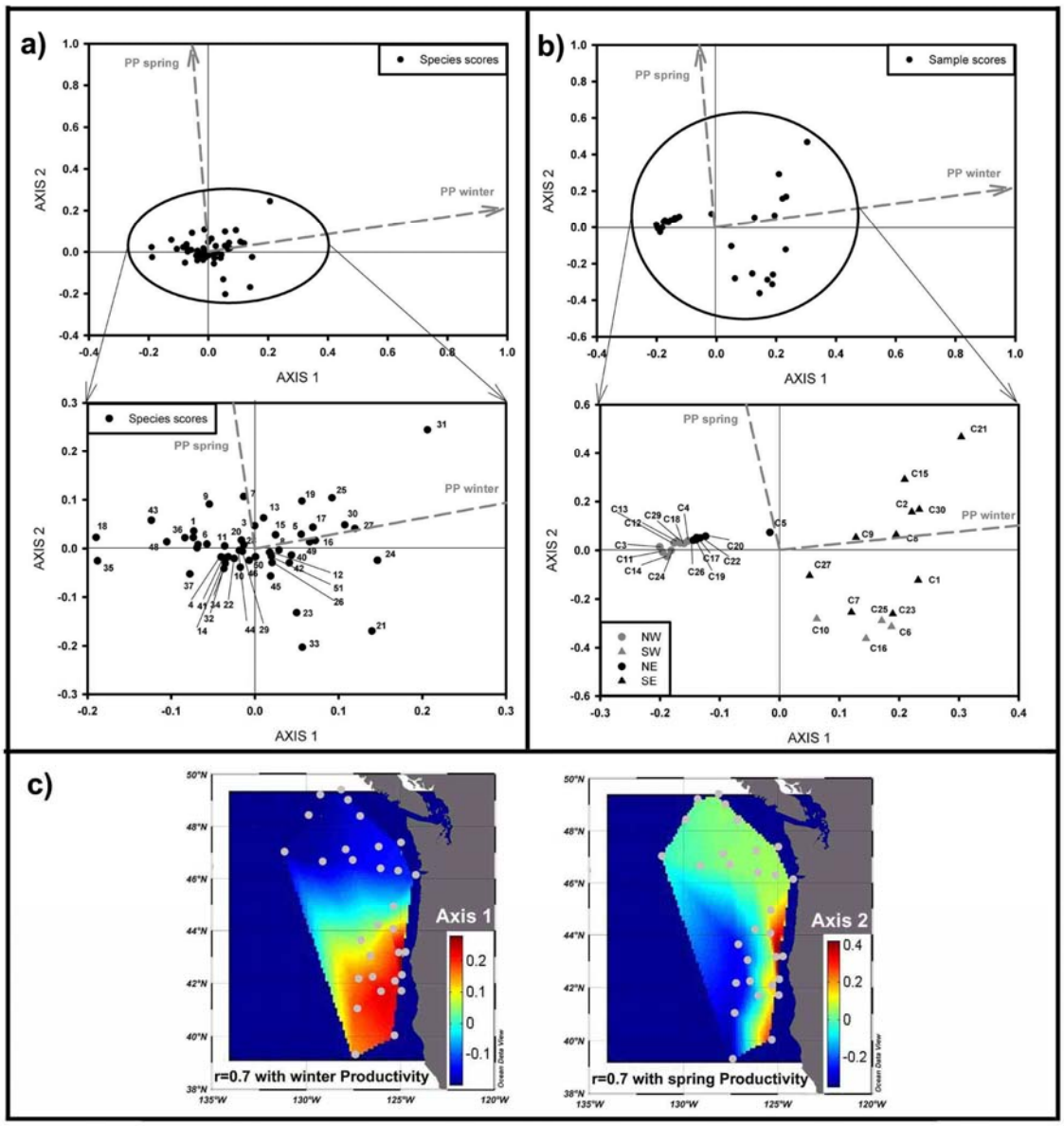

Figure 3.9 – Results for the "CCA_PP": a) standardized Canonical plot for species scores (see table 3.2 for a list of corresponding species number and names); b) standardized Canonical plot for sample scores and c) geographic distribution of sample scores and correlations between environmental variables and Canonical axes.

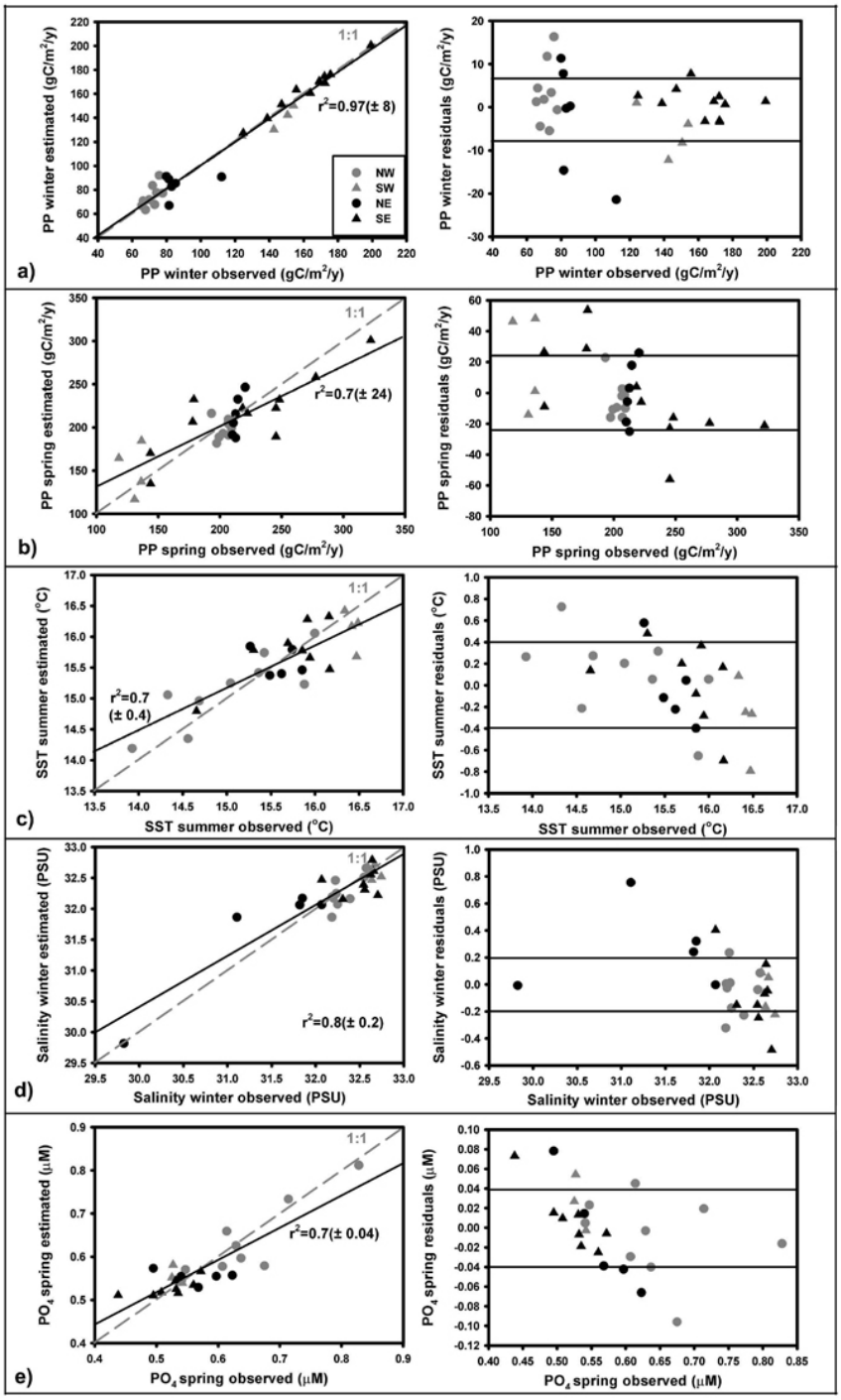

Figure 3.10 – Scatter plots for regression equations (gray line represents the 1:1 line) and residuals from modern transfer functions calibrations from CCA a) winter PP, b) spring PP, c) summer sea-surface temperature, d) winter salinity and e) spring PO_4. Sample symbols follow the division in figure 3.4.

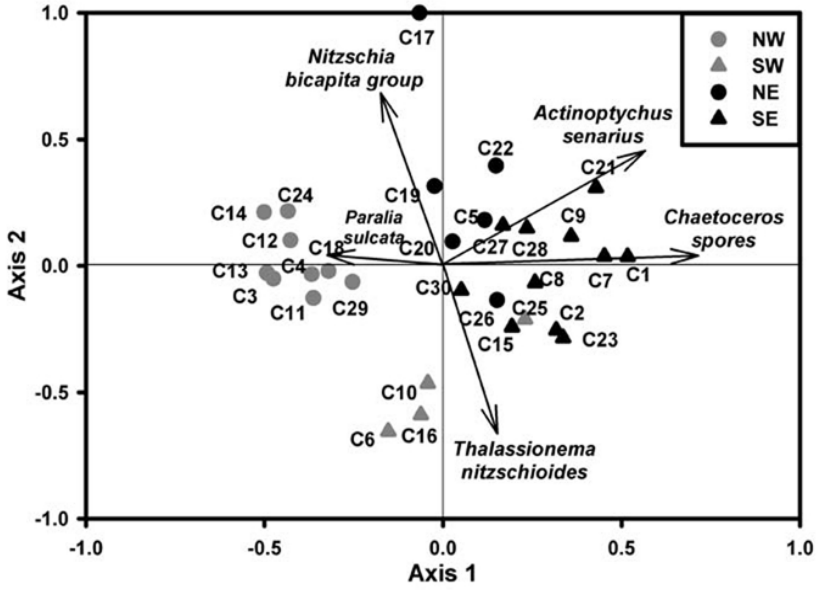

Figure 3.11 –Canonical plot showing the results for the Canonical Variate Analyses (see text for details). Sample symbols follow the division in figure 3.4.

4. PLEISTOCENE MEGA-FLOODS IN THE NORTHEAST PACIFIC

Cristina Lopes and Alan C. Mix

Variations in freshwater inputs to the oceans are known drivers of ocean and climate change. Late Pleistocene mega-floods from the Laurentide ice sheet and glacial Lake Agassiz (North America) likely disrupted the North Atlantic Deep Water formation and caused abrupt cooling (e.g. Clark et al., 2002; Bauer et al., 2004). Similar events may have occurred in the North Pacific drainage. Massive discharges of freshwater from the glacial lake Missoula are thought to have sculpted the so-called Channeled Scablands of eastern Washington and debouched via the Columbia River near 46^{o}N (e.g. Bretz, 1925; 1969). The dynamics and timing of these north Pacific mega-flood events remain poorly constrained, however, and the consequences of such discharges of freshwater in the northeast Pacific regional circulation remains unknown. Debate centers on whether these events occurred as a few brief (scale of weeks) but massive events (Shaw et al., 1999), or as a ~2000-year sequence of smaller but repeating jökulhlaups events (Wait, 1985; Atwater, 1987). Here we constrain the timing, mechanism, and impact of mega-floods in the northeast Pacific during the last glacial cycle based on oxygen isotopes and radiocarbon in foraminifera and abundances of freshwater diatoms in marine sediments. Anomalous freshwater plumes reduced surface-ocean salinities by 5-10 PSU more than 400 km to the south of the Columbia River (off northern California) frequently from 16,000 to 31,000 cal-yr BP. Mega-flood events were common during the advance of the Cordilleran Ice Sheet, prior to the existence of glacial lake Missoula, and the interval of flooding lasted 5-7 times longer than previously estimated.

The existence of mega-floods in the U.S. Pacific Northwest was first recognized in the wide-spread erosion of the Channeled Scablands of eastern Washington (Bretz, 1925). The presumed source of the mega-floods is an unstable ice dam of glacial Lake Missoula (northeast Idaho, at the southern margin of the Cordilleran Ice Sheet; Bretz, 1969; O'Connor and Baker, 1992), and perhaps other sources in British Columbia (Shaw et al., 1999). The only drainage path for the floodwaters is the Columbia River, and this has been hypothesized as the source of widespread flood and turbidite deposits on land and on the ocean floor off Washington

and Oregon (Benito and O'Connor, 2003; Zuffa et al., 2000; Normark and Reid, 2003).

Ideas on mechanisms for the Cordilleran mega-floods have changed over time, however. Originally, the erosional event was thought to reflect a single major event (or perhaps a few events) from Lake Missoula, lasting on the order of weeks or months and associated with the early retreat of the Cordilleran Ice Sheet (Bretz, 1969; Baker, 1973). Evidence in favor of the single flood hypothesis includes the presence of mammoth sand bars ripple marks, dry falls, and gravel deposits, all of which are difficult to reconcile with uniformitarian processes. More recently, flood events of the Channeled Scablands have been described as a sequence of 40-90 smaller jökulhlaups events in which unstable subglacial tunnels allowed lake Missoula to repeatedly fill and flush over a period of ~2,000-2,500 years, with an average repeat time of 10-60 years (Waitt, 1985; Atwater, 1987; Booth et al., 2004). Evidence in favor of the jökulhlaups hypothesis is the presence of rhythmically bedded backflood deposits. Some, however, consider the rhythmic beds to have been formed within single flood events, or perhaps a few flood events from several different freshwater sources (Shaw et al., 1999).

Timing of the mega-floods is also poorly known. The best-documented events are traced to glacial Lake Missoula, which formed behind an ice dam when the Purcell Lobe of the Cordilleran Ice Sheet was near its maximum. The Cordilleran ice sheet east of the Cascade Mountains reached its maximum extent around 18,000 cal-yr BP (15,000 ^{14}C yr BP, Clague and James, 2002), and dated lake deposits suggest that Lake Missoula existed for just a few thousand years, between 18,400-15,700 cal-yr BP (~15,300 and 12,700 ^{14}C yr BP; Wait, 1985). Radiocarbon dates on charcoal fragments from the Columbia plateau suggest that the earliest flood deposits may be older than 19,000 cal-yr BP; however these dates have been discounted because the materials are reworked (Benito and O'Connor, 2003). The early Lake Missoula floods may have been larger (more catastrophic) and less common than younger ones (Waitt, 1985; Atwater, 1987; O'Connor and Baker, 1992). The total quantity of freshwater drainage is estimated at $2x10^3$ km^3 (the volume of lake Missoula; Clarke et al., 1984)

to ~10^5 km^3 (including additional sources; Shaw et al., 1999). The rate of water discharge depends on the assumptions about duration of events, but fluxes on the order of 10^6 m^3/s to 10^7 m^3/s are thought to have reached the Pacific through the Columbia River valley (Benito and O'Connor, 2003). These flow rates are a factor of 100-1000 greater than peak seasonal flows of the modern Columbia River, which today accounts for 77% of the total drainage from western North America (Hickey et al., 1998). A freshwater balance based on the above values and assuming that the duration of the floods was about 15 days (Clarke et al., 1984) with a flood frequency of ten years (Booth et al, 2004), results in past fluxes that are 0.4 - 4 times the modern seasonal fluxes of the Columbia River.

Driven by seasonal wind-driven currents, the modern freshwater plume from the Columbia flows mostly to the north during winter and to the south during summer (Hickey et al., 1998), and can be recognized as a ~0.25-0.5 PSU reduction in surface salinities relative to ambient oceanic salinities of ~33 PSU as far as 600 km south of the Columbia mouth, and far as 400 km offshore (Berdeal et al., 2002). Smaller rivers in the region are the Umpqua, the Rogue, the Klamath and the Eel Rivers have no significant effect on offshore salinities (figure 4.1a).

The impact of the Pleistocene mega-floods in the Pacific Ocean is recognized by the extension of the turbidites that originated near the Columbia River mouth at 46°N and reach as far as 1100 km to the south (Zuffa et al., 2000). The dates of turbidite layers from the Escanaba Trough are poorly constrained, because the dated materials (wood fragments) are reworked. Estimates for the turbidite ages range from ~30,000 to less than 11,000 cal-yr BP; the younger turbidites (after around 19,000 cal-yr BP) are related to the Lake Missoula floods while the older ones (before 19,000 cal-yr BP) were not attributed to any particular source (Zuffa et al., 2000).

Thirty core-tops from the northeast Pacific (figure 4.1a and appendix D) document the response of fossil diatoms to freshwater input. Freshwater diatoms are most likely transported, and not actively living in the ocean, whereas brackish species may live in the plume itself. The percentage of freshwater diatoms tracks modern winter salinities ($r = -0.8$). The modern geographic ecological model can be estimated

by a transfer function (figure 4.1b) in which FD = -4.18 *Salinity+137.6, where FD are freshwater diatom percentages relative to the total diatom flora. The mean standard deviation of residuals for the paleosalinity estimations from the FD transfer function is 0.5 PSU.

Past variation in regional salinities over the last ~45,000 years is recorded at a site off northern California, near the southern limit of the modern Columbia River freshwater plume, which is sampled by ODP Holes 1019 C and D (41.683 N, 124.933 W, 978 m depth) and piston core MD02-2499 (41.683 N, 124.940 W, 904 m depth). Hole 1019D includes the late Holocene (0 to ~ 8,000 years B.P.), which is missing in core MD02-2499. Hole 1019C was analyzed for oxygen isotopes in foraminifera (Mix et al., 1999a). Freshwater diatoms are virtually absent in modern core-tops at this site.

Chronologies of the sediment cores are provided by 19 radiocarbon dates in the interval 0-45,000 cal-yr BP, and by benthic foraminiferal oxygen isotope stratigraphy (figure 4. 2 and appendix D). Estimates of paleosalinity based on freshwater diatoms document anomalous freshwater inputs from ~28,000-17,000 cal-yr BP, and perhaps again about 31,000 cal-yr BP, an interval that spans marine oxygen isotope stage (OIS) 2. Peak abundance of freshwater diatoms occurred at approximately 17,500, 21,000, 23,000 and 28,000 cal-yr BP, and reached values of more than 40% of the total diatom flora, which implies paleosalinity reductions of up to 10 PSU relative to modern regional background values of ~33 PSU.

Oxygen isotope ($\delta^{18}O$) data from the planktonic species *Neogloboquadrina pachyderma* (left coiling), when differenced against benthic foraminiferal $\delta^{18}O$ data, confirm the presence of anomalously low salinities from about 17,000-24,000 cal-yr BP. (figures 4.2b and d), with a maximum isotopic anomaly of –1.5 $^{0}/_{00}$. Assuming a modern $\delta^{18}O$ for Columbia River water of –10 to –14 $^{0}/_{00}$ VSMOW (Kendall and Coplen, 2001), a past $\delta^{18}O$ anomaly of –1.5 $^{0}/_{00}$ from such a source would imply a salinity anomaly of 4-5 PSU (larger if ice-age cooling contributed, smaller if ice-age freshwaters were more depleted in ^{18}O). This isotopic estimate of salinity change, about half of the magnitude of freshening implied by the freshwater diatom

percentages, likely reflects the tendency of marine foraminifera to avoid freshwater plumes either by living in shallow subsurface waters, or in seasonal or interannual settings with lower freshwater inputs.

The presence of a substantial freshwater plume as far south as the California-Oregon border during marine OIS 2 requires continued southward flow in the California Current, consistent with regional paleoceanographic reconstructions of the glacial maximum ocean (Ortiz et al., 1997). We reject a hypothesis that freshwater diatoms and isotopically depleted surface waters during the last glacial interval reflect local river runoff from the Rogue and/or Klamath Rivers. These rivers do not carry significant water to the ocean at present, had no anomalous freshwater sources during the glacial intervals, and provide no evidence for massive erosion during that time. Paleoclimate reconstructions based on pollen assemblages from Little Lake (44.17^{o}N; 123.58^{o}W; 127 m elevation; 45 km east of the Pacific coast) for OIS2 indicate that the precipitation was about half that at present (Worona and Whitlock, 1995; Whitlock and Grigg, 1999), suggesting that if anything, the small coastal rivers discharged less freshwater to the ocean, not more. Upper Klamath Lake (41.95^{o}N; 121.57^{o}W; 1263 m elevation; 210 km east of the Pacific coast) studies based on diatoms also indicate dryer and colder conditions for OIS2 with decreased river input and lower lake levels (Bradbury et al., 2004). We also reject an alternate hypothesis that the freshwater diatoms are eolian (Sancetta et al., 1992) because easterly winds required for such transport were likely confined to the region in Washington near the ice age (Hostetler and Bartlein, 1999), far to the north of our study site off northern California. Further, on the Gorda Ridge off Oregon, Lund and Mix (1998) found five thin sand layers in core W8709A-13PC (42.02^{o}N, 125.13^{o}W, 2712 m depth) dated at ~15,000, 16,000, 17,000, 20,000 and 22,000 cal-yr BP, and Zuffa et al. (2000) found turbidite layers perhaps as old as ~30,000 cal-yr BP. We infer that all of these deposits are consistent with extreme flood events, and not with eolian transport.

The younger age range of our inferred low salinity anomalies, from 19,000-17,000 cal-yr BP is a close match to terrestrial dates of mega-floods associated with Glacial Lake Missoula (e.g., Booth et al., 2004), as well as with the age of the

youngest turbidites in the Cascadia Basin that have been linked to the Missoula Floods (<19,000 cal-yr BP; Zuffa et al., 2000). However, the full range of ages for the freshwater diatoms, with significant salinity reductions as far back as 31,000 cal-yr BP, predate the existence of glacial lake Missoula, which existed only for about 2000-2500 years during the full advance of the Purcell Trench Lobe of the Cordilleran Ice Sheet between ~18,000 cal-yr BP and ~13,000 cal-yr BP (Clague, 1981; Atwater, 1987; Wait, 1985).

Earlier freshwater inputs must have come from a source other than Lake Missoula. The species of freshwater diatoms also suggest different freshwater sources and/or flooding mechanisms. The younger events were dominated by planktonic freshwater diatoms that are common in large lakes, including *Aulacoseira granulata* and *islandica* and *Cyclotella ocellata* and *comta*. At ages >25,000 (cal-yr BP), the percentages of benthic freshwater diatoms (mainly *Surirella linearis*) increases, consistent with a different source dominated by either shallow lakes or running water (figure 4.2). Possible sources for the older freshwater events include Lake Bonneville, for which poorly-dated early spillover events may date to ~30,000 years (Malde, 1968), or to periodic melting of a surging ice front during the growth phase of the Cordilleran Ice Sheet. Whatever the source, massive freshwater inputs to the Northeast Pacific appear to have been a common feature of the full extent of marine OIS 2 (the broadly defined Last Glacial Maximum).

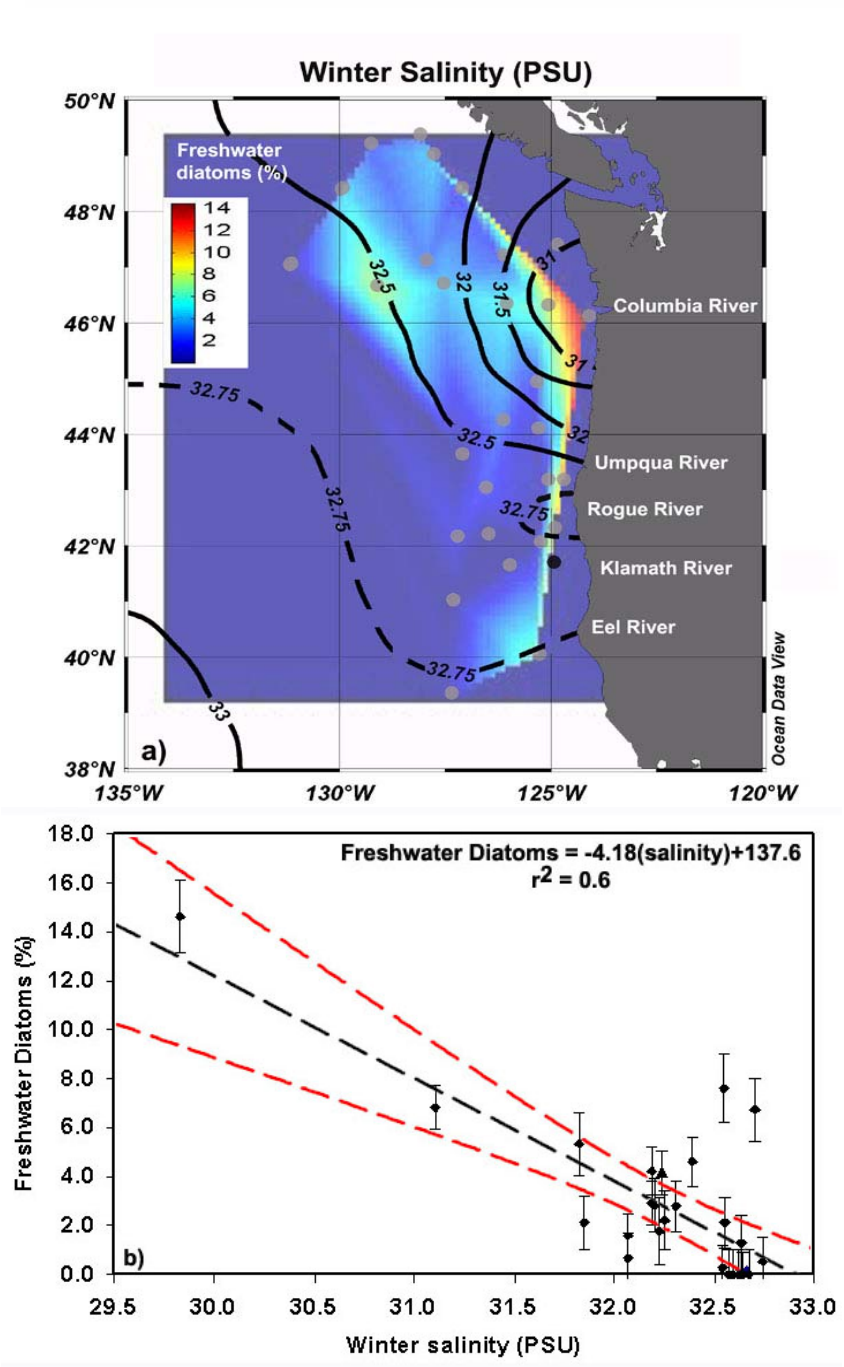

Figure 4.1 – a) Spatial distribution of freshwater diatom percentages (relative to total diatoms, gray scale) and winter sea-surface salinity (contours, from World Ocean Atlas 1998 (www.nodc.noaa.gov/OC5/woa98.html; July 2005). Gray dots are core-top locations and black dot locates the Pleistocene study site. b) Calibration of paleosalinity estimates from freshwater diatom percentages from the modern ecology model (error bars are relative to the total diatom assemblage, black dashed line is the regression and red dashed lines are the 95% confidence levels).

Figure 4.2 – Downcore observations from cores MD02-2499 (closed circles), ODP 1019D and C (open circles), a) benthic *Uvigerina sp*. $\delta^{18}O$ record for MD02-2499 and ODP 1019C; diamonds are calendar-corrected ^{14}C dates with $\pm$1-σ error bars for ODP 1019 (gray is 1019D and black is 1019C) and triangles are the same for MD02-2499; stars are isotope record correlations for both age models; b) planktonic left-coiling *Neogloboquadrina pachyderma* $\delta^{18}O$ record for ODP 1019 C; c) *Neogloboquadrina pachyderma* $\delta^{18}O$ record minus *Uvigerina sp*. $\delta^{18}O$ record from ODP 1019 C, d) freshwater diatom percentages for MD02-2499 (gray filling is % planktonic diatoms and black is % benthic diatoms) and winter salinity reconstructions and e) Greenland Summit (GISP-2) ice core $\delta^{18}O$ (‰ relative to SMOW), from Grootes et al. (1993). Additional symbols represent Gorda Ridge sand layers (black circles) from Lund and Mix, (1998) and black squares represent mega-flood turbidites from Zuffa et al. (2000). Y-D and B-A indicate the Younger Dryas and Bølling Allerød intervals.

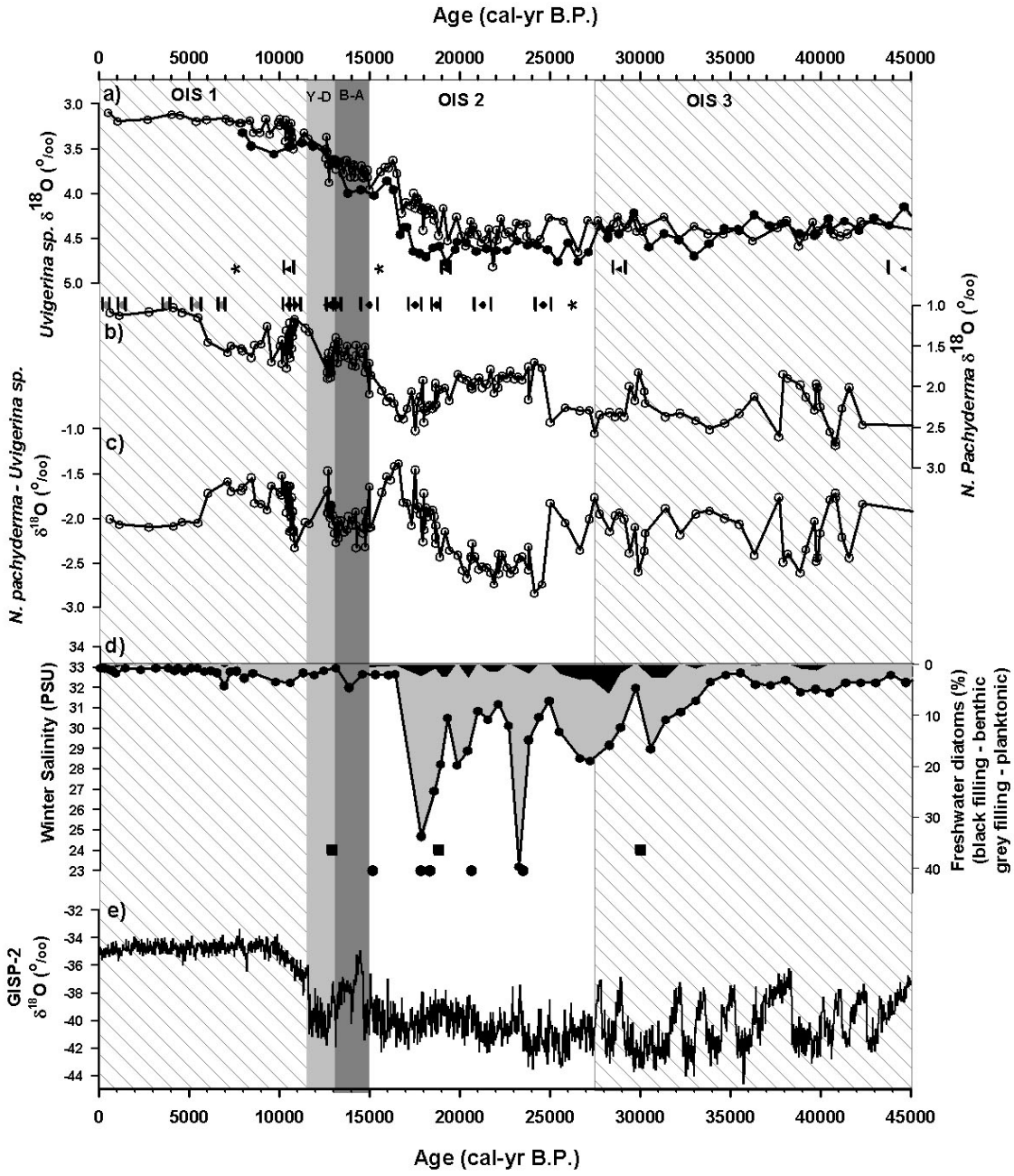
Age (cal-yr B.P.)
a)
OIS 1
Y-D
B-A
OIS 2
OIS 3
Uvigerina sp. δ18O (°/oo)
b)
N. Pachyderma δ18O (°/oo)
N. pachyderma - Uvigerina sp. δ18O (°/oo)
c)
d)
Winter Salinity (PSU)
Freshwater diatoms (%)
(black filling - benthic
grey filling - planktonic)
e)
GISP-2 δ18O (°/oo)
Age (cal-yr B.P.)

5. LATE PLEISTOCENE DIATOM ASSEMBLAGES IN NORTHEAST PACIFIC HAVE NO MODERN ANALOGS

Cristina Lopes and Alan C. Mix

Abstract

Fossil diatom assemblages from the past 60,000 years (B.P.) in the northeast Pacific (42°N, 129°W) have no modern analogs, which confounds attempts to reconstruct past conditions using traditional transfer-function methods. Removal of no-analog species from the dataset helps to circumvent the problem and yields conservative results (inside the modern calibration range) for environmental reconstructions. We infer a small decrease in primary productivity and sea-surface cooling 8,000 years ago, no evidence for regional millennial-scale oscillations during the deglaciation, and relatively high primary productivity during the Last Glacial Maximum in spite of a decrease in coastal upwelling. These findings contrast with previous findings of lower export production during cool climates, but could be reconciled if the glacial ecosystem was an inefficient exporter of organic matter, similar to the Alaska Gyre today. During Oxygen Isotope Stage 3, productivity and upwelling oscillations may reflect regional millennial–scale climate changes.

5.1 Introduction

The development of paleoecological transfer functions (TFs) assumes that the ecological relationships between environment and microorganisms remain the same in the past as it is recognized in modern calibrations. Core-top sediments provide modern analogs to be applied in the past. A no-analog situation occurs if past variability is outside the range of the modern calibration dataset, when different species occur in the past than in the present, or the microorganisms did not respond to the environment in the past in the same way as they respond today (Hutson, 1977; Mix et al., 1999b).

Here we document reconstructions of the past 60,000 years of sea-surface temperature, salinity, nutrients and productivity, using diatom TFs developed for the modern northeast Pacific upwelling system (Lopes et al, submitted, Chapter 3). Although the modern calibration showed promising results, their application to donwcore studies revealed no-analog conditions. We approached the no-analog issue using two different methods, each one with its advantages and disadvantages.

5.2.Modern regional setting

The study area (figure 5.1) is influenced by the positions of the north Pacific high and the Aleutian low-pressure cells. This atmospheric system interacts with the major north Pacific oceanic currents and creates fronts (figure 5.1). The atmospheric-ocean interaction also controls the upwelling and consequent productivity.

Two types of upwelling occur in the area: coastal upwelling driven by along-shore winds, and open-ocean upwelling driven by the curl of the wind-stress (Bakun and Nelson, 1991). The position of atmospheric pressure cells controls the seasonal distribution of coastal upwelling associated with the California current. Off Oregon, coastal upwelling occurs intermittently between April and August (Smith, 1983). Farther south (off California), coastal upwelling is more persistent and can even be present year-round (Huyer, 1983). The strongest coastal upwelling on an annual average occurs between 36^{o} N and 42^{o} N (Hostetler et al., 1999). Open-ocean upwelling is associated with wind jets or gradients over the ocean, especially in the Subarctic area off Washington and British Columbia (throughout the year) and off Oregon and California (in winter). Both coastal and open-ocean upwelling systems can be characterized by high productivity. Coastal upwelling favors intermittent blooms of larger phytoplankton that yield high export flux to the sediments, whereas open-ocean upwelling is often associated with the presence of small phytoplankton and low export to the sediments, due to efficient recycling of nutrients associated with high grazing activity (Miller et al., 1991) or limitation of micronutrients such as iron (Hutchins and Bruland, 1998).

The upwelled waters are a mixture of the Pacific Subarctic (cold, fresh and nutrient rich) water, the Equatorial Pacific water (warm saltier water) (Tibby, 1941; Sverdrup et al., 1942; Pickard, 1964), and North Pacific Intermediate Water (NPIW, 100 to 200 m deep) (Barber and Smith, 1981). The subsurface Davidson Current (or California Undercurrent) transports the Equatorial water at depths of 200 to 500 m northward along the margin, and may surface during winter (Hickey, 1979).

5.3 Data

5.3.1 Modern conditions

The modern dataset used for the diatom TFs development for the modern calibration (Lopes et al., submitted, Chapter 3) is comprised of 51 diatom species/groups and 30 samples (figure 5.1 and Appendix E). The environmental dataset include primary productivity (PP) (Antoine and Morel, 1996), sea-surface temperature (SST), salinity (SSS) and nutrients (NO_3, PO_4 and SiO_2) (World Ocean Atlas 98), divided into five temporal averages: annual mean, winter (January to March), spring (April to June), summer (July to September) and fall (October to December).

5.3.2 Downcore data

We used two cores for the downcore data: MD02-2499 Piston Core (41.653^{o}N, 124.940^{o}W, 904 m depth) and ODP 1019 D (41.683^{o}N, 124.933^{o}W, 978 m depth). These two cores are at essentially the same site (figure 5.1) but are both used because the top part of the MD core was highly disturbed (voids), and site 1019 had a confused stratigraphy in the older section of marine oxygen isotope stage 3 (OIS 3) (Lyle et al., 2000). The sedimentation rate for ODP 1019 D and MD02-2499 both average 30 cm/ky. Both cores were sampled every 20 cm for diatom analysis, representing a time interval of approximately 500 years.

For both the modern and the downcore species dataset, between 100 and 300 organisms were identified down to the species level (Appendix E). The number of identified organisms is a reflection of the abundance of diatoms in the samples. Our cutoff was decided on the basis that at least 100 organisms were needed and that we would not spend more than one day per sample, following previous practice (e.g. Abrantes and Sancetta, 1985; Nave et al., 2001). Sensitivity tests (F test on variances) showed that in our worse case scenario (only 100 identifications) species percentage variances are not significantly different than on counts of 300 specimens. The standard deviation of an individual species count in a sample of 100 specimens was 3% (at a 95% significance level).

5.4 Methods

5.4.1 Radiocarbon (age models) and isotopes

The age model for 1019 D was based on radiocarbon dates of Barron et al. (2003). Calendar corrections averaged the results from three methods: Calib version 5 (after Stuiver and Reimer, 1993), Fairbanks 0805 (Fairbanks et al., 2005) and CalPal (Weninger et al., 2002) (Table 2 in Appendix D).

Stable isotopic data ($\delta^{18}O$) for MD02-2499 were analyzed at the College of Oceanic and Atmospheric Sciences, Oregon State University using a Finnigan/MAT-252 mass spectrometer equipped with a Kiel-III carbonate device. Radiocarbon dates in MD02-2499 (Table 2 in Appendix D) were converted to calendar dates (B.P.) using averages from benthic and planktonic and from the conversion methods mentioned above. Further chronological constraints were made by tuning the benthic $\delta^{18}O$ record to Atlantic core MD95-2042, which is in turn synchronized to the GISP-2 ice core $\delta^{18}O$ record (Shackleton et al., 2000) and core 1019 C (Mix et al., 1999a). Tie points between the $\delta^{18}O$ records and calendar-corrected radiocarbon dates were then used to interpolate the ages for all the downcore samples (Table 2 in Appendix D).

The final age model is shown in figure 5.2. We cannot at this point confirm that the two cores overlap in age (the bottom age of ODP 1019D and the top age of MD02-2499 both result from age extrapolation) so they are plotted separately.

5.4.2 No-analog problem

Application of floral factors and quantitative TFs based on regional core-tops (Lopes et al., submitted, Chapter 3), to the downcore records of 1019 D and MD02-2499 revealed an apparent no-analog problem based on poor communalities (a measure of how well the sample raw information is described by the selected end-members or factors; Hutson, 1977). This no-analog condition is caused by the presence of 13 species in downcore samples at > 3 times their peak abundance in regional core-tops. In particular, the marine species *Stephanopyxis turris* is present at percentages up to 75% of the flora in MD02-2499, but at $< 2\%$ in regional core-tops (figure 5.3). *Stephanopyxis turris* is classified as a warm, subtropical species (Cupp,

1943) related to coastal upwelling and high productivity (Maruyama, 2000). Sediment trap studies from the Indian Ocean (Schiebel et al., 2004) found this species under areas of coastal upwelling, where the SSTs range between 20°C and 26°C. Other species that contribute to no-analog conditions include freshwater diatoms (maximum 36% downcore vs. maximum 14% core-top), *Actinocyclus curvatulus* (maximum 16% downcore, vs. maximum 2% core-top), *Actinoptychus senarius* (maximum 30% downcore vs. maximum 5% core-top), *Coscinodiscus oculus-iridis* (maximum 4% downcore vs. maximum 1% core-top), *Leptocylindrus spores* (maximum 12% downcore vs. maximum 4% core-top), *Melosira westi* (maximum 7% downcore vs. maximum 1% core-top), *Paralia sulcata* (maximum 18% downcore vs. maximum 9% core-top), and *Delphineis surillela* (maximum 21% downcore vs. maximum 2% core-top).

To address the no-analog problem we used two methods. The first method (Feldberg and Mix, 2002) combines regional core-top and downcore samples in order to improve the definition of floral factors, and as a result to improve the communalities while retaining the full species list. The second method follows Pisias et al. (1997) in removing the no-analog species from the dataset.

5.5 Results

5.5.1 Combining core-tops and downcore samples (method 1)

Application of the Feldberg and Mix (2002) approach resulted in new Q-mode factor analysis and new modern calibrations for the traditional transfer functions (I&K, Imbrie and Kipp, 1971). Transfer functions developed by Lopes et al. (submitted, Chapter 3) based on Canonical Correspondence Analysis (CCA, ter Braak and Smilauer, 1998) did not change because CCA does not provide a comparable measure of communalities and cannot incorporate down-core samples into the calibration scheme (Morey et al., 2005).

The resulting Q-mode factors are able to explain 95% of the total variance contained in all the samples. All communalities are > 0.7 except for a modern sample (C14 in figure 5.1, TT31-11 GC in Table 1 from Appendix D) which has a

communality of 0.6. The new factors are similar to those obtained for the modern calibration (Lopes et al, submitted, Chapter 3), but include an additional factor dominated by *Stephanodiscus turris* (Table 5.1 and figure 5.4). The factors based on the combination of downcore and core-top species are:

-Factor 1 (figure 5.4a) the "Upwelling factor", explains 53% of the total dataset. *Chaetoceros spores* dominate;

-Factor 2 (figure 5.4b) is now expressed by *Stephanopyxis turris*. This factor contributes with 29% of the total variance. The spatial distribution of this factor does not have much of an expression for the modern calibration. Because this species cannot be related to our modern oceanic conditions, we decided to name this factor the "Coastal warm/productivity factor" having in consideration the relation of this species in the Indian Ocean and its interpretation of past conditions in our area. The geographic pattern of factor 2 (figure 5.4b) is very similar to factor 1 (figure 5.4a). This is because not only the sample loadings for factor 2 are very low (in the core-tops), but also because *Chaetoceros spores* have the second most important loading for this factor (Table 5.1) and therefore influences the geographic pattern;

-Factor 3 (figure 5.4c) is our previous "Freshwater factor". It now has a secondary species (*Acinoptychus senarius*) and contributes with 7.4% for the total variance. Its geographic pattern (figure 5.4c) follows the same interpretation as in Lopes et al. (submitted, Chapter 3);

-Factor 4 (figure 5.4d) is the "Subarctic factor". It is still expressed by *Rhizosolenia. hebetata* but it has a secondary species: *Neodenticula seminae* which in the previous Q-mode analysis was expressing a factor by itself. This factor continues to indicate Subarctic conditions;

-Factor 5 (figure 5.4e) was our previous second most important factor. We related its dominant species (*Thalassionema nitzschioides*) with subtropical conditions and named this factor the "Subtropical factor". It now only contributes with 2.4% and its spatial distribution in modern conditions remains the same as before (Lopes et al. submitted, Chapter 3).

We recalculated all the TFs for the I&K method and we got the same oceanic properties and similar uncertainties (Table 5.2 and figure 5.5), although the new calibration dataset rejects a TF for annual salinity (Lopes et al., submitted, Chapter 3). Factor 2 (one of the no-analogs) contributes to the equations despite the fact that it does not have a strong expression in core-tops. Transfer functions were calibrated for winter primary productivity, winter salinity and spring PO_4.

5.5.2 Removal of no-analog species (method 2)

We created a new species dataset where species that have > three times the core-top abundances in the downcore samples were removed interactively. Each time a species was removed, its relative abundances were recalculated to a closure of 100% (the sum of all specie's relative abundances). This reduced dataset is comprised of 37 diatom species and will be named the "no-analog dataset" (Appendix E).

The Q-mode analysis resulting from the "no-analog dataset" shows that we can apply the I&K method in its classical form: calculate the Q-mode factors for the core-tops and apply them to our downcore samples (Imbrie and Kipp, 1971). In this case, our core-top factors are suitable to describe the species variability in our downcore samples. All communalities are > 0.7 and the resulting factors are able to explain 97 % of the total variance contained in the raw dataset. However, because of the removal of the freshwater group from the dataset, we no longer have a "Freshwater factor". Instead of five factors of Lopes et al. (submitted, Chapter 3), the "no-analog" dataset gives only four (Table 5.3):

-Factor 1 (figure 5.6a) the "Upwelling factor", explains 58% of the total variance. *Chaetoceros spores* dominate;

-Factor 2 (figure 5.6b) the "Subtropical factor" explains 19% and *Thalassionema nitzschioides* continues to be related to subtropical conditions ;

-Factor 3 (figure 5.6c) is the "Subarctic factor" and contributes with 10%. The species associated with this factor continues to be *Rhizosolenia hebetata (forma hebetata);*

-Factor 4 (figure 5.6d) is still expressed by *Neodenticula seminae* and reflects the "Mixture factor" contributing with 10%.

Factors 3 and 4 keep the same amount of variance explained as in Lopes et al. (submitted, Chapter 3). Factor 2 decreased from 19% to 16% and factor 1 increased from 56% to 58%.

Reduction of the species list requires recalibration of modern TFs for both the I&K and CCA methods. The only significant TF based on the I&K method is spring PO_4 (figure 5.7a). The salinity TF was lost because the new factors exclude freshwater diatoms.

The CCA TFs calculated with the reduced species dataset are similar to those of Lopes et al. (submitted, Chapter 3): winter and spring PP, summer SST, winter salinity and spring PO_4. The statistical properties of r^2 and RSME are somewhat worse with the new dataset, likely because smaller effective species counts retain more counting noise (figure 5.7b, c, d and e and Table 5.4).

5.6 Discussion

5.6.1) To analog or not to analog?

The comparison of the species relative percentages that dominate the Q-mode factors from sections 5.1 and 5.2 (considering only the common factors in the two methods) shows that the same general trend is kept (figure 5.8). However, the removal of species and recalculation of the relative percentages in the "no-analog dataset" made the species relative percentages increases and decreases more marked but the amplitude of the factors variations is less than in method 1(figure 5.9). Factors 2 and 3 do not differ much between the two methods. However, factor 1 shows an important difference between 15,000 and 24,000 years (B.P.) where a marked decrease in the upwelling flora in method 1 does not occur in method 2. This happens because removal of freshwater diatoms in method 2 yielded higher percentages for *Chaetoceros spores*.

The reconstructions from CCA TFs show that using method 2 the gradients in the environmental properties are more constrained and stay inside the modern calibration gradients (figure 5.10 and Table 2 from Appendix C). For winter and

spring PP (figures 5.10a and b), the two methods show similar reconstructions for the past 18,000 years (B.P.). Before 18,000 years (B.P.), however, method 1 shows reconstructed values that are three to four times higher than modern values, which is implausible for open-ocean productivity almost anywhere in the ocean. We thus reject method 1 for reconstruction of paleo-productivity in these samples. The reconstructions for SST, salinity and PO_4 (figures 5.10c, d and e) also vary by method. Summer SST reconstruction from method 1 yields higher values than method 2 for ages older than 18,000 years (B.P.). Although within the range of modern calibration temperatures, anomalous warmth during OIS 3 is not consistent with regional pollen and speleothem data (Whitlock and Grigg, 1999; Vacco et al., 2005), and as a result we reject method 1 for these temperature reconstructions. Similarly, for estimates of Salinity and PO_4 (figures 5.10c and d) method 1 gives higher ranges.

The I&K reconstructions from method 1 and 2 can only be compared for spring PO_4 (figure 5.11). While the reconstruction from method 1 (figure 5.11a) yields values for OIS 3 that are implausible (close to 30μM) the reconstruction from method 2 (figure 5.11b) stays inside the modern calibration range (close to 0.55 μM). We reject the method 1 no analog transfer function based on the implausibility of the results.

CCA TFs show better confinement to modern calibration ranges if we use method 2 to approach the no-analog problem. However, the exclusion of certain species does not solve the problem regarding the basic assumption of TFs. What is the environmental cause of such a shift in the species abundances? We know that the no-analog problem does not affect only diatoms. TFs based in other microorganisms such as foraminifera (Ortiz et al., 1997) and radiolaria (Pisias et al., 1997) also have no-analog problems for this area. However, the species dataset used by these authors also included samples from other regions. This fact allows the author to look for modern analogs that although not present in the modern study area, can be present in other areas. Unfortunately, due to the small size of our dataset, we cannot use this approach to solve our no-analog problems.

Lopes and Mix (Chapter 4) relate anomalous increases in freshwater diatoms and low $\delta^{18}O$ from planktonic foraminifera during the last glacial interval to mega floods emanating from the Columbia River. This implies that regional oceanic conditions under the freshwater plume were sufficiently different during the last ice age that regional calibration of transfer functions with modern conditions is not appropriate. We reject a hypothesis that anomalous species assemblages in the region result from lateral transport on the ocean floor (e.g. Barron et al., 2003), because there are no regional occurrences of the no-analog species to serve as sources for transport. Further, downcore samples in which *Stephanopyxis turris* comprise almost 80% of the species assemblage show good preservation and presence of fragile species. It may be possible that some anomalous increases in the no-analog species do not imply a dramatic change in the environmental conditions. Diatoms are highly competitive, and even a small change in turbulence, for example, can shift the dominant species without a major change in temperature or nutrients (Margalef, 1978).

5.6.2) Reconstruction of past oceanic conditions

Figure 5.12 shows the reconstructions we accepted for our study area, which are based on CCA transfer functions and Method 2 of the reduced species dataset.

During the Holocene (defined as the interval from modern to 12,000 years B.P. by Martinson et al., 1987), the winter and spring productivity (figures 5.12a and b) show some variability. While the winter productivity decreases from modern values, the spring productivity oscillates and returns to modern values during the Holocene. The Upwelling factor also shows some variability (figure 5.12d), although it remains constant from 2,000 to 8,000 years (B.P.). At 8,000 years (B.P.) there is an anomalous cooling event in summer SST ($1^{o}C$ less than modern values - within the calibration error of the transfer function figure 5.12d). Mix et al. (1999a) found the same anomalous cooling in their foraminifera study for core 1019 and in our case this decrease matches a strong increase in our Subarctic factor and in the PO_4 reconstruction (figures 5.9d and 5.10d). This summer SST cooling did not seem to affect the upwelling factor and productivity only decreases a little.

Our reconstructions do not seem to be affected by the Younger Dryas (Y-D, defined as the interval from 11,500 to 13,000 years B.P. from Alley et al., 1993) and the Bølling-Allerød (B-A, defined as the interval from 13,000 to 14,500 years B.P. from Alley et al., 1993). Other studies show that SST decreased during the Y-D and increased in the B-A and the productivity decreased during the Y-D and increased during the B-A (Mix et al., 1999a). In our case, the summer SST is higher in the Y-D than in the B-A (figure 5.12d). The upwelling factor does not change and only spring productivity show a slightly increase in the B-A period (figures 5.12b and c).

The marine oxygen isotope stage 2 (OIS 2) and the Last Glacial Maximum (LGM, chronozone level 2 from 18,000 to 24,000 years B.P. defined by Mix et al., 2001) have been characterized by previous studies as a period where coastal upwelling and consequent productivity decreased (Sancetta et al., 1992, Pisias et al., 2001, Barron et al., 2003), with less export of organic carbon, increased $CaCO_3$ (wt%) (Lyle et al., 2000) and colder SST (Prahl et al., 1995). Our SST reconstruction for OIS 2 shows a decrease of 1^oC from modern values with warm oscillations in between. This value is much lower than the ones reported in previous studies (e.g. Prahl et al., 1995; Ortiz et al., 1997) and it reflects summer SST as opposed to annual averages. In addition, the overall increases in our summer SST for the 60,000 years are always associated with decreases in the upwelling factor and productivity. This is the opposite of what is believed to be present in the California Upwelling System where peaks in productivity and upwelling are associated with warm intervals (e.g. Ortiz et al., 2004). The small magnitude in our SST oscillations and the correspondent oscillations in the upwelling factor and productivity might be the result of colder upwelled waters in summer rather than a signal given by the overall SST temperature.

Lopes and Mix (Chapter 4) report the possible consequences of the massive inputs of freshwater in the study area during OIS 2. The reconstructions we have accepted in this study removed that signal from the TFs (application of method 2 removed the anomalous freshwater signal). Previous methods applied (e.g. alkenones, radiolaria) were likely not as sensitive to the freshwater signal because these marine specific tracers tend to live either under freshwater plumes, or intermittently in seasons

or years with low freshwater fluxes. Our results show some contradictory trends than previous reported studies: we do not see a mark decrease in the upwelling factor for the LGM. Winter productivity remains constant during OIS 2 although with lower values than modern ones (figure 5.12a). Spring productivity (figure 5.12b) actually increases during late glacial, slightly decreasing in the LGM but always with higher values than modern ones.

Sancetta et al. (1992) suggested that although coastal upwelling (summer) decreased in the LGM, spring upwelling could actually have been stronger than modern. Ortiz et al. (1997) suggested that during LGM, our study area had similar conditions to the ones present in the modern Gulf of Alaska: productivity is a consequence of nutrient rich waters and strong open ocean curl induced upwelling. Our reconstructions show that it is possible that during OIS 2 and the LGM there was a high productive ecosystem in the study area. Lopes et al. (2006) showed that the upwelling factor dominant species (*Chaetoceros spores*) could not separate between the two types of upwelling (coastal and open ocean wind-stress curl) present in the northeast Pacific in modern days. If the upwelling conditions shifted from coastal to wind-stress induced in the LGM, it could have originated the same situation we see today in regions where wind-stress upwelling occurs: high surface productivity but less export production into the ocean floor (Miller et al., 1991). This could explain why our productivity reconstructions show contradictory results when compared to the organic carbon records in the area, in particular the one from 1019 (Lyle et al., 2000).

During OIS 3 there is agreement between peaks in the upwelling factor, increases in productivity, and in summer SST (figure 5.12). The reconstructions are mainly dominated by these oscillations, some of them with high amplitudes. There is a strong decrease in the upwelling factor at 30,000 years (B.P.) and strong decreases in productivity. The oscillations in OIS 3 seem to indicate that the upwelling (coastal and/or open ocean wind-stress) was intermittent. Hendy et al. (2004) also suggested that the California Upwelling System was intermittently active during OIS 3 for the area south of 35^{o}N, maybe due to the influence of Dansgaard-Oeschger events

(Dansgard et al., 1993). Pisias et al. (2001) also relates the variability found in their reconstructions for OIS 3 with millennial-scale climate variability.

5.7 Conclusions

The application of modern calibrated TFs to the long sediment cores reveals a no-analog condition. A cutoff value of three times the core-top abundances in the downcore samples shows that 13 species contribute for the existence of the no-analog situation.

Removal of the no-analog species (method 2) yielded more conservative reconstructed environmental properties for the past 60,000 years (B.P.) than inclusion of downcore samples in factor definitions. We reject I&K TFs for this region based on diatoms because no significant or stable equations were obtained.

We developed statistically significant transfer functions based on a reduced species set and CCA methods for winter and spring productivity and summer SST. Over the past 60,000 years most peaks in productivity are associated with decreases in summer SST and increases in the upwelling flora. During the early Holocene (at 8,000 years B.P.) however, cooling that does not match any increase in productivity or upwelling, but is associated with a peak in the Subarctic Factor, suggesting that different processes are responsible for regional oceanic change under glacial and interglacial regimes.

Diatoms indicate that LGM productivity did not decreased as much as reported from previous studies of preserved organic matter. Although winter productivity is slightly lower than modern values, spring productivity increased. Organic carbon records from ODP 1019 showed a marked decrease. To reconcile these findings, we speculate that upwelling conditions might have shifted from a modern coastal upwelling system that is efficient in exporting carbon to the sea floor, to a system driven by wind-stress curl upwelling that is not as efficient in exporting organic carbon to the sediments, as occurs in the Alaska Gyre today.

During OIS 3, our reconstructions show systematic oscillations in productivity, upwelling, and SST. Peaks in productivity match peaks in upwelling and decreases in

SST. This suggests that the inducing upwelling winds were intermittent during OIS 3. Previous authors found analogous oscillations off southern California and related then to hemispheric millennial-scale climate oscillations.

We speculate that the strong no-analog conditions in the glacial-age diatom floras documented here reflects anomalous input of freshwater via the Columbia River (Lopes and Mix, Chapter 4).

Table 5.1 - Factor scores from Q-mode analysis in method 1(gray boxes indicate highest score for each factor).

Species	Factor 1	Factor 2	Factor 3	Factor 4	Factor 5
Freshwater	-0.1055	0.0504	0.7153	0.1587	0.0164
Benthics	-0.0082	-0.0007	0.0662	-0.0066	0.0512
Actinocyclus curvatulus	-0.0292	0.0397	0.1718	0.0175	0.1025
Actinocyclus normanii	-0.0004	-0.0074	0.0367	0.0144	0.0324
Actinoptychus senarius	-0.0562	0.0373	0.5157	-0.1055	0.1394
Stephanodiscus rotula (f. minutula)	-0.0275	0.0179	0.1691	0.0229	0.0015
Bacteriastrum spp.	-0.0039	-0.0032	0.0279	0.0075	0.0263
Chaetoceros spores	0.9308	0.1371	0.1595	-0.0858	-0.2682
Coscinodiscus decrescens	-0.0050	-0.0004	-0.0074	0.0954	-0.0219
Coscinodiscus oculus iridis	0.0026	-0.0008	-0.0006	0.0049	-0.0040
Coscinodiscus marginatus	0.0037	-0.0073	0.0881	0.1847	-0.1109
Coscinodiscus radiatus	0.0014	0.0750	0.0621	0.2009	0.0116
Cyclotella litoralis	0.0164	-0.0030	-0.0139	0.0488	-0.0280
Cyclotella spp.	0.0062	-0.0044	0.0067	0.0338	0.0126
Cyclotella striata	0.0056	-0.0021	0.0002	-0.0011	0.0186
Hemidiscus cuneiformis	0.0052	-0.0012	-0.0062	0.0128	0.0077
Leptocylindrus spores	0.0478	-0.0029	-0.0058	0.0857	-0.0783
Melosira westi	-0.0119	-0.0061	0.0751	0.0058	-0.0138
Odontella aurita	0.0041	0.0003	0.0074	0.0131	0.0082
Paralia sulcata	0.0124	0.0583	0.0437	0.0371	0.1204
Rhizosolenia setigera	0.0015	-0.0003	-0.0012	-0.0002	0.0023
Rhizosolenia hebetata (f. hebetatata)	0.0072	-0.0121	-0.0616	0.7127	-0.2902
Rhizosolenia styliformis	0.0046	-0.0011	0.0021	-0.0055	0.0120
Roperia tesselata	0.0082	-0.0013	-0.0089	-0.0054	0.0297
Stephanopyxis turris	-0.1386	0.9803	-0.0963	-0.0179	-0.0390
Thalassiossira allenii	0.0020	-0.0006	-0.0014	0.0041	0.0030
Thalassiossira anguste-lineata	0.0045	-0.0010	-0.0037	0.0004	0.0088
Thalassiossira eccentrica	-0.0064	0.0190	0.1052	0.0991	0.1232
Thalassiossira leptotus	-0.0133	0.0273	0.0889	0.0422	-0.0005
Thalassiossira lineata	0.0068	-0.0020	0.0010	0.0431	-0.0374
Thalassiossira nanolineata	0.0012	0.0063	-0.0004	-0.0028	0.0005
Thalassiossira oestrupii	0.0045	0.0008	-0.0270	0.2601	-0.0481
Thalassiossira cf. *poroseriata*	0.0003	0.0021	-0.0021	0.0006	0.0074
Thalassiossira angulata and/or *pacifica*	0.0052	0.0036	-0.0018	-0.0024	0.0127
Thalassiossira cf. *trifulta*	-0.0026	0.0000	-0.0018	0.0320	-0.0095
Thalassiossira sp.1	-0.0043	-0.0019	-0.0084	0.1223	-0.0258
Thalassiossira sp.2	-0.0037	-0.0014	-0.0015	0.0894	-0.0476
Thalassiossira sp.6	-0.0023	0.0000	-0.0016	0.0279	-0.0083
Thalassiossira spp.	0.0010	-0.0025	-0.0099	0.1003	-0.0199
Delphineis surillela	-0.0202	0.0081	0.2360	-0.0737	0.0268
Delphineis karstenii	0.0029	0.0039	0.0096	-0.0074	0.0191
Fragilariopsis doliolus	0.0428	-0.0110	-0.0546	0.0900	0.1210
Gomphonema constrictum	-0.0029	-0.0018	0.0121	-0.0015	0.0191
Lioloma elongatum	0.0069	-0.0003	-0.0071	0.0683	-0.0228
Lioloma pacificum	0.0147	-0.0025	-0.0153	0.0553	-0.0115
Lioloma spp.	0.0030	-0.0023	-0.0116	0.1398	-0.0360
Neodenticula seminae	-0.0072	0.0083	0.0328	0.3649	0.0538
Nitzschia gp *bicapitata*	0.0042	-0.0023	0.0054	0.0098	0.0209
Raphoneis amphiceros	0.0007	0.0091	0.0688	-0.0258	0.0485
Thalassionema bacillare	0.0023	-0.0005	-0.0020	0.0035	0.0090
Thalassionema nitzschioides	0.3037	0.0590	-0.1203	0.2447	0.8515

Table 5.2 - Transfer function equations from CCA and I&K for method 1. Factors and axes refer to sample scores from respectively I&K and CCA analyses.

		r^2	error (RMSE)	Equation
I&K	PP winter	0.6	28 ($gC/m^2/y$)	estimated=111.5-1403.7(F2*F4)-428(F1*F3)+702(F2)
	Salinity winter	0.8	0.3 (PSU)	estimated=32.6-9(F2)^2
	PO_4 spring	0.8	0.04 (μM)	estimated=0.87+0.35(F4)^2+30.6(F2)^2-67(F2)+0.32(F4*F5)
CCA	PP winter	0.97	7.6 ($gC/m^2/y$)	estimated=112.7+36.2(A1)+31.7(A3)+7.9(A2)+25.6(A4)+ 10.3(A1*A2)+9.1(A1)^2+9.4(A1*A3)
	PP spring	0.7	24 ($gC/m^2/y$)	estimated=202.1+30.2(A2)+19.3(A3)
	SST summer	0.7	0.4 (^oC)	estimated=15.6-0.5(A3)-0.16(A2)-0.18(A2*A4)
	Salinity winter	0.8	0.2 (PSU)	estimated=32.2-0.6(A2)+0.3(A1)+0.05(A2)^2
	PO_4 spring	0.8	0.04 (μM)	estimated=0.6+0.06(A1)+0.02(A2)

Table 5.3 - Factor scores from Q-mode analysis in method 2 (gray boxes indicate highest score for each factor).

Species	Factor 1	Factor 2	Factor 3	Factor 4
Actinocyclus normanii	-0.0360	0.1032	-0.0210	0.0273
Bacteriastrum spp.	-0.0338	0.1095	0.0000	-0.0348
Chaetoceros spores	0.9717	0.0293	0.0583	0.1398
Coscinodiscus decrescens	-0.0355	0.0058	0.1377	0.0038
Coscinodiscus marginatus	0.0115	-0.0672	0.2509	-0.0604
Cyclotella litoralis	0.0169	-0.0060	0.0146	0.0059
Cyclotella spp.	0.0002	0.0274	0.0123	0.0215
Cyclotella striata	0.0096	0.0179	-0.0100	0.0013
Hemidiscus cuneiformis	0.0014	0.0080	0.0205	-0.0038
Odontella aurita	0.0029	0.0054	-0.0069	0.0260
Rhizosolenia setigera	0.0004	0.0060	-0.0014	-0.0022
Rhizosolenia hebetata (f. hebetatata)	-0.0065	-0.1523	0.7964	-0.1437
Rhizosolenia styliformis	0.0048	0.0164	-0.0068	-0.0094
Roperia tesselata	0.0045	0.0236	-0.0090	0.0009
Thalassiossira allenii	0.0020	0.0029	-0.0024	0.0057
Thalassiossira anguste-lineata	0.0047	-0.0001	-0.0094	0.0214
Thalassiossira eccentrica	-0.1467	0.3532	0.0736	-0.0122
Thalassiossira lineata	0.0005	-0.0098	-0.0089	0.0351
Thalassiossira nanolineata	0.0017	0.0020	-0.0008	-0.0016
Thalassiossira oestrupii	-0.0840	0.0207	0.3135	0.0979
Thalassiossira cf. *poroseriata*	-0.0047	0.0147	-0.0010	-0.0013
Thalassiossira angulata and/or *pacifica*	-0.0029	0.0030	-0.0077	0.0307
Thalassiossira cf. *trifulta*	-0.0152	0.0020	0.0464	0.0032
Thalassiossira sp.1	-0.0293	-0.0237	0.1592	0.0439
Thalassiossira sp.2	0.0205	-0.0586	0.1877	-0.1005
Thalassiossira sp.6	-0.0133	0.0017	0.0405	0.0028
Thalassiossira spp.	-0.0114	-0.0033	0.1352	-0.0119
Delphineis karstenii	-0.0031	0.0316	-0.0067	-0.0081
Fragilariopsis doliolus	-0.0526	0.1732	0.0132	0.1290
Gomphonema constrictum	-0.0245	0.0703	-0.0103	-0.0174
Lioloma elongatum	0.0007	-0.0145	0.0769	-0.0029
Lioloma pacificum	-0.0010	0.0091	0.0574	0.0001
Lioloma spp.	-0.0016	-0.0276	0.2145	-0.0455
Neodenticula seminae	-0.1310	-0.1899	0.0949	0.9425
Nitzschia gp *bicapitata*	0.0052	0.0246	0.0038	-0.0009
Thalassionema bacillare	-0.0010	0.0151	-0.0006	0.0004
Thalassionema nitzschioides	0.0217	0.8621	0.1666	0.1449

Table 5.4 - Transfer function equations from CCA and I&K for method 2. Factors and axes refer to sample scores from respectively I&K and CCA analyses.

		r^2	error (RMSE)	Equation
I&K	PO_4 spring	0.7	0.05 (μM)	estimated=0.52+0.34(F3)+-0.23(F1*F3)
CCA	PP winter	0.96	9 ($gC/m^2/y$)	estimated=112.4+37.6(A1)+37.9(A4)-16.2(A3)+ 11.8(A1*A4)+7.7(A1)^2+7.2(A2)-3.9(A1*A2)
	PP spring	0.7	25 ($gC/m^2/y$)	estimated=200.9+23.6(A2)+7.5(A1*A2)
	SST summer	0.6	0.4 (^oC)	estimated=15.6-0.4(A3)-0.2(A4)-0.1(A2)
	Salinity winter	0.7	0.3 (PSU)	estimated=32.2+0.3(A1)-0.3(A2)
	PO_4 spring	0.7	0.04 (μM)	estimated=0.57+0.05(A1)+0.02(A2)

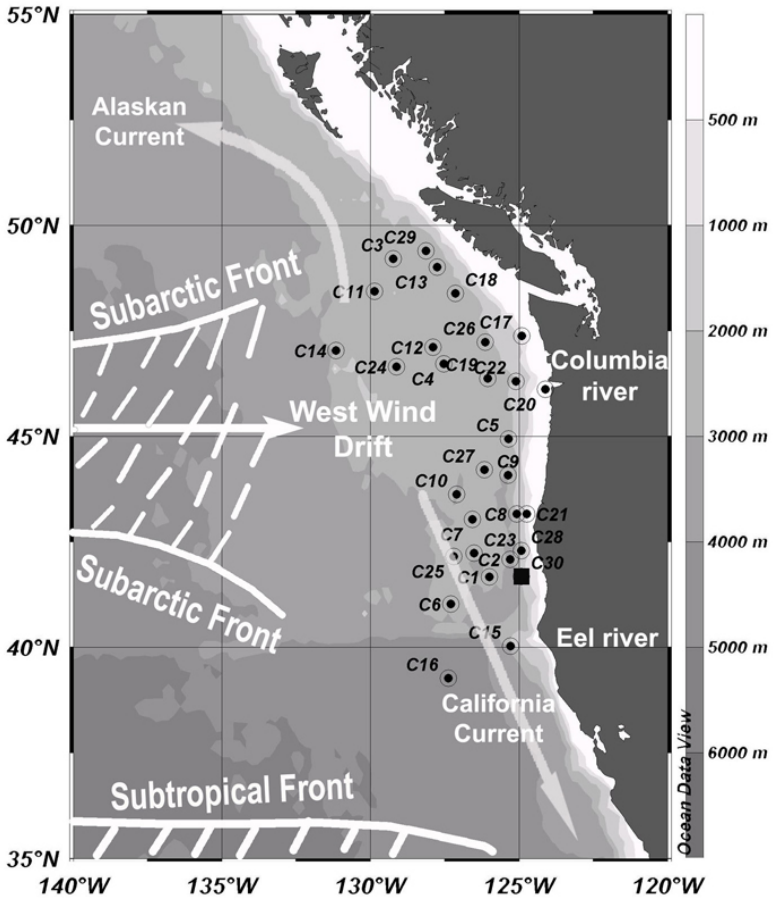

Figure 5.1 – Schematic of major oceanic currents and fronts in the NE Pacific system. Black dots are core-top sample locations and black square is location of the two downcores used in the reconstructions (1019 D and MD02-2499 are too close to show them separated). The range of positions for the Subarctic Front reflects summer (northern) and winter (southern) extremes. Shading reflects bathymetry.

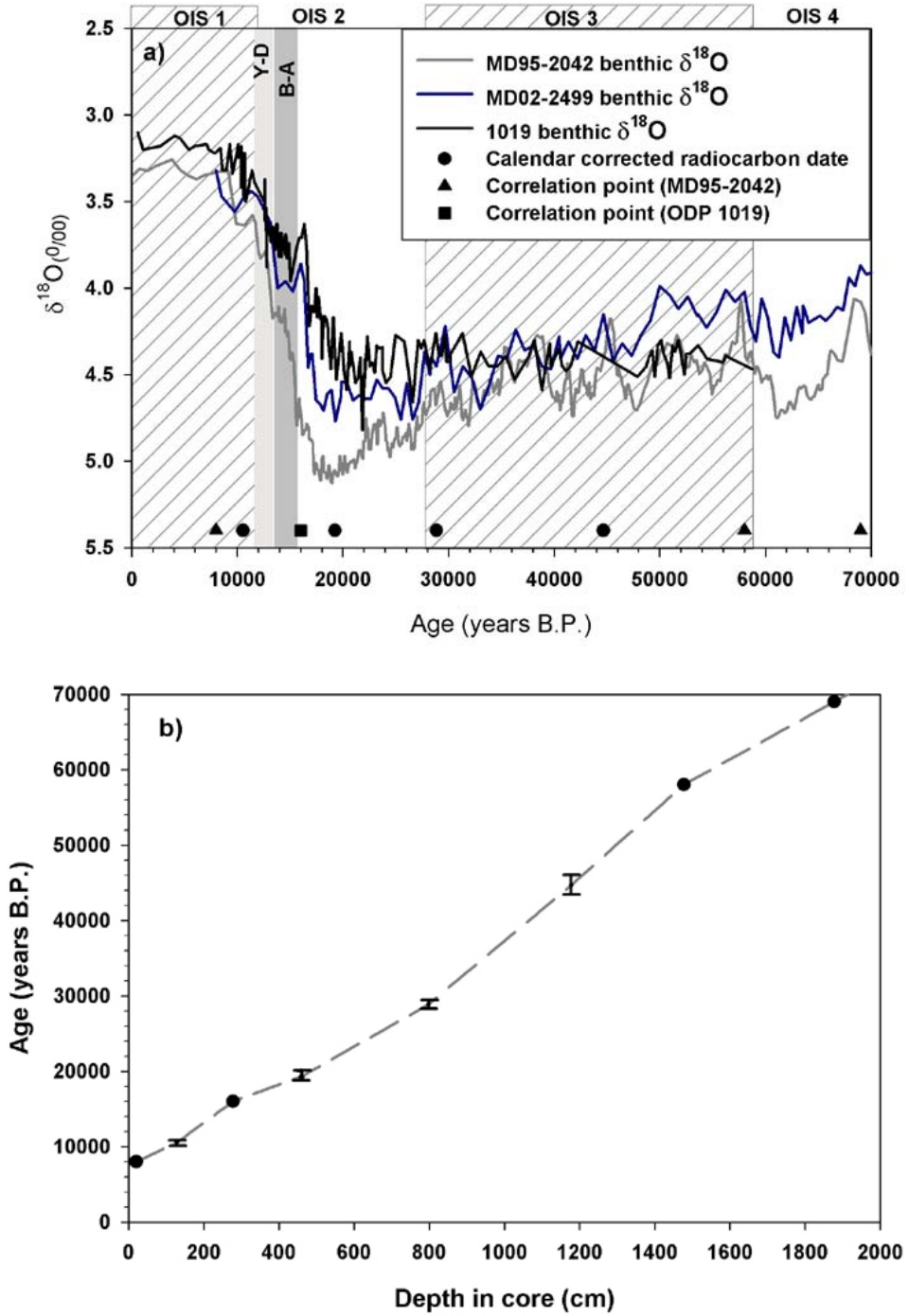

Figure 5.2 – Age model constrains for MD02-2499; a) constrain from MD95-2040 benthic $\delta^{18}O$, and b) correlation points (black dots) and radiocarbon constrains with correspondent error bars.

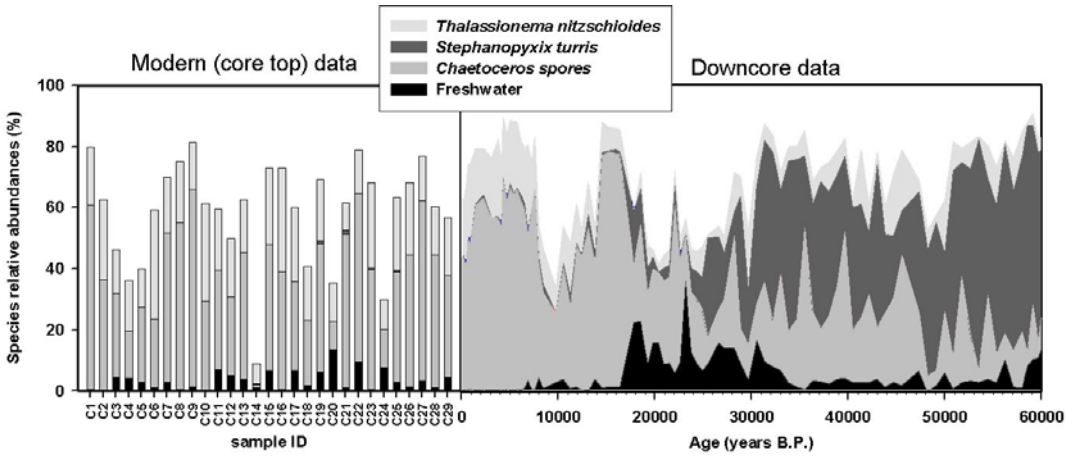

Figure 5.3 – Relative percent abundances of the most abundant diatom species from the modern calibration (histogram, left panel) and for our downcore samples (stacked area, right panel). Notice the increase of *Stephanopyxis turris* from 30,000 years to 60,000 years (B.P.) and its absence from the modern calibration.

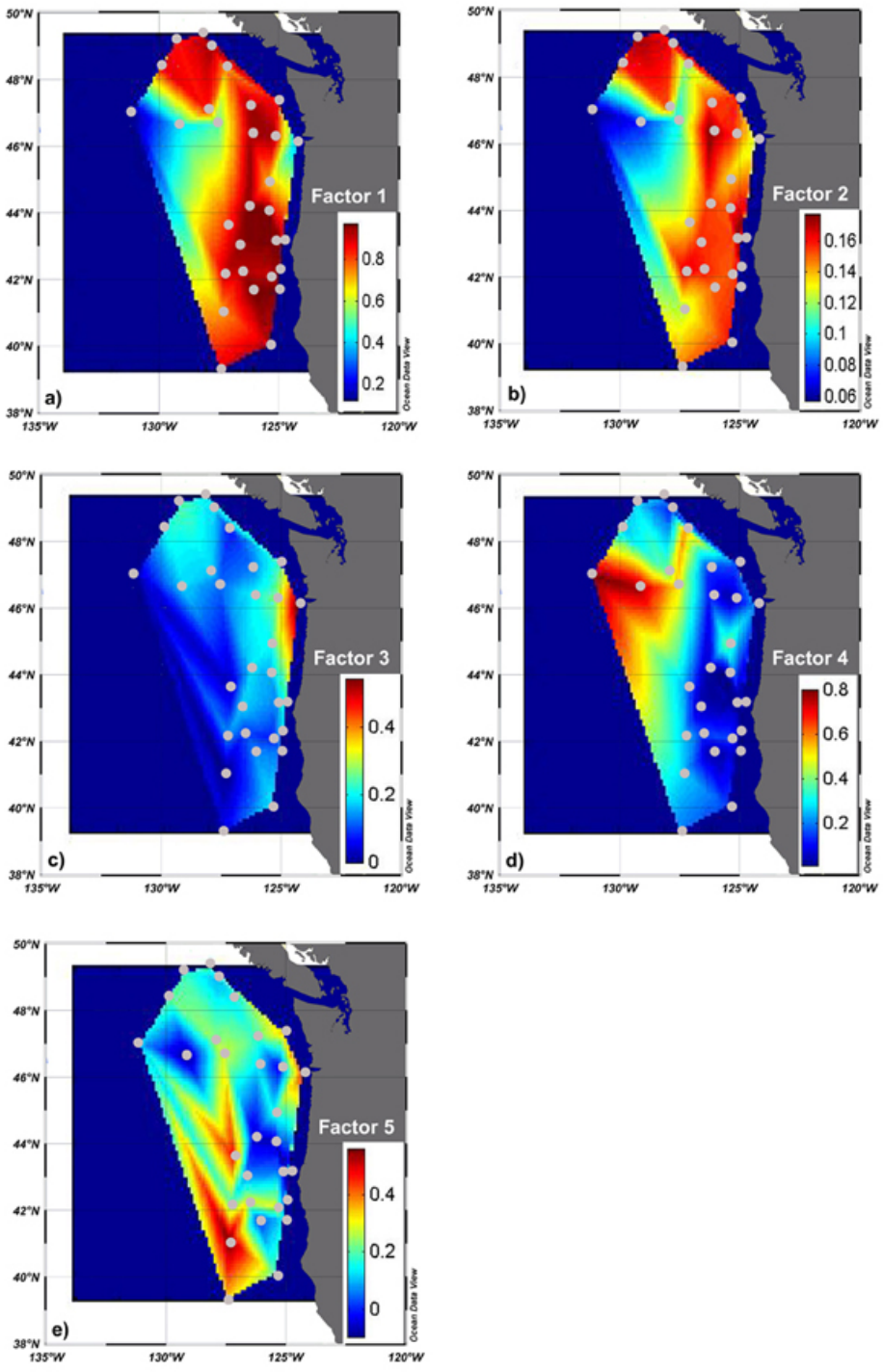

Figure 5.4 – Spatial distribution of factor loadings for the five factors obtained in method 1 (gray dots are the modern sample locations).

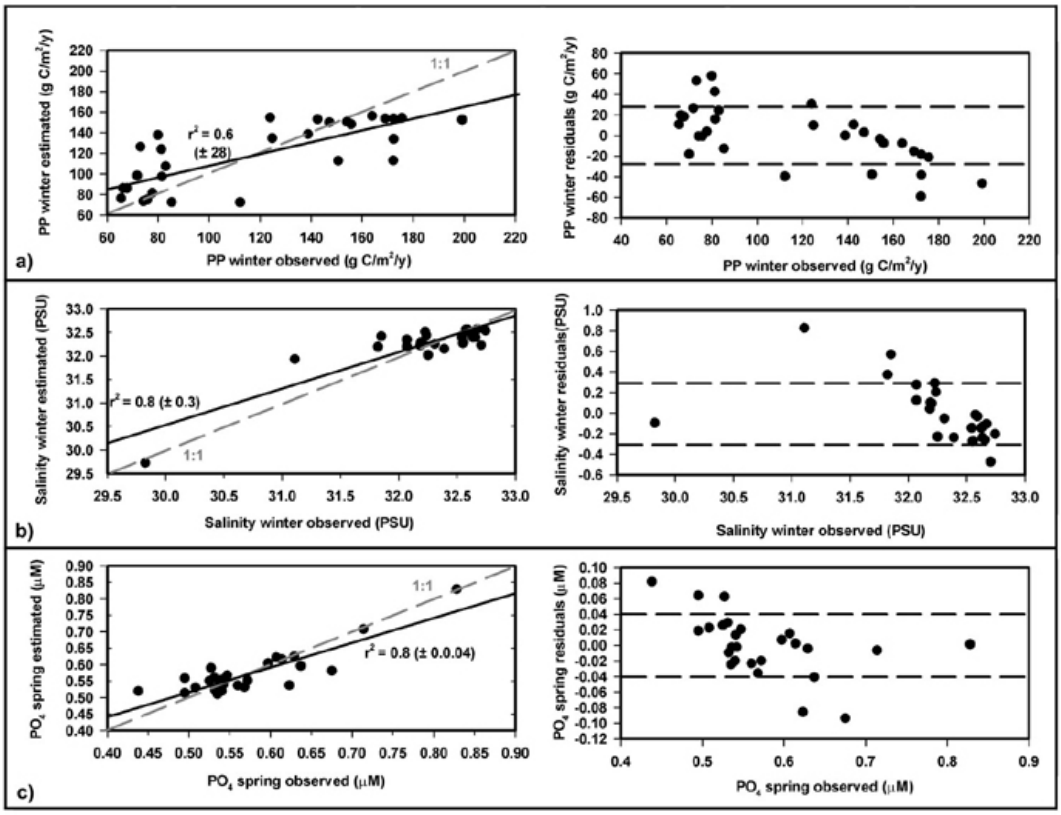

Figure 5.5 - Scatter plots for regression equations (gray line represents the 1:1 line) and residuals from modern transfer functions calibrations from Imbrie and Kipp and method 1: a) winter productivity, b) winter salinity and c) spring PO_4.

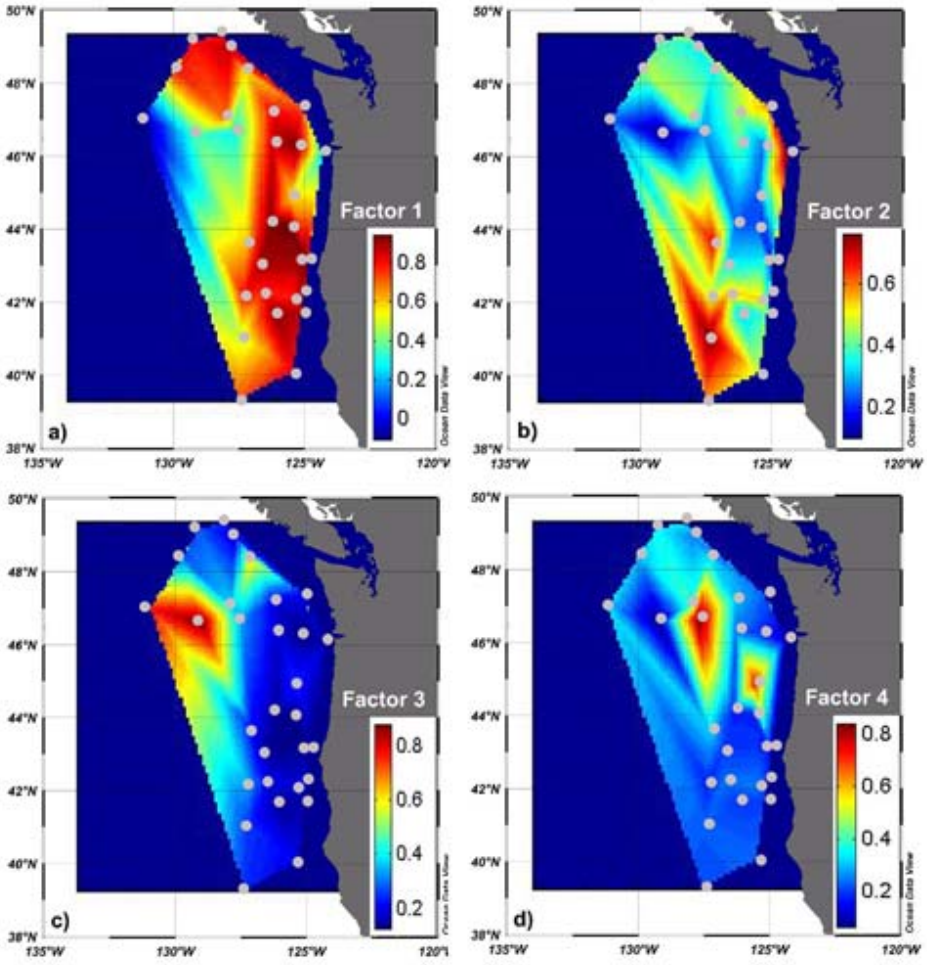

Figure 5.6 – Spatial distribution of factor loadings for the four factors obtained in method 2 (gray dots are the modern sample locations).

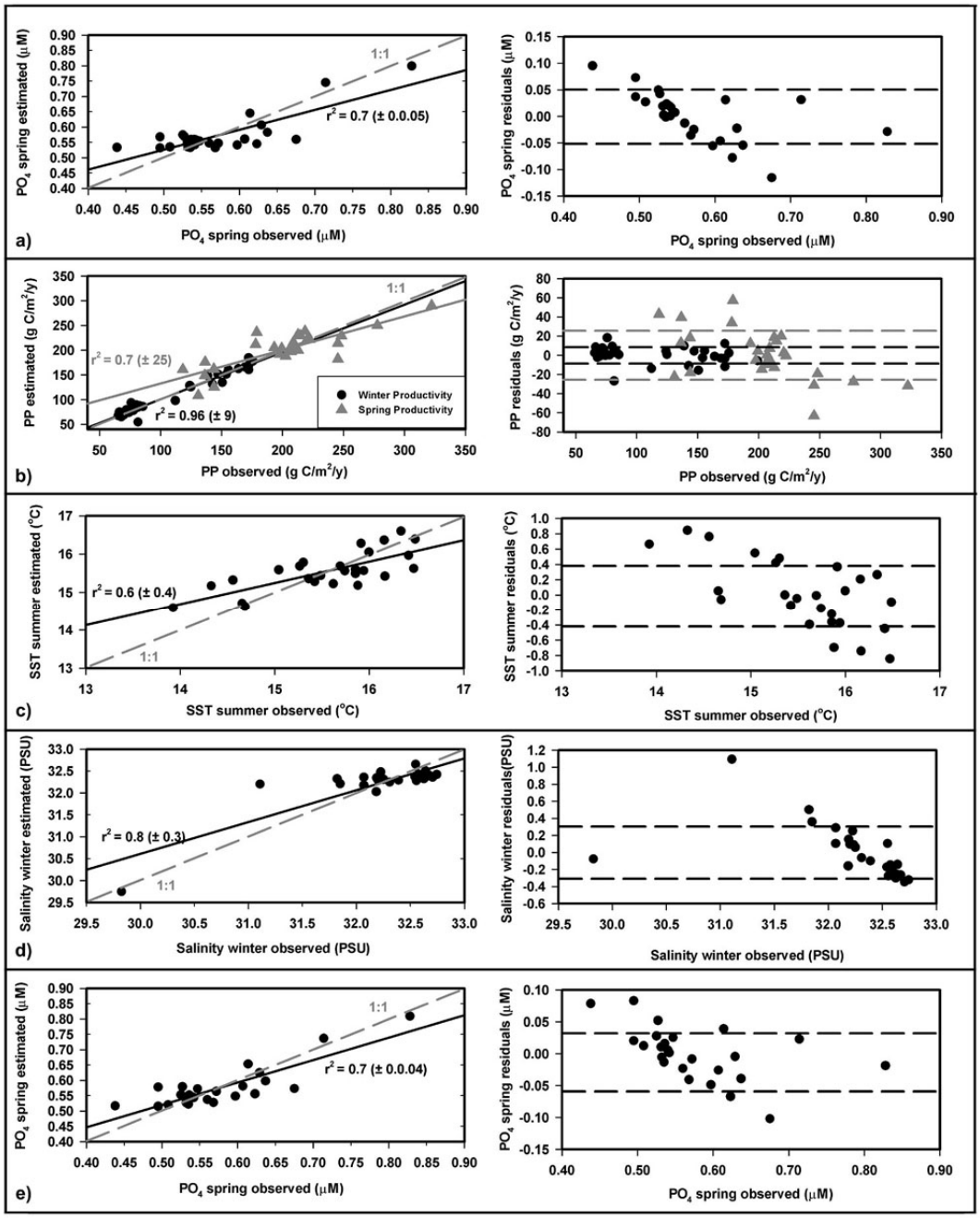

Figure 5.7 – Scatter plots for regression equations (gray line represents the 1:1 line) and residuals from modern transfer functions calibrations from method 1and: a) spring PO_4 from Imbrie and Kipp, b) winter (black dots) and spring (gray triangles) productivity from CCA, c) summer SST from CCA, d) winter salinity from CCA and e) spring PO_4 from CCA.

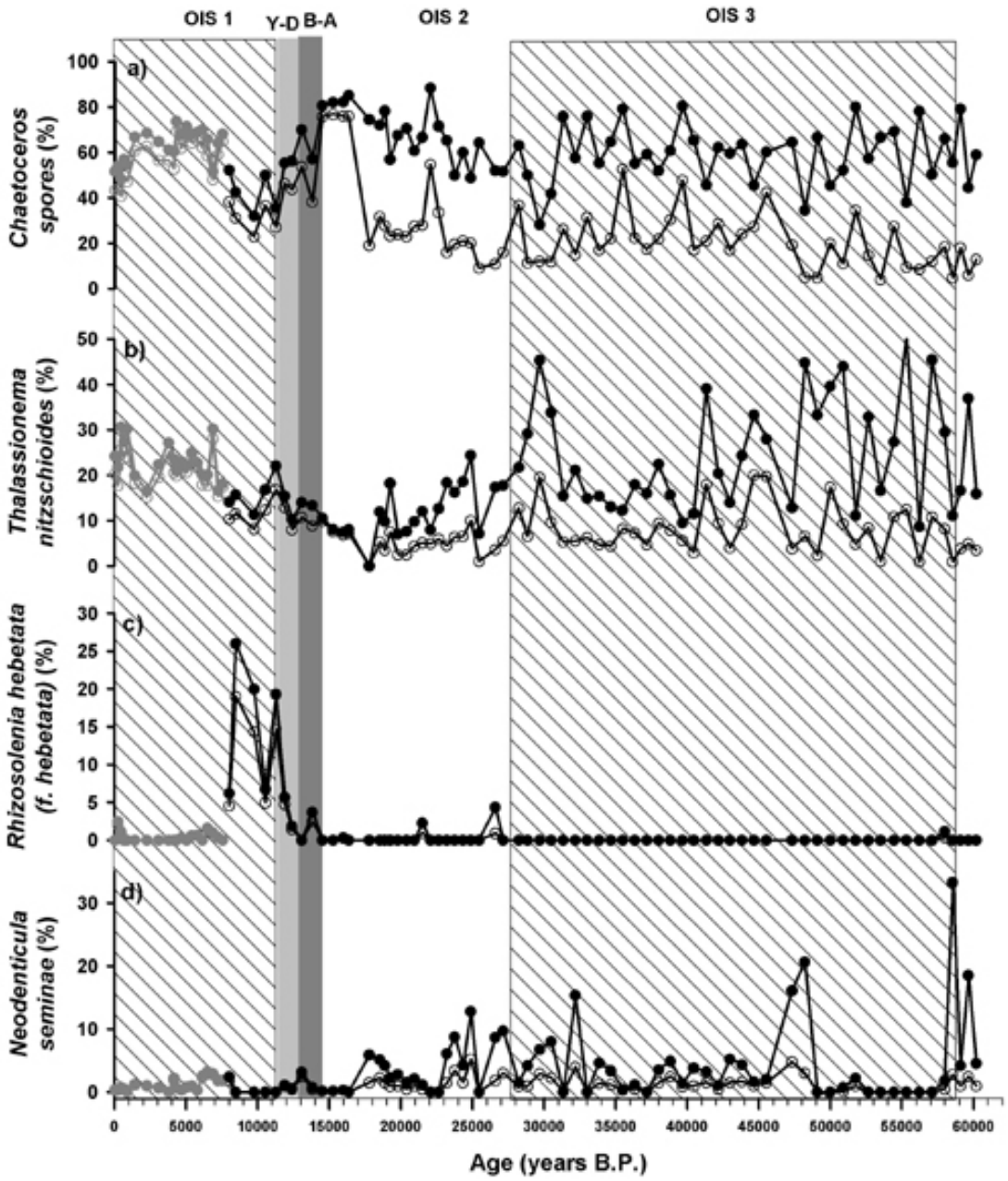

Figure 5.8 – Downcore species relative abundances for the Q-mode factor dominant species: a) *Chaetoceros spores*, b) *Thalassionema nitzschioides*, c) *Rhizosolenia hebetata (forma hebetata)* and d) *Neodenticula seminae*. Grey lines refer to core 1019 D and black lines refer to MD02-2499, open circles refer to method 1 and close circles refer to method 2.

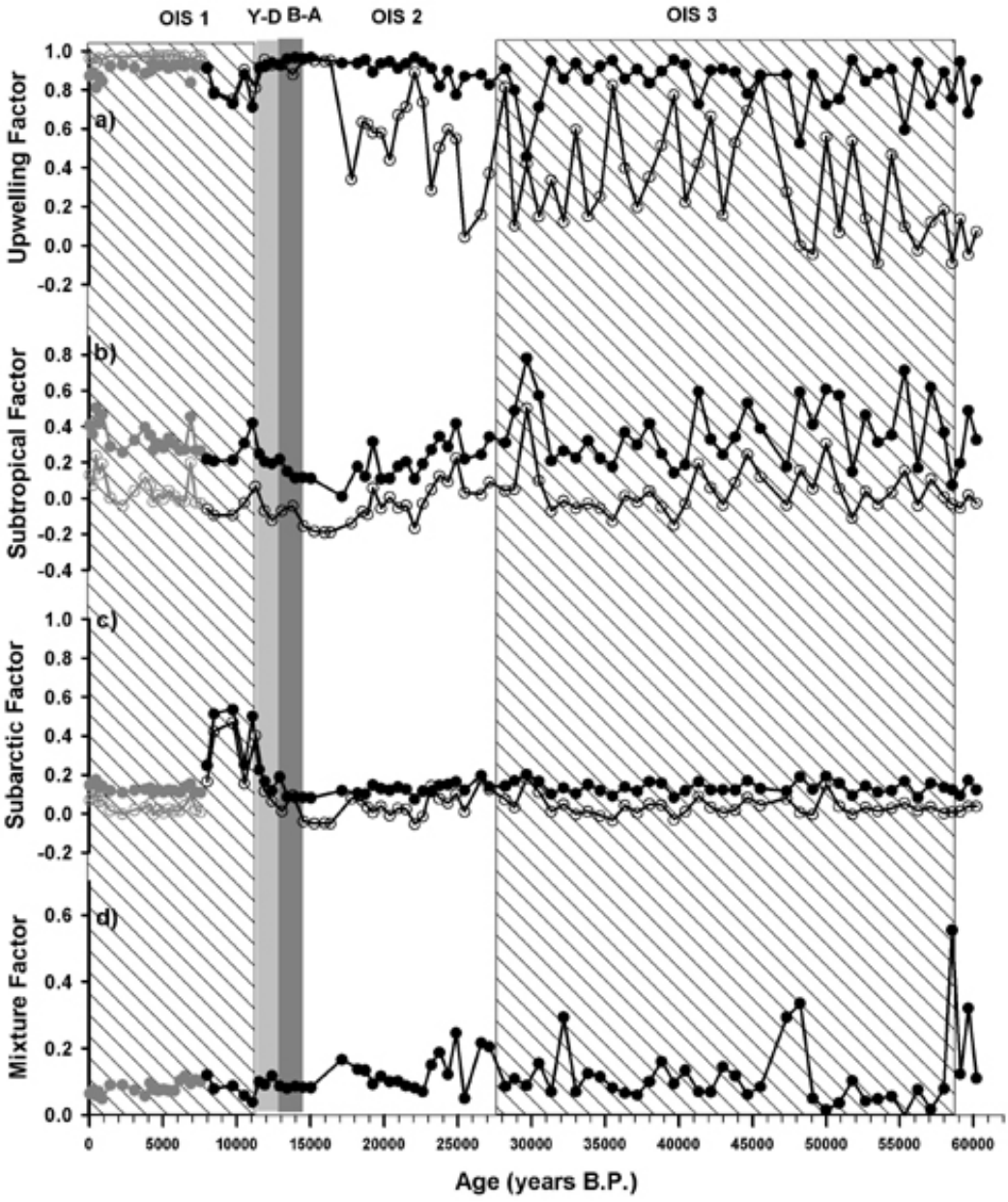

Figure 5.9 - Downcore plots of the factor loadings for Q-mode factors: a) Upwelling factor, b) Subtropical factor, c) Subarctic Factor and d) Mixture factor. Gray lines refer to core 1019 D and black lines refer to MD02-2499, open circles refer to method 1 and close circles refer to method 2.

Figure 5.10 – Plot of downcore reconstructions for CCA: a) winter productivity, b) spring productivity, c) winter salinity, d) spring PO_4 and e) summer SST. Gray lines refer to core 1019 D and black lines refer to MD02-2499, open circles refer to method 1 and close circles refer to method 2. Black arrows refer to modern values with correspondent error bars of estimation (black dash, when visible).

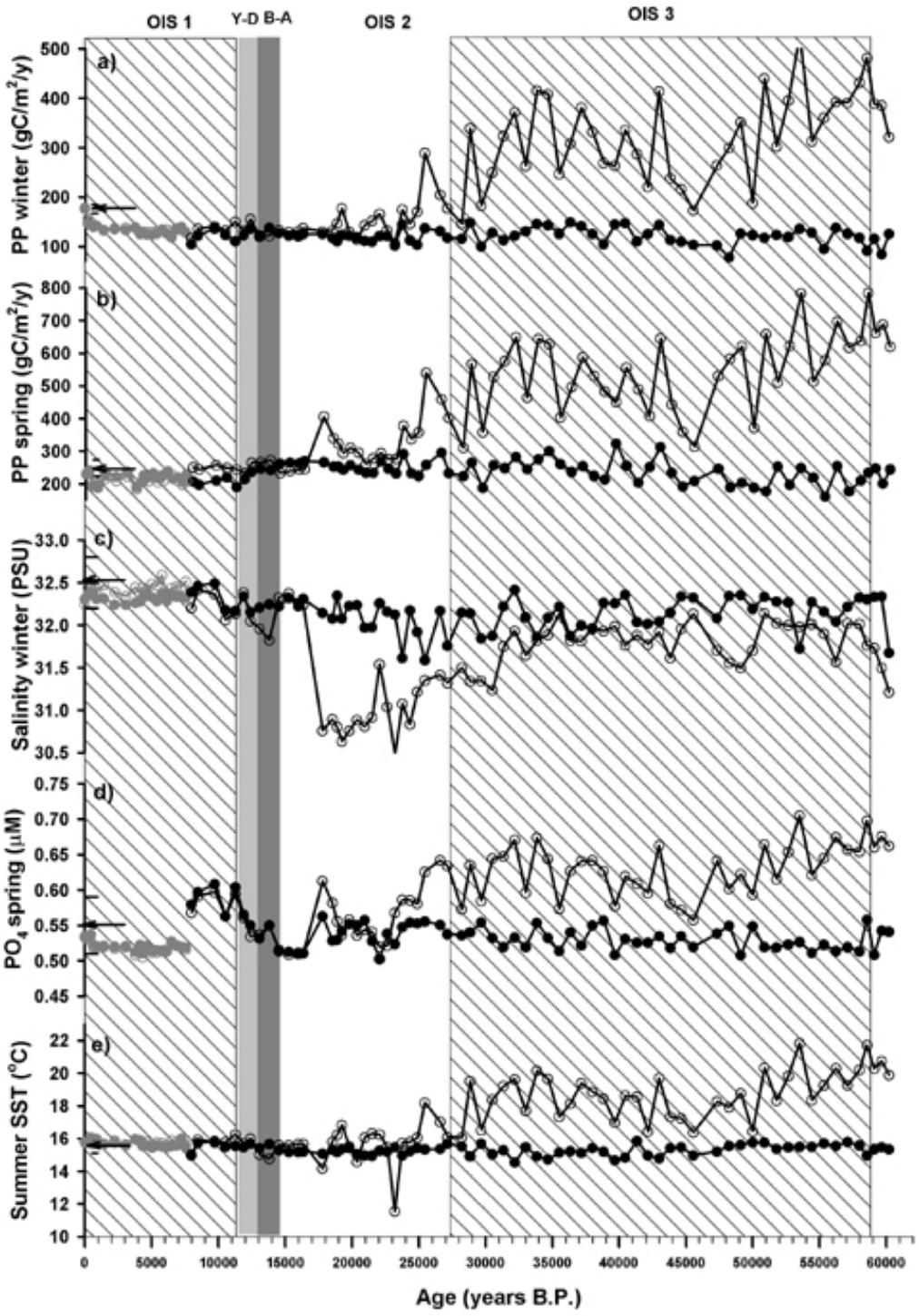
OIS 1
Y-D B-A
OIS 2
OIS 3
a)
PP winter (gC/m²/y)
b)
PP spring (gC/m²/y)
c)
Salinity winter (PSU)
d)
PO4 spring (µM)
e)
Summer SST (°C)
Age (years B.P.)

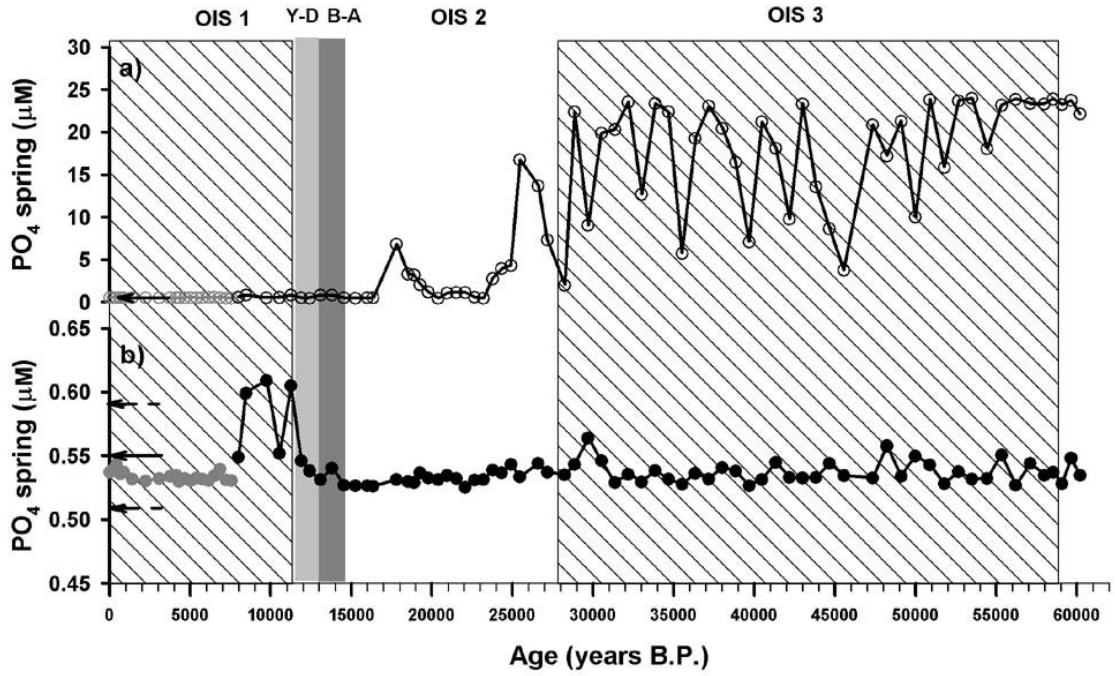

Figure 5.11 – Plot of downcore reconstructions for I&K: a) spring PO_4 from method 1 and b) spring PO_4 from method 2. Grey lines refer to core 1019 D and black lines refer to MD02-2499. Black arrows refer to modern values with correspondent error bars of estimation (black dash).

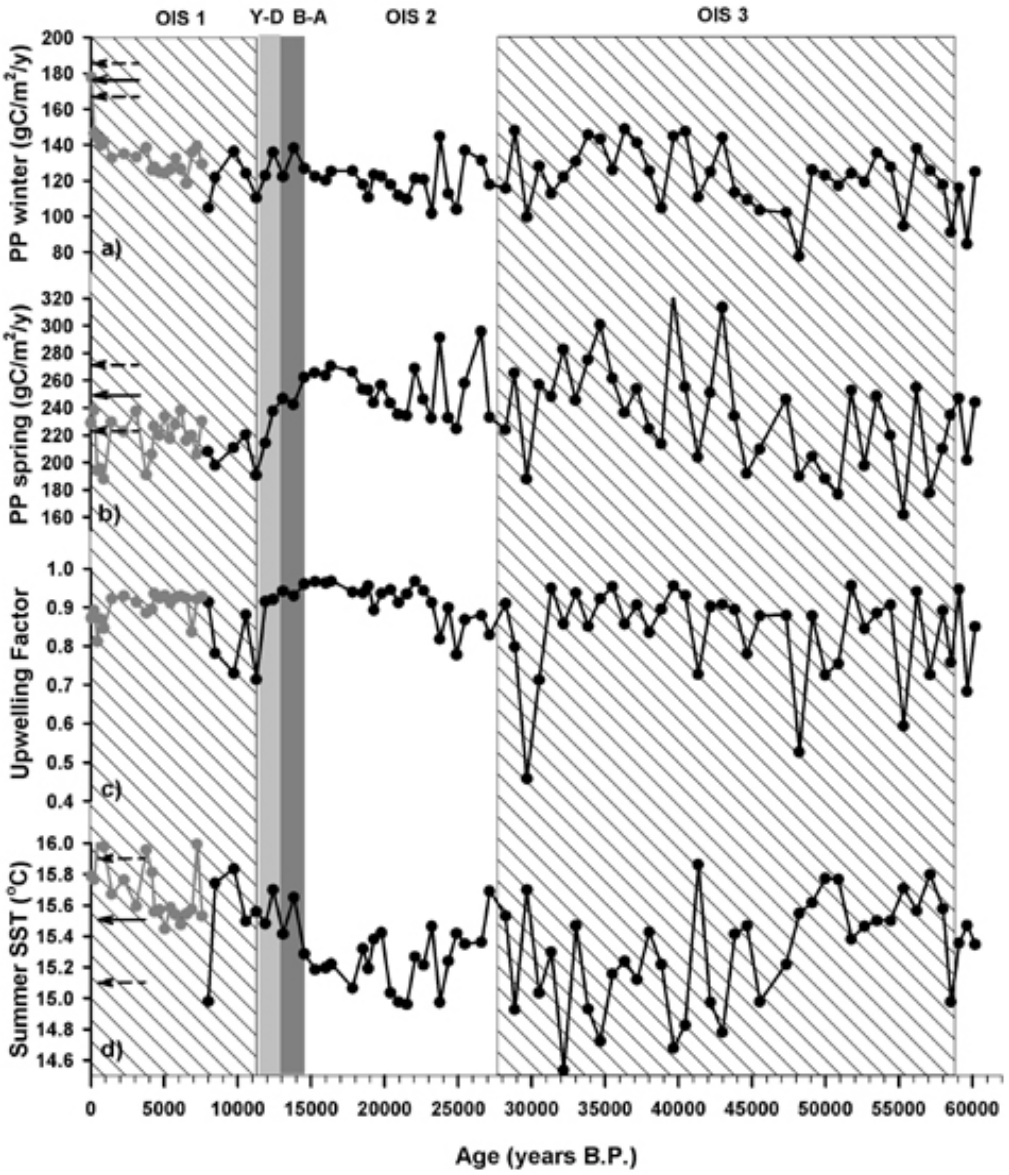

Figure 5.12 – Plot of downcore reconstructions for CCA and Upwelling factor from I&K: a) winter productivity, b) spring productivity, c) Upwelling factor and d) summer SST. Grey lines refer to core 1019 D and black lines refer to MD02-2499. Black arrows refer to modern values with correspondent error bars of estimation (dashed arrows).

6. NORTHEAST ATLANTIC PALEOCEANOGRAPHIC SEA-SURFACE TEMPERATURE AND CHLOROPHYLL RECONSTRUCTIONS

Cristina Lopes

6.1 Introduction

The Portuguese margin (northeast Atlantic) plays a significant role in the development of upwelling associated with the Canary Current System. Several studies from the Portuguese margin demonstrated that the geologic record of diatoms were good qualitative indicators of upwelling conditions, not only for modern conditions but also for the past conditions (e.g. Abrantes, 1991; Abrantes and Moita, 1997), although the development of quantitative environmental transfer functions (TFs) based on diatoms was never achieved

Here, I develop quantitative environmental TFs using the published dataset of Abrantes (1988). The TFs were developed using the same methods applied in the NE Pacific area (chapters 2 and 4, for more detailed explanation of the methods). Recommendations for improvement of the TFs presented here (derived from problems with the floral and environmental datasets) include refining taxonomic categories from genus to species, and developing environmental datasets near the coast at higher spatial higher resolution, to match the close spacing of the sediment cores in the small region.

6.2 Modern conditions

Off the Portuguese margin, upwelling occurs from April to October and results from the interaction between the trade winds, controlled by the Azores high and Greenland low pressure cells and the Canary Current, flowing southward parallel to the Portuguese coast (Fiúza, 1983). Due to the particular physiographic features of the coast, this process is not uniform along the entire region (Fiúza, 1983). The coastal upwelling along the Portuguese margin brings subsurface (60-120 m depth) waters to the surface. To the north of Nazaré canyon (≈ 39.5^0N; 9.5^0W), the ascending water is the Eastern North Atlantic Central Water (ENACW) with subpolar characteristics (colder and fresher), while south of Lisbon the same ENACW is saltier and warmer (Fiúza, 1983). This canyon marks the separation between the north wide shelf (≈ 200 km wide) and the narrow south shelf (≈ 60 km wide). Due to the morphological characteristics of this canyon (proximity to the coast and dimensions), a high amount

of sediments from land is transported to open ocean. Also, the proximity of two capes, Cape Carvoeiro and Cape da Roca (figure 6.1a), affects the coastal upwelling pattern by inducing the formation of filaments that reach more open ocean areas (Fiúza et al., 1998). The strongest upwelling area (North of Nazaré Canyon) is located in the region where the wind-stress curl is stronger (Bakun and Nelson, 1991).

6.3 Data

The core-top dataset is comprised of 161 samples. Most of them located on the shelf and upper slope (less than 500m depth) and extremely close to each other (figure 6.1a). Abrantes (1988) developed the diatom dataset compromising 27 species and/or groups of species (genus). The total diatom abundance (#valves/g of sediment) was used (Abrantes, 1988) to locate the stronger regions of the coastal upwelling (figure 6.1b and Table 6.1). From the 161 samples, 68 samples were used for diatom species identification (for taxonomic details see Abrantes, 1988). The environmental datasets used for the northeast Pacific (Antoine and Morel, 1996 and World Ocean Atlas, 1998) could not be used in the study presented here because of proximity to the coast and spatial sampling resolution less than 0.5^{o} latitude and longitude which is finer than the atlas produces typically have a spatial resolution of 1^{o} and effective spatial smoothing of a few degrees. As a result, only 28 samples could be paired with environmental information (sea-surface temperature, (SST), salinity and nutrients) retrieved from the WOA 98 database. Because of spatial smoothing, only 11 unique environmental values could be obtained, which is insufficient for transfer function development as it does not cover the entire study area. Although satellite data on primary production is of higher resolution (Antoine and Morel, 1996), because of spatial smoothing many of the samples yield identical productivity values. As a result, the spatial gradients in productivity, where available, are too small for effective TF calibration.

The only environmental data that can be used together with the diatom dataset is comprised of in-situ measurements of SST and chlorophyll (figure 6.2) for annual average, winter (September to March), summer (April to September) and seasonal

range (summer minus winter). These measurements were obtained from cruises along the Portuguese margin during 1985 and 1986 and represent surface water conditions in just two years, which may not be representative of long-term means (data from Abrantes, personal communication). With this dataset, 62 of the 68 samples selected (from the species dataset) have in-situ environmental data for chlorophyll and SST (Table 6.2 and Appendix F). The compilation of information for the wind-stress curl was also not possible because of the closeness of the samples regarding the coast (the values closer to the coast are missing). However, we will refer to Bakun and Nelson (1991) maps for qualitative comparison.

Sediment core KS11 (40.69^{o}N, 10.21^{o}W, 3590 m depth), which was previously studied by Abrantes (1991) was selected for downcore study. Its published diatom dataset uses a taxonomy that is consistent with that of the core-tops. The downcore sampling resolution cannot be comparable to the core studied in the northeast Pacific (Chapter 4) because KS11 has a much lower sampling resolution.

6.4 Modern calibration and Transfer Functions

6.4.1 Imbrie and Kipp (I&K, Imbrie and Kipp, 1971)

The application of Q-mode analysis returned six factors that explained 97% of the raw species information in the core-tops. All communalities are higher than 0.7 except for sample 55, which only has a communality of 0.5. This sample was therefore removed from the Q-mode analysis. The factors loadings are in Table 6.3 and the factor description is as follows:

-Factor 1 (figure 6.3a) is dominated by *Paralia sulcata* and explains 54% of the total dataset. This factor is most common over the shelf, and is negatively correlated with annual, summer and seasonal range of SST (Table 6.4). Because of these characteristics this factor will be designated as the “shelf factor”. Abrantes (1988) related *Paralia sulcata* with upwelling conditions, considering that this species would increase its size if the nutrients were more available. Because we do not have a significant correlation with chlorophyll, however, we cannot infer about the link between this species and productivity for this area.

-Factor 2 (figure 6.3b) is dominated by *Chaetoceros spores* with 17% of the total dataset. *Chaetoceros spores* have been strongly associated with coastal upwelling off the Portuguese margin, especially with the position of the upwelling front (e.g. Abrantes 1988). This factor has significant negative correlations with SST for annual, winter and summer (Table 6.4) and its loadings are focused in three regions: the north coast (41^{o}N) where it mimics the geographic pattern of the diatom abundances (figure 6.1b), the central coast (39^{o}N) where offshore abundances track upwelling filaments associated with Cabo da Roca (Fiúza et al., 1998) and the south coast (37.5^{o}N) where cool filaments are associated with Cabo de São Vicente (figure 6.1a). Because of the association of this species to coastal upwelling and its reasonable agreement with the chlorophyll maps (figure 6.2), this factor will be designated as "coastal upwelling factor".

-Factor 3 (figure 6.3c) is dominated by *Thalassionema spp., and explains* 10% of the total dataset. This factor has significant negative correlations with chlorophyll and significant positive correlations with SST (Table 6.4). Its geographic distribution is confined to the southern and open-ocean areas. The presence of this species points to warmer and less productive waters, either related to the presence of Mediterranean water (warmer and saltier) or to the subtropical gyre. This factor can be designated as "subtropical factor". Abrantes (1988) suggests that this species can be related with weaker upwelling conditions. However, the positive correlations with SST do not support this.

-Factor 4 (figure 6.3d) is dominated by *Leptocylindrus spores* and accounts for 6% of the total dataset. This factor has a significant positive correlation with winter chlorophyll and a significant negative correlation with winter SST (Table 6.4). High loadings of this factor coincides with the area of stronger wind-stress curl reported for winter by Bakun and Nelson (1991). The correlations and the geographic pattern of this factor suggest a link to upwelling derived from the wind-stress curl and therefore it will be designated as the "curl upwelling factor".

-Factor 5 (figure 6.3e) is dominated by *Diploneis spp.* and accounts for 6% of the total dataset. This factor does not have any significant correlations with SST or chlorophyll (Table 6.4). The genus *Diploneis* is considered benthic (Abrantes, 1988) and high loadings are found near the mouth of the Sado River. The depths for samples with higher relative percentages of this species are less than 200m (figure 6.4). This factor is named the "benthic factor".

-Factor 6 (figure 6.3f) is controlled by *Thalassiossira spp.*, and accounts for 4% of the total dataset. This factor also does not have any significant correlations with SST or chlorophyll (Table 6.4). High loadings are confined to the north coastal region where it maybe be related to the stronger river input present in that area. Abrantes (1988) also suggested this relationship. Therefore, with no strong indication of other type of environment this factor will be named the "river input factor".

6.4.2 Canonical Correspondence Analysis (CCA, ter Braak and Smilauer, 1998)

Following the same approach as in Chapter 2, two CCA analyses are used to separate SST from chlorophyll. The correlation values for the environmental variables are presented in Table 6.5. The CCA returned significant correlations for annual and winter chlorophyll (figure 6.5) and winter and summer SST (figure 6.6). Although the CCA for the chlorophyll has a significance level of 0.001, only 7% of the species variance can be related to the canonical axis and therefore with the respective chlorophyll data. This indicates weak gradients and therefore the correlations between the canonical axis and the chlorophyll dataset will not be very useful. This can be observed in the canonical plot (figures 6.5a and b) where the samples and species scores are scattered and do not indicate a preferential position relatively to the environmental arrows. The only significant correlation that was found is $r = 0.4$ between Axis 1 and annual and winter chlorophyll. The sample scores for CCA Axes 1 and 2 do not have any significant geographical pattern (figure 6.5c and d). The species percent fit is in Table 6.6.

The CCA for SST also has a significance level of 0.001. However, the amount of species variance related to SST (winter and summer) is 20% and this leads to a

significant correlation between Axis 1 and summer SST (r = 0.7). Some of the samples align with the summer SST environmental arrow (figure 6.6a). Some species, such as *Thalassionema spp*. and *Melosira spp*., also track this gradient (figure 6.6b). The geographic pattern for Axis 1 is very similar to the pattern of the summer SST observed values (figure 6.6c and d). The species percent fit is in Table 6.7.

6.4.3. Transfer functions from modern calibration

Six TFs were developed for the modern calibration. Two TFs resulted from the Imbrie and Kipp (1971), or I&K, method (section 4.1) for annual and summer SST (figures 6.7a and b and Table 6.8). Both TFs have an r^2 of 0.7 and the residuals overestimate higher observed values and underestimate lower ones. No TFs from I&K yield significant results for chlorophyll. The TFs developed from CCA (section 4.2) correspond to winter and summer SST and annual and winter chlorophyll. The r^2 for the SST TFs are 0.9 for winter and 0.7 for summer respectively (figures 6.7c and d and Table 6.8). The residuals indicate that the TF for summer SST also overestimates warmer observed values and underestimates cooler ones. The TFs for chlorophyll have r^2 of 0.8 and 0.7 for annual and winter seasons respectively (figures 6.7e and f, Table 6.8). For both chlorophyll seasons the residuals are scattered and do not have any particular trend.

6.5 Downcore reconstructions

The classical I&K approach (Imbrie and Kipp, 1971) was used for the downcore samples and the factors obtained for the core-tops (modern) samples were applied to the downcore samples with communalities all > 0.70), suggesting that modern samples provide good analogs for past variability. Only factors one to three have strong variability in the downcore samples (figure 6.8). The application of the TFs to the downcore samples is presented in figure 6.9, where factors 1, 2 and 3 were also plotted.

6.6 Discussion

Both the CCA and I&K approach are more effective in capturing the variance related with SST (20%) than chlorophyll (7%). The lack of strong gradients is also revealed by the weak or non-existent correlations between the canonical axis and the environmental properties. Nevertheless, six TFs were developed which have significant modern calibrations.

Although the reconstructions for core KS11 go back to 60,000 years (B.P.), the sampling resolution only allows having significant interpretations for Oxygen Isotope Stage 2 (OIS 2, defined from 12,000 to 28,000 years B.P. (Shackleton et al., 2000). During OIS 2 factors 1, 2, 3 and 4 have strong variability (figure 6.8). The most significant trend is the sharp increase in factor 2, the only that has been related to coastal upwelling conditions (figure 6.8b). Factor 1 decreased during IOS 2 relative to the top of the core, with peaks that mirror the peaks in factor 2 (figures 6.8a and b). The mirror effect between factors 1 and 2 might suggest that factor 1 can increase with the presence of nutrients that would not be enough to sustain the necessary ecology for Chaetoceros to develop (factor 2). As the nutrients become more available, Chaetoceros would dominate the flora and *Paralia sulcata* (factor 1) would be overcome by competition.

Factor 3 is related to warmer and less productive areas. This factor is relatively rare during OIS 2 except for a peak present at the early stage of OIS 2 (figure 6.8c). This is in good agreement with factors 1 and 2 as they indicate an increase in productivity during IOS 2 compared to modern conditions, and as the SST decreased (e.g. Pailler and Bard, 2002). The peak in factor 3 at approximately 24,000 years (B.P.) has a correspondent decrease in factor 2 (figures 6.8b and c). Factor 4, the factor associated with upwelling induced by the curl of wind-stress, has some variability (figure 6.8d). However, the general trend of this factor during OIS 2 is to be lower than modern conditions. Comparison of factors 2 and 4 suggest that coastal upwelling increased during the LGM while wind-stress curl upwelling decreased. In case of factor 4, the controlling species is more indicative of this trend than the factor itself (figure 6.8d).

Factors 5 and 6 are indirectly connected with the presence of rivers. The fact that core KS11 has benthic diatoms at its top (about 3.5% of the total diatom assemblage) is problematic because this core is at 3590 m deep in the open ocean. The presence of benthic diatoms suggests that there is bottom lateral transport of sediments (Lopes et al., 2006). Alternatively, a relatively freshwater river plume could transport these benthic species seaward. We cannot check this possibility, because we have no salinity data to relate to the core-tops. Factor 5 does not have much impact in the downcore samples, with values close to zero (figure 6.8e). The relative percentages of benthic diatoms vary between 0.5 and 1% (figure 6.8e). A peak with higher than modern values is present at around 20,000 years (B.P.). At the same time, there is also a peak in the species associated with factor 6 and that are also linked to river influence (figure 6.8f). It is possible that around 20,000 years (B.P.) the core location suffered a strong river influence, maybe due to the sea level decrease. This core is presently at 95 km from the coast and during the maximum sea level decrease it was 35 km closer to the coast (Abrantes et al., 1994). Alternatively, the brief input of freshwater indicators during may reflect a discrete down-slope transport event.

I&K style TFs reconstruct annual and summer SST and the CCA reconstructs annual and summer SST and annual and winter chlorophyll (figure 6.9). For CCA, the annual SST did not change much from modern conditions (figure 6.8c). This can be a consequence of the weak gradients that CCA was able to extract. The summer season has more variability, with a decrease of about 0.6^{o}C during OIS 2, which is much less than the decreases in SST reported from other studies (e.g. 6 to 8^{o}C less than modern conditions in Pailler and Bard, 2002). These reconstructions demonstrate how dependent the CCA is on finding sharp gradients in the modern calibration in order to express those variations in downcore reconstructions. However, this can also be a consequence of the species dataset homogenization due to the species grouping into genus. The I&K reconstructions, for annual and summer (figure 6.9), indicate stronger variability than the ones from CCA. For summer, I&K underestimates modern SST by about 4^{o}C. The lowest values for the summer SST reconstruction are < 0^{o}C, which is unrealistic. The reconstruction for annual SST also underestimated modern values by

about 2^{o}C. However, for the annual reconstruction, the gradient between the top of the core and OIS 2 is about 8^{o}C, which is very close to the ones reported by previous authors based on the organic geochemical $U^{k'}_{37}$ tracer (Pailler and Bard, 2002). The annual SST peaks at about 24,000 years ago are driven by the peak in factor 3, which is associated with warmer subtropical waters (figures 6.8c and 9e).

Winter chlorophyll reconstructions from CCA suggest no major changes in the past (figure 6.9d). However, a strong increase (almost double) is present in annual chlorophyll at 20,000 years (B.P.) and higher than modern values were present until 30,000 years (B.P.) (figure 6.9d). If both seasonal reconstructions are correct, summer chlorophyll must have increased dramatically in the past. Although factor 2 (coastal upwelling factor) increases sharply during OIS 2 (figure 6.8b), there is only an increase in chlorophyll at an early stage of OIS 2 (figure 6.9d). The peak in chlorophyll coincides with the peaks in river influence mentioned before (figures 6.8e and f) and it also coincides with a peak in export productivity inferred by Abrantes et al. (1994). The increase in upwelling during OIS 2 is thought to be related to an increase in the trade winds (e.g. Abrantes 1991; Sancetta, 1992). However, not all the upwelling increase is associated to increases in export productivity and/or chlorophyll. We speculate that the diatom productivity response relates to micronutrients such as iron (e.g. Hutchins and Bruland, 1998), which is in turn related to the presence of river influence.

The preservation of diatoms in the sediments is the result of a balance between productivity at the surface and dissolution in the water column and/or in the sediments (Abrantes, 1991). The increase of upwelling related species in the sediments during OIS 2 could be related to better preservation conditions in the past and not increased productivity. However, Abrantes (1991) concluded that this is not the case and that the preservation conditions in the sediments during OIS 2 are not significantly different from today.

The results obtained here are limited by the available information from the core-top diatom and the environmental datasets. The grouping of species into genus can be problematic because not all the species from the same group have the same

environmental preferences. Refinement of the taxonomic concepts may improve this situation.

The modern environmental dataset also limits this study. Almost 85% of the samples did not have corresponding environmental data because of the proximity to the coast and/or because the samples would fall inside the same WOA 98 grid value. Almost all core-tops had a corresponding modern productivity value (Antoine and Morel, 1996). However, groups of core-tops would have the identical value because they where in the same grid box. The predicted values from adjacent core-top samples were not only different but also typically fell outside the error range (results not presented here).

The only possible environmental information that could be used at this point is the in-situ measurements for SST and chlorophyll (indirect productivity indicator) obtained during a two-year cruise. Although not representative of long-term environmental conditions, the use of this environmental dataset resulted in TFs that could still be developed and used for past reconstructions. No information is available for modern nutrients and salinity. Nevertheless, it may be possible in the future to get information regarding nutrients and salinity from a previous study (Moita, 2001).

6.7 Recommendations and Conclusions

The diatom species dataset used here is dominated by genera rather than individual species. This yields problems because the homogenization of the diatom species might cause a reduction and/or undetected spatial environmental gradients, and not all the species from a certain genus might have the same environmental preferences. The recommendation in this case is to ungroup the diatom species in a taxonomically refined dataset.

The core-top sample distribution also needs revision. In order to use the WOA 98 and productivity datasets used in chapter 2, more samples with a wider grid distribution need to be recovered. More samples from open ocean environment are needed in order to cover a broader range of environmental conditions.

Q-mode analysis returned six factors. Although some factors might be related with other oceanic properties besides SST and chlorophyll, factors 1, 2, 3 and 4 have significant correlations with these two oceanic properties. Factor 1 is related with shelf conditions and some coastal upwelling. Factor 2 is considered the traditional coastal upwelling indicator while factor 3 is related with warmer and less productive waters from south. Factor 4 indicates another type of upwelling that has not been considered in previous studies in this area: wind-stress curl induced upwelling. Factors 5 and 6 have no significant correlation with SST and chlorophyll. However, factor 5 is dominated by a benthic genus and factor 6 by a genus that likes river input because of nutrients. Although not directly given by freshwater diatoms, factors 5 and 6 might serve as an indirect indicator of river influence.

The TFs developed with the information that is available at this point indicate promising results for the modern calibration. However, the weak gradients that exist in the modern calibration need to be overcome. The I&K method is only able to produce TFs for SST and although the CCA method captures gradients related with chlorophyll and SST, these gradients are very small. Even more, the variance in the species dataset that can be explained by the chlorophyll gradient is only 7%. The correlation between the canonical axis and the environmental variables are also not very significant. For SST, both the I&K and the CCA methods have comparable results.

The downcore factors derived from the modern core-tops indicate that only the first 4 factors have strong variability in the past. The sampling resolution limits the interpretations to a discussion between the top of the core (1,000 years B.P.) and OIS 2. Factor 2 increases during IOS 2 suggesting an increase in the coastal upwelling conditions. In addition, the wind-stress curl upwelling factor decreases during IOS 2 suggesting weaker conditions in the past. Factor 3, the “subtropical factor” decreases except at the early stage of IOS 2 where factor 2 decreases. This suggests that warmer and less productive conditions were present. Although factors 5 and 6 do not vary at all in the past, the corresponding dominant species of these factors have a peak at approximately 20,000 years (B.P.) suggestive of a strong river influence, maybe due to

the sea level drop and/or higher river runoff due to increase precipitation on land, or due to downslope transport.

The SST reconstructions, either from I&K or CCA, do not agree with values from other studies. SST from CCA reconstruction barely changed from modern conditions. I&K results have more variations and gradients between the modern and OIS 2 that are close in magnitude with the ones previously reported for the area. However, I&K underestimates the modern SST values by close to 2^{o}C.

For the past 20,000 years, CCA estimates of chlorophyll were similar to modern values, despite the sharp increase in the coastal upwelling. Chlorophyll values only doubled at around 20,000 years (B.P.). This peak is in good agreement with a productivity export reconstruction based on organic carbon concentration and matches the peaks in the river influence. This suggests that although coastal upwelling increased, the ecosystem might have turned into a high nutrient low chlorophyll (HNLC) system. The peak in chlorophyll can be due to an increase in the supply of iron (micronutrient) from river runoff that allowed the system to use the nutrients more effectively than before.

Table 6.1 - Core-top locations and correspondent diatom abundances (Laboratory code from Department of Marine Geology, INETI, Lisbon).

Laboratory code	Core	Longitude (W)	Latitude (N)	Diatom abundances (10^6 valves/g sediment)
116	VB024	-8.87	41.58	4.49
120	VB028	-9.02	41.58	2.92
123	VB031	-9.16	41.59	1.10
124	VB032	-9.19	41.58	0.13
165	VB073	-9.20	40.81	0.89
167	VB075	-9.08	40.81	0.70
168	VB076	-9.02	40.81	1.63
170	VB078	-8.93	40.81	12.00
172	VB080	-8.82	40.81	5.00
174	VB082	-8.73	40.81	0.30
215	VB123	-9.07	39.72	0.41
218	VB126	-9.18	39.72	0.90
219	VB127	-9.23	39.72	0.76
221	VB129	-9.33	39.72	0.09
224	VB132	-9.43	39.72	0.18
226	VB134	-9.50	39.72	0.19
242	VB150	-9.45	39.09	1.05
244	VB152	-9.53	39.08	1.20
246	VB154	-9.58	39.08	0.30
248	VB156	-9.67	39.08	0.45
249	VB157	-9.70	39.08	0.60
252	VB160	-9.77	39.08	0.59
254	VB162	-9.83	39.08	0.10
256	VB164	-9.94	39.09	0.29
273	LV001	-7.50	37.14	11.10
276	LV004	-7.50	37.07	0.09
277	LV005	-7.50	37.04	0.17
278	LV006	-7.50	37.00	0.18
280	LV008	-7.50	36.95	0.07
282	LV010	-7.50	36.91	0.16
287	LV015	-7.80	36.91	0.28
317	LV045	-8.17	36.84	0.07
326	LV054	-8.87	36.89	0.18

(continued on next page)

Table 6.1 (continued)

Laboratory code	Core	Longitude (W)	Latitude (N)	Diatom abundances (10^6 valves/g sediment)
338	LV066	-8.67	37.06	0.18
339	LV067	-8.67	37.05	0.91
341	LV069	-8.67	37.03	2.50
343	LV071	-8.67	37.00	0.13
345	LV073	-8.67	36.97	0.07
347	LV075	-8.67	36.93	0.18
349	LV077	-8.67	36.90	0.14
351	LV079	-8.67	36.88	0.33
369	LV097	-9.05	36.92	0.70
386	LV114	-8.87	37.58	0.21
387	LV115	-8.88	37.58	0.25
388	LV116	-8.90	37.58	1.03
389	LV117	-8.92	37.59	0.79
393	LV121	-8.98	37.59	0.10
395	LV123	-9.02	37.58	0.31
397	LV125	-9.05	37.58	0.31
415	LV143	-8.94	37.92	0.26
426	LV154	-8.90	38.08	0.25
445	LV167B	-9.20	37.81	0.85
451	LV172	-8.97	38.22	0.11
453	LV174	-8.91	38.23	0.20
455	LV176	-8.87	38.24	0.21
457	LV178	-8.83	38.25	1.00
458	LV179	-8.81	38.25	21.50
698	FM-3	-9.53	40.19	0.05
700	FM-5	-9.40	40.19	0.08
702	FM-7	-9.19	40.21	0.57
703	FM-8	-9.11	40.20	2.69
704	FM-9	-9.07	40.20	1.95
706	FM-11	-8.99	40.19	0.50
708	FM-13	-8.93	40.19	1.50
709	FM-14	-8.89	40.14	0.74
1327	KS012	-10.34	40.57	0.47

(continued on next page)

Table 6.1 (continued)

Laboratory code	Core	Longitude (W)	Latitude (N)	Diatom abundances (10^6 valves/g sediment)
1343	KC003	-9.34	36.83	0.07
1363	KC027	-7.82	36.85	0.20
1937	TG070	-6.57	36.75	0.55
1938	TG071	-6.54	36.74	0.29
1939	TG072	-6.70	36.74	1.54
1940	TG079	-7.21	37.10	0.13
1941	TG080	-7.30	37.09	0.00
2351	SO11KG	-9.33	37.53	0.17
2353	SO09KG	-9.85	37.84	0.27
2354	SO13KG	-9.27	37.56	0.51
2356	SO15KG	-9.42	37.58	0.17
2357	SO16KS	-9.42	37.58	0.00
2360	SO25KG	-9.55	37.86	0.02
2362	SO30KG	-9.60	37.46	0.13
2393	TM06	-9.10	38.32	0.12
2394	TM07	-9.13	38.07	0.00
2861	SO-83-07GK	-9.71	37.84	0.43
2863	SO-83-09GK	-9.37	37.81	0.10
2864	SO-83-10GK	-9.25	37.82	0.00
2865	SO-83-11GK	-9.08	37.82	0.70
2968	PO01(2)	-9.11	37.33	0.00
2969	PO03(1)	-9.31	37.33	0.00
2970	PO04(1)	-9.52	37.32	0.06
2972	PO05(1)	-9.27	37.90	0.00
2974	PO06(1)	-9.50	37.82	0.00
2977	PO07(1)	-9.64	37.70	0.00
2979	PO08(2)	-9.93	37.64	2.26
2981	PO09(1)	-10.05	37.61	0.23
2984	PO12(1)	-9.67	39.64	0.00
2985	PO13(1)	-9.76	39.63	0.04
2987	PO14(1)	-9.84	39.62	0.19
2989	PO15(2)	-9.93	39.63	0.03
2992	PO17(1)	-9.97	40.04	0.00

(continued on next page)

Table 6.1 (continued)

Laboratory code	Core	Longitude (W)	Latitude (N)	Diatom abundances (10^6 valves/g sediment)
2995	PO20(1)	-9.71	40.09	0.00
2997	PO21(1)	-9.68	40.55	0.00
2999	PO22(1)	-9.65	40.56	0.06
3001	PO23(1)	-9.56	40.59	0.00
3003	PO24(1)	-9.48	40.57	0.00
3006	PO25(2)	-9.42	40.55	0.00
3008	PO27(2)	-9.73	41.43	0.10
3010	PO28(1)	-9.72	41.49	0.06
3012	PO29(1)	-9.57	41.54	0.00
3014	PO30(1)	-9.52	41.55	0.00
3016	PO31(1)	-9.52	41.60	0.00
3019	PO32(2)	-9.48	41.63	0.10
3021	PO33(2)	-9.43	41.67	0.00
3040	MD95-2039	-10.35	40.63	0.00
3082	MD95-2042	-10.17	37.80	0.01
3083	M39002-3	-7.78	36.03	0.71
3085	M39003-2	-7.22	36.11	0.08
3087	M39004-2	-7.73	36.24	2.05
3089	M39016-2	-7.71	36.78	0.83
3090	M39017-4	-7.41	36.65	0.22
3092	M39021-5	-8.25	36.61	0.00
3093	M39022-1	-8.26	36.71	0.15
3094	M39022-3	-8.26	36.71	0.24
3095	M39023-3	-8.26	36.74	0.22
3096	M39029-6	-8.23	36.05	0.36
3098	M39035-3	-9.50	37.82	0.12
3100	M39058-1	-10.68	39.04	0.53
3101	M39059-2	-10.54	39.07	0.17
3102	M39070-1	-9.39	43.62	0.00
3103	M39072-1	-9.44	43.79	1.06
3104	MD95-2040	-9.86	40.58	0.13
3105	MD95-2041	-9.51	37.83	0.00
1316	KS1	-12.41	41.74	0.04

(continued on next page)

Table 6.1 (continued)

Laboratory code	Core	Longitude (W)	Latitude (N)	Diatom abundances (10^6 valves/g sediment)
1318	KS3	-9.67	42.24	0.16
1322	KS7	-9.33	41.15	0.00
1323	KS8	-9.42	41.05	0.00
1324	KS9	-9.57	40.95	0.04
1325	KS10	-10.03	40.72	0.27
1327	KS12	-10.34	40.57	0.47
1330	KS14	-9.83	39.93	0.00
1331	KS16	-9.78	39.91	0.06
1335	KS20	-10.50	37.37	0.07
1337	KS22	-9.71	37.23	0.00
1338	KS23	-9.52	37.24	0.00
1339	KS24	-9.40	37.26	0.00
1340	KS25	-9.33	37.28	0.06
1377	KS26	-9.29	37.30	0.00
1354	KC14	-7.51	36.89	0.00
1355	KC15	-7.50	36.87	0.00
1358	KC18	-7.66	36.62	0.00
1360	KC24	-7.83	36.67	0.00
1361	KC25	-7.81	36.74	0.02
1362	KC26	-7.81	36.79	0.00
1363	KC27	-7.82	36.85	0.20
1365	KC29	-7.82	36.90	0.19
1366	KC30	-8.01	36.77	0.02
1367	KC31	-7.95	36.75	0.00
1368	KC32	-7.93	36.69	0.03
1369	KC33	-7.88	36.63	0.11
1370	KC35	-8.24	36.74	0.00
1371	KC36	-8.25	36.73	0.00
1373	KC38	-8.23	36.58	0.00

Table 6.2 - Core-top samples that have species identifications available (gray boxes mark samples without environmental information). Laboratory code from Department of Marine Geology, INETI, Lisbon.

ID # for this study	Laboratory code	Core	Longitude (W)	Latitude (N)	Water Depth (m)
1	116	VB024	-8.8717	41.5833	40
2	120	VB028	-9.0150	41.5817	85
3	123	VB031	-9.1633	41.5883	100
4	124	VB032	-9.1917	41.5750	105
5	165	VB073	-9.2033	40.8083	140
6	167	VB075	-9.0817	40.8100	95
7	168	VB076	-9.0233	40.8083	85
8	170	VB078	-8.9250	40.8083	50
9	172	VB080	-8.8150	40.8083	35
10	174	VB082	-8.7317	40.8083	10
11	215	VB123	-9.0700	39.7183	20
12	218	VB126	-9.1783	39.7167	70
13	219	VB127	-9.2267	39.7183	100
14	221	VB129	-9.3333	39.7167	130
15	224	VB132	-9.4250	39.7167	130
16	226	VB134	-9.5000	39.7150	145
17	242	VB150	-9.4450	39.0867	30
18	244	VB152	-9.5283	39.0833	52
19	246	VB154	-9.5817	39.0833	62
20	248	VB156	-9.6650	39.0833	94
21	249	VB157	-9.7000	39.0833	94
22	252	VB160	-9.7667	39.0833	116
23	254	VB162	-9.8333	39.0833	144
24	256	VB164	-9.9417	39.0850	154
25	276	LV004	-7.5017	37.0650	47
26	277	LV005	-7.5017	37.0383	74
27	278	LV006	-7.5017	37.0033	95
28	280	LV008	-7.4983	36.9500	180
29	282	LV010	-7.5000	36.9100	405
30	287	LV015	-7.8000	36.9083	235
31	317	LV045	-8.1700	36.8383	95
32	326	LV054	-8.8667	36.8900	110
33	338	LV066	-8.6667	37.0583	33
34	339	LV067	-8.6667	37.0483	36
35	341	LV069	-8.6667	37.0267	38
36	343	LV071	-8.6667	37.0000	63
37	345	LV073	-8.6667	36.9683	80
38	347	LV075	-8.6667	36.9333	98
39	349	LV077	-8.6667	36.8967	105
40	351	LV079	-8.6667	36.8750	110
41	369	LV097	-9.0450	36.9167	93

(continued on next page)

Table 6.2 (continued)

ID # for this study	Laboratory code	Core	Longitude (W)	Latitude (N)	Water Depth (m)
42	386	LV114	-8.8667	37.5817	95
43	387	LV115	-8.8817	37.5800	110
44	388	LV116	-8.9000	37.5817	118
45	389	LV117	-8.9167	37.5850	129
46	393	LV121	-8.9833	37.5850	160
47	395	LV123	-9.0183	37.5817	190
48	397	LV125	-9.0533	37.5833	245
49	415	LV143	-8.9417	37.9167	105
50	426	LV154	-8.8983	38.0833	112
51	445	LV167B	-9.1967	37.8133	450
52	451	LV172	-8.9683	38.2183	140
53	453	LV174	-8.9083	38.2317	120
54	455	LV176	-8.8683	38.2400	105
55	457	LV178	-8.8333	38.2467	60
56	458	LV179	-8.8083	38.2500	35
57	698	FM-3	-9.5267	40.1917	158
58	700	FM-5	-9.4033	40.1917	135
59	702	FM-7	-9.1883	40.2050	100
60	703	FM-8	-9.1083	40.2033	85
61	704	FM-9	-9.0650	40.1950	65
62	706	FM-11	-8.9883	40.1883	45
63	708	FM-13	-8.9333	40.1850	18
64	709	FM-14	-8.8900	40.1433	10
65	1327	KS012	-10.3417	40.5733	3380
66	1333	KS018	-10.8167	39.8167	4950
67	1343	KC003	-9.3350	36.8333	787
68	1363	KC027	-7.8167	36.8500	618

Table 6.3 - Factor scores from Q-mode analysis (gray boxes indicate highest score for each factor).

Species and/or group	Species #	Factor 1	Factor 2	Factor 3	Factor 4	Factor 5	Factor 6
Actinocyclus spp.	1	0.005	0.006	0.013	0.014	0.001	-0.003
Actinoptychus spp.	2	0.049	0.002	0.017	0.082	-0.032	-0.006
Azpeitia spp.	3	0.015	-0.002	0.018	-0.004	0.015	-0.002
Biddulphia spp.	4	0.005	0.006	0.002	0.005	0.007	0.014
Cerataulus spp.	5	0.001	-0.003	0.019	0.003	0.041	0.002
Chaetoceros spores	6	-0.111	0.992	0.010	-0.021	-0.017	-0.013
Coscinodiscus spp.	7	0.049	0.003	0.059	0.018	-0.015	0.063
Hyalodiscus spp.	8	0.079	0.012	-0.009	-0.085	-0.007	0.320
Leptocylindrus spores	9	-0.009	0.015	-0.010	0.941	0.020	-0.253
Melosira spp.	10	-0.002	0.004	0.161	-0.043	0.055	0.103
Paralia sulcata	11	0.984	0.109	0.023	0.016	-0.058	-0.023
Psammodiscus nitidus	12	-0.003	-0.007	0.021	0.000	0.137	-0.004
Thalassiosira spp.	13	-0.011	0.019	0.150	0.301	0.094	0.880
Triceratium spp.	14	0.009	0.009	0.002	-0.011	0.027	-0.003
Cocconeis spp.	15	-0.023	0.034	-0.016	0.016	0.344	-0.060
Delphineis spp.	16	0.024	0.025	-0.001	-0.005	0.029	-0.063
Diploneis spp.	17	0.061	0.008	0.022	-0.042	0.880	-0.080
Fragilaria spp.	18	-0.003	0.004	0.000	0.017	0.022	0.008
Grammatophora spp.	19	0.015	0.022	-0.003	-0.022	0.038	0.020
Navicula spp.	20	0.012	0.004	-0.007	-0.005	0.141	-0.040
Navicula directa	21	0.037	-0.004	0.003	-0.043	0.172	0.034
Nitzschia spp.	22	0.020	0.005	0.013	-0.015	0.094	0.044
Nitzschia marina	23	0.007	0.005	0.011	0.003	0.002	0.000
Opephora spp.	24	-0.003	0.001	-0.004	0.006	0.042	-0.009
Plagiogramma spp.	25	0.007	0.008	-0.003	0.000	0.037	-0.014
Thalassionema spp.	26	-0.026	-0.016	0.972	-0.032	-0.040	-0.156
Trachyneis aspera	27	0.021	0.000	0.007	-0.020	0.049	0.027

Table 6.4 - Correlation values for the environmental variables and the factors (gray boxes indicate significant correlations for p=0.05).

	Annual Chlorophyll (mg/m3)	Winter chlorophyll (mg/m3)	Summer chlorophyll (mg/m3)	Seasonal range chlorophyll (mg/m3)	Annual SST (°C)	Winter SST (°C)	Summer SST (°C)	Seasonal range SST (°C)
Factor 1	0.24	0.23	0.20	0.17	-0.38	-0.20	-0.37	-0.32
Factor 2	0.21	0.13	0.19	0.17	-0.37	-0.37	-0.30	-0.19
Factor 3	-0.36	-0.34	-0.31	-0.26	0.77	0.50	0.73	0.60
Factor 4	0.20	0.39	0.14	0.08	-0.25	-0.43	-0.15	0.00
Factor 5	0.04	-0.14	0.06	0.08	-0.10	0.14	-0.17	-0.23
Factor 6	-0.09	0.03	-0.09	-0.10	0.05	-0.12	0.10	0.16

Table 6.5 - Correlation values for the environmental variables (gray boxes indicate significant correlations for p=0.05).

	Annual Chlorophyll (mg/m3)	Winter chlorophyll (mg/m3)	Summer chlorophyll (mg/m3)	Seasonal range chlorophyll (mg/m3)	Annual SST (°C)	Winter SST (°C)	Summer SST (°C)	Seasonal range SST (°C)
Annual Chlorophyll (mg/m3)	1	0.19	0.99	0.95	-0.68	-0.35	-0.68	-0.59
Winter chlorophyll (mg/m3)		1	0.04	-0.12	-0.31	-0.46	-0.20	-0.05
Summer chlorophyll (mg/m3)			1	0.99	-0.64	-0.28	-0.66	-0.60
Seasonal range chlorophyll (mg/m3)				1	-0.59	-0.21	-0.62	-0.59
Annual SST (°C)					1	0.60	0.96	0.81
Winter SST (°C)						1	0.35	0.01
Summer SST (°C)							1	0.94
Seasonal range SST (°C)								1

Table 6.6 - Cumulative species fit as % of environmental variance explained by each species for CCA chlorophyll.

Species #	Species and/or groups	CCA axis 1	CCA axis 2	species variability	% variance explained
10	*Melosira spp.*	0.23	0.25	2.8	24.5
26	*Thalassionema spp.*	0.18	0.18	7.6	17.7
2	*Actinoptychus spp.*	0.17	0.17	2.6	17.5
9	*Leptocylindrus spores*	0.11	0.14	1.5	13.8
21	*Navicula directa*	0.02	0.11	3.3	10.8
1	*Actinocyclus spp.*	0.00	0.09	2.4	8.6
11	*Paralia sulcata*	0.08	0.08	0.3	7.8
27	*Trachyneis aspera*	0.01	0.07	2.8	6.7
18	*Fragilaria spp.*	0.01	0.07	12.7	6.7
3	*Azpeitia spp.*	0.00	0.07	1.8	6.6
16	*Delphineis spp.*	0.03	0.06	3.1	5.7
25	*Plagiogramma spp.*	0.05	0.05	2.7	5.0
13	*Thalassiosira spp.*	0.00	0.04	0.6	3.6
17	*Diploneis spp.*	0.00	0.03	1.2	3.1
12	*Psammodiscus nitidus*	0.02	0.03	5.1	2.8
8	*Hyalodiscus spp.*	0.02	0.02	1.1	1.9
19	*Grammatophora spp.*	0.00	0.01	2.5	1.4
14	*Triceratium spp.*	0.00	0.01	2.6	1.3
4	*Biddulphia spp.*	0.00	0.01	5.2	1.3
22	*Nitzschia spp.*	0.01	0.01	1.3	1.0
6	*Chaetoceros spores*	0.01	0.01	2.5	0.7
24	*Opephora spp.*	0.00	0.01	21.3	0.7
23	*Nitzschia marina*	0.00	0.01	5.2	0.6
7	*Coscinodiscus spp.*	0.00	0.00	1.1	0.5
5	*Cerataulus spp.*	0.00	0.00	7.6	0.3
15	*Cocconeis spp.*	0.00	0.00	8.1	0.2
20	*Navicula spp.*	0.00	0.00	3.2	0.2

Table 6.7 - Cumulative species fit as % of environmental variance explained by each species for CCA SST.

Species #	Species and/or groups	CCA axis 1	CCA axis 2	species variability	% variance explained
10	*Melosira spp.*	0.60	0.60	2.8	60.0
26	*Thalassionema spp.*	0.54	0.54	7.6	54.2
9	*Leptocylindrus spores*	0.07	0.16	1.5	15.8
25	*Plagiogramma spp.*	0.11	0.15	2.7	14.9
13	*Thalassiosira spp.*	0.05	0.14	0.6	14.3
5	*Cerataulus spp.*	0.05	0.13	7.6	13.4
17	*Diploneis spp.*	0.02	0.12	1.2	12.4
16	*Delphineis spp.*	0.11	0.11	3.1	10.8
15	*Cocconeis spp.*	0.05	0.10	8.1	10.2
11	*Paralia sulcata*	0.09	0.09	0.3	9.3
6	*Chaetoceros spores*	0.06	0.08	2.5	7.9
24	*Opephora spp.*	0.04	0.07	21.3	7.4
7	*Coscinodiscus spp.*	0.03	0.06	1.1	6.1
2	*Actinoptychus spp.*	0.04	0.06	2.6	5.7
20	*Navicula spp.*	0.05	0.05	3.2	5.5
19	*Grammatophora spp.*	0.00	0.05	2.5	5.0
3	*Azpeitia spp.*	0.03	0.05	1.8	4.8
12	*Psammodiscus nitidus*	0.00	0.04	5.1	3.9
27	*Trachyneis aspera*	0.00	0.04	2.8	3.6
22	*Nitzschia spp.*	0.00	0.02	1.3	2.0
4	*Biddulphia spp.*	0.02	0.02	5.2	1.8
1	*Actinocyclus spp.*	0.00	0.01	2.4	1.2
18	*Fragilaria spp.*	0.01	0.01	12.7	1.1
14	*Triceratium spp.*	0.01	0.01	2.6	1.0
21	*Navicula directa*	0.00	0.00	3.3	0.5
23	*Nitzschia marina*	0.00	0.00	5.2	0.0
8	*Hyalodiscus spp.*	0.00	0.00	1.1	0.0

Table 6.8 - Compilation of the TFs developed for this study (F is from factors and A is from CCA axis).

Method		r2	RMSE	Equation (TF)
I&K	Annual SST	0.7	0.4 (^{o}C)	estimated=15.2+12.8(F3)-6.1F1*F6)-10.3(F2^2)-2.4(F1*F5)-6.5(F6^2)
I&K	Summer SST	0.7	0.8 (^{o}C)	estimated=16.4+24.3(F3)-13.3(F1*F6)-20(F2^2)-13.5(F6^2)
CCA	Winter SST	0.9	0.1 (^{o}C)	estimated=14+0.4(A1)-0.26(A2)-0.8(A4)+0.4(A3)-0.06(A1*A4)-0.1(A2*A3)+0.03(A2^2)+0.05(A3^2)
CCA	Summer SST	0.7	0.8 (^{o}C)	estimated=17.2+1.2(A1)-0.8(A4)-0.7(A3*A4)
CCA	Annual chlorophyll	0.8	0.1(mg/m^{3})	estimated=0.56+0.2(A1)+0.4(A3)+0.09(A2)+0.1(A2*A3)+0.08(A1*A2)+0.2(A1*A3)+0.3(A3^2)-0.06(A3*A4)+0.03(A1^2)
CCA	Winter chlorophyll	0.7	0.06 (mg/m^{3})	estimated=0.4+0.03(A1)+0.1(A3)-0.03(A2)-0.05(A2*A3)-0.08(A3^2)+0.01(A4^2)

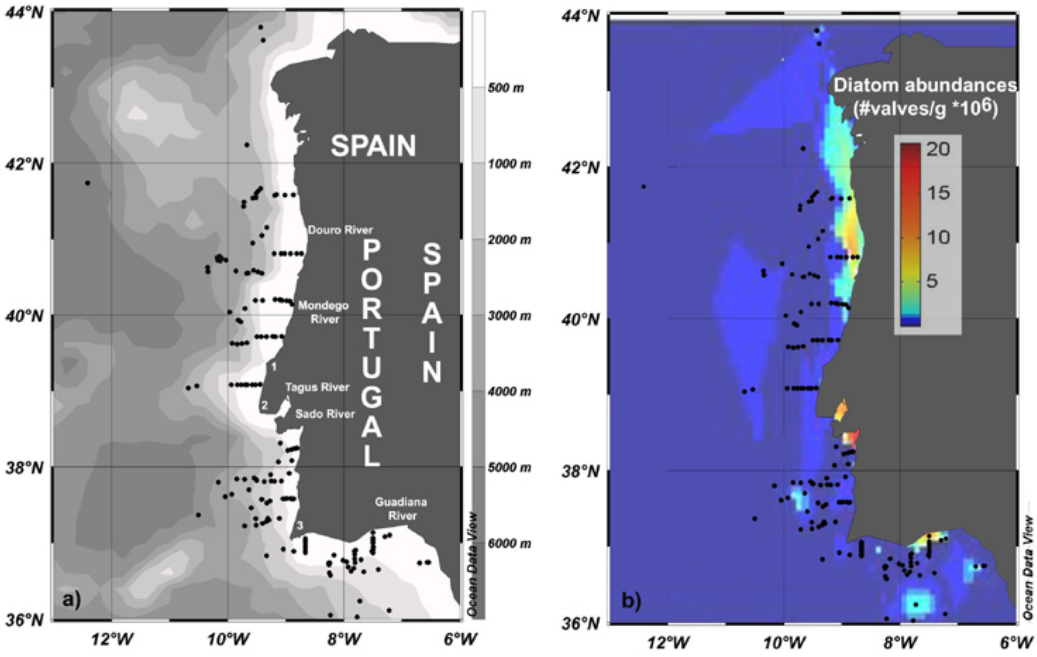

Figure 6.1 – Maps of the study area, a) sample locations (black dots) from core-tops and core KS11 (black polygon), major rivers and 1- Cape Carvoeiro, 2- Cape da Roca and 3 – Cape de São Vicente.(shading reflects bathymetry); b) spatial distribution of total diatom abundances (3valves/g of sediment).

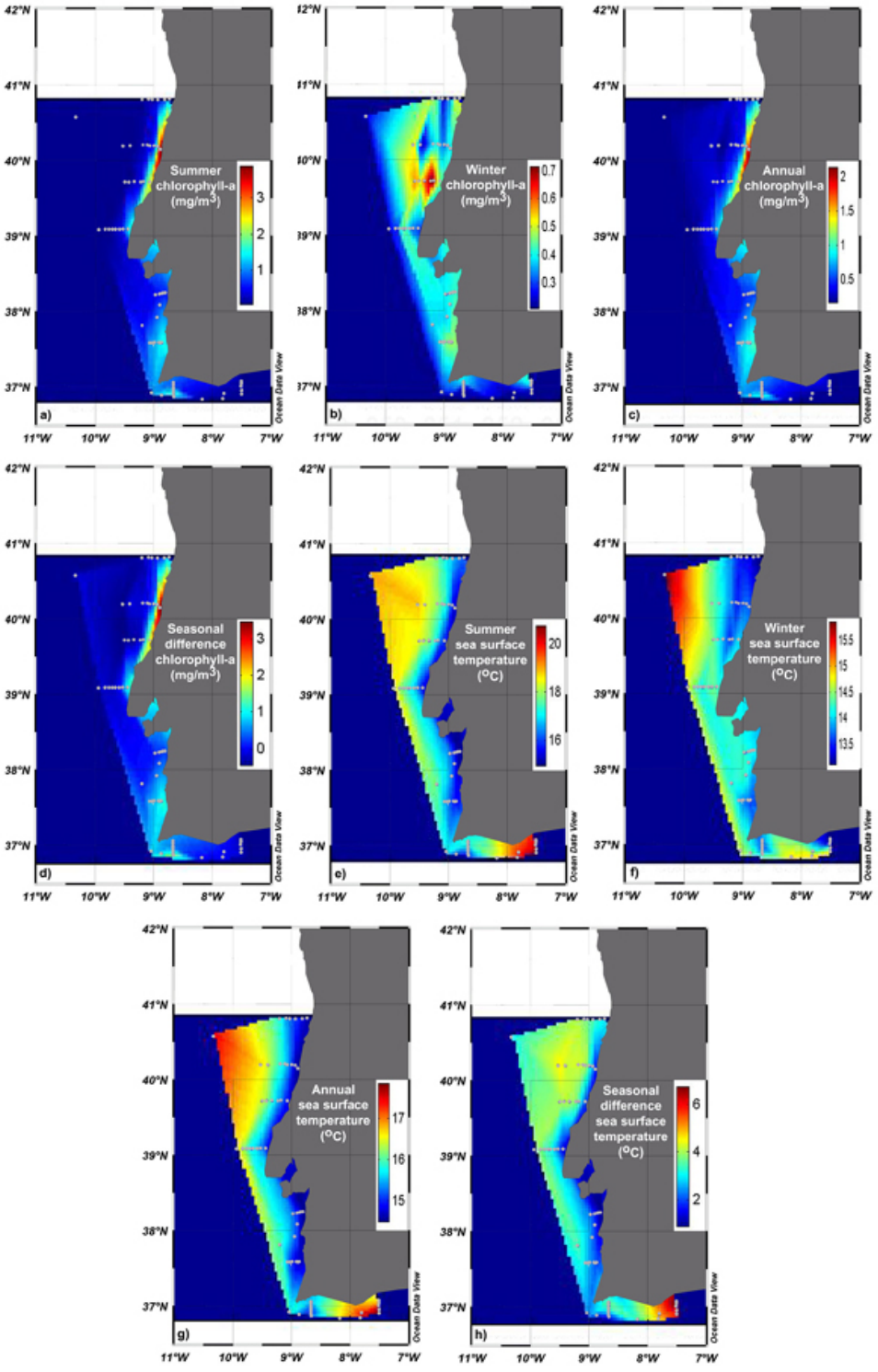

Figure 6.2 – Spatial distribution of in-situ measurements for chlorophyll (a, b, c and d) and sea-surface temperature (e, f, g and h). Grey dots are sample locations.

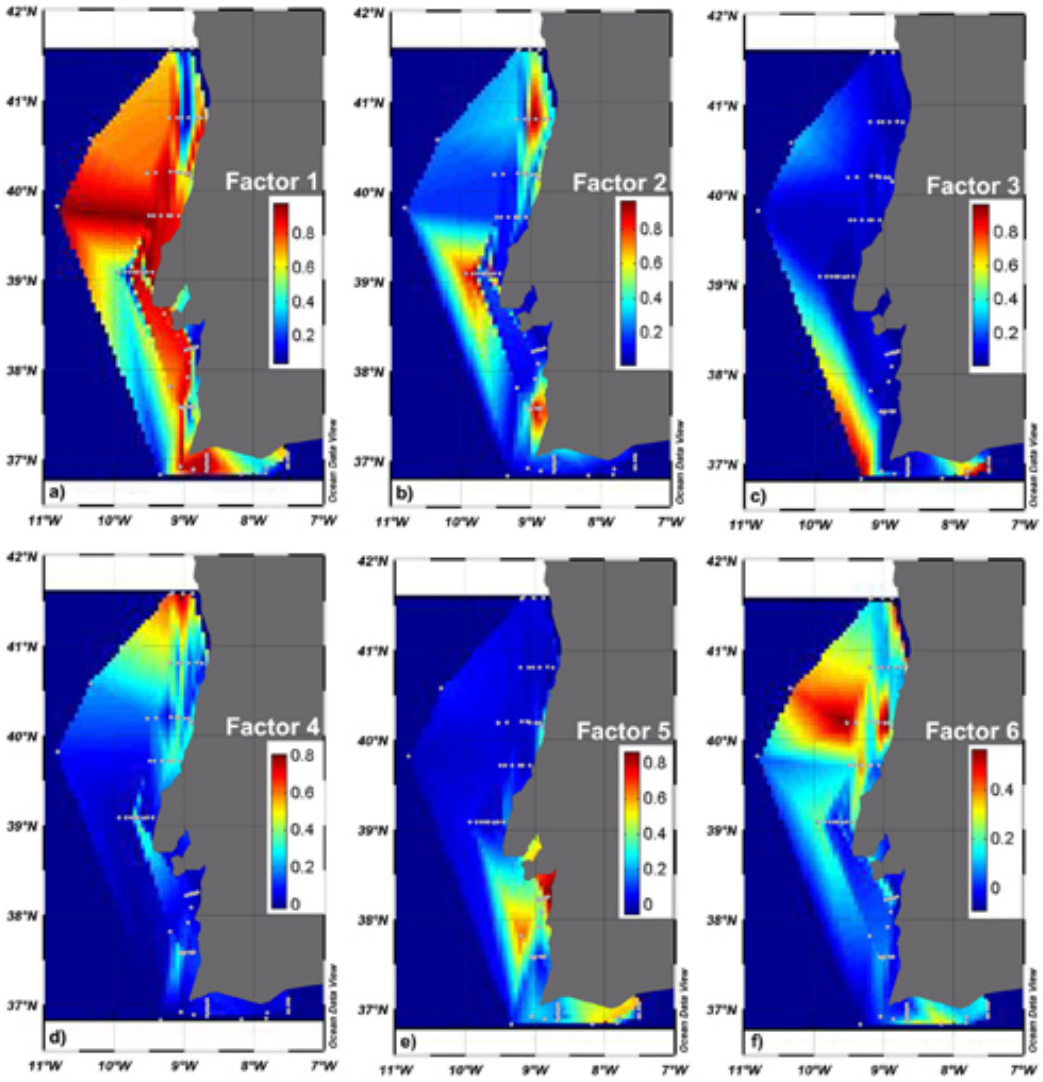

Figure 6.3 – Spatial distribution of factor loadings for the six factors. Grey dots are sample locations.

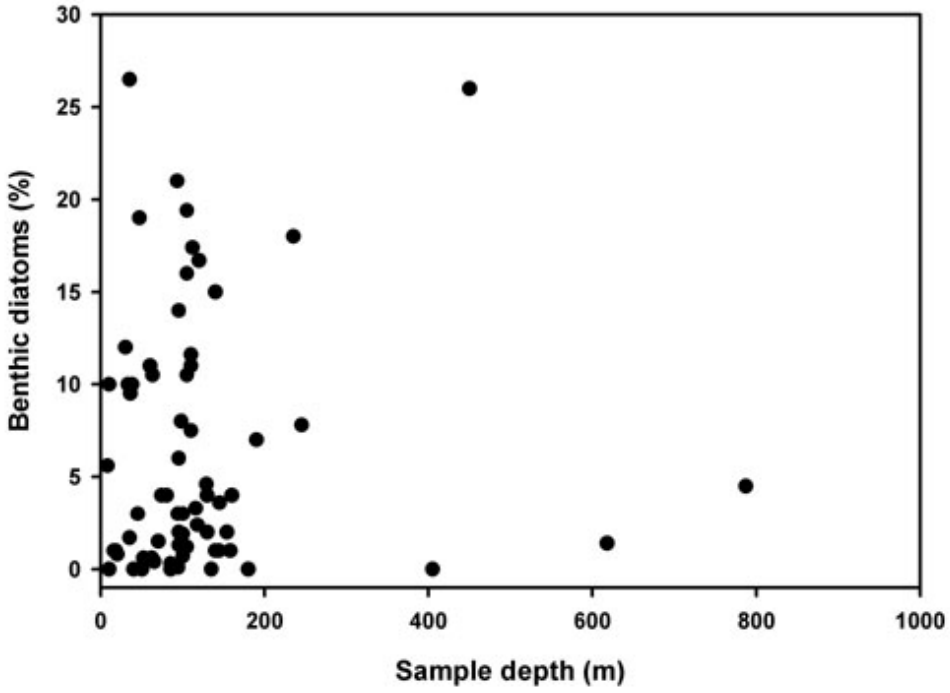

Figure 6.4 – Benthic diatom relative abundances (percentage) plotted versus sample depth (m).

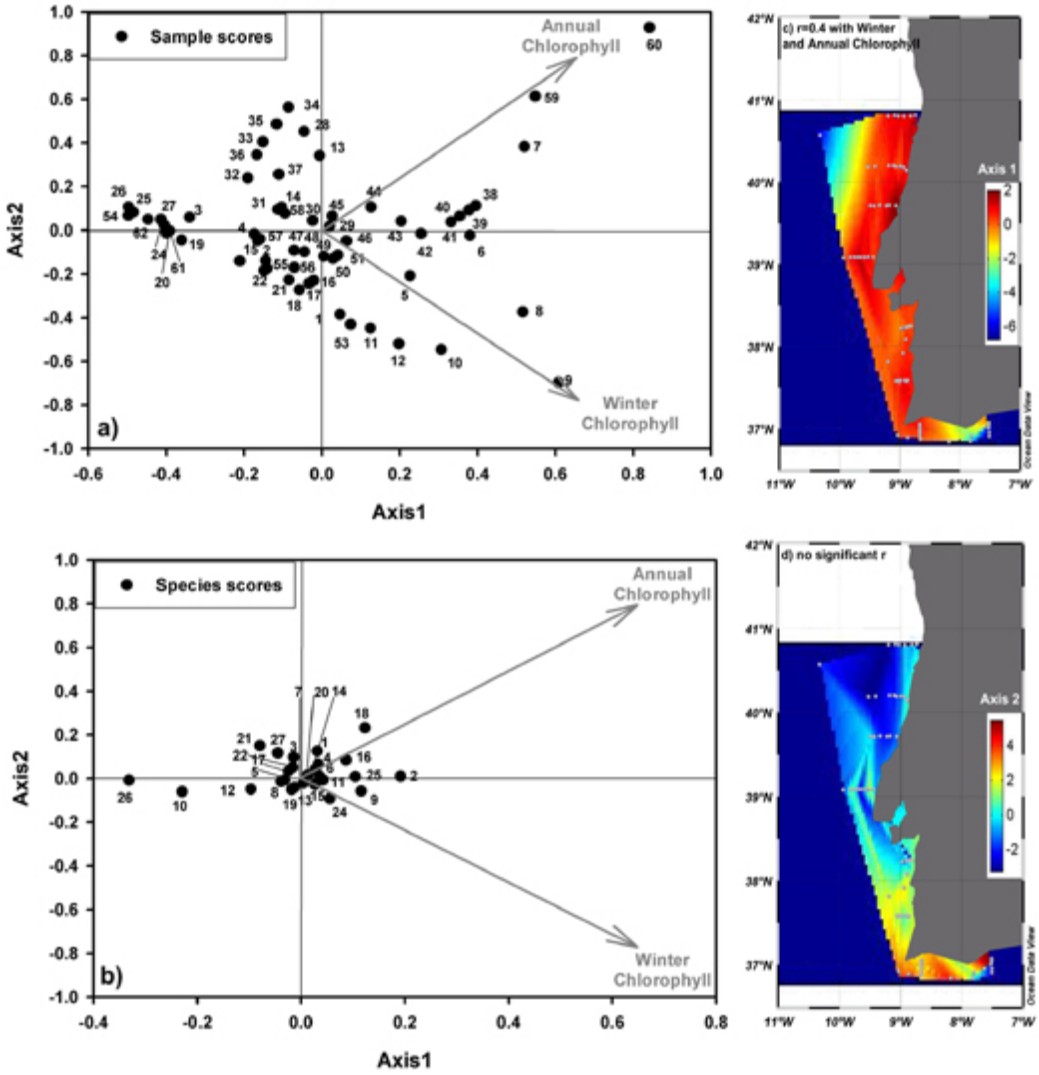

Figure 6.5 - Results for the chlorophyll CCA: a) standardized Canonical plot for sample scores (see Appendix F for a list of corresponding samples number); b) standardized Canonical plot for species scores (see Table 6.2 for a list of corresponding species numbers and names and names); c and d) geographic distribution of sample scores and correlations between environmental variables and Canonical axes.

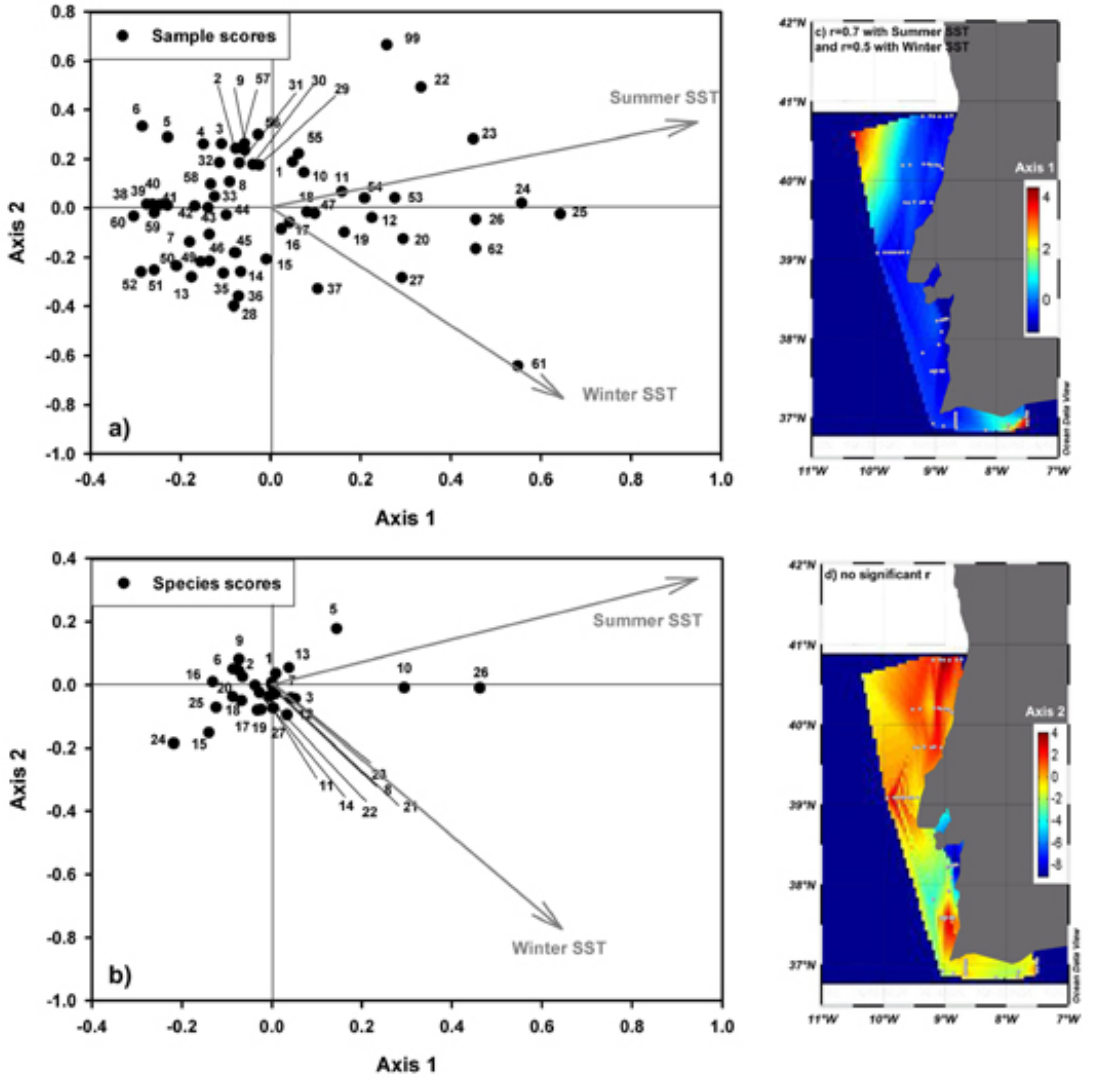

Figure 6.6 - Results for the SST CCA: a) standardized Canonical plot for sample scores (see Appendix F for a list of corresponding samples number); b) standardized Canonical plot for species scores (see Table 6.2 for a list of corresponding species numbers and names and names); c and d) geographic distribution of sample scores and correlations between environmental variables and Canonical axes.

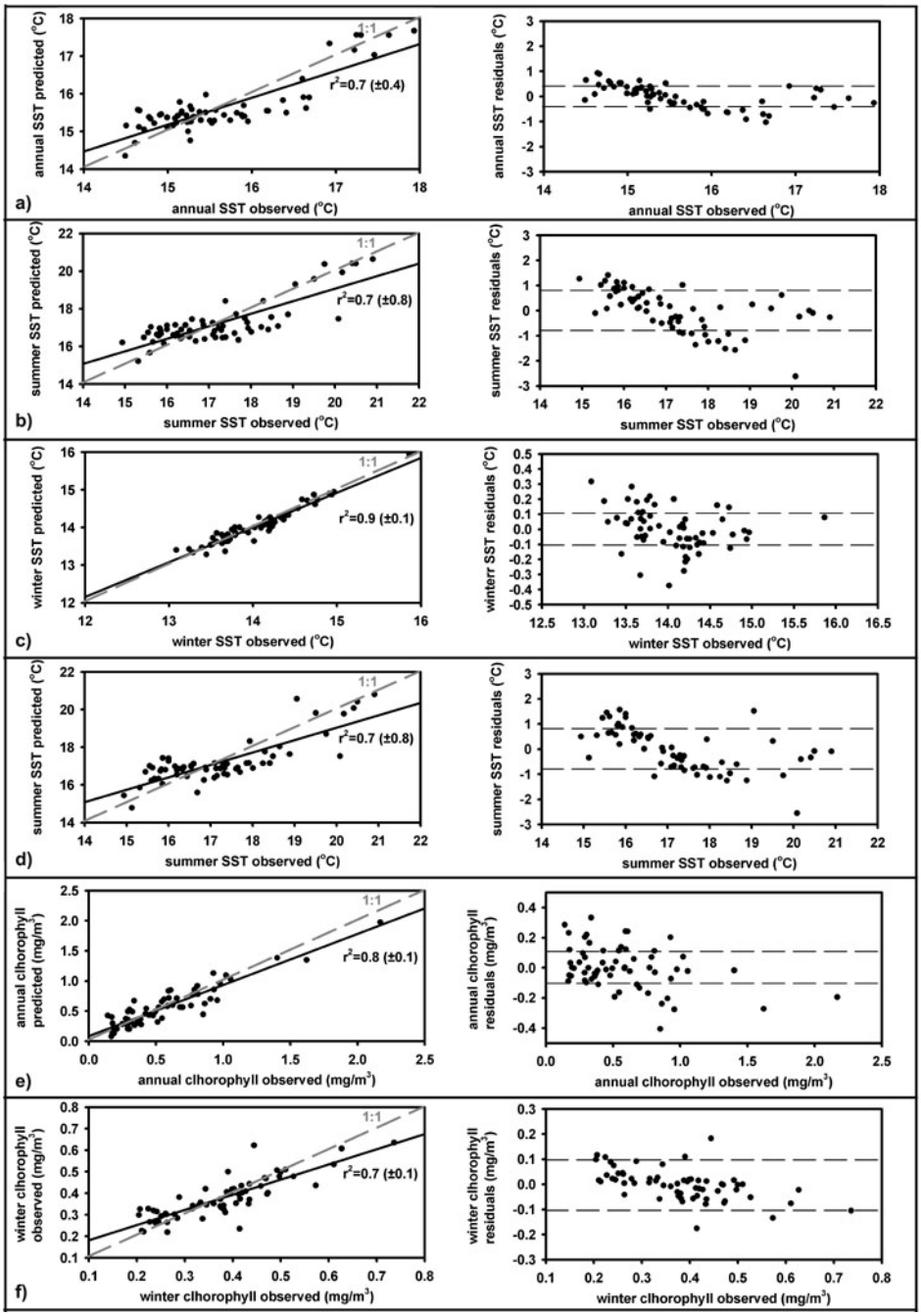

Figure 6.7 - Scatter plots for regression equations (gray line represents the 1:1 line) and residuals from modern transfer functions calibrations from Imbrie and Kipp method: a) annual SST, b) winter SST; and from CCA: c) winter SST, d) summer SST, e) annual chlorophyll and f) winter chlorophyll.

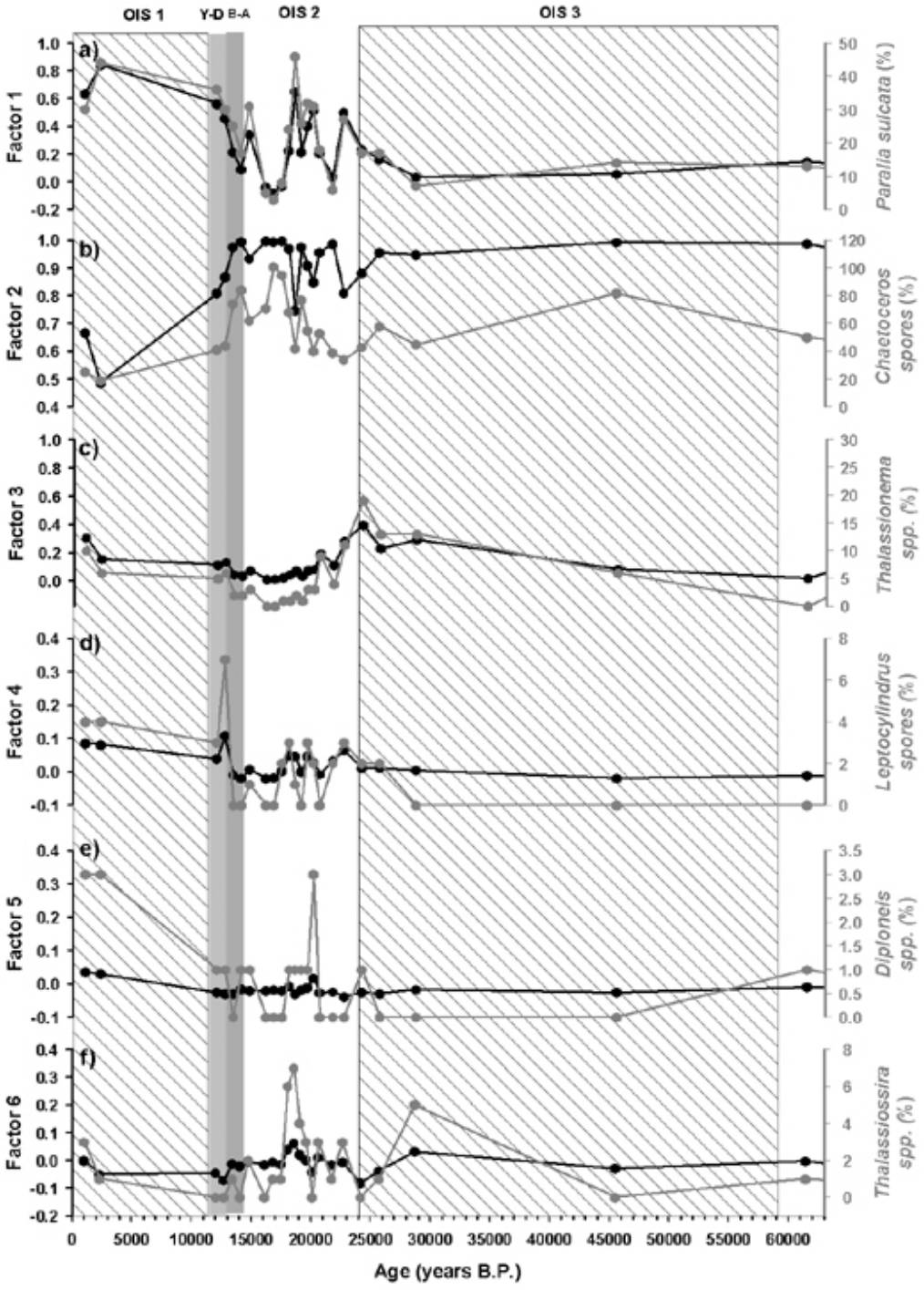

Figure 6.8 – Downcore factors (black lines) and correspondent species relative percentages (gray lines) for core KS-11.

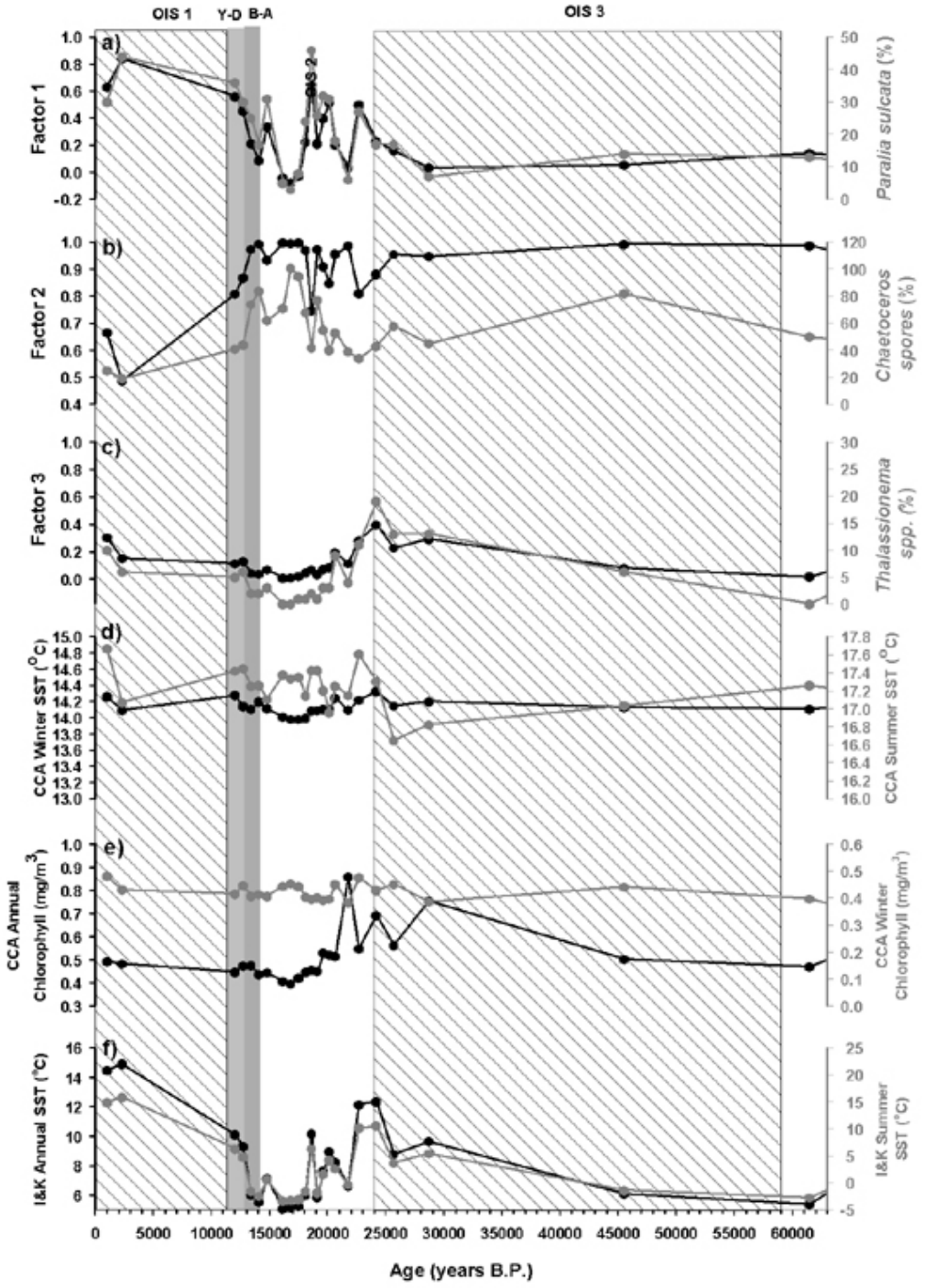

Figure 6.9 – Downcore factors and environmental reconstructions for core KS11: a) factor 1 (black line) and correspondent species (gray line), b) factor 2 (black line) and correspondent species (gray line), c) factor 3 (black line) and correspondent species (gray line), d) SST reconstruction from CCA for winter (black line) and summer (gray line), e) chlorophyll reconstructions from CCA for annual (black line) and winter (gray line) and e) SST reconstruction from I&K for annual (black line) and winter (gray line).

7. CONCLUSIONS

Diatom assemblages from marine sediments record modern oceanographic conditions and therefore can be used in paleoceanographic reconstructions. Although the work presented here focuses on upwelling areas, the approach can be extended to any oceanic area with sufficient diatom preservation in the sediments.

A first step in this work was to develop new quantitative databases on diatom species distributions based on modern taxonomies in core-tops from the northeast Pacific off Washington, Oregon, and northern California, and to assemble similar data from the Northeast Atlantic off Portugal, with sufficient spatial detail to resolve coastal and offshore upwelling systems. Along with these geologic data, I assembled complementary data on modern oceanographic properties that facilitate quantitative analyses of the physical controls on the ecosystem.

With these new datasets, I developed diatom transfer functions to reconstruct quantitatively seasonal and annual primary productivity, sea-surface temperature, salinity and nutrients in the Northeast Pacific and Northeast Atlantic. A strength of multivariate transfer function methods is the ability to reconstruct more than one environmental property, as long as the environmental properties are sufficiently independent of each other. A weakness is possible instability in response to so-called no-analog conditions, which occur if the flora of the past is comprised of a blend of species outside the range of modern spatial variability.

Transfer functions developed here are based on traditional (Imbrie and Kipp, 1971) methods of factor analysis followed by multiple linear regressions, and on canonical correspondence (CCA, weighted average) methods. CCA proved to be a more robust method (relative to extrapolation and the presence of weak no-analogs) for extracting patterns of species assemblages that relate directly to environmental variables than the Imbrie and Kipp method. Both methods, however, were sensitive to the no-analog problem in the northeast Pacific. After exploring two possible ways of circumventing this situation, I conclude that removing the no-analog species from the

dataset yields more conservative results for the severe no-analog conditions encountered in Pleistocene sediments of the northeast Pacific.

The presence of high abundances of freshwater diatoms in the marine realm during the last ice age suggests that the no-analog condition was created by the massive freshwater inputs from Pleistocene mega-floods, which entered the northeast Pacific via the Columbia River. A key finding of this dissertation is that these megafloods spanned the time of the advance of the Cordilleran Ice Sheet, from ~31,000-~16,000 years ago, unlike previous inferences that flooding events were limited to ~2500 years (dated in the incomplete land record from18,400-15,700 years ago).

The reconstructions of productivity and sea-surface temperature for the past 60,000 years in the northeast Pacific suggest that temperature in the coastal upwelling region was relatively stable, and that productivity did not decrease significantly at the Last Glacial Maximum. This finding contrasts with inferences based on organic carbon concentrations and geochemical temperature proxies in sediments, which suggested both cooler temperatures and lower export production. The new temperature results suggest that regional ice-age cooling was offset by weaker coastal upwelling during the upwelling season. The apparently conflicting results on productivity can be reconciled if the major change was in export production (as recorded by organic carbon contents) rather than primary productivity (as recorded by diatom assemblages). This implies that open-ocean upwelling driven by wind-stress curl, rather than coastal upwelling dominated the region during the Last Glacial Maximum (consistent with previous model predictions of changes in coastal upwelling off Oregon and California from Ortiz et al., 1997 and Pisias et al., 2001). This condition is similar to that of the modern Alaska Gyre, in which organic matter is efficiently recycled in near-surface waters. Millennial-scale climate oscillations that affected the winds are a possible explanation for observed oscillations in upwelling, productivity and sea-surface temperature during Oxygen Isotope Stage 3 (~30,000-60,000 years ago).

Quantitative reconstructions also yielded new insights into the history of the Portuguese upwelling system. During the Last Glacial Maximum and Oxygen Isotope Stage 2 the coastal upwelling was stronger than today, but chlorophyll and productivity only increased briefly at 20,000 years ago, coincident with a peak in river influence. I infer that when the rivers brought micronutrients (such as iron) into the area and the upwelling system was able to utilize the existing nutrients, high productivity developed. During this time, upwelling driven by wind-stress curl was relatively weak off Portugal.

This dissertation brings a new understanding on the dynamics of upwelling along the coast (driven by along-shore winds) versus offshore (driven by wind-stress curl) and corresponding responses of the ecosystem via diatom productivity. The type of upwelling present in a certain area plays an important role in atmospheric carbon dioxide sequestration. Coastal upwelling systems are thought to export carbon to the deep sea more efficiently than offshore upwelling systems driven by wind-stress curl. The comparison of the two upwelling areas studied here revealed the importance of regional controls of upwelling and productivity. In the northeast Pacific, coastal upwelling decreased during the Last Glacial Maximum and was replaced by wind-stress curl upwelling. The primary productivity remained close to modern values, however the system was less efficient in exporting organic matter into the sediments. In the northeast Atlantic region off Portugal, coastal upwelling was stronger during the Last Glacial interval than at present, and upwelling induced by wind-stress curl was weaker. Such differences document that these two upwelling areas in the northern hemisphere responded differently to global climate changes, and underscore the need to understand regional mechanisms of climate and ecological change.

BIBLIOGRAPHY

Abrantes, F.,1988. Diatom assemblages as upwelling indicators in surface sediments off Portugal. *Marine Geology*, **85**, 15-39.

Abrantes, F., 1991. Increased upwelling off Portugal during the last glaciation: Diatom evidence. *Marine Micropaleontology*, **17**, 285-310.

Abrantes, F., 2000. 200,000-yr diatom records from Atlantic upwelling sites reveal maximum productivity during LGM and a shift in phytoplankton community structure at 185,000 yr. *Earth and Planetary Science Letters*, **176**, 7-16.

Abrantes, F. G., Sancetta, C., 1985. Diatom assemblages in surface sediments reflect coastal upwelling off Southern Portugal. *Oceanologica Acta*, **8** (1), 7-12.

Abrantes, F., Winn, K., Sarnthein, M., 1994. Late Quaternary Paleoproductivity Variations in the NE and Equatorial Atlantic: Diatom and Corg Evidence. *In* Zahn R., Pederson, T. F., Kaminski, M. A., Labeyrie, L. (Eds.), *Carbon Cycling in the Glacial Ocean: Constrains on the Ocean's Role in Global Change*, NATO ASI Series, **I** (17), Springer-Verlag, New York, 425-442.

Abrantes, F., Moita, M. T., 1997. Water column and recent sediment data on diatoms and coccolithophorids, off Portugal, confirm sediment record of upwelling events. *Oceanologica Acta*, **22** (3), 319-334.

Abrantes, F., Gil, I., Lopes, C., Castro, M., 2004. Quantitative diatom analyses-a faster cleaning procedure. *Deep-Sea Research I*, **52**, 189-198.

Alley, R. B., Meese, D. A., Shuman, C. A., Gow, A. J., Taylor, K. C., Grootes, P. M., White, J. W. C., Ram, M., Waddington, E. D., Mayewski, P. A., Zielinski, G. A., 1993. Abrupt increase in Greenland snow accumulation in the end of the Younger Dryas event. *Nature*, **362**, 527-529.

Anderson, G.C., 1964. The seasonal and geographic distribution of primary productivity off the Washington and Oregon coasts. *Limnology and Oceanography*, **9** (3), 284-302.

Antoine, D., Morel, A., 1996. Ocean primary production. 1) Adaptation of a spectral light-photosynthesis model in view of application to satellite chlorophyll observations. *Global Biogeochemical Cycles*, **18** (1), 43-55.

Atwater, B. F., 1987. Status of Glacial Lake Columbia during the Last Floods from Glacial Lake Missoula. *Quaternary Research*, **27**, 182-201.

Baker, V. R., 1973. Paleohydrology and Sedimentology of Lake Missoula Flooding in Eastern Washington. *Geological Society of America Special Paper 144*.

Bakun, A., Nelson, C.S., 1991. The seasonal cycle of wind-stress curl in subtropical eastern boundary current regions. *Journal of Physical Oceanography*, **21**, 1815-1834.

Barber, R.T., Smith, R.L., 1981. Coastal Upwelling Ecosystems. *In* Longhurst, A. R. (Ed.), *Analysis of Marine Ecosystems*, Academic Press, London, 31-68.

Barron, J.A., Heusser, L., Herbert, T., Lyle, M., 2003. High-resolution climatic Evolution of coastal northern California during the past 16,000 years. *Paleoceanography*, **18** (1), 20(1)-20(14).

Battarbee, R.W., 1973. A New Method for the Estimation of Absolute Microfossil Numbers, with Reference Especially to Diatoms. *Limnology and Oceanography*, **18** (4), 647-653.

Bauer, E., Ganopolski, A., Montoya, M., 2204. Simulation of the cold climate event 8200 years ago by meltwater outburst from Lake Agassiz. *Paleoceanography*, **19**, PA3014.

Benito, G., O'Connor, J. E., 2003. Number and size of last-glacial Missoula floods in the Columbia River valley between the Pasco Basin, Washington, and Portland, Oregon. *Geological Society of America Bulletin*, **115** (5), 624-638.

Berdeal, I. G., Hickey, B. N., Kawase, M., 2002. Influence of wind-stress and ambient flow on a high discharge river plume. *Journal of Geophysical Research*, **107** (9), 13-1 – 13-24.

Berger, W.H., Wefer, G., 1991. Productivity of the Glacial Ocean: discussion of the Iron hypothesis. *Limnology and Oceanography*, **36** (8), 1 899-1 918.

Blasco, D., Estrada, M., Jones, B.H., 1980. Relationship between the phytoplankton and the hydrography in the Northwest African Upwelling region near Cabo Carvoeiro. *Deep Sea Research*, **27**A, 799-821.

Bograd, S.J., Lynn, R.J., 2003. Anomalous Subarctic influence in the southern California Current during 2002. *Geophysical Research Letters*, **30** (15), CCR 2-1 to CCR 2-4.

Booth, D. B., Troost, K. G., Clague, J. J., Waitt, R. B., 2004. The Cordilleran Ice Sheet. *In* Gillespie, A. R., Porter, S. C. and Atwater, B. F. (Eds.), *The Quaternary Period in the United States*, Amsterdam, Elsevier, 17-43.

Bradbury, J. P., Colman, S. M., Dean, W. E., 2004. Limnological and climatic environments at Upper Klamath Lake, Oregon during the past 45 000 years. *Journal of Paleolimnology*, **31**, 167-188.

Bretz, J. H., 1925. The Spokane flood beyond the Channeled Scabland. *Journal of Geology*, **33**, 97-115.

Bretz, J. H., 1969. The Lake Missoula floods and the Channeled Scabland. *Journal of Geology*, **77**, 505-543.

Brink, K.H., Cowles, T.J., 1991. The coastal transition zone program. *Journal of Geophysical Research*, **14** (96), 14 637-14 647.

Cattell, R. B., Vogelmann, S., 1977. A comprehensive trial of the scree and KG criteria for determining the number of factors. *Multivariate Behavioral Research*, **12**, 289-325.

Clague, J.J., 1981. Late Quaternary geology and geochronology of British Columbia, Part 2. *Geological Survey of Canada Paper* **80**-3, 1-41.

Clague, J. J., James, T. S., 2002. History and isostatic effects of the last ice sheet in southern British Columbia. *Quaternary Science Reviews*, **21**, 71-87.

Clark, P. U., Pisias, N. G., Stocker, T. F., Weaver, A. J., 2002. The role of the thermohaline circulation in abrupt climate change. *Nature*, **415**, 863-869.

Clarke, G.K.C., Mathews, W. H., Pack, R.T., 1984. Outburst floods from glacial lake Missoula. *Quaternary Research*, **22**, 289-299.

Grootes, P. M., Stuiver, M., White, J. W. C., Johnsen, S. J., Jouzel, J., 1993. Comparison of oxygen isotope records from the GISP2 and GRIP Greenland ice cores. *Nature*, **366**, 552-554.

Cupp, E. 1943. Marine plankton diatoms of the west coast of North America. *Bulletin of the Scripps Institution of Oceanography of the University of California*, **5**, 1.

Dansgaard, W., Johnsen, S. J., Clausen, H. B., Dahl-Jensen, D., Gundestrup, N. S., Hammer, C. U., Hvidberg, C. S., Steffensen, J. P., Sveinbjörnsdottir, A. E., Jouzel, J. and Bond, G., 1993. Evidence for general instability of past climate from 250-kyr ice-core record. *Nature*, **364**, 218-220

Davis, J.C., 2002. Statistics and data analysis in geology. Gerder, M. (Ed.), John Wiley & Sons, New York.

Devore, J., Peck, R., 1986. The exploration and analysis of data. West Publishing Company, Minnesota, 110-124.

Dugdale, R.C., Goering, J.J., 1967. Uptake of new and regenerated forms of nitrogen in primary productivity. *Limnology and Oceanography*, **12**, 196-206.

Fairbanks, R. G., Mortlock, R. A., Chiu, T.-C., Cao, L., Kaplan, A., Guilderson, T. P., Fairbanks, T. W., Bloom, A. L., 2005. Marine Radiocarbon Calibration Curve Spanning 0 to 50,000 Years B. P. Based on Paired ^{230} Th/^{234} U/^{238} U and ^{14}C Dates on Pristine Corals. *Quaternary Science Reviews*, **24**, 1781-1796.

Feldberg, M., Mix, A. C., 2002. Sea-surface temperatures estimates in the Southeast Pacific based on planktonic foraminiferal species: modern calibration and Last Glacial Maximum. *Marine Micropaleontology*, **44**, 1-29.

Fenner, J., 1982. Diatoms in the Eocene and Oligocene sediments off NW Africa, their stratigraphic and paleogeographic occurrences. Dissertation Thesis, University of Kiel, Germany.

Fiúza, A., 1983. Upwelling patterns of Portugal. *In* Suess, E., Thiede, J. (Eds.), *Coastal Upwelling-Its sediment Record, Part A: responses of the sedimentary regime to present coastal upwelling*, NATO Conference Series **IV**, Plenum Press, New York, 85-98.

Fiúza, A. F. G., Hamann, M., Ambar, I., del Rio, G. D., González, N., Cabanas, J., 1998. Water masses and their circulation off Western Iberia during May 1993. *Deep Sea research I*, **45**, 1127-1160.

Gardner, J.V., Dean, W.E., Dartnell, P., 1997. Biogenic sedimentation beneath the California Current system for the past 30 ky and its paleoceanographic significance. *Paleoceanography*, **12** (2), 207-225.

Grantham, B.A., Chan, F., Nielsen, K.,J., Fox, D.S., Barth, J.A., Huyer, A., Lubchenco, J., Menge, B.A., 2004. Upwelling-driven nearshore hypoxia signals ecosystem and oceanographic changes in the northeast Pacific. *Nature*, **429**, 749-754.

Haidvogel, D.B., Beckmann, A., Hedstrom, K.S., 1991. Dynamic simulations of filament formation and evolution in the coastal transition zone. *Journal of Geophysical Research*, **96**, 15,017-15,040.

Hales, B., Takahashi, T., Bandstra, L., 2005. Atmospheric CO_2 uptake by a coastal upwelling system. *Global Biogeochemical Cycles*, **19**, GB1009.

Hasle, G.R., 1977. Distributional features of some marine planktonic diatoms. *In* Dunbard, M.J. (Ed.), *Polar Oceans*, McGill University, 549-552.

Hendy, I. L., Pedersen, T. F., Kennett, J. P., Tada, R., 2004. Intermittent existence of a southern Californian upwelling cell during submillennial climate change of the past 60 kyr. *Paleoceanography*, **19**, PA3007.

Hickey, B.M., 1979. The California Current System-hypotheses and facts. *Progress in Oceanography*, **8**, 191-279.

Hickey, B.M., 1998. Coastal Oceanography of Western North America from the yip of Baja California to Vancouver Island. *In* Robinson, A.R. and Brink, K.H. (Eds.), *The Sea*, **11**, Wiley & Sons, New York, 345-393.

Hickey, B. M., Pietrafesa, L. J., Jay, D. A., Boicourt, W. C., 1998. The Columbia River Plume Study: Subtidal variability in the velocity and salinity fields. *Journal of Geophysical Research*, **103** (5), 10339-10368.

Hood, R.R., Abbott, M.R., Huyer, A., Kosro, P.M., 1990. Surface Patterns in Temperature, Flow, Phytoplankton Biomass, and Species Composition in the Coastal Transition Zone off Northern California. *Journal of Geophysical Research*, **95**, 18 081-18 094.

Hostetler, S. W., Bartlein, P. J. 1999. Simulation of the Potential Responses of Regional Climate and Surface Processes in Western North America to a Canonical

Heinrich Event. *In* Clark, P. U., Webb, R. S., Keigwin, L. D. (Eds.), *Mechanisms of Global Climate Change at Millennial Time Scales,* AGU Monograph **112**, American Geophysical Union, Washington DC, 313-327.

Hostetler, S.W., Clark, P.U., Bartlein, P.J., Mix, A.C., Pisias, N J., 1999. Atmospheric transmission of North Atlantic Heinrich events. *Journal of Geophysical Research*, **104** (D4), 3 947-3 952.

Hustedt, F., 1930. Die Kieselalgen Deutschlands, Ősterreichs, und der Schweiz unter Berűcksichtigung der űbrigen Länder Europas sowie der angrenzenden Meeresgebiete, Band VIII, Teil 1: Akademische Verlagsgesellschaft m. b. h. Leipzig.

Hustedt, F., 1959. Die Kieselalgen Deutschlands, Ősterreichs, und der Schweiz unter Berűcksichtigung der űbrigen Länder Europas sowie der angrenzenden Meeresgebiete, Band VIII, Teil 2: Akademische Verlagsgesellschaft m. b. h. Leipzig.

Hutchins, D. A., Bruland, K., 1998. Iron-limited growth and Si:N uptake ratios in a coastal upwelling regime. *Science*, **393**, 561-564.

Hutson, W. H., 1977. Transfer Functions under No-Analog Conditions: experiments with Indian Ocean Planktonic Foraminifera. *Quaternary Research*, **8**, 355-367.

Huyer, A., 1983. Coastal Upwelling in the California Current System. *Progress in Oceanography*, **12**, 259-284.

Imbrie, J., Kipp, N.G., 1971. A new micropaleontological method for quantitative paleoclimatology: application to a late Pleistocene Caribbean core. *In* Turekian, K. (Ed.), *Late Cenozoic Glacial Ages*. Yale University Press, New Haven, CT, 71-181.

Jackson, D. A., 1993. Stopping rules in principal component analysis: A comparison of heuristical and statistical approaches. *Ecology*, **74**, 2204-2214.

Jiang, H., Björck, S., Svensson, N.-O., 1998. Reconstruction of Holocene sea-surface salinity in the Skagerrak-Kattegat: a climatic and environmental record of Scandinavia. *Journal of Quaternary Science*, **13** (2), 107-114.

Jöckel, K.-H., Rothe, G., Sendler, W. (Eds.), 1992. Bootstrapping and Related Techniques. Proceedings of an International Conference Held in Trier, FRG, June 4-8, 1990. Springer-Verlag, Berlin, Germany.

Jousé, A.P., Kozlova, O.G., Muhina, V.V., 1971. Distribution of diatoms in the surface layer of sediment from the Pacific Ocean. *In* Riedel, W.R., Funnell, B. (Eds.), *The Micropaleontology of Oceans*, Cambridge University Press, Cambridge, 263-269.

Kendall, C., Coplen, T. B., 2001. Distribution of oxygen-18 and deuterium in river waters across the United States. *Hydrological Processes*, **15**, 1363-1393.

Kucera, M., Weinelt, M., Kiefer, T., Pflaumann, U., Hayes, A., Weinelt, M., Chen, M., Mix, A. C., Barrows, T. T., Cortijo, E., Duprat, J., Juggins, S., Waelbroeck, C., 2005. Reconstruction of sea-surface temperatures from assemblages of planktonic foraminifera: multi-technique approach based on geographically constrained calibration data sets and its application to glacial Atlantic and Pacific Oceans. *Quaternary Science Reviews*, **24**, 951-998.

Lepŝ, J., Ŝmilauer, P, 2003. Multivariate Analysis of Ecological Data using CANOCO. Cambridge University Press, Cambridge, U.K.

Lopes, C., Mix, A. C., Abrantes, F., Submitted. Northeast Pacific Diatom-Based Transfer Functions: Imbrie and Kipp Versus Canonical Correspondence Analysis. Quaternary Science Reviews.

Lopes, C., Mix, A. C, Abrantes, F., 2006. Diatoms in northeast Pacific surface sediments as paleoceanographic proxies. *Marine Micropaleontology*, **60** (1), 45-65.

Lund, D. C, Mix, A. C., 1998. Millennial-scale deep water oscillations: Reflections of the North Atlantic in the deep Pacific from 10 to 60 ka. *Paleoceanography*, **13** (1), 10-19.

Lyle, M., Mix, A., Ravelo, C., Andreasen, D., Heusser, L. and Olivarez, A., 2000. Millennial-Scale $CaCO_3$ and C_{ORG} Events along the Northern and Central California Margins: Stratigraphy and Origins. *Proceedings of the Ocean Drilling Program, Scientific Results*, **167**, 163-182.

Lynn, R.J., Simpson, J.J., 1987. The California Current system: the seasonal variability of its physical characteristics. *Journal of Geophysical Research*, **92**, C12, 12 947-12 966.

Malde, H. E., 1968. The Catastrophic Late Pleistocene Bonneville Flood in the Snake River Plain, Idaho. *Geological Survey Professional Paper* **596**, 1-56.

Margalef, R., 1978. Life-forms of phytoplankton as survival alternatives in an unstable environment. *Oceanologica Acta*, **1** (4), 493-508.

Martinson, D. G., Pisias, N. G., Hays, J. D., Imbrie, J., Moore Jr., T. C., Shackleton, N. F., 1987. Age Dating and the Orbital Theory of the Ice Ages: Development of a High-Resolution 0 to 300,000-Year Chronostratigraphy. *Quaternary Research*, **27**, 1-29.

Maruyama, T., 2000. Middle Miocene to Pleistocene Diatom Stratigraphy of Leg 167. *Proceedings of the Ocean Drilling Program, Scientific Results*, **167**, 63-110.

McCune, B., Mefford, M. J., 1999. PC-ORD. Multivariate Analysis of Ecological Data, Version 4.0. MjM Software Design, Gleneden Beach, Oregon, U.S.A.

McCune, B., Grace, J. B., 2002. Analysis of Ecological Communities. MjM Software Design, Gleneden Beach, Oregon, U.S.A.

McGarigal, K., Cushman, S., Stafford, S., 2000. Multivariate Statistics for Wildlife and Ecology Research. Springer Science+Bussiness Media Inc, New York, U.S.A.

Miller, C.B., Frost, B.W., Booth, P.A., 1991. Ecological processes in the subarctic Pacific: Iron limitation cannot be the whole story. *Oceanography*, **4**, 71-78.

Mix, A. C., Lund, D. C., Pisias, N. G., Bodén, P., Bornmalm, L., Lyle, M., Pike, J., 1999a. Rapid climate oscillations in the Northeast Pacific during the last deglaciation reflect northern and southern hemisphere sources. *In* Clark, P. U., Webb, R. S., Keigwin, L. D. (Eds.), *Mechanisms of Global Climate Change at Millennial Time Scales*, AGU Monograph **112**, American Geophysical Union, Washington DC, 127-148.

Mix, A. C., Morey, A. E., Pisias, N. G., 1999b. Foraminiferal faunal estimates of paleotemperature: Circumventing the no-analog problem yields cool ice age tropics. *Paleoceanography*, **14** (3), 350-359.

Mix, A. C., Bard, E. and Schneider, R., 2001. Environmental processes of the ice age: land, oceans, glaciers (EPILOG). *Quaternary Science Reviews*, **20**, 627-657.

Moita, M. T., 2001. Estrutura, Variabilidade e Dinâmica do Fitoplâncton na Costa de Portugal Continental. Lisbon, Ph. D. thesis.

Mooers, C.N.K., Robinson, A.R., 1984. Turbulent jets and eddies in the California Current and inferred cross-shore transports. **Science**, New Series, **223** (4631), 51-53.

Morey, A. E., Mix, A. C., Pisias, N. G., 2005. Planktonic foraminiferal assemblages preserved in surface sediments correspond to multiple environment variables. *Quaternary Science Reviews*, **24**, 925-950.

Mullenbach, B.L., Nittrouer, C.A., 2000. Rapid deposition on fluvial sediment in the Eel Canyon, northern California. *Continental Shelf Research*, **20**, 2 191-2 212.

Nave, S., Freitas, P., Abrantes, F., 2001. Coastal upwelling in the Canary Island region: spatial variability reflected by the surface sediment diatom record. *Marine Micropaleontology*, **42**, 1-23.

Normark, W. R., Reid, J. A., 2003. Extensive Deposits on the Pacific Plate from Late Pleistocene North American Lake Outbursts. *Journal of Geology*, **111**, 617-637.

O'Connor, J. E., Baker, V. R., 1992. Magnitudes and implications of peak discharges from glacial Lake Missoula. *Geological Society of America Bulletin*, **104**, 267-279.

Ogston, A.S., Guerra, J.V., Sternberg, R.W., 2004. Interannual variability of nearbed sediment flux on the Eel River shelf, northern California. *Continental Shelf Research*, **24**, 117-136.

Ortiz, J., Mix, A., Hostler, S., Kashgarian, M., 1997. The California Current of the last glacial maximum: Reconstruction at 42^{o}N based on multiple proxies. *Paleoceanography*, **12** (2), 191-205.

Ortiz, J. D., O'Connell, S. B., DelViscio, J., Dean, W, Carriquiry, J. D., Marchitto, T., Zheng, Y., van Geen, A., 2004. Enhanced marine productivity off western North America during warm climate intervals of the past 52 k.y. *Geological Society of America*, **32** (6), 521-524.

Pailler, D., Bard, E., 2002. High frequency palaeoceanographic changes during the past 140 000 yr recorded by the organic matter in sediments of the Iberian Margin. *Palaeogeography, Palaeoclimatology, Palaeoecology*, **181**, 431-452.

Palmer, M. W., 1993. Putting things in even better order: the advantages of Canonical Correspondence Analysis. *Ecology*, **17** (8), 2215-2230.

Pickard, G. L., 1964. Descriptive Physical Oceanography, Pergamon, New York.

Pisias, N. G., Roelofs, A., Weber, M., 1997. Radiolarian-based transfer functions for estimating mean surface ocean temperatures and seasonal range. *Paleoceanography*, **12** (3), 365-379.

Pisias, N. G., Mix, A. C., Heusser, L., 2001. Millennial scale climate variability of the northeast Pacific Ocean and northwest North America based on radiolaria and pollen. *Quaternary Science Reviews*, **20**, 1561-1576.

Pokras, E.M., Mix, A.C., 1985. Eolian evidence for spatial variability of late Quaternary climates in Tropical Africa. *Quaternary Research*, **24**, 137-149.

Prahl, F. G., Pisias, N., Sparrow, M. A., Sabin, A., 1995. Assessment of sea-surface temperature at 42^{o}N in the California Current over the last 30,000 years. *Paleoceanography*, **10** (4), 763-773.

Roden, G. I., 1975. On North Pacific temperature, salinity, sound velocity and density fronts and their relation to the wind and energy flux fields. *Journal of Physical Oceanography*, **5**, 557-571.

Sancetta, C., 1979. Oceanography of the north Pacific during the last 18,000 years: Evidence from fossil diatoms. *Marine Micropaleontology*, **4**, 103-123.

Sancetta, C., 1992. Comparison of phytoplankton in sediment trap time series and surface sediments along a productivity gradient. *Paleoceanography*, **7** (2), 183-194.

Sancetta, C., Silvestri, S., 1986. Pliocene-Pleistocene evolution of the north Pacific ocean-atmosphere system, interpreted from fossil diatoms. *Paleoceanography*, **1** (2), 163-180.

Sancetta, C., Lyle, M., Heusser, L., Zahn, R., Bradbury, J. P., 1992. Late-glacial to Holocene changes in winds, upwelling and seasonal production of the northern California Current system. *Quaternary Research*, **38**, 359-370.

Schiebel, R., Zeltner, A., Treppke, U. F., Waniek, J. J., Bollmann, J., Rixen, T., Hemleben, C., 2004. Distribution of diatoms, coccolithophores and planktic foraminifers along a trophic gradient during a SW monsoon in the Arabian Sea. *Marine Micropaleontology*, **51**, 345-371.

Schlitzer, R., Ocean Data View, http://www.awi-bremenhaven.de/GEO/ODV, 2004

Schrader, H., 1972. Kieselsaure-Skelette in Sedimenten des ibero-marokkanischen Kontinentalrandes und angrenzender Tiefsee-Ebenen. "Meteor" Forschungsergeb., Reihe C (8), 10-36.

Schrader, H., Gersonde, R., 1978. Diatoms and silicoflagellates. *Utrecht Micropaleontological Bulletins*, **17**, 129-176.

Schuette, G., Schrader, H., 1981a. Diatoms in surface sediments: a reflection of coastal upwelling. *In* Richards, F. A. (Ed.), *Coastal Upwelling*, American Geophysical Union, Washington, 372-380.

Schuette, G., Schrader, H., 1981b. Diatom taphocoenoses in coastal upwelling areas of South West Africa. *Marine Micropaleontology*, **6**, 131-155.

Semina, H.J., Tarkhova, I.A., 1972. Ecology of phytoplankton in the north Pacific Ocean. *In* Takenouti, A.Y. (Ed.), *Biological oceanography of the northern north Pacific Ocean*, Idemitsu Shoten, Tokyo, 117-124.

Shackleton, N. J., Hall, M. A., Vincent, E., 2000. Phase relationship between millennial-scale events 64,000-24,000 years ago. *Paleoceanography*, **15** (6), 565-569.

Shaw, J., Munro-Stasiuk, M., Sawyer, B., Beaney, C., Lesemann, J.-E., Musacchio, A., Rains, B., Young, R. R., 1999. The Channeled Scabland: Back to Bretz? *Geology*, **27**, 605-608.

Smith, R.L., 1983. Circulation patterns in upwelling regimes. *In* Suess, E., Thiede, J. (Eds.), *Coastal Upwelling-Its sediment Record, Part A: responses of the sedimentary regime to present coastal upwelling*, NATO Conference Series **IV**, Plenum Press, New York, 13-60.

Stuiver, M., Reimer, P. J., 1993. Extended ^{14}C database and revised CALIB radiocarbon calibration program. *Radiocarbon*, **35**, 215-230.

Sverdrup, H.U., Johnson, M.W., Fleming, R.H., 1942. The Oceans, Their Physics, Chemistry, and General Biology, Prentice Hall, Englewood Cliffs, New Jersey.

Talley, L.D., 1993. Distribution and formation of north Pacific intermediate water. *Journal of Physical Oceanography*, **23**, 517-537.

Telford, R. J., Birks, H. J. B., 2005. The secret assumption of transfer functions: problems with spatial autocorrelation in evaluating model performance. *Quaternary Science Reviews*, **24**, 2173-2179.

ter Braak, C. J. F., 1986. Canonical Correspondence Analysis: A New eigenvector Technique for Multivariate Direct Gradient Analysis. *Ecology*, **67** (5), 1167-1179.

ter Braak, C. J. F., Verdonschot, P. F. M., 1995. Canonical correspondence analysis and related multivariate methods in aquatic ecology. *Aquatic Sciences*, **57** (3), 255-289.

ter Braak, C. J. F., Smilauer, P., 1998. CANOCO Reference Manual and User's Guide to Canoco for Windows: Software for Canonical Community Ordination (Version 4.0). Microcomputer Power, Ithaca, New York, U.S.A.

Tibby, R.B., 1941. The water masses off the west coast of north America. *Journal of Marine Research*, **IV** (2), 112-121.

Tomas, C.R. (Ed.), 1996. Identifying Marine Diatoms and Dinoflagellates. Academic Press, California.

Traganza, E.D., Silva, V.M., Austin, D.M.; Hanson, W.L., Bonsik, S.H., 1983. Nutrient mapping and recurrence of coastal upwelling centers by satellite remote sensing: It's implication top primary production and the sediment record. *In* Suess, E., Thiede, J. (Eds.), *Coastal Upwelling-Its sediment Record, Part A: responses of the sedimentary regime to present coastal upwelling*, NATO Conference Series **IV**, Plenum Press, New York, 61-83.

Vacco, D. A., Clark, P. U., Mix, A. C., Cheng, H., Edwards, R. L., 2005. A speleothem record of Younger Dryas cooling, Klamath Mountains, Oregon, USA. *Quaternary Research*, **64**, 249-256.

Waitt, R. B., 1985. Case for periodic, colossal jökulhlaups from Pleistocene glacial Lake Missoula. *Geological Society of America Bulletin*, **96**, 1271-1286.

Weninger, B., Jöris, O., Danzeglocke, U., 2002. http://www.calpal-online.de.

Wheeler, P.A., Huyer, A., Fleischbein, J., 2003. Cold halocline, increased nutrients and higher chlorophyll off Oregon in 2002. *Geophysical Research Letters*, **30** (15), CCR3-1 to CCR3-4.

Whitlock, C., Grigg, L. D., 1999. Paleoecological Evidence of Milankovitch and Sub-Milankovitch Climate Variations in the Western U.S. During Late Quaternary. *In* Clark, P. U., Webb, R. S., Keigwin, L. D. (Eds.), *Mechanisms of Global Climate Change at Millennial Time Scales*, AGU Monograph **112**, American Geophysical Union, Washington DC, 227-241.

World Ocean Atlas (WOA), 1998, www.nodc.noaa.gov/OC5/woa98.html, September 2002.

Worona, M. A., Whitlock, C., 1995. Late Quaternary vegetation and climate history near Little Lake, central Coast Range, Oregon. *Geological Society of America Bulletin,* **107**, 867-876.

Zuffa, G. G., Normark, W. R., Serra, F., Brunner, C. A., 2000. Turbidite Megabeds in an Oceanic Rift Valley Recording Jökulhlaups of Late Pleistocene Glacial Lakes of the Western United States. *Journal of Geology*, **108**, 253-274.

APPENDIX A: Taxonomic notes.

Most of the taxonomic references were taken from Hustedt (1930 and 1959), Cupp (1943) and Tomas (1996). Exceptions and special issues are noted here.

- "spp." designations were used if the authors were not able to check all the morphologic characteristics that would allow an unambiguous species designation, for example due to the position of the frustules. In most cases the diatom in question belongs to one of the previous species found;
- "cf" designations were used when one of the morphologic characteristics would not fit the taxonomic description. In most cases it was a discrepancy between sizes or position of processes;
- *Thalassiossira sp1*: Valve flat or slightly convex, circular (~23 μm diameter). Areolae (5 in 10 μm distance) decreasing in size towards the margin (7 in 10 μm distance). Arrangement of aerolae in linear rows with sparse processes close to the valve center. One ring of marginal processes (9 in 10 μm distance). No apparent labial process;
- *Thalassiossira sp2*: Valve slightly convex, circular (~37 μm diameter). Areolae (6 to 7 in 10 μm distance) with no particular orientation and sparse processes half way from the margin to center. One ring of marginal processes (2 in 10 μm distance). No apparent labial process. Otherwise similar to *Coscinodsicus marginatus*;
- *Thalassiossira sp3*: Valve flat, circular (~18 μm diameter). Aerolae arrangement very similar to *Thalassiossira eccentrica* (8 in 10 μm). Three or more central processes randomly arranged. Spines on the edge of the valve and with one series of processes (2 to 3 in 10 μm distance);
- *Thalassiossira sp4*: Valve flat or slightly convex, circular (~25 μm diameter). Central aerolae (4 in 10 μm distance) with no particular arrangement and variable size. Two central processes located half way from center to the valve edge. Aerolae decrease in size towards the edge and assume almost a centric

arrangement. One ring of marginal processes (4 in 10 μm distance) and spines. No apparent labial process;

- *Thalassiossira sp5*: Valve flat, circular (~16 μm diameter). One small central process. Aerolae (6 to 7 in 10 μm distance) with almost linear arrangement. Aerolae do not decrease in size towards the valve edge. Spines on the edge and no edge processes. No apparent labial process;
- *Thalassiossira sp6*: Valve flat or slightly convex, circular (~25 μm in diameter). Areolae (5 in 10 μm distance) decreasing in size towards the margin (6 in 10 μm distance). Arrangement of aerolae in linear rows with sparse processes all over the valve, becoming more curvilinear towards the margin. No apparent ring of marginal processes. No apparent labial process. Similar to *Thalassiossira sp1* but with more random processes on the valve;
- *Cocconeis sp1:* Elliptical cell 80 μm long and 40 μm wide. Five transapical striae and 6 aerolae in 10 μm distance. Valve appears depressed on the edges. No apparent edge chamber present. The raphe valve has central hyaline area and the raphe reaches the edge of the valve.
- Some differences were found between the species reported here and previous studies (e.g. Sancetta, 1992, Barron 2003). The most significant differences regard the species *Thalassiotrix longuissima* and *Thalassiossira pacifica*. The first species was reported for the NE Pacific, however we believe that past authors have identified *Lioloma elongatum* and *Lioloma pacificum* as *Thalassiotrix longuissima*. We found *Thalassiotrix longuissima*, but the separation from *Lioloma* results in the elimination of *Thalassiotrix* in the Q-mode Factor Analysis due to its low relative abundance percentages (<2% in all samples examined here). *Thalassiossira pacifica* was not found in the samples used in this study. However, after a review of our identifications, it is possible that some of our counts of *Thalassiossira angulata* can include some *Thalassiossira pacifica* as these species can be very similar.

APPENDIX B: Supplementary data for Chapter 2.

Table B.1 – Core-top locations, depths and diatom abundances (GC - Gravity, PC-Piston, MG -Multicorer, AC - Trigger). Gray boxes indicate samples used for species identifications.

Core ID	Core ID # Figure 2.4	latitude (N)	longitude (W)	water depth (m)	Diatom Abundances (#valves/g)	Chaetoceros abundances (#valves/g)
W8209B-1 GC	25	39.632	-132.062	4560	2.22E+05	0.00E+00
W8209B-19 GC	26	39.272	-127.380	4355	4.04E+06	1.01E+06
W8209B-21 GC	27	39.273	-130.047	4474	3.75E+05	1.50E+05
L6-85-NC 7 GC	28	40.525	-127.705	3195	8.20E+05	2.34E+05
TT34-1 GC	29	40.517	-130.050	3287	6.66E+05	3.33E+05
Y73-10 100 GC	30	40.032	-125.298	1935	1.40E+06	2.34E+05
L6-85-NC 3 GC	31	41.028	-127.308	2983	1.26E+07	2.57E+06
W8809A-11 GC	32	41.672	-126.003	3020	1.99E+07	9.26E+06
W8809A-29 GC	33	41.803	-129.005	3288	4.30E+05	1.72E+05
W8809A-31 GC	34	41.678	-130.007	3136	0.00E+00	0.00E+00
W8809A-36 GC	36	41.270	-133.347	3844	0.00E+00	0.00E+00
W8809A-38 GC	37	41.078	-134.655	3928	0.00E+00	0.00E+00
W8809A-51 GC	38	41.662	-128.352	3159	5.14E+05	0.00E+00
W8909A-48 GC	39	41.333	-132.667	3670	0.00E+00	0.00E+00
W8809A-19GC	40	42.230	-126.517	2669	2.76E+06	1.00E+06
W8809A-26 GC	41	42.213	-128.007	3034	3.37E+05	0.00E+00
W8909A-24 GC	42	42.082	-125.302	2790	4.80E+07	2.78E+07
W8909A-31 GC	43	42.155	-127.208	2800	5.05E+06	1.12E+06
W8909A-7 GC	44	42.295	-124.930	1100	5.81E+06	3.06E+06
7407 Y-1 GC	45	43.628	-127.100	2918	1.43E+07	4.00E+06
W7905A-160 GC	47	43.165	-125.087	1476	5.86E+06	2.82E+06
W7905A-163 GC	48	43.167	-124.752	308	2.29E+06	1.22E+06
W8508AA-9 GC	49	43.030	-126.578	3092	8.74E+06	3.81E+06
W7610B-7 MG	51	44.213	-126.177	2893	6.75E+05	4.35E+05
W7905A-106 GC	52	44.230	-124.658	522	2.73E+05	0.00E+00
W8306A-1 GC	53	44.938	-125.362	2511	2.81E+07	8.77E+06
W9205A 1 GC	54	44.085	-125.373	3020	6.77E+06	3.74E+06
AT9009-2 GC	55	45.137	-125.438	2650	2.55E+06	1.02E+06
SAC9610-14 GC	56	45.523	-123.902	100	0.00E+00	0.00E+00
W7809C-34 GC	57	45.013	-124.235	1216	0.00E+00	0.00E+00
TT03-02 PC	59	46.985	-132.003	3109	0.00E+00	0.00E+00

(continued on next page)

Table B.1 (continued)

Core ID	Core ID #	latitude (N)	longitude (W)	water depth (m)	Diatom Abundances (#valves/g)	Chaetoceros abundances (#valves/g)
TT17-1 GC	60	46.633	-134.267	3909	0.00E+00	0.00E+00
TT29-18 PC	61	46.433	-128.383	2742	1.89E+05	0.00E+00
TT39-5 AC	62	46.720	-127.542	2665	1.16E+07	3.48E+06
Y6908-5A GC	65	46.652	-129.133	2600	4.26E+06	3.28E+05
Y7409-15 24 GC	66	46.118	-124.125	200	5.16E+06	7.94E+05
AT8408-17 GC	68	47.228	-126.145	2390	7.52E+06	3.51E+06
TT03-07 PC	69	47.095	-132.068	3210	0.00E+00	0.00E+00
TT29-22 AC	71	47.113	-127.907	2555	7.22E+06	1.15E+06
TT31-007 GC	72	47.000	-130.050	2614	0.00E+00	0.00E+00
TT31-11 GC	73	47.033	-131.158	3056	3.40E+06	0.00E+00
TT39-22 PC	74	47.587	-129.507	2566	1.14E+06	0.00E+00
TT39-23 PC	75	47.630	-128.667	2625	5.60E+05	0.00E+00
TT68-18 AC	76	47.383	-124.913	1240	3.04E+06	7.01E+05
TT39-17 PC	79	48.230	-130.030	2793	6.31E+05	0.00E+00
TT39-18 AC	80	48.437	-129.870	2765	1.28E+07	3.45E+06
TT39-19 PC	81	48.390	-127.153	2555	1.71E+06	2.14E+05
TT39-21 AC	82	48.063	-128.057	2575	1.64E+06	0.00E+00
TT90-33 GC	83	48.098	-126.017	1474	9.73E+05	4.87E+05
TT39-11 AC	85	49.013	-127.767	2480	1.35E+07	3.68E+06
TT39-12 AC	86	49.397	-128.140	2341	1.60E+07	5.50E+06
TT39-15 AC	87	49.210	-129.243	2396	9.44E+06	2.36E+06
MD02-2499 PC	99	41.653	-124.940	905	not available	not available

Table B.2 - Sample scores from Q-mode analysis.

Sample	Communalities	Factor 1	Factor 2	Factor 3	Factor 4	Factor 5
W8209B-19 GC	0.991	0.919	0.127	0.307	0.174	0.081
Y73-10 100 GC	0.986	0.744	0.184	0.571	0.240	0.126
L6-85-NC 3 GC	0.929	0.757	0.266	0.340	0.367	0.186
W8809A-11 GC	0.970	0.284	0.334	0.261	0.836	0.107
W8809A-19GC	0.980	0.579	0.247	0.211	0.726	0.110
W8909A-24 GC	0.991	0.455	0.245	0.801	0.213	0.194
W8909A-31 GC	0.976	0.894	0.137	0.330	0.188	0.116
W8909A-7 GC	0.995	0.908	0.122	0.340	0.173	0.101
7407 Y-1 GC	0.994	0.946	0.122	0.230	0.161	0.075
W7905A-160 GC	0.986	0.575	0.202	0.705	0.301	0.165
W7905A-163 GC	0.986	0.772	0.272	0.433	0.295	0.205
W8508AA-9 GC	0.981	0.688	0.368	0.447	0.376	0.178
W7610B-7 MG	0.981	0.868	0.186	0.326	0.244	0.163
W8306A-1 GC	0.765	-0.092	0.764	0.144	0.371	0.122
W9205A 1 GC	0.974	0.797	0.211	0.444	0.214	0.225
TT39-5 AC	0.987	0.708	0.236	0.606	0.189	0.161
TT068-27 PC	0.960	0.707	0.196	0.548	0.203	0.283
W7905A-109 GC	0.920	0.555	0.614	0.376	0.293	0.092
Y6908-5A GC	0.985	0.848	0.185	0.392	0.216	0.181
Y7409-15 24 GC	0.996	0.277	0.183	0.228	0.130	0.904
AT8408-17 GC	0.984	0.951	0.123	0.157	0.163	0.118
TT29-22 AC	0.991	0.933	0.134	0.219	0.167	0.163
TT31-11 GC	0.993	0.754	0.204	0.551	0.230	0.161
TT68-18 AC	0.909	0.343	0.876	0.125	0.037	0.085
TT39-18 AC	0.989	0.773	0.330	0.482	0.170	0.146
TT39-19 PC	0.989	0.814	0.187	0.421	0.289	0.175
TT39-11 AC	0.996	0.943	0.147	0.214	0.161	0.114
TT39-12 AC	0.980	0.881	0.181	0.336	0.208	0.123
TT39-15 AC	0.987	0.791	0.234	0.392	0.328	0.212
MD02-2499 PC	0.923	0.870	0.193	0.271	0.184	0.149

Table B.3 - Species found in core-top samples and corresponding references.

Species name	Taxonomic Reference
Actinocyclus curvatulus	Janisch
Actinocyclus normanii	(Greg.) Husted
Actinoptychus senarius	(Ehr.) Ehrenberg
Actinoptychus adriaticus	Grunow
Actinoptychus splendens	(Shadbolt) Ralfs (1861)
Actinoptychus spp.	
Stephanodiscus rotula (forma minutula)	(Kutz) Grunow
Asterolampra grevillei	(Wallich) Greville
Asterolampra marylandica	Ehrenberg
Asterolampra spp.	
Asteromphalus robustus	Castracane (1875)
Asteromphalus heptachis	(de Brebisson) Ralfs
Asteromphalus sarcophagus	Wallich
Asteromphalus spp.	
Aulacoseira islandica	(O. Mull.) Simonsen
Aulacoseira granulata	(Thwaites) Crawford/ (Her.) Thwaites
Aulacoseira spp.	
Azpetia africana	(Janisch ex. Schmidt) Fryxell & Watkins
Azpetia neocrenulata	(VanLandingham) Fryxell & Watkins in Fryxell et al.
Azpetia nodulifera	(Schmidt) Fryxell & Simonsen
Bactriastrum cf delicatum	Cleve
Bacteriastrum spp.	Shadbolt
Chaetoceros resting spores	
Coscinodiscus asteromphalus	Ehrenberg
Coscinodiscus decrescens	Grunow
Coscinodiscus denarius	A. Schmidt
Coscinodiscus granii	Gough
Coscinodiscus oculus iridis	Ehrenberg
Coscinodiscus marginatus	Ehrenberg
Coscinodiscus radiatus	Ehrenberg/(Schmidt)
Coscinodiscus zadiatus	Schmidt
Cyclotella litoralis	Lange & Syvertsen
Cyclotella meneghiniana	Kutzing
Cyclotella ocellata	Pantocsek
Cyclotella comta	Ehrenberg (Kutzing)
Cyclotella spp.	
Cyclotella striata	(Kutz.) Grunow
Hemidiscus cuneiformis	Wallich
Leptocylindrus resting spores	Cleve

(continued on next page)

Table B.3 (continued)

Species name	Taxonomic Reference
Melosira ambigua	(Grunow) Simonsen
Melosira westi	W. Smith 1856
Melosira spp.	
Odontella aurita	(Lyngbye) C. A. Agardh
Odontella spp.	
Paralia sulcata	(Ehr.) Cleve
Rhizosolenia aciculares	Sundstrom
Rhizosolenia borealis	Sundstrom
Rhizosolenia castracanei	Peragallo
Rhizosolenia spp.	
Rhizosolenia hebetata (forma semispina)	(Hensen) Gran
Rhizosolenia setigera	Brightwell
Rhizosolenia cf simplex	
Rhizosolenia simplex	Karsten
Rhizosolenia hebetata (forma hebetatata)	Bailey 1856
Rhizosolenia styliformis	Brightwell
Roperia tesselata	(Roper) Grunow ex Van Heurck
Stephanopyxis turris	(Arnot in Greville) Ralfs in Pritchard
Thalassiossira allenii	Takano
Thalassiossira anguste-lineata	(A. Schmi.) Fryxell & Hasle
Thalassiossira angulata	Gregory
Thalassiossira dichotomica	(Kozlova) Fryxell & Hasle
Thalassiossira endoseriata	Hasle & Fryxell
Thalassiossira cf eccentricas	
Thalassiossira eccentrica	(Ehr.) Cleve
Thalassiossira exigua	Fryxell & Hasle
Thalassiossira hendeyi	Hasle & G. Fryxell
Thalassiossira leptotus	Hasle & Fryxell
Thalassiossira lineata	Jouse
Thalassiossira lundiana	Fryxell
Thalassiossira cf mendiolana	
Thalassiossira mendiolana	Hasle & Heimdal
Thalassiossira cf nanolineata	
Thalassiossira nanolineata	(Mann) Fryxell & Hasle
Thalassiossira nordenskioeldii	Cleve
Thalassiossira oestrupii	(Ostenf.) Hasle
Thalassiossira oceanica	Hasle
Thalassiossira cf poroseriata	(Ramsfjell) Hasle
Thalassiosira cf punctigera	(Castracane) Hasle
Thalassiossira cf sacketii	Fryxell

(continued on next page)

Table B.3 (continued)

Species name	Taxonomic Reference
Thalassiossira cf simonsenii	Hasle & Fryxell
Thalassiossira subtilis	(Ostenfeld) Gran
Thalassiossira trifulta	Fryxell
Thalassiossira cf trifulta	
Thalassiossira sp1	See taxonomic notes
Thalassiossira sp2	See taxonomic notes
Thalassiossira sp3	See taxonomic notes
Thalassiossira sp4	See taxonomic notes
Thalassiossira sp5	See taxonomic notes
Thalassiossira sp6	See taxonomic notes
Thalassiossira spp.	
Triceratum alternans	Bailey
Achnantes lanceolata	(Breb) Grunow
Achnantes spp.	
Amphora comutata	Grunow
Amphora spp.	
Cocconeis diminuta	Pantocsek
Cocconeis cf nitida	
Cocconeis nitida	Gregory
Cocconeis disculus	(Schuman) Cleve
Cocconeis placentula	Ehrenberg
Cocconeis scutellum	Ehrenberg
Cocconeis spp.	
Cocconeis sp1	See taxonomic notes
Delphineis surilella	(Ehr.) Andrews
Diploneis chersonensis	(Grunow) Cleve
Diploneis constrita	Grunow
Epithemia turgida	(Her.) Kutz
Epithemia spp.	
Eunotia monodom	Ehrenberg
Eunotia spp.	
Fragilaria brevistriata	Grunow
Fragilaria construens	(Ehr.) Grunow
Delphineis karstenii	(Boden) Fryxell
Fragilaria inflata	(Heiden) Hustedt
Fragilaria leptostauron	(Her.) Husted
Fragilaria pinnata	Ehrenberg
Fragilaria spp.	
Fragilariopsis doliolus	(Wallich) Medin & Sims
Gomphonema acuminatum	Ehrenberg

(continued on next page)

Table B.3 (continued)

Species name	Taxonomic Reference
Gomphonema olivaceum	Cleve
Gomphonema constrictum	Ehrenberg
Lioloma elongatum	(Grunow) Hasle
Lioloma pacificum	(Cupp) Hasle
Lioloma spp.	
Navicula commutabilis	
Navicula distans	(W. Smith) Ralphs in Pritchard
Navicula gibbula	Cleve
Navicula lundstronii	
Navicula gp lyratae	Ehrenberg
Navicula spp.	
Neodenticula seminae	(Simonsen & Kanaya) Akiba & Yanagisawa
Nitzschia dietrichii	Simonsen
Nitzschia amphibia	Grunow
Nitzschia gp bicapitata	Cleve
Nitzschia bifurcata	Kaczmarska & Licea
Pleurosigma nicobaricum	Grunow
Pleurosigma spp.	
Opephora martyi	Heribaud
Raphoneis amphiceros	Ehrenberg/(Gregory) Grunow
Raphoneis cf nitida	(Gregory) Grunow
Raphoneis spp.	
Surirella linearis	W. Smith
Synedra ulna	(Nitzsch.) Ehrenberg
Tetracyclus rupestris	(Braun) Grunow
Thalassionema bacillare	Heiden in Heiden & Kolbe
Thalassionema nitzschioides	Grunow
Thalassionema nitzschioides parva	Heiden & Kolbe
Thalassiotrix longissima	Cleve & Grunow

Table B.4 – Relative percentages for species that have >2% for 100% closure.

	Grouped as Benthic		Grouped as Freshwater		
Species	W8809-11GC	W8909-24GC	TT39-15 REF	TT39-5AC REF	W8306-A1-RKC*
Actinocyclus curvatulus	0.53	0.31	1.91	0.00	0.91
Actinocyclus normanii	1.32	0.31	1.59	1.19	1.37
Actinoptychus senarius	1.85	1.88	2.23	0.30	3.19
Stephanodiscus rotula (forma minutula)	0.00	0.00	0.00	0.00	0.46
Aulacoseira islandica	0.00	0.00	0.95	1.19	0.00
Aulacoseira granulata	0.00	0.00	0.32	0.89	0.00
Aulacoseira spp.	0.00	0.00	0.00	0.00	0.00
Bacteriastrum spp.	0.00	0.00	0.00	0.30	0.00
Chaetoceros resting spores	60.16	36.42	27.34	15.50	24.57
Coscinodiscus decrescens	0.00	0.00	0.00	0.00	0.00
Coscinodiscus marginatus	0.53	0.00	3.50	1.19	0.91
Coscinodiscus radiatus	0.53	5.97	7.00	4.17	5.46
Cyclotella litoralis	0.00	1.57	0.32	0.00	0.46
Cyclotella ocellata	0.00	0.00	0.00	0.00	0.00
Cyclotella spp.	0.53	0.00	2.23	0.00	1.37
Cyclotella striata	0.53	0.00	0.32	0.30	0.46
Hemidiscus cuneiformis	1.06	1.57	0.32	0.00	0.00
Leptocylindrus resting spores	1.32	0.31	0.00	0.30	2.73
Melosira ambigua	0.00	0.00	0.00	0.00	0.00
Odontella aurita	0.00	0.31	0.00	0.00	2.28
Paralia sulcata	0.00	0.00	9.22	1.49	2.73
Rhizosolenia setigera	0.00	0.31	0.00	0.00	0.00
Rhizosolenia hebetata (forma hebetatata)	1.32	1.57	2.86	4.47	2.73
Rhizosolenia styliformis	0.00	0.31	0.32	0.00	0.00
Roperia tesselata	1.06	0.63	0.32	0.00	0.46
Thalassiossira allenii	0.00	0.00	0.32	0.00	0.46
Thalassiossira anguste-lineata	0.79	2.51	0.32	0.89	0.46
Thalassiossira angulata	0.53	0.94	0.95	1.49	0.00
Thalassiossira eccentrica	0.00	0.00	0.95	1.49	1.82
Thalassiossira leptotus	0.26	0.00	0.00	0.00	0.00
Thalassiossira lineata	0.00	0.00	0.00	0.00	2.28
Thalassiossira nanolineata	0.00	0.00	0.00	0.00	0.00
Thalassiossira oestrupii	0.79	0.94	2.86	4.17	1.37
Thalassiossira cf poroseriata	0.00	0.00	0.64	0.00	0.00
Thalassiossira cf trifulta	0.00	0.00	0.00	0.00	0.00
Thalassiossira sp1	0.00	1.26	0.95	2.98	0.46
Thalassiossira sp2	0.53	0.00	0.32	0.00	0.00
Thalassiossira sp6	0.00	0.00	0.00	0.00	0.00
Thalassiossira spp.	0.00	0.31	0.00	0.00	0.00
Cocconeis placentula	0.00	0.00	0.64	0.00	0.00
Cocconeis sp1	0.00	0.00	0.00	0.00	0.00
Delphineis surilella	0.00	0.00	0.00	0.00	0.00
Epithemia turgida	0.00	0.00	0.16	0.15	0.11
Fragilaria construens	0.00	0.00	0.00	1.94	1.48
Fragilariopsis doliolus	4.22	7.69	2.23	4.92	3.75
Gomphonema constrictum	0.00	0.00	0.00	0.00	0.00
Lioloma elongatum	0.40	0.47	0.79	0.60	0.46
Lioloma pacificum	0.40	0.63	0.32	0.75	0.57
Lioloma spp.	0.00	0.00	0.00	0.89	0.68
Neodenticula seminae	0.79	1.57	5.72	29.06	22.18
Nitzschia gp bicapitata	0.00	0.00	0.32	0.30	0.23
Raphoneis amphiceros	0.26	1.41	0.00	0.00	0.00
Thalassionema bacillare	0.26	1.73	0.00	0.00	0.00
Thalassionema nitzschioides	19.13	26.22	14.63	16.39	12.51

(continued on next page)

Table B.4 (continued)

Grouped as Benthic | Grouped as Freshwater

Species	LG-85-NC 3GC	W8508-9GC	W7905-160G	W9205-1GC	7407Y-1 REF
Actinocyclus curvatulus	0.66	0.00	0.31	0.00	0.00
Actinocyclus normanii	0.99	0.32	0.31	0.00	1.95
Actinoptychus senarius	0.00	2.59	1.56	1.36	0.33
Stephanodiscus rotula (forma minutula)	0.33	0.00	0.93	0.34	0.00
Aulacoseira islandica	0.00	0.00	0.00	0.00	0.00
Aulacoseira granulata	0.00	0.00	0.00	0.00	0.00
Aulacoseira spp.	0.00	0.00	0.00	0.00	0.00
Bacteriastrum spp.	0.00	0.00	0.00	0.00	0.00
Chaetoceros resting spores	22.44	48.95	54.52	64.52	28.99
Coscinodiscus decrescens	0.00	0.00	0.00	0.00	0.00
Coscinodiscus marginatus	0.33	0.00	0.62	0.68	0.00
Coscinodiscus radiatus	2.97	3.57	1.25	1.70	2.61
Cyclotella litoralis	0.00	0.00	0.00	0.00	0.00
Cyclotella ocellata	0.00	0.00	0.00	0.00	0.00
Cyclotella spp.	0.99	0.65	0.31	0.68	0.33
Cyclotella striata	0.33	0.32	1.25	0.68	0.33
Hemidiscus cuneiformis	0.33	0.32	0.00	0.34	0.98
Leptocylindrus resting spores	1.32	0.32	1.56	1.02	0.00
Melosira ambigua	0.00	0.65	0.00	0.34	0.00
Odontella aurita	0.00	0.00	0.00	0.00	0.33
Paralia sulcata	0.66	0.97	2.18	1.36	0.33
Rhizosolenia setigera	0.00	0.00	0.00	0.00	0.00
Rhizosolenia hebetata (forma hebetatata)	2.97	0.00	0.31	1.70	0.33
Rhizosolenia styliformis	0.00	6.81	0.00	0.00	0.00
Roperia tesselata	1.32	0.00	0.00	1.02	2.28
Thalassiossira allenii	0.33	0.00	0.00	0.00	0.00
Thalassiossira anguste-lineata	0.33	0.32	1.87	0.68	0.33
Thalassiossira angulata	0.33	0.00	0.00	0.00	0.65
Thalassiossira eccentrica	2.31	0.65	0.00	0.34	1.63
Thalassiossira leptotus	0.00	0.00	0.00	0.00	0.00
Thalassiossira lineata	0.66	0.00	0.00	1.36	0.00
Thalassiossira nanolineata	0.00	0.00	0.31	0.00	0.00
Thalassiossira oestrupii	2.31	2.92	0.93	0.34	4.56
Thalassiossira cf poroseriata	1.65	0.00	0.00	0.00	0.00
Thalassiossira cf trifulta	0.00	0.00	0.00	0.00	0.00
Thalassiossira sp1	0.33	0.00	0.31	0.34	0.00
Thalassiossira sp2	0.00	0.00	0.00	0.00	0.00
Thalassiossira sp6	0.00	0.00	0.00	0.00	0.00
Thalassiossira spp.	0.00	0.00	0.00	0.34	0.00
Cocconeis placentula	0.00	0.49	0.31	0.00	0.00
Cocconeis sp1	0.00	0.00	0.00	0.00	0.00
Delphineis surilella	0.33	0.81	0.62	0.68	0.65
Epithemia turgida	0.00	0.00	0.00	0.00	0.00
Fragilaria construens	0.00	0.00	0.00	0.00	0.00
Fragilariopsis doliolus	11.06	0.97	3.43	1.36	11.40
Gomphonema constrictum	0.00	0.00	0.00	0.00	0.00
Lioloma elongatum	0.50	0.97	0.31	0.17	0.49
Lioloma pacificum	1.32	1.78	0.31	0.17	0.65
Lioloma spp.	1.49	1.30	0.78	0.51	0.98
Neodenticula seminae	0.33	0.65	0.00	0.51	3.91
Nitzschia gp bicapitata	0.17	0.00	0.00	0.00	0.33
Raphoneis amphiceros	0.00	0.49	0.31	0.00	0.00
Thalassionema bacillare	0.33	0.00	0.31	0.00	0.65
Thalassionema nitzschioides	35.81	18.31	19.94	15.45	31.92

(continued on next page)

Table B.4 (continued)

Grouped as Benthic

Grouped as Freshwater

Species	TT39-18 AC REF	TT29-22 AC REF	TT39-11 AC REF	TT31-011 GC REF	Y73-10-100 GC
Actinocyclus curvatulus	0.68	0.38	0.32	1.37	0.90
Actinocyclus normanii	1.03	0.38	1.26	0.00	0.00
Actinoptychus senarius	0.34	0.00	0.32	0.00	0.90
Stephanodiscus rotula (forma minutula)	0.00	0.75	0.00	0.34	0.00
Aulacoseira islandica	1.03	1.13	1.58	0.00	0.00
Aulacoseira granulata	1.03	0.38	0.32	0.00	0.00
Aulacoseira spp.	0.34	0.00	0.32	0.00	0.90
Bacteriastrum spp.	0.00	0.00	0.00	0.00	0.90
Chaetoceros resting spores	32.53	25.66	41.32	1.03	41.26
Coscinodiscus decrescens	0.00	0.38	0.00	6.84	4.48
Coscinodiscus marginatus	1.03	0.75	0.32	2.74	0.00
Coscinodiscus radiatus	3.08	3.02	3.15	6.15	3.59
Cyclotella litoralis	2.05	2.26	0.63	0.34	0.00
Cyclotella ocellata	0.00	0.00	0.32	0.00	0.00
Cyclotella spp.	2.40	2.26	0.00	1.03	0.00
Cyclotella striata	0.00	0.38	2.52	0.00	0.00
Hemidiscus cuneiformis	0.34	0.00	0.32	1.03	0.00
Leptocylindrus resting spores	0.00	1.51	0.32	0.00	0.90
Melosira ambigua	1.03	0.75	0.00	0.00	0.00
Odontella aurita	0.00	0.00	0.00	0.00	0.00
Paralia sulcata	4.11	1.89	6.62	0.00	0.00
Rhizosolenia setigera	0.00	0.00	0.00	0.00	0.00
Rhizosolenia hebetata (forma hebetatata)	3.42	6.04	2.21	10.60	1.79
Rhizosolenia styliformis	0.00	0.00	0.00	0.00	0.00
Roperia tesselata	0.34	0.38	0.00	0.00	0.00
Thalassiossira allenii	0.00	0.00	1.58	0.00	0.90
Thalassiossira anguste-lineata	0.00	0.00	0.32	0.00	0.00
Thalassiossira angulata	0.00	0.00	1.58	0.00	0.00
Thalassiossira eccentrica	1.71	1.89	0.00	7.86	1.79
Thalassiossira leptotus	0.68	0.38	0.00	2.74	0.00
Thalassiossira lineata	0.00	0.00	0.00	0.00	0.00
Thalassiossira nanolineata	0.00	0.00	0.00	0.00	1.79
Thalassiossira oestrupii	4.45	3.02	1.26	15.73	0.00
Thalassiossira cf poroseriata	0.00	0.00	0.00	0.00	0.00
Thalassiossira cf trifulta	0.00	0.00	0.00	2.74	0.00
Thalassiossira sp1	0.00	0.00	2.21	6.15	0.90
Thalassiossira sp2	0.00	0.00	0.32	0.00	0.00
Thalassiossira sp6	0.00	0.00	0.00	2.39	0.00
Thalassiossira spp.	0.00	1.13	0.00	3.42	0.00
Cocconeis placentula	0.17	0.38	0.47	0.00	0.00
Cocconeis sp1	0.00	0.00	0.00	0.00	0.00
Delphineis surilella	0.34	0.38	0.00	0.00	0.90
Epithemia turgida	0.00	0.00	0.00	0.00	0.00
Fragilaria construens	0.34	0.00	1.10	0.00	5.83
Fragilariopsis doliolus	2.23	0.94	1.26	4.27	0.90
Gomphonema constrictum	0.00	0.00	0.00	0.00	0.00
Lioloma elongatum	0.17	0.38	1.10	1.37	0.90
Lioloma pacificum	0.51	0.94	0.16	1.20	0.00
Lioloma spp.	1.03	2.83	0.00	3.76	2.69
Neodenticula seminae	4.45	7.92	3.15	7.35	2.24
Nitzschia gp bicapitata	0.51	1.51	0.79	0.00	0.00
Raphoneis amphiceros	0.00	0.00	0.00	0.00	0.45
Thalassionema bacillare	1.03	0.38	0.79	0.17	0.00
Thalassionema nitzschioides	20.03	19.06	17.35	6.67	25.11

(continued on next page)

Table B.4 (continued)

		Grouped as Benthic		Grouped as Freshwater	
Species	W8209-19 GC	TT68-18 AC	TT39-19 REF	TT68-PC 27 REF	Y7409-15 24GC
Actinocyclus curvatulus	0.00	0.00	0.89	0.89	1.01
Actinocyclus normanii	0.00	0.75	0.89	0.00	4.04
Actinoptychus senarius	0.35	3.74	0.00	0.89	4.04
Stephanodiscus rotula (forma minutula)	1.05	1.87	1.79	1.79	4.04
Aulacoseira islandica	0.00	1.12	0.00	0.89	3.03
Aulacoseira granulata	0.00	1.87	0.00	0.00	0.00
Aulacoseira spp.	0.00	0.00	0.00	0.00	3.03
Bacteriastrum spp.	0.00	0.37	0.00	0.00	5.05
Chaetoceros resting spores	38.39	29.16	21.43	41.96	9.09
Coscinodiscus decrescens	0.00	0.00	2.68	0.00	0.00
Coscinodiscus marginatus	0.70	1.12	1.79	0.00	0.00
Coscinodiscus radiatus	2.79	3.36	0.00	2.68	1.01
Cyclotella litoralis	0.00	0.00	0.89	0.00	0.00
Cyclotella ocellata	0.35	0.75	0.00	0.00	2.02
Cyclotella spp.	0.35	1.12	0.00	0.89	1.01
Cyclotella striata	0.70	1.50	0.00	0.89	1.01
Hemidiscus cuneiformis	0.00	0.37	0.89	0.00	0.00
Leptocylindrus resting spores	1.75	0.00	0.00	1.79	1.01
Melosira ambigua	0.00	0.37	0.89	1.79	2.02
Odontella aurita	0.00	0.37	0.89	0.89	1.01
Paralia sulcata	2.44	0.75	0.89	0.00	4.04
Rhizosolenia setigera	0.35	0.00	0.00	0.00	0.00
Rhizosolenia hebetata (forma hebetatata)	4.89	1.12	16.07	0.89	0.00
Rhizosolenia styliformis	0.00	0.00	0.00	0.00	1.01
Roperia tesselata	0.00	0.00	0.00	0.00	0.00
Thalassiossira allenii	1.05	0.00	0.00	0.00	0.00
Thalassiossira anguste-lineata	0.00	0.00	0.00	0.00	0.00
Thalassiossira angulata	0.00	0.37	0.00	0.00	0.00
Thalassiossira eccentrica	0.00	0.75	0.89	0.00	14.14
Thalassiossira leptotus	0.00	1.50	1.79	0.89	0.00
Thalassiossira lineata	0.00	0.00	0.00	0.00	0.00
Thalassiossira nanolineata	0.00	0.00	0.00	0.00	0.00
Thalassiossira oestrupii	0.00	0.00	0.89	2.68	0.00
Thalassiossira cf poroseriata	0.00	0.00	0.00	0.00	0.00
Thalassiossira cf trifulta	0.00	0.00	0.00	0.00	0.00
Thalassiossira sp1	0.00	0.00	1.79	1.79	0.00
Thalassiossira sp2	0.00	0.00	0.00	0.00	0.00
Thalassiossira sp6	0.00	0.00	0.00	0.00	0.00
Thalassiossira spp.	1.75	1.87	7.14	0.89	0.00
Cocconeis placentula	0.35	1.50	0.00	0.45	4.04
Cocconeis sp1	0.00	0.00	0.00	0.00	2.02
Delphineis surilella	0.00	0.00	0.00	0.00	1.94
Epithemia turgida	0.17	1.50	0.00	0.89	3.54
Fragilaria construens	0.00	0.00	0.89	1.79	1.01
Fragilariopsis doliolus	2.44	2.24	1.34	3.13	0.00
Gomphonema constrictum	0.00	0.00	0.00	0.00	3.03
Lioloma elongatum	0.17	0.00	2.23	0.00	0.00
Lioloma pacificum	1.22	0.75	2.23	0.89	0.00
Lioloma spp.	0.70	0.00	2.68	1.34	0.00
Neodenticula seminae	0.87	0.93	8.48	1.79	0.00
Nitzschia gp bicapitata	0.17	6.54	0.45	2.23	0.00
Raphoneis amphiceros	0.87	1.12	0.00	0.89	1.52
Thalassionema bacillare	0.17	0.56	0.00	0.00	0.00
Thalassionema nitzschioides	34.21	24.11	17.41	20.09	12.63

(continued on next page)

Table B.4 (continued)

	Grouped as Benthic		Grouped as Freshwater		
Species	W7905-163G	W7905-109G	W8809A-19GC	Y6908-5A	W8909-31
Actinocyclus curvatulus	1.63	0.00	0.99	1.84	0.00
Actinocyclus normanii	0.00	0.00	0.00	0.00	0.00
Actinoptychus senarius	4.60	1.83	1.97	0.00	2.24
Stephanodiscus rotula (forma minutula)	0.00	0.61	0.00	0.46	0.00
Aulacoseira islandica	0.00	2.74	0.00	3.23	0.37
Aulacoseira granulata	0.32	0.00	0.00	3.23	0.00
Aulacoseira spp.	0.00	0.00	0.00	0.00	0.00
Bacteriastrum spp.	0.98	0.30	0.00	0.92	0.37
Chaetoceros resting spores	50.49	55.10	39.14	12.44	36.26
Coscinodiscus decrescens	0.00	0.00	0.00	0.00	0.00
Coscinodiscus marginatus	0.65	0.00	0.66	9.68	1.12
Coscinodiscus radiatus	2.28	1.22	4.28	0.92	4.86
Cyclotella litoralis	1.95	0.91	0.00	0.00	1.50
Cyclotella ocellata	0.00	0.00	0.00	0.00	0.00
Cyclotella spp.	0.00	2.74	0.66	0.00	1.50
Cyclotella striata	0.98	0.30	0.00	0.00	0.00
Hemidiscus cuneiformis	0.65	0.30	0.00	0.00	0.37
Leptocylindrus resting spores	3.91	0.30	0.33	0.00	0.00
Melosira ambigua	0.00	3.04	0.00	0.46	0.00
Odontella aurita	2.93	0.30	0.99	0.00	0.00
Paralia sulcata	5.54	2.13	0.33	0.46	1.87
Rhizosolenia setigera	0.00	0.30	1.64	0.00	0.00
Rhizosolenia hebetata (forma hebetatata)	1.63	1.22	2.30	23.96	8.22
Rhizosolenia styliformis	0.00	0.00	0.00	0.00	0.00
Roperia tesselata	0.98	0.00	1.97	0.00	0.37
Thalassiossira allenii	0.00	0.00	0.00	0.00	0.00
Thalassiossira anguste-lineata	0.32	0.00	0.00	0.00	0.00
Thalassiossira angulata	0.00	0.00	0.00	0.00	0.00
Thalassiossira eccentrica	2.28	1.22	2.63	0.00	1.50
Thalassiossira leptotus	0.32	0.00	0.99	0.46	1.87
Thalassiossira lineata	0.32	0.00	0.00	0.00	0.00
Thalassiossira nanolineata	0.00	0.00	0.00	0.00	0.00
Thalassiossira oestrupii	0.65	0.30	0.99	3.23	2.24
Thalassiossira cf poroseriata	0.00	0.00	0.00	0.00	0.00
Thalassiossira cf trifulta	0.00	0.00	0.00	0.00	0.00
Thalassiossira sp1	0.00	0.61	0.99	2.76	0.00
Thalassiossira sp2	0.00	0.00	0.00	9.22	1.50
Thalassiossira sp6	0.00	0.00	0.00	0.00	0.00
Thalassiossira spp.	0.32	0.30	0.00	0.92	0.37
Cocconeis placentula	0.00	0.15	0.00	0.00	0.00
Cocconeis sp1	0.00	0.00	0.00	0.00	0.00
Delphineis surilella	0.00	0.00	0.00	0.00	0.00
Epithemia turgida	0.16	0.00	0.00	0.00	0.00
Fragilaria construens	0.00	0.76	0.00	0.23	0.00
Fragilariopsis doliolus	1.47	0.61	5.59	0.23	1.87
Gomphonema constrictum	0.00	0.00	0.00	0.00	0.00
Lioloma elongatum	0.16	0.30	0.49	2.07	0.00
Lioloma pacificum	0.49	0.00	0.82	1.15	1.87
Lioloma spp.	0.65	0.76	0.82	6.45	2.24
Neodenticula seminae	0.00	0.91	1.81	3.69	0.37
Nitzschia gp bicapitata	0.00	1.52	0.16	0.46	0.00
Raphoneis amphiceros	0.65	2.13	0.33	0.00	1.12
Thalassionema bacillare	0.00	0.00	0.00	0.00	0.00
Thalassionema nitzschioides	8.96	14.31	28.13	9.68	23.93

(continued on next page)

Table B.4 (continued)

	Grouped as Benthic		Grouped as Freshwater		
Species	AT8408-17	W7610B1-7MGREF	W89097GC	TT39-AC12REF	MD02-2499
Actinocyclus curvatulus	0.35	1.32	1.50	1.58	0.47
Actinocyclus normanii	0.00	0.00	0.00	1.27	0.00
Actinoptychus senarius	1.06	1.32	1.85	0.82	3.27
Stephanodiscus rotula (forma minutula)	0.35	0.00	0.00	0.00	0.00
Aulacoseira islandica	0.71	0.33	0.00	1.27	0.47
Aulacoseira granulata	0.00	0.00	0.37	0.00	0.00
Aulacoseira spp.	0.00	0.00	0.00	0.00	0.00
Bacteriastrum spp.	0.00	0.00	0.75	1.27	0.00
Chaetoceros resting spores	43.26	58.88	43.44	33.54	36.70
Coscinodiscus decrescens	0.00	0.00	0.00	0.00	0.00
Coscinodiscus marginatus	0.00	0.00	1.17	0.99	7.53
Coscinodiscus radiatus	1.77	1.32	4.87	1.90	5.18
Cyclotella litoralis	0.71	1.32	0.00	0.63	0.00
Cyclotella ocellata	0.71	0.33	0.00	0.00	0.47
Cyclotella spp.	0.00	0.99	0.75	1.58	8.47
Cyclotella striata	0.35	0.66	2.62	0.00	0.00
Hemidiscus cuneiformis	0.00	0.00	0.75	0.00	0.94
Leptocylindrus resting spores	1.77	3.29	2.62	3.16	6.12
Melosira ambigua	0.00	0.66	0.00	0.00	0.00
Odontella aurita	0.35	0.33	0.37	0.00	0.47
Paralia sulcata	0.71	2.63	0.75	3.80	2.82
Rhizosolenia setigera	0.00	0.00	0.00	0.00	0.00
Rhizosolenia hebetata (forma hebetatata)	0.71	2.96	2.25	2.21	1.41
Rhizosolenia styliformis	0.00	0.00	0.00	0.00	0.00
Roperia tesselata	0.00	0.00	1.50	0.00	0.00
Thalassiossira allenii	0.00	0.00	0.00	0.00	0.00
Thalassiossira anguste-lineata	0.00	0.00	0.37	0.00	0.00
Thalassiossira angulata	0.00	0.00	0.00	0.00	0.00
Thalassiossira eccentrica	3.90	1.64	2.25	4.43	0.94
Thalassiossira leptotus	1.06	0.33	1.87	0.00	0.00
Thalassiossira lineata	0.00	0.00	0.00	0.00	0.47
Thalassiossira nanolineata	0.00	0.00	0.00	0.00	0.00
Thalassiossira oestrupii	3.19	0.00	1.50	1.90	1.41
Thalassiossira cf poroseriata	0.00	0.00	0.00	0.00	0.00
Thalassiossira cf trifulta	0.00	0.00	0.00	0.00	0.00
Thalassiossira sp1	0.35	0.00	0.00	1.27	0.00
Thalassiossira sp2	1.42	0.00	0.00	0.00	0.00
Thalassiossira sp6	0.00	0.00	0.00	0.00	0.00
Thalassiossira spp.	0.71	0.00	1.87	2.53	1.41
Cocconeis placentula	0.89	0.00	0.00	0.32	0.24
Cocconeis sp1	0.00	0.00	0.00	0.00	0.00
Delphineis surilella	0.00	0.00	0.00	0.00	0.00
Epithemia turgida	0.00	0.16	0.00	0.32	0.47
Fragilaria construens	0.00	0.99	0.00	0.00	0.00
Fragilariopsis doliolus	2.48	0.33	5.61	2.37	0.47
Gomphonema constrictum	0.00	0.00	0.00	0.00	0.00
Lioloma elongatum	0.18	0.16	0.00	0.32	0.94
Lioloma pacificum	0.35	0.49	0.37	0.32	1.65
Lioloma spp.	0.35	1.51	0.37	0.63	0.24
Neodenticula seminae	5.68	0.82	1.12	6.01	0.24
Nitzschia gp bicapitata	0.35	0.33	0.37	0.47	0.00
Raphoneis amphiceros	0.00	1.51	0.37	0.32	0.47
Thalassionema bacillare	0.00	0.00	0.00	0.32	0.24
Thalassionema nitzschioides	23.58	14.47	15.74	18.67	13.40

Table B.5 – Correlation coefficients between ocean properties and factors for sub-areas north and south of 46°N (gray boxes indicate significant correlations for p=0.05).

South of 46°N		Factor 1	Factor 2	Factor 3	Factor 4	Factor 5
	annual	0.49	-0.49	-0.53	-0.01	-0.33
	winter	0.27	0.21	-0.16	-0.56	0.16
Productivity	spring	0.30	-0.45	-0.32	0.20	-0.11
	summer	0.51	-0.60	-0.61	0.09	-0.54
	fall	0.69	-0.51	-0.73	-0.29	-0.45
	annual	-0.35	0.55	0.44	-0.25	0.38
	winter	-0.28	0.58	0.38	-0.30	0.56
Temperature	spring	-0.05	0.66	0.26	-0.26	-0.26
	summer	-0.26	0.25	0.24	-0.05	-0.15
	fall	-0.38	0.59	0.48	-0.26	0.45
	annual	-0.22	0.69	0.32	-0.46	0.65
	winter	-0.18	0.69	0.25	-0.50	0.58
Salinity	spring	-0.24	0.71	0.33	-0.47	0.64
	summer	-0.26	0.64	0.37	-0.38	0.69
	fall	-0.21	0.66	0.31	-0.42	0.65
	annual	0.38	-0.60	-0.52	0.29	-0.64
	winter	0.34	-0.60	-0.40	0.29	-0.24
Chlorophyll	spring	0.38	-0.77	-0.49	0.41	-0.59
	summer	0.33	-0.45	-0.48	0.21	-0.63
	fall	0.39	-0.54	-0.53	0.23	-0.57
	annual	0.21	-0.50	-0.33	0.37	-0.64
	winter	0.21	-0.52	-0.34	0.33	-0.68
Nitrate	spring	0.07	-0.15	-0.16	0.20	-0.30
	summer	0.08	-0.30	-0.18	0.35	-0.45
	fall	0.19	-0.36	-0.21	0.28	-0.15
	annual	-0.04	0.13	0.11	-0.02	0.39
	winter	0.24	-0.53	-0.33	0.32	-0.49
Silicate	spring	-0.22	0.41	0.33	-0.14	0.56
	summer	-0.23	0.48	0.36	-0.22	0.68
	fall	-0.01	0.19	0.08	-0.11	0.43
	annual	0.26	-0.70	-0.38	0.46	-0.65
	winter	0.13	-0.53	-0.27	0.42	-0.72
Phosphate	spring	0.27	-0.74	-0.37	0.47	-0.62
	summer	0.29	-0.68	-0.41	0.42	-0.69
	fall	0.24	-0.49	-0.25	0.31	-0.12

(continued on next page)

Table B.5 (continued)

North of 46^{0}N		Factor 1	Factor 2	Factor 3	Factor 4	Factor 5
	annual	0.22	0.01	-0.50	-0.09	0.47
	winter	0.13	-0.02	-0.46	-0.12	0.47
Productivity	spring	0.43	0.23	-0.69	-0.03	0.43
	summer	0.01	0.00	0.25	0.09	-0.21
	fall	-0.10	-0.28	-0.24	-0.15	0.51
	annual	-0.31	-0.40	0.08	-0.06	0.27
	winter	-0.23	-0.37	-0.05	-0.11	0.36
Temperature	spring	-0.05	-0.21	-0.27	-0.15	0.51
	summer	-0.42	-0.44	0.28	0.03	0.06
	fall	-0.48	-0.50	0.33	0.01	0.07
	annual	-0.08	0.09	0.55	0.30	-0.85
	winter	-0.03	0.14	0.51	0.33	-0.87
Salinity	spring	-0.08	0.10	0.54	0.31	-0.84
	summer	-0.12	0.06	0.58	0.26	-0.82
	fall	-0.14	0.03	0.59	0.31	-0.86
	annual	0.33	0.11	-0.69	-0.27	0.70
	winter	0.47	0.42	-0.47	-0.14	0.21
Chlorophyll	spring	0.43	0.24	-0.71	-0.25	0.62
	summer	0.20	-0.03	-0.61	-0.27	0.72
	fall	0.24	-0.01	-0.64	-0.26	0.72
	annual	0.14	0.26	-0.01	0.04	-0.15
	winter	0.22	0.35	-0.09	0.04	-0.13
Nitrate	spring	-0.31	-0.10	0.49	0.10	-0.36
	summer	0.27	0.32	-0.20	-0.08	0.00
	fall	0.42	0.43	-0.35	0.02	0.01
	annual	-0.31	-0.01	0.56	0.06	-0.43
	winter	-0.02	0.28	0.30	0.06	-0.38
Silicate	spring	-0.65	-0.40	0.78	0.11	-0.39
	summer	-0.47	-0.24	0.64	0.06	-0.35
	fall	0.50	0.54	-0.37	-0.07	-0.03
	annual	0.42	0.31	-0.62	-0.21	0.52
	winter	0.38	0.28	-0.62	-0.21	0.56
Phosphate	spring	-0.33	-0.38	-0.21	-0.31	0.84
	summer	0.53	0.43	-0.61	-0.16	0.35
	fall	0.54	0.45	-0.53	-0.09	0.20

(continued on next page)

Table B.5 (continued)

South of 46^{0}N		Factor 1	Factor 2	Factor 3	Factor 4	Factor 5
	annual	0.45	-0.69	-0.49	0.26	-0.31
	winter	0.32	-0.47	-0.44	0.14	0.01
wind stress	spring	0.42	-0.67	-0.33	0.27	-0.24
curl	summer	0.45	-0.60	-0.58	0.21	-0.28
	fall	0.35	-0.63	-0.34	0.27	-0.44
	annual	0.61	0.67	-0.55	0.00	0.65
	winter	0.58	0.66	-0.55	0.03	0.71
wind stress	spring	0.44	0.45	-0.39	-0.09	0.40
curl	summer	0.66	0.52	-0.61	-0.07	0.39
	fall	0.28	0.51	-0.22	0.05	0.54

Table B.6 – Correlation coefficients between ocean properties and factors for sub-areas west and east of 127°W (gray boxes indicate significant correlations for p=0.05).

West of 127°W		Factor 1	Factor 2	Factor 3	Factor 4	Factor 5
	annual	-0.02	-0.46	0.19	0.34	-0.18
	winter	0.13	0.78	-0.37	-0.32	0.15
Productivity	spring	-0.07	-0.76	0.32	0.39	-0.18
	summer	-0.12	-0.78	0.38	0.33	-0.18
	fall	0.09	0.78	-0.35	-0.30	0.13
	annual	-0.14	0.61	-0.12	-0.21	-0.08
	winter	-0.03	0.67	-0.21	-0.25	-0.01
Temperature	spring	0.00	0.70	-0.24	-0.19	-0.02
	summer	-0.33	0.44	0.07	-0.12	-0.21
	fall	-0.18	0.57	-0.07	-0.23	-0.08
	annual	-0.30	0.36	0.15	-0.50	-0.06
	winter	-0.29	0.42	0.12	-0.48	-0.08
Salinity	spring	-0.31	0.34	0.15	-0.50	-0.03
	summer	-0.28	0.20	0.20	-0.52	-0.06
	fall	-0.26	0.47	0.05	-0.41	-0.08
	annual	0.57	0.14	-0.49	0.21	0.21
	winter	0.39	-0.39	-0.13	0.12	0.24
Chlorophyll	spring	0.37	-0.37	-0.13	0.31	0.05
	summer	0.33	0.66	-0.52	0.00	0.16
	fall	0.47	0.76	-0.67	-0.06	0.24
	annual	0.06	-0.65	0.17	0.21	0.10
	winter	0.02	-0.69	0.22	0.28	0.00
Nitrate	spring	-0.26	-0.73	0.42	0.12	-0.01
	summer	0.18	-0.55	0.06	0.14	0.14
	fall	0.36	-0.41	-0.13	0.16	0.32
	annual	-0.24	-0.80	0.48	0.21	-0.16
	winter	-0.12	-0.76	0.37	0.30	-0.14
Silicate	spring	-0.72	-0.73	0.78	0.14	-0.43
	summer	-0.46	-0.57	0.54	-0.08	-0.07
	fall	0.34	-0.39	-0.06	0.11	0.15
	annual	0.36	-0.41	-0.13	0.19	0.24
	winter	0.40	-0.34	-0.20	0.17	0.33
Phosphate	spring	-0.37	-0.80	0.48	0.36	-0.18
	summer	0.42	-0.37	-0.17	0.17	0.21
	fall	0.53	-0.25	-0.29	0.10	0.34

(continued on next page)

Table B.6 (continued)

East of 127^{0}W		Factor 1	Factor 2	Factor 3	Factor 4	Factor 5
	annual	0.19	0.25	-0.12	0.00	-0.33
	winter	0.30	0.42	-0.17	-0.13	-0.41
Productivity	spring	-0.18	0.07	0.28	0.14	0.14
	summer	0.13	0.06	-0.23	0.05	-0.24
	fall	0.35	0.20	-0.24	-0.05	-0.48
	annual	0.23	0.02	-0.20	-0.06	-0.29
	winter	0.15	0.34	-0.01	-0.09	-0.25
Temperature	spring	-0.14	-0.08	-0.11	-0.08	0.09
	summer	0.25	-0.40	-0.41	0.02	-0.26
	fall	0.33	0.13	-0.15	-0.04	-0.41
	annual	0.60	0.56	-0.02	0.06	-0.76
	winter	0.64	0.49	-0.05	0.12	-0.83
Salinity	spring	0.61	0.57	-0.03	0.04	-0.76
	summer	0.52	0.63	0.07	-0.01	-0.64
	fall	0.56	0.55	-0.01	0.07	-0.74
	annual	-0.43	-0.27	-0.08	0.16	0.30
	winter	-0.54	-0.27	0.23	0.07	0.63
Chlorophyll	spring	-0.48	-0.57	0.04	0.09	0.59
	summer	-0.18	0.02	-0.15	0.13	-0.04
	fall	-0.24	-0.02	-0.08	0.15	0.03
	annual	-0.33	-0.23	0.10	0.07	0.39
	winter	-0.24	-0.39	-0.04	0.08	0.31
Nitrate	spring	-0.13	0.43	0.29	0.15	-0.01
	summer	-0.44	-0.08	0.20	0.02	0.50
	fall	-0.47	-0.01	0.30	0.00	0.56
	annual	-0.25	0.24	0.33	-0.11	0.37
	winter	-0.27	-0.23	0.12	0.00	0.40
Silicate	spring	-0.05	0.34	0.33	-0.10	0.15
	summer	-0.08	0.51	0.36	-0.15	0.13
	fall	-0.25	0.47	0.37	-0.15	0.32
	annual	-0.58	-0.45	0.09	0.00	0.71
	winter	-0.58	-0.46	0.03	0.00	0.69
Phosphate	spring	-0.58	-0.57	0.06	0.03	0.71
	summer	-0.51	-0.44	0.06	0.03	0.62
	fall	-0.58	-0.20	0.23	-0.08	0.74

(continued on next page)

Table B.6 (continued)

West of 127^{0}W		Factor 1	Factor 2	Factor 3	Factor 4	Factor 5
	annual	0.13	-0.54	0.13	0.34	0.10
	winter	0.17	-0.48	0.05	0.32	0.22
wind stress	spring	-0.09	-0.74	0.37	0.36	-0.15
curl	summer	0.16	-0.36	0.05	0.38	0.06
	fall	0.23	-0.47	0.03	0.24	0.22
East of 127^{0}W		**Factor 1**	**Factor 2**	**Factor 3**	**Factor 4**	**Factor 5**
	annual	0.02	-0.25	0.13	0.12	0.47
	winter	0.08	-0.03	0.14	-0.05	0.65
wind stress	spring	-0.03	-0.24	0.19	0.15	0.48
curl	summer	-0.06	-0.11	0.12	0.09	0.42
	fall	0.08	-0.48	-0.02	0.20	-0.01

APPENDIX C: Supplementary data for Chapter 3.

Table C.1 - Relative percentages for species that have >1% for 100% closure.

	Grouped as Benthic		Grouped as Freshwater		
Sample ID in figure 3.1	C1	C2	C3	C4	C5
Species	W8809-11GC	W8909-24GC	TT39-15 REF	TT39-5AC REF	W8306-A1-RKC*
Actinocyclus curvatulus	0.53	0.31	1.91	0.00	0.91
Actinocyclus normanii	1.32	0.31	1.59	1.19	1.37
Actinoptychus senarius	1.85	1.88	2.23	0.30	3.19
Stephanodiscus rotula (forma minutula)	0.00	0.00	0.00	0.00	0.46
Aulacoseira islandica	0.00	0.00	0.95	1.19	0.00
Aulacoseira granulata	0.00	0.00	0.32	0.89	0.00
Aulacoseira spp.	0.00	0.00	0.00	0.00	0.00
aulacosira italica	0.00	0.00	0.00	0.00	0.00
Bacteriastrum spp.	0.00	0.00	0.00	0.30	0.00
Chaetoceros resting spores	60.16	36.42	27.34	15.50	24.57
Coscinodiscus decrescens	0.00	0.00	0.00	0.00	0.00
Coscinodiscus oculus iridis	0.00	0.00	0.00	0.00	0.00
Coscinodiscus marginatus	0.53	0.00	3.50	1.19	0.91
Coscinodiscus radiatus	0.53	5.97	7.00	4.17	5.46
cyclotella kutzingiana	0.00	0.00	0.00	0.00	0.00
Cyclotella litoralis	0.00	1.57	0.32	0.00	0.46
Cyclotella ocellata	0.00	0.00	0.00	0.00	0.00
Cyclotella comta	0.00	0.00	0.00	0.00	0.00
Cyclotella spp.	0.53	0.00	2.23	0.00	1.37
Cyclotella striata	0.53	0.00	0.32	0.30	0.46
Hemidiscus cuneiformis	1.06	1.57	0.32	0.00	0.00
Leptocylindrus resting spores	1.32	0.31	0.00	0.30	2.73
Melosira ambigua	0.00	0.00	0.00	0.00	0.00
Melosira westi	0.00	0.00	1.27	0.00	0.00
melosira distans	0.00	0.00	0.00	0.00	0.00
Odontella aurita	0.00	0.31	0.00	0.00	2.28
Paralia sulcata	0.00	0.00	9.22	1.49	2.73
Rhizosolenia setigera	0.00	0.31	0.00	0.00	0.00
Rhizosolenia hebetata (forma hebetatata)	1.32	1.57	2.86	4.47	2.73
Rhizosolenia styliformis	0.00	0.31	0.32	0.00	0.00
Roperia tesselata	1.06	0.63	0.32	0.00	0.46
Stephanopyxis turris	0.00	0.00	0.00	0.00	0.00
Thalassiossira allenii	0.00	0.00	0.32	0.00	0.46
Thalassiossira anguste-lineata	0.79	2.51	0.32	0.89	0.46
Thalassiossira angulata/pacifica	0.53	0.94	0.95	1.49	0.00
Thalassiossira eccentrica	0.00	0.00	0.95	1.49	1.82
Thalassiossira leptotus	0.26	0.00	0.00	0.00	0.00
Thalassiossira lineata	0.00	0.00	0.00	0.00	2.28
Thalassiossira nanolineata	0.00	0.00	0.00	0.00	0.00
Thalassiossira oestrupii	0.79	0.94	2.86	4.17	1.37
Thalassiossira cf poroseriata	0.00	0.00	0.64	0.00	0.00
Thalassiossira cf trifulta	0.00	0.00	0.00	0.00	0.00
Thalassiossira sp1	0.00	1.26	0.95	2.98	0.46
Thalassiossira sp2	0.53	0.00	0.32	0.00	0.00
Thalassiossira sp6	0.00	0.00	0.00	0.00	0.00
Thalassiossira spp.	0.00	0.31	0.00	0.00	0.00
Cocconeis placentula	0.00	0.00	0.64	0.00	0.00
Cocconeis scutellum	0.00	0.00	0.32	0.00	0.00
Cocconeis sp1	0.00	0.00	0.00	0.00	0.00
Delphineis surilella	0.00	0.00	0.00	0.00	0.00
Epithemia turgida	0.00	0.00	0.16	0.15	0.11
Fragilaria construens	0.00	0.00	0.00	1.94	1.48
Delphineis karstenii	0.00	0.00	0.32	0.00	0.00
Fragilaria inflata	0.00	0.00	0.00	0.00	0.00
Fragilaria pinnata	0.00	0.00	0.00	0.00	0.00
Fragilariopsis doliolus	4.22	7.69	2.23	4.92	3.75
Gomphonema constrictum	0.00	0.00	0.00	0.00	0.00

(continued on next page)

Table C.1 (continued)

	Grouped as Benthic		Grouped as Freshwater		
Sample ID in figure 3.1	C6	C7	C8	C9	C10
Species	LG-85-NC 3GC	W8508-9GC	W7905-160G	W9205-1GC	7407Y-1 REF
Actinocyclus curvatulus	0.66	0.00	0.31	0.00	0.00
Actinocyclus normanii	0.99	0.32	0.31	0.00	1.95
Actinoptychus senarius	0.00	2.59	1.56	1.36	0.33
Stephanodiscus rotula (forma minutula)	0.33	0.00	0.93	0.34	0.00
Aulacoseira islandica	0.00	0.00	0.00	0.00	0.00
Aulacoseira granulata	0.00	0.00	0.00	0.00	0.00
Aulacoseira spp.	0.00	0.00	0.00	0.00	0.00
aulacosira italica	0.00	0.00	0.00	0.00	0.00
Bacteriastrum spp.	0.00	0.00	0.00	0.00	0.00
Chaetoceros resting spores	22.44	48.95	54.52	64.52	28.99
Coscinodiscus decrescens	0.00	0.00	0.00	0.00	0.00
Coscinodiscus oculus iridis	0.33	0.00	0.00	0.00	0.00
Coscinodiscus marginatus	0.33	0.00	0.62	0.68	0.00
Coscinodiscus radiatus	2.97	3.57	1.25	1.70	2.61
cyclotella kutzingiana	0.00	0.00	0.00	0.00	0.00
Cyclotella litoralis	0.00	0.00	0.00	0.00	0.00
Cyclotella ocellata	0.00	0.00	0.00	0.00	0.00
Cyclotella comta	0.00	0.00	0.00	0.00	0.00
Cyclotella spp.	0.99	0.65	0.31	0.68	0.33
Cyclotella striata	0.33	0.32	1.25	0.68	0.33
Hemidiscus cuneiformis	0.33	0.32	0.00	0.34	0.98
Leptocylindrus resting spores	1.32	0.32	1.56	1.02	0.00
Melosira ambigua	0.00	0.65	0.00	0.34	0.00
Melosira westi	0.00	0.00	0.00	0.00	0.00
melosira distans	0.00	0.00	0.00	0.00	0.00
Odontella aurita	0.00	0.00	0.00	0.00	0.33
Paralia sulcata	0.66	0.97	2.18	1.36	0.33
Rhizosolenia setigera	0.00	0.00	0.00	0.00	0.00
Rhizosolenia hebetata (forma hebetatata)	2.97	0.00	0.31	1.70	0.33
Rhizosolenia styliformis	0.00	6.81	0.00	0.00	0.00
Roperia tesselata	1.32	0.00	0.00	1.02	2.28
Stephanopyxis turris	0.00	0.00	0.00	0.00	0.00
Thalassiossira allenii	0.33	0.00	0.00	0.00	0.00
Thalassiossira anguste-lineata	0.33	0.32	1.87	0.68	0.33
Thalassiossira angulata/pacifica	0.33	0.00	0.00	0.00	0.65
Thalassiossira eccentrica	2.31	0.65	0.00	0.34	1.63
Thalassiossira leptotus	0.00	0.00	0.00	0.00	0.00
Thalassiossira lineata	0.66	0.00	0.00	1.36	0.00
Thalassiossira nanolineata	0.00	0.00	0.31	0.00	0.00
Thalassiossira oestrupii	2.31	2.92	0.93	0.34	4.56
Thalassiossira cf poroseriata	1.65	0.00	0.00	0.00	0.00
Thalassiossira cf trifulta	0.00	0.00	0.00	0.00	0.00
Thalassiossira sp1	0.33	0.00	0.31	0.34	0.00
Thalassiossira sp2	0.00	0.00	0.00	0.00	0.00
Thalassiossira sp6	0.00	0.00	0.00	0.00	0.00
Thalassiossira spp.	0.00	0.00	0.00	0.34	0.00
Cocconeis placentula	0.00	0.49	0.31	0.00	0.00
Cocconeis scutellum	0.00	0.00	0.16	0.00	0.00
Cocconeis sp1	0.00	0.00	0.00	0.00	0.00
Delphineis surilella	0.33	0.81	0.62	0.68	0.65
Epithemia turgida	0.00	0.00	0.00	0.00	0.00
Fragilaria construens	0.00	0.00	0.00	0.00	0.00
Delphineis karstenii	0.33	0.00	0.78	0.00	0.16
Fragilaria inflata	0.00	1.46	0.00	0.34	0.00
Fragilaria pinnata	0.00	0.00	0.00	0.00	0.00
Fragilariopsis doliolus	11.06	0.97	3.43	1.36	11.40
Gomphonema constrictum	0.00	0.00	0.00	0.00	0.00

(continued on next page)

Table C.1 (continued)

		Grouped as Benthic		Grouped as Freshwater	
Sample ID in figure 3.1	C11	C12	C13	C14	C15
Species	TT39-18 AC REF	TT29-22 AC REF	TT39-11 AC REF	TT31-011 GC REF	Y73-10-100 GC
Actinocyclus curvatulus	0.68	0.38	0.32	1.37	0.90
Actinocyclus normanii	1.03	0.38	1.26	0.00	0.00
Actinoptychus senarius	0.34	0.00	0.32	0.00	0.90
Stephanodiscus rotula (forma minutula)	0.00	0.75	0.00	0.34	0.00
Aulacoseira islandica	1.03	1.13	1.58	0.00	0.00
Aulacoseira granulata	1.03	0.38	0.32	0.00	0.00
Aulacoseira spp.	0.34	0.00	0.32	0.00	0.90
aulacosira italica	0.00	0.00	0.00	0.00	0.00
Bacteriastrum spp.	0.00	0.00	0.00	0.00	0.90
Chaetoceros resting spores	32.53	25.66	41.32	1.03	41.26
Coscinodiscus decrescens	0.00	0.38	0.00	6.84	4.48
Coscinodiscus oculus iridis	1.03	0.00	0.00	0.00	0.00
Coscinodiscus marginatus	1.03	0.75	0.32	2.74	0.00
Coscinodiscus radiatus	3.08	3.02	3.15	6.15	3.59
cyclotella kutzingiana	0.00	0.00	0.00	0.00	0.00
Cyclotella litoralis	2.05	2.26	0.63	0.34	0.00
Cyclotella ocellata	0.00	0.00	0.32	0.00	0.00
Cyclotella comta	0.00	0.00	0.00	0.00	0.00
Cyclotella spp.	2.40	2.26	0.00	1.03	0.00
Cyclotella striata	0.00	0.38	2.52	0.00	0.00
Hemidiscus cuneiformis	0.34	0.00	0.32	1.03	0.00
Leptocylindrus resting spores	0.00	1.51	0.32	0.00	0.90
Melosira ambigua	1.03	0.75	0.00	0.00	0.00
Melosira westi	0.00	0.00	0.63	0.00	0.00
melosira distans	0.00	0.00	0.00	0.00	0.00
Odontella aurita	0.00	0.00	0.00	0.00	0.00
Paralia sulcata	4.11	1.89	6.62	0.00	0.00
Rhizosolenia setigera	0.00	0.00	0.00	0.00	0.00
Rhizosolenia hebetata (forma hebetatata)	3.42	6.04	2.21	10.60	1.79
Rhizosolenia styliformis	0.00	0.00	0.00	0.00	0.00
Roperia tesselata	0.34	0.38	0.00	0.00	0.00
Stephanopyxis turris	0.00	0.00	0.00	0.34	0.00
Thalassiossira allenii	0.00	0.00	1.58	0.00	0.90
Thalassiossira anguste-lineata	0.00	0.00	0.32	0.00	0.00
Thalassiossira angulata/pacifica	0.00	0.00	1.58	0.00	0.00
Thalassiossira eccentrica	1.71	1.89	0.00	7.86	1.79
Thalassiossira leptotus	0.68	0.38	0.00	2.74	0.00
Thalassiossira lineata	0.00	0.00	0.00	0.00	0.00
Thalassiossira nanolineata	0.00	0.00	0.00	0.00	1.79
Thalassiossira oestrupii	4.45	3.02	1.26	15.73	0.00
Thalassiossira cf poroseriata	0.00	0.00	0.00	0.00	0.00
Thalassiossira cf trifulta	0.00	0.00	0.00	2.74	0.00
Thalassiossira sp1	0.00	0.00	2.21	6.15	0.90
Thalassiossira sp2	0.00	0.00	0.32	0.00	0.00
Thalassiossira sp6	0.00	0.00	0.00	2.39	0.00
Thalassiossira spp.	0.00	1.13	0.00	3.42	0.00
Cocconeis placentula	0.17	0.38	0.47	0.00	0.00
Cocconeis scutellum	0.00	0.00	0.00	0.00	0.00
Cocconeis sp1	0.00	0.00	0.00	0.00	0.00
Delphineis surilella	0.34	0.38	0.00	0.00	0.90
Epithemia turgida	0.00	0.00	0.00	0.00	0.00
Fragilaria construens	0.34	0.00	1.10	0.00	5.83
Delphineis karstenii	0.34	0.19	0.00	0.00	0.00
Fragilaria inflata	0.00	0.57	0.00	0.00	0.00
Fragilaria pinnata	0.86	0.00	0.00	0.00	0.00
Fragilariopsis doliolus	2.23	0.94	1.26	4.27	0.90
Gomphonema constrictum	0.00	0.00	0.00	0.00	0.00

(continued on next page)

Table C.1 (continued)

	Grouped as Benthic		Grouped as Freshwater		
Sample ID in figure 3.1	C16	C17	C18	C19	C20
Species	W8209-19 GC	TT68-18 AC	TT39-19 REF	TT68-PC 27 REF	Y7409-15 24GC
Actinocyclus curvatulus	0.00	0.00	0.89	0.89	1.01
Actinocyclus normanii	0.00	0.75	0.89	0.00	4.04
Actinoptychus senarius	0.35	3.74	0.00	0.89	4.04
Stephanodiscus rotula (forma minutula)	1.05	1.87	1.79	1.79	4.04
Aulacoseira islandica	0.00	1.12	0.00	0.89	3.03
Aulacoseira granulata	0.00	1.87	0.00	0.00	0.00
Aulacoseira spp.	0.00	0.00	0.00	0.00	3.03
aulacosira italica	0.00	0.00	0.00	0.00	0.00
Bacteriastrum spp.	0.00	0.37	0.00	0.00	5.05
Chaetoceros resting spores	38.39	29.16	21.43	41.96	9.09
Coscinodiscus decrescens	0.00	0.00	2.68	0.00	0.00
Coscinodiscus oculus iridis	0.00	0.00	0.00	0.00	0.00
Coscinodiscus marginatus	0.70	1.12	1.79	0.00	0.00
Coscinodiscus radiatus	2.79	3.36	0.00	2.68	1.01
cyclotella kutzingiana	0.00	0.00	0.00	0.00	0.00
Cyclotella litoralis	0.00	0.00	0.89	0.00	0.00
Cyclotella ocellata	0.35	0.75	0.00	0.00	2.02
Cyclotella comta	0.00	0.00	0.00	0.00	0.00
Cyclotella spp.	0.35	1.12	0.00	0.89	1.01
Cyclotella striata	0.70	1.50	0.00	0.89	1.01
Hemidiscus cuneiformis	0.00	0.37	0.89	0.00	0.00
Leptocylindrus resting spores	1.75	0.00	0.00	1.79	1.01
Melosira ambigua	0.00	0.37	0.89	1.79	2.02
Melosira westi	0.00	0.00	0.00	0.00	0.00
melosira distans	0.00	0.00	0.00	0.00	0.00
Odontella aurita	0.00	0.37	0.89	0.89	1.01
Paralia sulcata	2.44	0.75	0.89	0.00	4.04
Rhizosolenia setigera	0.35	0.00	0.00	0.00	0.00
Rhizosolenia hebetata (forma hebetatata)	4.89	1.12	16.07	0.89	0.00
Rhizosolenia styliformis	0.00	0.00	0.00	0.00	1.01
Roperia tesselata	0.00	0.00	0.00	0.00	0.00
Stephanopyxis turris	0.00	0.00	0.00	0.89	0.00
Thalassiossira allenii	1.05	0.00	0.00	0.00	0.00
Thalassiossira anguste-lineata	0.00	0.00	0.00	0.00	0.00
Thalassiossira angulata/pacifica	0.00	0.37	0.00	0.00	0.00
Thalassiossira eccentrica	0.00	0.75	0.89	0.00	14.14
Thalassiossira leptotus	0.00	1.50	1.79	0.89	0.00
Thalassiossira lineata	0.00	0.00	0.00	0.00	0.00
Thalassiossira nanolineata	0.00	0.00	0.00	0.00	0.00
Thalassiossira oestrupii	0.00	0.00	0.89	2.68	0.00
Thalassiossira cf poroseriata	0.00	0.00	0.00	0.00	0.00
Thalassiossira cf trifulta	0.00	0.00	0.00	0.00	0.00
Thalassiossira sp1	0.00	0.00	1.79	1.79	0.00
Thalassiossira sp2	0.00	0.00	0.00	0.00	0.00
Thalassiossira sp6	0.00	0.00	0.00	0.00	0.00
Thalassiossira spp.	1.75	1.87	7.14	0.89	0.00
Cocconeis placentula	0.35	1.50	0.00	0.45	4.04
Cocconeis scutellum	0.00	0.00	0.00	0.00	0.00
Cocconeis sp1	0.00	0.00	0.00	0.00	2.02
Delphineis surilella	0.00	0.00	0.00	0.00	1.94
Epithemia turgida	0.17	1.50	0.00	0.89	3.54
Fragilaria construens	0.00	0.00	0.89	1.79	1.01
Delphineis karstenii	0.35	1.50	0.00	0.45	0.97
Fragilaria inflata	0.00	0.75	0.00	0.00	0.00
Fragilaria pinnata	0.00	0.00	0.00	0.00	0.00
Fragilariopsis doliolus	2.44	2.24	1.34	3.13	0.00
Gomphonema constrictum	0.00	0.00	0.00	0.00	3.03

(continued on next page)

Table C.1 (continued)

		Grouped as Benthic		Grouped as Freshwater	
Sample ID in figure 3.1	C21	C22	C23	C24	C25
Species	W7905-163G	W7905-109G	W8809A-19GC	Y6908-5A	W8909-31
Actinocyclus curvatulus	1.63	0.00	0.99	1.84	0.00
Actinocyclus normanii	0.00	0.00	0.00	0.00	0.00
Actinoptychus senarius	4.60	1.83	1.97	0.00	2.24
Stephanodiscus rotula (forma minutula)	0.00	0.61	0.00	0.46	0.00
Aulacoseira islandica	0.00	2.74	0.00	3.23	0.37
Aulacoseira granulata	0.32	0.00	0.00	3.23	0.00
Aulacoseira spp.	0.00	0.00	0.00	0.00	0.00
aulacosira italica	0.00	0.00	0.00	0.00	0.00
Bacteriastrum spp.	0.98	0.30	0.00	0.92	0.37
Chaetoceros resting spores	50.49	55.10	39.14	12.44	36.26
Coscinodiscus decrescens	0.00	0.00	0.00	0.00	0.00
Coscinodiscus oculus iridis	0.00	0.00	0.00	0.00	0.00
Coscinodiscus marginatus	0.65	0.00	0.66	9.68	1.12
Coscinodiscus radiatus	2.28	1.22	4.28	0.92	4.86
cyclotella kutzingiana	0.00	0.00	0.00	0.00	0.00
Cyclotella litoralis	1.95	0.91	0.00	0.00	1.50
Cyclotella ocellata	0.00	0.00	0.00	0.00	0.00
Cyclotella comta	0.00	0.00	0.00	0.46	0.00
Cyclotella spp.	0.00	2.74	0.66	0.00	1.50
Cyclotella striata	0.98	0.30	0.00	0.00	0.00
Hemidiscus cuneiformis	0.65	0.30	0.00	0.00	0.37
Leptocylindrus resting spores	3.91	0.30	0.33	0.00	0.00
Melosira ambigua	0.00	3.04	0.00	0.46	0.00
Melosira westi	0.00	0.00	0.00	0.00	0.00
melosira distans	0.00	0.00	0.00	0.00	0.00
Odontella aurita	2.93	0.30	0.99	0.00	0.00
Paralia sulcata	5.54	2.13	0.33	0.46	1.87
Rhizosolenia setigera	0.00	0.30	1.64	0.00	0.00
Rhizosolenia hebetata (forma hebetatata)	1.63	1.22	2.30	23.96	8.22
Rhizosolenia styliformis	0.00	0.00	0.00	0.00	0.00
Roperia tesselata	0.98	0.00	1.97	0.00	0.37
Stephanopyxis turris	1.30	0.00	0.33	0.00	0.37
Thalassiossira allenii	0.00	0.00	0.00	0.00	0.00
Thalassiossira anguste-lineata	0.32	0.00	0.00	0.00	0.00
Thalassiossira angulata/pacifica	0.00	0.00	0.00	0.00	0.00
Thalassiossira eccentrica	2.28	1.22	2.63	0.00	1.50
Thalassiossira leptotus	0.32	0.00	0.99	0.46	1.87
Thalassiossira lineata	0.32	0.00	0.00	0.00	0.00
Thalassiossira nanolineata	0.00	0.00	0.00	0.00	0.00
Thalassiossira oestrupii	0.65	0.30	0.99	3.23	2.24
Thalassiossira cf poroseriata	0.00	0.00	0.00	0.00	0.00
Thalassiossira cf trifulta	0.00	0.00	0.00	0.00	0.00
Thalassiossira sp1	0.00	0.61	0.99	2.76	0.00
Thalassiossira sp2	0.00	0.00	0.00	9.22	1.50
Thalassiossira sp6	0.00	0.00	0.00	0.00	0.00
Thalassiossira spp.	0.32	0.30	0.00	0.92	0.37
Cocconeis placentula	0.00	0.15	0.00	0.00	0.00
Cocconeis scutellum	0.00	0.00	0.00	0.00	0.00
Cocconeis sp1	0.00	0.00	0.00	0.00	0.00
Delphineis surilella	0.00	0.00	0.00	0.00	0.00
Epithemia turgida	0.16	0.00	0.00	0.00	0.00
Fragilaria construens	0.00	0.76	0.00	0.23	0.00
Delphineis karstenii	0.00	0.76	0.33	0.00	0.00
Fragilaria inflata	0.00	0.00	0.00	0.00	0.37
Fragilaria pinnata	0.00	0.00	0.00	0.00	0.00
Fragilariopsis doliolus	1.47	0.61	5.59	0.23	1.87
Gomphonema constrictum	0.00	0.00	0.00	0.00	0.00

(continued on next page)

Table C.1 (continued)

	Grouped as Benthic		Grouped as Freshwater		
Sample ID in figure 3.1	C26	C27	C28	C29	C30
Species	AT8408-17	W7610B1-7MGREF	W89097GC	TT39-AC12REF	ODP 1019
Actinocyclus curvatulus	0.35	1.32	1.50	1.58	0.93
Actinocyclus normanii	0.00	0.00	0.00	1.27	0.93
Actinoptychus senarius	1.06	1.32	1.85	0.82	1.24
Stephanodiscus rotula (forma minutula)	0.35	0.00	0.00	0.00	0.62
Aulacoseira islandica	0.71	0.33	0.00	1.27	0.00
Aulacoseira granulata	0.00	0.00	0.37	0.00	0.00
Aulacoseira spp.	0.00	0.00	0.00	0.00	0.00
aulacosira italica	0.00	0.00	0.00	0.00	0.00
Bacteriastrum spp.	0.00	0.00	0.75	1.27	0.00
Chaetoceros resting spores	43.26	58.88	43.44	33.54	43.30
Coscinodiscus decrescens	0.00	0.00	0.00	0.00	0.00
Coscinodiscus oculus iridis	0.00	0.00	0.00	0.00	0.31
Coscinodiscus marginatus	0.00	0.00	1.17	0.99	1.87
Coscinodiscus radiatus	1.77	1.32	4.87	1.90	2.18
cyclotella kutzingiana	0.00	0.00	0.00	0.00	0.00
Cyclotella litoralis	0.71	1.32	0.00	0.63	3.43
Cyclotella ocellata	0.71	0.33	0.00	0.00	0.00
Cyclotella comta	0.00	0.00	0.00	0.00	0.00
Cyclotella spp.	0.00	0.99	0.75	1.58	0.00
Cyclotella striata	0.35	0.66	2.62	0.00	0.00
Hemidiscus cuneiformis	0.00	0.00	0.75	0.00	1.25
Leptocylindrus resting spores	1.77	3.29	2.62	3.16	3.12
Melosira ambigua	0.00	0.66	0.00	0.00	0.00
Melosira westi	0.00	0.00	0.00	0.00	0.00
melosira distans	0.00	0.00	0.00	0.00	0.00
Odontella aurita	0.35	0.33	0.37	0.00	0.93
Paralia sulcata	0.71	2.63	0.75	3.80	2.49
Rhizosolenia setigera	0.00	0.00	0.00	0.00	0.00
Rhizosolenia hebetata (forma hebetatata)	0.71	2.96	2.25	2.21	0.00
Rhizosolenia styliformis	0.00	0.00	0.00	0.00	0.00
Roperia tesselata	0.00	0.00	1.50	0.00	2.49
Stephanopyxis turris	0.00	0.00	0.00	0.00	0.00
Thalassiossira allenii	0.00	0.00	0.00	0.00	0.00
Thalassiossira anguste-lineata	0.00	0.00	0.37	0.00	0.31
Thalassiossira angulata/pacifica	0.00	0.00	0.00	0.00	0.00
Thalassiossira eccentrica	3.90	1.64	2.25	4.43	1.56
Thalassiossira leptotus	1.06	0.33	1.87	0.00	0.62
Thalassiossira lineata	0.00	0.00	0.00	0.00	0.31
Thalassiossira nanolineata	0.00	0.00	0.00	0.00	0.00
Thalassiossira oestrupii	3.19	0.00	1.50	1.90	0.93
Thalassiossira cf poroseriata	0.00	0.00	0.00	0.00	0.00
Thalassiossira cf trifulta	0.00	0.00	0.00	0.00	0.00
Thalassiossira sp1	0.35	0.00	0.00	1.27	0.00
Thalassiossira sp2	1.42	0.00	0.00	0.00	0.00
Thalassiossira sp6	0.00	0.00	0.00	0.00	0.00
Thalassiossira spp.	0.71	0.00	1.87	2.53	0.00
Cocconeis placentula	0.89	0.00	0.00	0.32	0.93
Cocconeis scutellum	0.00	0.00	0.00	0.00	0.00
Cocconeis sp1	0.00	0.00	0.00	0.00	0.00
Delphineis surilella	0.00	0.00	0.00	0.00	0.00
Epithemia turgida	0.00	0.16	0.00	0.32	0.00
Fragilaria construens	0.00	0.99	0.00	0.00	0.00
Delphineis karstenii	0.50	0.82	0.00	0.42	0.31
Fragilaria inflata	0.00	0.00	0.00	0.00	0.00
Fragilaria pinnata	0.00	0.00	0.00	0.73	0.00
Fragilariopsis doliolus	2.48	0.33	5.61	2.37	2.49
Gomphonema constrictum	0.00	0.00	0.00	0.00	0.00

(continued on next page)

Table C.1 (continued)

Grouped as Benthic | Grouped as Freshwater

Sample ID in figure 3.1	C1	C2	C3	C4	C5
Species	W8809-11GC	W8909-24GC	TT39-15 REF	TT39-5AC REF	W8306-A1-RKC*
Lioloma elongatum	0.40	0.47	0.79	0.60	0.46
Lioloma pacificum	0.40	0.63	0.32	0.75	0.57
Lioloma spp.	0.00	0.00	0.00	0.89	0.68
Neodenticula seminae	0.79	1.57	5.72	29.06	22.18
Nitzschia gp bicapitata	0.00	0.00	0.32	0.30	0.23
Raphoneis amphiceros	0.26	1.41	0.00	0.00	0.00
Surirella linearis	0.13	0.00	0.79	0.00	0.00
Tetracyclus rupestris	0.00	0.00	0.16	0.00	0.00
Thalassionema bacillare	0.26	1.73	0.00	0.00	0.00
Thalassionema nitzschioides	19.13	26.22	14.63	16.39	12.51
Sample ID in figure 3.1	C6	C7	C8	C9	C10
Species	LG-85-NC 3GC	W8508-9GC	W7905-160G	W9205-1GC	7407Y-1 REF
Lioloma elongatum	0.50	0.97	0.31	0.17	0.49
Lioloma pacificum	1.32	1.78	0.31	0.17	0.65
Lioloma spp.	1.49	1.30	0.78	0.51	0.98
Neodenticula seminae	0.33	0.65	0.00	0.51	3.91
Nitzschia gp bicapitata	0.17	0.00	0.00	0.00	0.33
Raphoneis amphiceros	0.00	0.49	0.31	0.00	0.00
Surirella linearis	0.00	0.00	0.31	0.00	0.00
Tetracyclus rupestris	0.00	0.00	0.00	0.00	0.00
Thalassionema bacillare	0.33	0.00	0.31	0.00	0.65
Thalassionema nitzschioides	35.81	18.31	19.94	15.45	31.92
Sample ID in figure 3.1	C11	C12	C13	C14	C15
Species	TT39-18 AC REF	TT29-22 AC REF	TT39-11 AC REF	TT31-011 GC REF	Y73-10-100 GC
Lioloma elongatum	0.17	0.38	1.10	1.37	0.90
Lioloma pacificum	0.51	0.94	0.16	1.20	0.00
Lioloma spp.	1.03	2.83	0.00	3.76	2.69
Neodenticula seminae	4.45	7.92	3.15	7.35	2.24
Nitzschia gp bicapitata	0.51	1.51	0.79	0.00	0.00
Raphoneis amphiceros	0.00	0.00	0.00	0.00	0.45
Surirella linearis	0.00	0.00	0.63	0.00	0.00
Tetracyclus rupestris	0.17	0.00	0.00	0.00	0.00
Thalassionema bacillare	1.03	0.38	0.79	0.17	0.00
Thalassionema nitzschioides	20.03	19.06	17.35	6.67	25.11
Sample ID in figure 3.1	C16	C17	C18	C19	C20
Species	W8209-19 GC	TT68-18 AC	TT39-19 REF	TT68-PC 27 REF	Y7409-15 24GC
Lioloma elongatum	0.17	0.00	2.23	0.00	0.00
Lioloma pacificum	1.22	0.75	2.23	0.89	0.00
Lioloma spp.	0.70	0.00	2.68	1.34	0.00
Neodenticula seminae	0.87	0.93	8.48	1.79	0.00
Nitzschia gp bicapitata	0.17	6.54	0.45	2.23	0.00
Raphoneis amphiceros	0.87	1.12	0.00	0.89	1.52
Surirella linearis	0.00	0.00	0.00	0.00	0.00
Tetracyclus rupestris	0.00	0.37	0.00	0.00	0.00
Thalassionema bacillare	0.17	0.56	0.00	0.00	0.00
Thalassionema nitzschioides	34.21	24.11	17.41	20.09	12.63
Sample ID in figure 3.1	C21	C22	C23	C24	C25
Species	W7905-163G	W7905-109G	W8809A-19GC	Y6908-5A	W8909-31
Lioloma elongatum	0.16	0.30	0.49	2.07	0.00
Lioloma pacificum	0.49	0.00	0.82	1.15	1.87
Lioloma spp.	0.65	0.76	0.82	6.45	2.24
Neodenticula seminae	0.00	0.91	1.81	3.69	0.37
Nitzschia gp bicapitata	0.00	1.52	0.16	0.46	0.00
Raphoneis amphiceros	0.65	2.13	0.33	0.00	1.12
Surirella linearis	0.49	0.30	0.00	0.00	0.56
Tetracyclus rupestris	0.00	0.00	0.00	0.46	0.00
Thalassionema bacillare	0.00	0.00	0.00	0.00	0.00
Thalassionema nitzschioides	8.96	14.31	28.13	9.68	23.93

(continued on next page)

Table C.1 (continued)

		Grouped as Benthic		Grouped as Freshwater	
Sample ID in figure 3.1	C26	C27	C28	C29	C30
Species	AT8408-17	W7610B1-7MGREF	W89097GC	TT39-AC12REF	ODP 1019
Lioloma elongatum	0.18	0.16	0.00	0.32	0.93
Lioloma pacificum	0.35	0.49	0.37	0.32	1.25
Lioloma spp.	0.35	1.51	0.37	0.63	0.62
Neodenticula seminae	5.68	0.82	1.12	6.01	0.31
Nitzschia gp bicapitata	0.35	0.33	0.37	0.47	0.16
Raphoneis amphiceros	0.00	1.51	0.37	0.32	1.40
Surirella linearis	0.71	0.33	0.00	0.60	0.00
Tetracyclus rupestris	0.00	0.16	0.00	0.00	0.31
Thalassionema bacillare	0.00	0.00	0.00	0.32	0.00
Thalassionema nitzschioides	23.58	14.47	15.74	18.67	20.25

Table C.2 – Environmental variables (PP - Productivity in $gC/m^2/y$ from Antoine and Morel 1996 and SST (^oC), Salinity (PSU), NO_3 (µmol/l), PO_4 (µM) and SiO2 (µmol/L) from WOA 98). Gray boxes are missing values.

sample	PP annual	PP winter	PP spring	PP summer	PP fall	SST annual	SST winter	SST spring	SST summer	SST fall
C1	180.25	169.08	177.96	220.08	153.89	13.054	10.673	12.265	15.693	13.554
C2	215.1	172.35	245.45	279.27	163.31	12.411	10.154	11.874	15.303	12.669
C3	135.36	65.53	202.56	204.22	69.18	10.85	7.841	9.794	14.559	11.183
C4	142.18	77.75	209.43	204.86	76.66	12.135	9.021	11.118	15.88	12.523
C5	172.51	112.16	220.57	229.75	127.55	12.577	9.668	11.977	15.855	12.808
C6	134.35	154.06	130.89	129.54	122.9	13.425	10.82	12.412	16.337	14.09
C7	153.6	138.77	143.85	186.23	145.54	12.854	10.022	11.994	16.159	13.241
C8	209.59	163.9	222.38	285.19	166.87	12.729	9.997	12.091	15.942	12.899
C9	200.19	147.12	218.45	271.89	163.29	12.577	9.668	11.977	15.855	12.808
C10	129.85	123.96	136.26	136.61	122.59	13.031	10.1	11.944	16.487	13.569
C11	134.24	66.3	197.53	203.82	69.33	11.237	8.119	10.05	15.043	11.706
C12	141.51	74.23	207.07	208.54	76.2	11.69	8.644	10.777	15.36	11.98
C13	140.58	73.1	208.88	208.14	72.21	10.432	7.812	9.702	13.926	10.629
C14	133.34	67.77	193.26	201.28	71.04	11.517	8.375	9.991	15.424	12.214
C15	206.54	172.19	277.77	222.83	153.37	12.73	10.846	12.212	14.656	13.204
C16	117.97	142.53	118.21	103.67	107.47	14.048	11.752	13.058	16.471	14.913
C17	142.7	81.48	212.84	200.31	76.15	-100	-100	-100	-100	-100
C18	139.05	75.79	206.7	201.97	71.77	11.159	8.243	10.373	14.686	11.335
C19	142.46	81.29	211	200.39	77.12	12.148	9.097	11.384	15.743	12.366
C20	145.74	85.35	214.69	201.63	81.29	12.266	9.336	12.068	15.487	12.174
C21	277.3	199.21	322.28	395.98	191.72	-100	-100	-100	-100	-100
C22	143.75	82.98	212.72	200.62	78.67	12.2	9.215	11.712	15.621	12.252
C23	155.39	155.69	143.67	178.91	143.29	12.929	10.324	12.106	15.914	13.347
C24	138.11	69.96	199.4	208.02	75.03	12.11	8.919	10.71	15.998	12.735
C25	137.37	150.59	136.5	137.88	124.5	13.218	10.447	12.168	16.417	13.804
C26	141.23	79.93	210.25	199.61	75.13	11.742	8.778	11.083	15.265	11.843
C27	161.66	124.76	178.89	195.47	147.49	12.688	9.709	11.826	16.167	13.048
C28	215.1	172.35	245.45	279.27	163.31	-100	-100	-100	-100	-100
C29	138.36	71.81	207.01	204.69	69.93	10.767	7.866	9.88	14.329	10.978
C30	212.8	175.62	248.32	268.27	158.98	-100	-100	-100	-100	-100
sample	Salinity annual	Salinity winter	Salinity spring	Salinity summer	Salinity fall	NO3 annual	NO3 winter	NO3 spring	NO3 summer	NO3 fall
C1	32.562	32.658	32.556	32.401	32.609	0.89	1.318	1.071	0.323	0.848
C2	32.477	32.641	32.395	32.213	32.583	1.733	2.936	1.707	0.899	1.391
C3	32.157	32.25	32.112	32.063	32.186	4.063	7.165	3.336	1.983	3.77
C4	32.105	32.236	31.983	31.959	32.243	2.163	4.896	1.655	0.801	1.301
C5	31.816	32.069	31.451	31.55	32.194	1.739	4.019	1.177	0.654	1.107
C6	32.578	32.67	32.612	32.413	32.599	0.761	1.29	0.924	0.229	0.6
C7	32.31	32.556	32.229	31.968	32.453	1.27	3.031	1.015	0.315	0.721
C8	32.273	32.543	32.124	31.797	32.412	1.21	3.122	0.855	0.234	0.631
C9	31.816	32.069	31.451	31.55	32.194	1.739	4.019	1.177	0.654	1.107
C10	32.401	32.592	32.399	32.109	32.48	1.171	2.89	0.997	0.227	0.572
C11	32.295	32.39	32.271	32.206	32.291	3.412	6.418	3.23	1.583	2.418
C12	32.09	32.2	31.947	32.005	32.207	2.661	5.539	2.016	1.268	1.821
C13	32.089	32.189	31.941	32.111	32.149	3.754	6.747	2.621	2.43	3.219
C14	32.522	32.575	32.556	32.467	32.464	3.465	6.161	4.259	1.667	1.773
C15	32.691	32.705	32.665	32.677	32.716	0.571	0	0.906	0.224	1.153
C16	32.724	32.744	32.755	32.688	32.708	0.396	0.272	0.425	0.288	0.6
C17	-100	-100	-100	-100	-100	-100	-100	-100	-100	-100
C18	32.108	32.225	31.954	32.062	32.191	3.202	6.17	2.337	1.837	2.464
C19	31.765	31.821	31.48	31.688	32.069	2.198	4.948	1.398	0.963	1.483
C20	30.267	29.825	29.367	30.611	31.265	2.424	5.24	1.166	1.371	1.917
C21	-100	-100	-100	-100	-100	-100	-100	-100	-100	-100
C22	31.218	31.108	30.69	31.29	31.785	2.269	5.043	1.218	1.153	1.662
C23	32.476	32.625	32.446	32.202	32.561	1.216	2.346	1.206	0.435	0.879
C24	32.454	32.549	32.472	32.32	32.425	2.319	4.935	2.49	0.806	1.046
C25	32.502	32.635	32.525	32.257	32.549	0.994	2.12	1.016	0.243	0.596
C26	31.814	31.85	31.534	31.806	32.066	2.681	5.575	1.682	1.493	1.974
C27	32.077	32.308	31.903	31.796	32.303	1.528	3.746	1.067	0.433	0.868
C28	-100	-100	-100	-100	-100	-100	-100	-100	-100	-100
C29	32.102	32.185	32.009	32.029	32.147	3.896	6.885	2.895	2.149	3.654
C30	-100	-100	-100	-100	-100	-100	-100	-100	-100	-100

(continued on next page)

Table C.2 (continued)

sample	PO4 annual	PO4 winter	PO4 spring	PO4 summer	PO4 fall	SiO2 annual	SiO2 winter	SiO2 spring	SiO2 summer	SiO2 fall
C1	0.577	0.61	0.535	0.507	0.657	4.715	7.717	3.218	3.558	4.366
C2	0.622	0.725	0.56	0.494	0.71	5.819	8.752	4.295	5.24	4.989
C3	0.728	1.002	0.607	0.575	0.727	10.529	13.572	6.473	10.117	11.954
C4	0.663	0.913	0.629	0.478	0.632	6.537	8.873	6.152	6.121	5.003
C5	0.546	0.742	0.495	0.383	0.564	7.409	10.157	7.428	6.967	5.084
C6	0.549	0.576	0.525	0.493	0.602	4.262	7.762	2.739	3.004	3.543
C7	0.541	0.684	0.508	0.405	0.566	5.219	8.076	4.357	4.715	3.727
C8	0.483	0.637	0.438	0.332	0.527	5.573	8.323	4.899	5.375	3.696
C9	0.546	0.742	0.495	0.383	0.564	7.409	10.157	7.428	6.967	5.084
C10	0.553	0.69	0.536	0.433	0.554	4.495	7.438	3.506	3.842	3.195
C11	0.735	0.991	0.675	0.581	0.693	8.427	11.088	6.852	8.024	7.742
C12	0.702	0.965	0.637	0.502	0.703	7.862	10.114	6.418	7.874	7.043
C13	0.713	0.983	0.541	0.495	0.831	12.028	13.91	5.756	13.691	14.753
C14	0.791	1.007	0.828	0.672	0.659	6.762	9.345	8.683	5.099	3.921
C15	0.633	0.605	0.572	0.604	0.75	4.411	5.802	3.312	2.984	5.546
C16	0.532	0.479	0.542	0.535	0.574	3.501	6.214	2.56	2.154	3.076
C17	-100	-100	-100	-100	-100	-100	-100	-100	-100	-100
C18	0.725	0.993	0.614	0.513	0.777	9.701	11.811	6.261	10.436	10.297
C19	0.655	0.908	0.597	0.459	0.656	7.709	10.1	7.208	7.37	6.158
C20	0.644	0.906	0.54	0.448	0.684	12.05	14.829	12.594	11.145	9.634
C21	-100	-100	-100	-100	-100	-100	-100	-100	-100	-100
C22	0.65	0.906	0.568	0.449	0.675	9.314	11.83	9.076	8.859	7.49
C23	0.572	0.661	0.531	0.464	0.63	5.031	8.108	3.67	4.246	4.098
C24	0.706	0.941	0.714	0.56	0.608	5.286	7.574	5.89	4.389	3.292
C25	0.551	0.633	0.527	0.461	0.583	4.385	7.717	2.99	3.454	3.378
C26	0.709	0.976	0.623	0.491	0.745	8.679	10.872	6.986	8.865	7.992
C27	0.564	0.754	0.532	0.407	0.563	5.978	8.63	5.64	5.501	4.14
C28	-100	-100	-100	-100	-100	-100	-100	-100	-100	-100
C29	0.702	0.975	0.547	0.523	0.762	11.563	14.037	6.156	12.044	14.016
C30	-100	-100	-100	-100	-100	-100	-100	-100	-100	-100

Table C.3- Sample scores from Q-mode analysis.

Sample	Communalities	Factor 1	Factor 2	Factor 3	Factor 4	Factor 5
W8209B-19 GC	0.99	0.9222	0.2953	0.1283	0.1769	0.0809
Y73-10 100 GC	0.99	0.7494	0.5627	0.1817	0.2433	0.1247
L6-85-NC 3 GC	0.93	0.7508	0.3126	0.2783	0.3629	0.2435
W8809A-11 GC	0.97	0.2870	0.2564	0.3286	0.8417	0.1019
W8809A-19GC	0.98	0.5777	0.1985	0.2467	0.7282	0.1270
W8909A-24 GC	0.99	0.4635	0.7915	0.2445	0.2146	0.2106
W8909A-31 GC	0.98	0.8961	0.3114	0.1417	0.1905	0.1413
W8909A-7 GC	0.99	0.9113	0.3275	0.1236	0.1750	0.1049
7407 Y-1 GC	0.99	0.9481	0.2172	0.1242	0.1635	0.0783
W7905A-160 GC	0.99	0.5827	0.6973	0.1992	0.3033	0.1703
W7905A-163 GC	0.98	0.7688	0.4038	0.2790	0.2954	0.2494
W8508AA-9 GC	0.98	0.6865	0.4213	0.3722	0.3784	0.2214
W7610B-7 MG	0.98	0.8721	0.3121	0.1880	0.2481	0.1647
W8306A-1 GC	0.77	-0.0984	0.1522	0.7581	0.3726	0.1372
W9205A 1 GC	0.98	0.8042	0.4333	0.2116	0.2196	0.2201
TT39-5 AC	0.99	0.7147	0.5976	0.2345	0.1927	0.1601
TT068-27 PC	0.96	0.7112	0.5294	0.2028	0.2062	0.2953
W7905A-109 GC	0.92	0.5586	0.3726	0.6088	0.3030	0.0772
Y6908-5A GC	0.99	0.8514	0.3775	0.1885	0.2208	0.1844
Y7409-15 24 GC	0.99	0.2915	0.2294	0.1867	0.1356	0.8954
AT8408-17 GC	0.98	0.9505	0.1455	0.1250	0.1646	0.1189
TT29-22 AC	0.99	0.9306	0.1958	0.1424	0.1708	0.1874
TT31-11 GC	0.99	0.7596	0.5411	0.2039	0.2326	0.1660
TT68-18 AC	0.91	0.3353	0.1079	0.8833	0.0424	0.0813
TT39-18 AC	0.99	0.7763	0.4644	0.3338	0.1741	0.1710
TT39-19 PC	0.99	0.8188	0.4119	0.1851	0.2915	0.1700
TT39-11 AC	1.00	0.9447	0.2009	0.1489	0.1649	0.1186
TT39-12 AC	0.98	0.8834	0.3256	0.1827	0.2100	0.1234
TT39-15 AC	0.99	0.7898	0.3688	0.2401	0.3286	0.2523
1019 D PC	0.99	0.8703	0.3891	0.1424	0.1914	0.1433

Table C.4 – Correlation coefficients between environmental variables (gray boxes indicate significant correlations at p=0.05%).

	PP annual	PP winter	PP spring	PP summer	PP fall	SST annual	SST winter
PP annual	1.0						
PP winter	0.64	1.00					
PP spring	0.57	-0.19	1.00				
PP summer	0.78	0.05	0.81	1.00			
PP fall	0.76	0.94	-0.07	0.26	1.00		
SST annual	0.21	0.78	-0.49	-0.35	0.68	1.00	
SST winter	0.33	0.87	-0.39	-0.29	0.75	0.96	1.00
SST spring	0.36	0.81	-0.32	-0.20	0.73	0.95	0.95
SST summer	-0.05	0.45	-0.62	-0.38	0.43	0.85	0.68
SST fall	0.13	0.75	-0.56	-0.43	0.63	0.98	0.95
Salinity annual	0.07	0.42	-0.32	-0.21	0.32	0.26	0.34
Salinity winter	0.13	0.43	-0.30	-0.13	0.38	0.25	0.31
Salinity spring	0.02	0.37	-0.34	-0.24	0.27	0.22	0.30
Salinity summer	-0.07	0.29	-0.28	-0.31	0.13	0.16	0.27
Salinity fall	0.20	0.60	-0.34	-0.20	0.51	0.46	0.54
NO3 annual	-0.37	-0.86	0.35	0.24	-0.77	-0.96	-0.97
NO3 winter	-0.37	-0.89	0.33	0.27	-0.76	-0.91	-0.98
NO3 spring	-0.33	-0.71	0.25	0.17	-0.65	-0.83	-0.83
NO3 summer	-0.36	-0.80	0.36	0.18	-0.76	-0.94	-0.90
NO3 fall	-0.28	-0.70	0.39	0.19	-0.67	-0.92	-0.84
PO4 annual	-0.40	-0.81	0.39	0.10	-0.82	-0.84	-0.82
PO4 winter	-0.38	-0.92	0.42	0.25	-0.82	-0.91	-0.96
PO4 spring	-0.43	-0.63	0.15	-0.06	-0.65	-0.46	-0.51
PO4 summer	-0.34	-0.35	0.11	-0.21	-0.49	-0.36	-0.27
PO4 fall	-0.12	-0.46	0.49	0.16	-0.54	-0.75	-0.59
SiO2 annual	-0.22	-0.72	0.44	0.28	-0.64	-0.84	-0.82
SiO2 winter	-0.25	-0.68	0.33	0.24	-0.60	-0.79	-0.79
SiO2 spring	-0.13	-0.66	0.46	0.34	-0.52	-0.51	-0.61
SiO2 summer	-0.21	-0.70	0.42	0.29	-0.61	-0.85	-0.83
SiO2 fall	-0.22	-0.59	0.38	0.17	-0.58	-0.84	-0.74

	SST spring	SST summer	SST fall	Salinity annual	Salinity winter	Salinity spring	Salinity summer
SST winter							
SST spring	1.00						
SST summer	0.73	1.00					
SST fall	0.88	0.84	1.00				
Salinity annual	0.06	0.14	0.40	1.00			
Salinity winter	0.05	0.16	0.38	0.98	1.00		
Salinity spring	0.01	0.12	0.37	1.00	0.98	1.00	
Salinity summer	-0.03	-0.01	0.32	0.95	0.89	0.96	1.00
Salinity fall	0.28	0.28	0.58	0.97	0.96	0.96	0.90
NO3 annual	-0.95	-0.73	-0.93	-0.32	-0.31	-0.28	-0.22
NO3 winter	-0.89	-0.58	-0.91	-0.46	-0.42	-0.41	-0.40
NO3 spring	-0.93	-0.62	-0.72	0.05	0.03	0.10	0.16
NO3 summer	-0.89	-0.82	-0.92	-0.34	-0.36	-0.30	-0.19
NO3 fall	-0.85	-0.88	-0.90	-0.28	-0.30	-0.24	-0.14
PO4 annual	-0.87	-0.70	-0.77	-0.14	-0.20	-0.10	0.05
PO4 winter	-0.89	-0.61	-0.90	-0.43	-0.42	-0.39	-0.33
PO4 spring	-0.61	-0.24	-0.34	0.12	0.05	0.15	0.27
PO4 summer	-0.49	-0.45	-0.22	0.35	0.22	0.38	0.58
PO4 fall	-0.64	-0.91	-0.74	-0.14	-0.21	-0.13	0.06

(continued on next page)

Table C.4 (continued)

	SST spring	SST summer	SST fall	Salinity annual	Salinity winter	Salinity spring	Salinity summer
SiO2 annual	-0.68	-0.74	-0.90	-0.68	-0.67	-0.66	-0.57
SiO2 winter	-0.64	-0.66	-0.85	-0.70	-0.68	-0.67	-0.61
SiO2 spring	-0.39	-0.29	-0.59	-0.86	-0.85	-0.85	-0.78
SiO2 summer	-0.69	-0.74	-0.91	-0.63	-0.60	-0.60	-0.54
SiO2 fall	-0.70	-0.87	-0.86	-0.41	-0.42	-0.38	-0.27

	PO4 winter	PO4 spring	PO4 summer	PO4 fall	SiO2 annual	SiO2 winter	SiO2 spring
PO4 annual							
PO4 winter	1.00						
PO4 spring	0.63	1.00					
PO4 summer	0.34	0.79	1.00				
PO4 fall	0.60	0.35	0.55	1.00			
SiO2 annual	0.79	0.13	0.06	0.66	1.00		
SiO2 winter	0.75	0.08	0.01	0.59	0.98	1.00	
SiO2 spring	0.70	0.32	-0.01	0.24	0.73	0.72	1.00
SiO2 summer	0.78	0.07	0.00	0.67	0.99	0.96	0.65
SiO2 fall	0.67	0.06	0.20	0.81	0.92	0.88	0.42

	SiO2 summer
SiO2 spring	
SiO2 summer	1.00
SiO2 fall	0.93

APPENDIX D: Supplementary data for Chapter 4.

Table D.1 – Core-top locations, depths, diatom abundances and winter salinities (GC - Gravity, PC- Piston , MG -Multicorer, AC - Trigger).

Core ID #	Core ID	latitude (N)	longitude (W)	water depth (m)	Freshwater diatoms(%)	Winter Salinity from WOA (PSU)
C1	W8809-11 GC	41.672	-126.003	3020	0.13	32.66
C2	W8909-24 GC	42.082	-125.302	2790	0.00	32.64
C3	TT39-15 AC	49.210	-129.243	2396	2.23	32.25
C4	TT39-5 AC	46.720	-127.542	2665	4.17	32.24
C5	W8306A-1 GC	44.938	-125.362	2511	1.59	32.07
C6	L6-85-NC 3 GC	41.028	-127.308	2983	0.00	32.67
C7	W8508-9 GC	43.030	-126.578	3092	2.11	32.56
C8	W7905-160 GC	43.165	-125.087	1476	0.31	32.54
C9	W9205-1 GC	44.085	-125.373	3020	0.68	32.07
C10	7407 Y-1 GC	43.628	-127.100	2918	0.00	32.59
C11	TT39-18 AC	48.437	-129.870	2765	4.62	32.39
C12	TT29-22 AC	47.113	-127.907	2555	2.83	32.20
C13	TT39-11 AC	49.013	-127.767	2480	4.26	32.19
C14	TT31-11 GC	47.033	-131.158	3056	0.00	32.58
C15	Y73-10 100 GC	40.032	-125.298	1935	6.73	32.71
C16	W8209B-19 GC	39.272	-127.380	4355	0.52	32.74
C17	TT68-18 AC	47.383	-124.913	1240	6.36	no information
C18	TT39-19 PC	48.390	-127.153	2555	1.79	32.2
C19	TT68-27 PC	46.372	-126.063	2050	5.36	31.8
C20	Y7409-15 24 GC	46.118	-124.125	200	14.65	29.8
C21	W7905A-163 GC	43.167	-124.752	308	0.97	no information
C22	W7905A-109 GC	46.300	-125.115	1670	6.84	31.11
C23	W8809A-19 GC	42.230	-126.517	2669	0.00	32.63
C24	Y6908-5A GC	46.652	-129.133	2600	7.61	32.55
C25	W8909A-31 GC	42.155	-127.208	2800	1.30	32.64
C26	AT8408-17 GC	47.228	-126.145	2390	2.13	31.85
C27	W7610B-7 MG	44.213	-126.177	2893	2.80	32.31
C28	W8909A-7 GC	42.295	-124.930	1100	0.37	no information
C29	TT39-12 AC	49.397	-128.140	2341	2.92	32.19
C30	ODP1019D	41.683	-124.933	978	0.00	no information

Table D.2 - Radiocarbon data from cores ODP 1019 C and D and MD02-2499.

CORE	Material (foraminifers)	Depth (mcd)	Revised depth (mcd)	^{14}C Age (years B.P.)	Reservoir Age (years)
ODP 1019D	*Globobulimina* spp.	0.16	0.16	2040±40	1750
ODP 1019D	mixed benthic forams	0.16	0.16	2130±40	1750
ODP 1019D	*Globobulimina* spp.	0.57	0.57	3040±40	1750
ODP 1019D	mixed benthic forams	1.16	1.27	5100±700	1750
ODP 1019D	mixed benthic forams	2.07	2.21	6400±40	1750
ODP 1019C	bark	2.84	2.84	6030+150	
ODP 1019C	mixed planktic forams	4.17	4.17	9950+110	720
ODP 1019C	mixed planktic forams	4.92	4.92	10210+120	720
ODP 1019C	mixed planktic forams	5.16	5.16	11410+170	720
ODP 1019C	mixed planktic forams	5.81	5.81	11580+140	720
ODP 1019C	mixed planktic forams	6.21	6.21	11950+110	720
ODP 1019C	mixed planktic forams	7.11	7.11	13350+120	720
ODP 1019C	mixed planktic forams	8.21	8.21	15080+120	720
ODP 1019C	mixed planktic forams	9.54	9.54	16040+140	720
ODP 1019C	mixed planktic forams	10.55	10.55	18550+210	720
ODP 1019C	mixed planktic forams	12.15	12.15	21240+280	720
MD02-2499	*Uvigerina* spp.	1.28	1.28	10950±50	1750
MD02-2499	mixed planktic forams	1.28	1.28	10100±65	720
MD02-2499	*Uvigerina* spp.	4.58	4.58	17850±80	1750
MD02-2499	mixed planktic forams	4.58	4.58	16750±140	720
MD02-2499	mixed benthic forams	7.98	7.98	25800±180	1750
MD02-2499	mixed planktic forams	7.98	7.98	24900±120	720
MD02-2499	*Uvigerina* spp.	11.78	11.78	47300±930	1750
MD02-2499	mixed planktic forams	11.78	11.78	38600±540	720

(continued on next page)

Table D.2 (continued)

CORE	Reservoir Corrected Age (years B.P.)	calendar age (years B.P.)	Final depth (mcd)	average calendar age (years B.P.)	Reference
ODP 1019D	290±40	310±80	0.16	333±190	Barron et al. (2003)
ODP 1019D	380±40	430±90			Barron et al. (2003)
ODP 1019D	1290±40	1250±60	0.57	1216±205	Barron et al. (2003)
ODP 1019D	3350±700	3670±910	1.27	3677±205	Barron et al. (2003)
ODP 1019D	4650±40	5430±90	2.21	5342±257	Barron et al. (2003)
ODP 1019C		6741±183	2.84	6741±183	Mix et al. (1999) and this study
ODP 1019C	9230±228	10458±301	4.17	10458±301	Mix et al. (1999) and this study
ODP 1019C	9490±233	10805±308	4.92	10805±308	Mix et al. (1999) and this study
ODP 1019C	10690±263	12566±333	5.16	12566±333	Mix et al. (1999) and this study
ODP 1019C	10860±244	12804±259	5.81	12804±259	Mix et al. (1999) and this study
ODP 1019C	11230±228	13135±219	6.21	13135±219	Mix et al. (1999) and this study
ODP 1019C	12630±233	14917±473	7.11	14917±473	Mix et al. (1999) and this study
ODP 1019C	14360±233	17457±359	8.21	17457±359	Mix et al. (1999) and this study
ODP 1019C	15320±244	18624±247	9.54	18624±247	Mix et al. (1999) and this study
ODP 1019C	17830±290	21200±470	10.55	21200±470	Mix et al. (1999) and this study
ODP 1019C	20520±344	24553±443	12.15	24553±443	Mix et al. (1999) and this study
MD02-2499	9200±206	10384±267	1.28	10549±279	This study
MD02-2499	9380±210	10624±301			This study
MD02-2499	16100±215	19277±203	4.58	19260±237	This study
MD02-2499	16030±244	19213±231			This study
MD02-2499	24050±269	28624±299	7.98	28858±348	This study
MD02-2499	24180±233	28762±263			This study
MD02-2499	45550±951	48815±1879	11.78	44669±898	This study
MD02-2499	37880±576	42705±430			This study

Table D.3 - Calendar (cal) corrections for Lund and Mix (1998) age model (“m pf” is mixed planktonic foraminifera, “m bf” is mixed benthic foraminifera).

Source	Depth (cm)	material	measured 14C age (years)	measured 14C error (years)	Modern Reservoir age (years)	Modern reservoir error
Lund and Mix, 1998	198.75	m pf	13000	900	720	200
	198.75	m bf	14700	250	2310	200
	212.5	*G. bulloides*	13700	700	720	200
	227.5	m pf	15270	220	720	200
	301.25	m pf	16710	120	720	200
	301.25	m bf	18360	200	2310	200
	303.75	m pf	17030	150	720	200
	303.75	m bf	18630	180	2310	200
	332.5	m pf	18370	270	720	200
	382	*G. bulloides*	22140	140	720	200

Source	Depth (cm)	material	delta R	Reservoir Corrected 14C	Reservoir corrected 14C error	Calib 5.0.2 cal age (years B.P.)
Lund and Mix, 1998	198.75	m pf	320	12280	921.9544457	14405.5
	198.75	m bf	1910	12390	320.1562119	14463.5
	212.5	*G. bulloides*	320	12980	728.0109889	15191
	227.5	m pf	320	14550	297.3213749	17518.5
	301.25	m pf	320	15990	233.2380758	19182
	301.25	m bf	1910	16050	282.8427125	19223
	303.75	m pf	320	16310	250	19409.5
	303.75	m bf	1910	16320	269.0724809	19420
	332.5	m pf	320	17650	336.0059523	20848.5
	382	*G. bulloides*	320	21420	244.1311123	out of range

Source	Depth (cm)	material	Calib 5.0.2 error (years B.P.)	Fairbanks 0805 cal age (years B.P.)	Fairbanks 0805 error (years B.P.)	CALPAL 2005 SFCP cal age (years B.P.)
Lund and Mix, 1998	198.75	m pf	1146.5	14428	1220	14919
	198.75	m bf	460.5	14462	497	14693
	212.5	*G. bulloides*	1016	15369	1062	15651
	227.5	m pf	502.5	17691	461	17882
	301.25	m pf	199	19178	222	19213
	301.25	m bf	236	19230	263	19309
	303.75	m pf	195.5	19462	238	19580
	303.75	m bf	198	19472	258	19600
	332.5	m pf	445.5	20984	488	21117
	382	*G. bulloides*	out of range	25763	351	25657

Source	Depth (cm)	material	CALPAL 2005 SFCP error (years B.P.)	Average cal age (years B.P.) Calib, Fairbanks and CALPAL	Average error Calib, Fairbanks and CALPAL (years B.P.)	Average cal age (years B.P.) pf and pb
Lund and Mix, 1998	198.75	m pf	1408	14584	1258	
	198.75	m bf	617	14540	525	14562 (±892)
	212.5	*G. bulloides*	1166	15404	1081	
	227.5	m pf	354	17697	439	
	301.25	m pf	272	19191	231	
	301.25	m bf	347	19254	282	19223 (±257)
	303.75	m pf	379	19484	271	
	303.75	m bf	400	19497	285	19491 (±278)
	332.5	m pf	508	20983	481	
	382	*G. bulloides*	468	25710	410	

Table D.4 – Corrected calendar ages (years B.P.) for sand layers.

Source	sand layer depth (cm)	age (cal years BP) at the base of sand layer
Lund and Mix, 1998	206-208	15128
	230-232	17790
	252-256	18287
	322-325	20594
	355-358	23464

Table D.5 - Calendar (cal) corrections for Zuffa et al. (2000) age model ("m pf" is mixed planktonic foraminifera at the top of the turbidites).

Source	Depth (cm)	material	measured 14C age (years)	measured 14C error (years)	Modern Reservoir age (years)	Modern reservoir error
Zuffa et al, 2000	21.57	m pf	11600	85	720	200
	121.5	m pf	16200	100	720	200
	262.25	m pf	25700	160	720	200
Source	Depth (cm)	material	delta R	Reservoir Corrected 14C	Reservoir corrected 14C error	Calib 5.0.2 cal age (years B.P.)
Zuffa et al, 2000	21.57	m pf	320	10880	217.3131381	12877
	121.5	m pf	320	15480	223.6067977	18790
	262.25	m pf	320	24980	256.1249695	out range
Source	Depth (cm)	material	Calib 5.0.2 error (years B.P.)	Fairbanks 0805 cal age (years B.P.)	Fairbanks 0805 error (years B.P.)	CALPAL 2005 SFCP cal age (years B.P.)
Zuffa et al, 2000	21.57	m pf	215	12821	216	12827
	121.5	m pf	168	18734	187	18726
	262.25	m pf	out range	29983	530	29929
Source	Depth (cm)	material	CALPAL 2005 SFCP error (years B.P.)	Average cal age (years B.P.) Calib, Fairbanks and CALPAL	Average error Calib, Fairbanks and CALPAL (years B.P.)	
Zuffa et al, 2000	21.57	m pf	212	12842	214	
	121.5	m pf	322	18750	255	
	262.25	m pf	337	29956	434	

Table D.6 - List of relative percentages of freshwater diatoms for downcore samples (modern calibration samples are in appendix C, table 1). Age is in years B. P.

Centric Planktonic
Pennate and/or Benthic

CORE	Age	*Aulacoseira islandica*	*Aulacoseira granulata*	*Aulacoseira spp.*	*Aulacosira italica*	*Cyclotella kutzingiana*	*Cyclotella ocellata*
CL30/1019D	31	0.0	0.0	0.0	0.0	0.0	0.0
1019D	247	0.0	0.0	0.0	0.0	0.0	0.0
1019D	462	0.0	0.0	0.0	0.0	0.0	0.0
1019D	678	0.0	0.0	0.0	0.0	0.0	0.0
1019D	893	0.0	0.0	0.0	0.0	0.0	0.3
1019D	1423	0.0	0.0	0.0	0.0	0.0	0.0
1019D	2260	0.0	0.0	0.0	0.0	0.0	0.0
1019D	3093	0.0	0.0	0.0	0.0	0.0	0.0
1019D	3787	0.0	0.0	0.0	0.0	0.0	0.0
1019D	4153	0.5	0.0	0.0	0.0	0.0	0.0
1019D	4336	0.0	0.0	0.0	0.0	0.0	0.0
1019D	4683	0.0	0.6	0.0	0.0	0.0	0.0
1019D	5050	0.0	0.0	0.0	0.0	0.0	0.0
1019D	5415	0.0	0.0	0.0	0.0	0.0	0.0
1019D	5781	0.3	0.3	0.0	0.0	0.0	0.0
1019D	6148	0.0	0.3	0.0	0.0	0.0	0.0
1019D	6513	0.0	0.0	0.0	0.0	0.0	0.0
1019D	6879	0.9	0.0	0.0	0.0	0.0	0.0
1019D	7244	0.0	0.0	0.0	0.3	0.0	0.0
1019D	7574	0.0	0.3	0.0	0.0	0.0	0.0
MD02-2499	8000	1.0	0.0	0.0	0.0	0.0	0.0
MD02-2499	8472	0.0	0.0	0.0	0.0	0.0	0.0
MD02-2499	9747	0.0	2.9	0.0	0.0	0.0	0.0
MD02-2499	10549	1.0	2.0	0.0	0.0	0.0	0.0
MD02-2499	11276	0.5	0.5	0.0	0.0	0.0	0.0
MD02-2499	11894	0.0	0.0	0.0	0.0	0.5	0.0
MD02-2499	12421	0.5	0.0	0.0	0.0	0.0	0.0
MD02-2499	13093	0.0	0.0	0.0	0.0	0.0	0.0
MD02-2499	13820	2.0	0.5	0.0	0.0	0.0	0.0
MD02-2499	14546	0.3	0.0	0.0	0.0	0.3	0.0
MD02-2499	15273	0.0	0.0	0.0	0.0	0.0	0.0
MD02-2499	16000	0.0	0.0	0.0	0.0	0.0	0.0
MD02-2499	16362	0.3	0.0	0.0	0.3	0.0	0.0
MD02-2499	17811	8.0	12.0	0.0	0.0	0.0	12.0
MD02-2499	18536	6.0	7.6	0.0	0.0	0.0	2.5
MD02-2499	18898	2.5	5.0	0.0	0.0	0.0	4.0
MD02-2499	19260	1.6	2.2	0.0	0.0	0.0	1.2
MD02-2499	19796	7.0	2.0	0.0	0.0	1.0	4.0
MD02-2499	20389	4.0	2.0	0.0	0.0	0.0	1.0
MD02-2499	20954	3.9	2.9	0.0	0.0	0.0	0.0
MD02-2499	21519	3.4	1.0	0.0	1.0	0.0	1.4
MD02-2499	22083	2.5	0.5	0.0	0.0	0.0	1.5
MD02-2499	22648	0.0	2.0	0.0	0.0	0.0	2.0
MD02-2499	23213	11.9	10.0	0.0	1.0	0.0	5.0
MD02-2499	23777	2.9	2.0	0.0	2.9	0.0	2.0
MD02-2499	24342	1.0	1.0	0.0	0.0	0.0	1.0

(continued on next page)

Table D.6 (continued)

Centric Planktonic
Pennate and/or Benthic

CORE	age	*Cyclotella comta*	*Melosira ambigua*	*Melosira distans*	*Epithemia turgida*	*Fragilaria construens*	*Fragilaria inflata*
CL30/1019D	31	0.0	0.0	0.0	0.0	0.0	0.0
1019D	247	0.0	0.0	0.0	0.0	0.0	0.0
1019D	462	0.0	0.0	0.0	0.0	0.0	0.0
1019D	678	0.0	0.3	0.0	0.0	0.0	0.0
1019D	893	0.0	0.0	0.0	0.0	0.0	0.0
1019D	1423	0.0	0.0	0.0	0.0	0.0	0.0
1019D	2260	0.0	0.0	0.0	0.0	0.3	0.0
1019D	3093	0.0	0.0	0.0	0.0	0.0	0.0
1019D	3787	0.0	0.0	0.0	0.0	0.0	0.0
1019D	4153	0.0	0.0	0.0	0.0	0.0	0.0
1019D	4336	0.0	0.0	0.0	0.0	0.0	0.0
1019D	4683	0.0	0.0	0.0	0.0	0.0	0.0
1019D	5050	0.0	0.0	0.0	0.0	0.0	0.0
1019D	5415	0.0	0.0	0.0	0.0	0.0	0.0
1019D	5781	0.0	0.0	0.0	0.0	0.0	0.0
1019D	6148	0.0	0.0	0.0	0.0	0.0	0.0
1019D	6513	0.0	1.0	0.0	0.0	0.0	0.0
1019D	6879	0.0	1.8	0.0	0.0	0.0	0.0
1019D	7244	0.3	0.0	0.0	0.0	0.0	0.0
1019D	7574	0.0	0.0	0.0	0.0	0.0	0.0
MD02-2499	8000	0.0	1.0	0.0	0.0	0.0	0.0
MD02-2499	8472	0.0	1.0	0.0	0.0	0.0	0.0
MD02-2499	9747	0.0	0.0	0.0	0.0	0.0	0.0
MD02-2499	10549	0.0	0.0	0.0	0.0	0.0	0.0
MD02-2499	11276	0.0	0.0	0.0	0.0	0.0	0.0
MD02-2499	11894	0.0	0.0	0.5	0.0	0.0	0.5
MD02-2499	12421	0.0	0.0	0.0	0.0	0.0	0.0
MD02-2499	13093	0.0	0.0	0.0	0.0	0.0	0.0
MD02-2499	13820	0.0	1.5	0.0	0.0	0.0	0.0
MD02-2499	14546	0.0	0.0	0.0	0.0	0.6	0.0
MD02-2499	15273	0.0	0.0	0.6	0.0	0.0	0.0
MD02-2499	16000	0.0	0.9	0.0	0.0	0.3	0.0
MD02-2499	16362	0.0	0.3	0.0	0.0	0.0	0.0
MD02-2499	17811	0.0	0.0	0.0	0.5	0.0	0.0
MD02-2499	18536	4.0	4.0	0.0	0.0	1.0	0.0
MD02-2499	18898	3.5	2.5	0.0	0.0	0.5	1.2
MD02-2499	19260	1.2	1.6	0.0	0.0	1.1	0.8
MD02-2499	19796	1.0	5.0	0.0	0.0	0.0	0.0
MD02-2499	20389	1.0	6.0	0.0	0.0	0.0	3.0
MD02-2499	20954	2.0	0.0	0.0	0.0	0.0	0.0
MD02-2499	21519	1.0	1.4	0.0	0.0	1.0	0.5
MD02-2499	22083	0.5	1.0	0.0	0.0	1.0	0.5
MD02-2499	22648	3.9	1.0	3.0	0.0	0.0	0.0
MD02-2499	23213	4.0	8.0	0.0	0.0	1.0	0.0
MD02-2499	23777	2.0	1.0	0.0	0.0	0.0	0.0
MD02-2499	24342	3.0	4.0	0.0	0.0	0.0	0.0

(continued on next page)

Table D.6 (continued)

Centric Planktonic
Pennate and/or Benthic

CORE	age	*Fragilaria pinnata*	*Surirella linearis*	Total FW	Salinity (PSU)
CL30/1019D	31	0.0	0.0	0.00	32.93
1019D	247	0.0	0.0	0.00	32.93
1019D	462	0.0	0.2	0.16	32.90
1019D	678	0.0	0.1	0.44	32.83
1019D	893	0.0	0.8	1.10	32.67
1019D	1423	0.0	0.0	0.00	32.93
1019D	2260	0.0	0.0	0.32	32.86
1019D	3093	0.0	0.0	0.00	32.93
1019D	3787	0.0	0.0	0.00	32.93
1019D	4153	0.0	0.0	0.48	32.82
1019D	4336	0.0	0.0	0.00	32.93
1019D	4683	0.0	0.0	0.63	32.78
1019D	5050	0.0	0.0	0.00	32.93
1019D	5415	0.0	0.0	0.00	32.93
1019D	5781	0.0	0.0	0.63	32.78
1019D	6148	0.2	0.0	0.49	32.82
1019D	6513	0.0	0.0	0.95	32.71
1019D	6879	0.0	0.9	3.62	32.07
1019D	7244	0.0	0.0	0.66	32.78
1019D	7574	0.0	0.3	0.61	32.79
MD02-2499	8000	0.0	0.0	2.02	32.45
MD02-2499	8472	0.0	0.0	1.00	32.69
MD02-2499	9747	0.0	0.0	2.87	32.25
MD02-2499	10549	0.0	0.0	2.97	32.22
MD02-2499	11276	0.0	0.0	0.95	32.71
MD02-2499	11894	0.0	0.0	1.43	32.59
MD02-2499	12421	0.0	0.0	0.49	32.82
MD02-2499	13093	0.0	0.0	0.00	32.93
MD02-2499	13820	0.0	0.0	3.97	31.98
MD02-2499	14546	0.0	0.0	1.22	32.64
MD02-2499	15273	0.0	0.6	1.29	32.62
MD02-2499	16000	0.0	0.3	1.43	32.59
MD02-2499	16362	0.0	0.3	1.28	32.63
MD02-2499	17811	2.0	0.0	34.50	24.68
MD02-2499	18536	0.0	0.0	25.19	26.90
MD02-2499	18898	0.0	0.7	19.80	28.19
MD02-2499	19260	0.0	0.6	10.26	30.48
MD02-2499	19796	0.0	0.0	19.90	28.17
MD02-2499	20389	0.0	0.0	16.92	28.88
MD02-2499	20954	0.0	0.0	8.82	30.82
MD02-2499	21519	0.0	0.0	10.63	30.39
MD02-2499	22083	0.0	0.0	7.39	31.16
MD02-2499	22648	0.0	0.0	11.82	30.10
MD02-2499	23213	0.0	0.0	40.80	23.17
MD02-2499	23777	2.0	0.0	14.71	29.41
MD02-2499	24342	0.0	0.0	10.00	30.54

(continued on next page)

Table D.6 (continued)

Centric Planktonic
Pennate and/or Benthic

CORE	age	*Aulacoseira islandica*	*Aulacoseira granulata*	*Aulacoseira spp.*	*Aulacosira italica*	*Cyclotella kutzingiana*	*Cyclotella ocellata*
MD02-2499	24906	1.0	1.9	0.0	0.0	0.0	0.0
MD02-2499	25471	0.0	1.0	0.0	2.0	0.0	4.0
MD02-2499	26600	2.7	0.0	0.0	0.9	0.0	2.7
MD02-2499	27165	3.0	0.0	0.0	1.0	0.0	5.0
MD02-2499	28238	0.9	0.9	0.0	0.0	0.0	1.8
MD02-2499	28859	0.0	0.9	0.0	0.0	0.0	2.8
MD02-2499	29691	2.7	0.9	0.0	0.0	0.0	0.4
MD02-2499	30523	1.8	1.8	0.0	0.9	0.0	0.0
MD02-2499	31355	0.0	1.0	0.0	0.0	0.0	1.0
MD02-2499	32187	2.0	2.0	0.0	0.0	0.0	1.0
MD02-2499	33020	0.0	1.0	0.0	0.0	0.0	0.0
MD02-2499	33852	0.9	0.0	0.0	0.0	0.0	0.0
MD02-2499	34684	0.3	0.3	0.0	0.3	0.0	0.0
MD02-2499	35516	0.0	0.3	0.0	0.0	0.0	0.3
MD02-2499	36348	0.5	0.5	0.0	0.0	0.5	0.0
MD02-2499	37180	0.0	0.0	0.0	1.2	0.0	0.3
MD02-2499	38012	0.0	1.0	0.0	0.0	1.0	0.0
MD02-2499	38844	1.0	0.0	0.0	0.0	0.0	1.0
MD02-2499	39676	1.0	0.3	0.0	0.0	0.0	0.0
MD02-2499	40467	0.0	0.0	0.0	0.0	0.0	2.0
MD02-2499	41341	0.0	1.0	0.0	0.0	0.0	0.0
MD02-2499	42173	1.5	0.0	0.0	0.5	0.5	0.0
MD02-2499	43005	0.0	0.0	0.0	1.0	0.0	0.0
MD02-2499	43837	0.0	0.9	0.0	0.0	0.0	0.0
MD02-2499	44669	1.0	0.0	0.0	0.0	0.0	0.0
MD02-2499	45558	0.0	0.0	0.0	1.0	0.0	0.0
MD02-2499	47335	0.0	1.9	0.0	0.0	0.0	1.0
MD02-2499	48224	0.0	0.0	0.0	0.0	0.0	0.0
MD02-2499	49113	0.0	0.0	0.0	0.0	0.0	0.0
MD02-2499	50001	2.6	0.9	0.0	0.0	0.0	0.0
MD02-2499	50890	0.3	0.3	0.0	0.0	0.0	0.0
MD02-2499	51779	0.0	1.0	0.0	0.0	0.0	1.0
MD02-2499	52668	0.3	0.9	0.0	0.0	0.0	0.0
MD02-2499	53512	1.0	1.0	0.0	0.0	0.0	1.0
MD02-2499	54445	0.9	0.0	0.0	0.4	0.0	0.4
MD02-2499	55334	0.0	0.0	0.0	0.0	0.5	0.0
MD02-2499	56223	3.8	1.9	0.0	0.0	0.0	0.0
MD02-2499	57111	1.0	0.0	0.0	0.0	0.0	0.0
MD02-2499	58000	0.3	0.0	0.0	0.0	0.0	0.0
MD02-2499	58550	1.9	1.9	0.0	0.0	1.9	0.9
MD02-2499	59100	3.8	0.0	0.0	0.9	0.0	0.0
MD02-2499	59650	2.0	1.0	0.0	2.0	0.0	2.0
MD02-2499	60200	6.9	2.9	0.0	0.0	0.0	2.9

(continued on next page)

Table D.6 (continued)

Centric Planktonic
Pennate and/or Benthic

CORE	age	*Cyclotella comta*	*Melosira ambigua*	*Melosira distans*	*Epithemia turgida*	*Fragilaria construens*	*Fragilaria inflata*
MD02-2499	24906	2.9	1.0	0.0	0.0	0.0	0.0
MD02-2499	25471	2.0	2.0	0.0	0.0	0.0	0.0
MD02-2499	26600	3.6	1.8	3.6	0.0	0.5	0.0
MD02-2499	27165	2.0	0.0	5.0	0.0	1.0	0.0
MD02-2499	28238	2.6	3.5	0.0	0.0	0.9	0.0
MD02-2499	28859	0.0	6.5	0.0	0.0	0.9	0.0
MD02-2499	29691	0.0	0.0	0.0	0.0	0.0	0.0
MD02-2499	30523	2.8	6.4	0.0	0.9	1.8	0.0
MD02-2499	31355	1.9	3.9	0.0	1.0	0.0	1.0
MD02-2499	32187	1.0	3.0	0.0	0.0	0.0	0.0
MD02-2499	33020	1.0	3.8	0.0	0.0	0.0	0.0
MD02-2499	33852	0.0	1.9	0.0	0.0	0.0	0.0
MD02-2499	34684	0.0	0.6	0.0	0.0	0.0	0.0
MD02-2499	35516	0.0	0.3	0.0	0.0	0.0	0.0
MD02-2499	36348	0.5	1.0	0.0	0.0	0.0	0.0
MD02-2499	37180	0.0	2.1	0.0	0.0	0.0	0.0
MD02-2499	38012	0.0	0.5	0.0	0.0	0.0	0.0
MD02-2499	38844	0.0	2.0	0.0	0.0	1.0	0.0
MD02-2499	39676	0.3	1.3	0.0	0.0	1.3	0.0
MD02-2499	40467	1.0	2.0	0.0	0.0	0.0	0.0
MD02-2499	41341	0.0	2.0	0.0	0.0	0.0	0.0
MD02-2499	42173	0.0	0.5	0.0	0.0	0.0	0.0
MD02-2499	43005	1.0	1.0	0.0	0.0	0.0	0.0
MD02-2499	43837	0.5	0.0	0.0	0.0	0.0	0.0
MD02-2499	44669	0.0	2.0	0.0	0.0	0.0	0.0
MD02-2499	45558	0.5	0.0	0.0	0.5	0.0	0.0
MD02-2499	47335	1.0	3.8	0.0	0.0	0.0	0.0
MD02-2499	48224	0.0	0.0	0.0	0.0	0.0	0.0
MD02-2499	49113	0.0	1.9	0.0	0.0	0.0	0.0
MD02-2499	50001	0.0	2.6	0.0	0.0	0.0	0.0
MD02-2499	50890	0.0	0.3	0.0	0.0	0.0	0.0
MD02-2499	51779	1.9	0.0	0.0	0.0	0.0	0.0
MD02-2499	52668	0.6	0.9	0.0	0.0	0.3	0.0
MD02-2499	53512	0.0	1.0	0.0	0.0	0.0	0.0
MD02-2499	54445	0.0	2.6	0.0	0.0	0.0	0.0
MD02-2499	55334	0.0	1.9	0.0	0.0	0.0	0.0
MD02-2499	56223	0.0	3.8	0.0	0.0	0.0	0.0
MD02-2499	57111	0.0	0.5	0.0	0.0	0.0	0.0
MD02-2499	58000	0.0	0.7	0.0	0.0	0.0	0.0
MD02-2499	58550	0.0	2.8	0.0	0.0	0.0	0.0
MD02-2499	59100	0.9	4.7	0.0	0.0	0.0	0.0
MD02-2499	59650	2.0	3.9	0.0	0.0	0.0	0.0
MD02-2499	60200	1.0	4.9	0.0	0.0	0.0	0.0

(continued on next page)

Table D.6 (continued)

Centric Planktonic
Pennate and/or Benthic

CORE	age	*Fragilaria pinnata*	*Surirella linearis*	Total FW	Salinity (PSU)
MD02-2499	24906	0.0	0.0	6.67	31.34
MD02-2499	25471	0.0	2.0	13.00	29.82
MD02-2499	26600	0.0	2.7	18.55	28.49
MD02-2499	27165	0.0	2.0	19.00	28.39
MD02-2499	28238	0.0	5.3	15.79	29.15
MD02-2499	28859	0.0	0.9	12.15	30.03
MD02-2499	29691	0.0	0.0	4.04	31.97
MD02-2499	30523	0.0	0.0	16.51	28.98
MD02-2499	31355	0.0	1.0	10.63	30.39
MD02-2499	32187	0.0	0.0	9.00	30.78
MD02-2499	33020	0.0	1.0	6.67	31.34
MD02-2499	33852	0.0	0.0	2.82	32.26
MD02-2499	34684	0.0	0.0	1.43	32.59
MD02-2499	35516	0.0	0.0	0.95	32.71
MD02-2499	36348	0.0	0.5	3.40	32.12
MD02-2499	37180	0.0	0.0	3.52	32.09
MD02-2499	38012	0.0	0.0	2.49	32.34
MD02-2499	38844	0.0	0.0	4.90	31.76
MD02-2499	39676	0.0	0.0	4.32	31.90
MD02-2499	40467	0.0	0.0	5.00	31.74
MD02-2499	41341	0.0	0.0	3.00	32.22
MD02-2499	42173	0.0	0.0	2.96	32.22
MD02-2499	43005	0.0	0.0	3.00	32.22
MD02-2499	43837	0.0	0.0	1.42	32.59
MD02-2499	44669	0.0	0.0	2.93	32.23
MD02-2499	45558	0.0	0.0	1.95	32.47
MD02-2499	47335	0.0	0.0	7.66	31.10
MD02-2499	48224	0.0	0.0	0.00	32.93
MD02-2499	49113	0.0	0.0	1.93	32.47
MD02-2499	50001	0.0	0.0	6.06	31.48
MD02-2499	50890	0.0	0.0	0.94	32.71
MD02-2499	51779	0.0	0.0	3.83	32.02
MD02-2499	52668	0.0	0.3	3.43	32.11
MD02-2499	53512	0.0	0.0	3.96	31.99
MD02-2499	54445	0.0	0.0	4.42	31.88
MD02-2499	55334	0.0	0.5	2.82	32.26
MD02-2499	56223	0.0	0.9	10.33	30.46
MD02-2499	57111	0.0	0.0	1.44	32.59
MD02-2499	58000	0.0	0.0	1.00	32.69
MD02-2499	58550	0.0	0.0	9.35	30.70
MD02-2499	59100	0.0	0.0	10.38	30.45
MD02-2499	59650	0.0	0.0	12.81	29.87
MD02-2499	60200	0.0	0.0	18.63	28.47

Table D.7 - MD02-2499 $\delta^{18}O$ record from *Uvigerina sp.*

depth (cm composite)	age cal (years BP)	*Uvigerina sp.* $\delta^{18}O$	depth (cm composite)	age cal (years BP)	*Uvigerina sp.* $\delta^{18}O$
20	8000	3.32	780	28351	4.40
40	8472	3.47	798	28859	4.45
94	9747	3.56	818	29691	4.22
128	10549	3.48	838	30523	4.60
148	11276	3.44	858	31355	4.45
165	11894	3.47	878	32187	4.52
198	13093	3.62	898	33020	4.70
218	13820	4.00	918	33852	4.56
238	14546	3.96	938	34684	4.39
258	15273	4.02	958	35516	4.41
278	16000	3.86	978	36348	4.24
298	16362	3.96	998	37180	4.36
318	16724	4.46	1018	38012	4.33
330	16942	4.38	1038	38844	4.45
338	17087	4.38	1058	39676	4.47
358	17449	4.65	1077	40467	4.28
378	17811	4.67	1080	40592	4.41
398	18173	4.71	1098	41341	4.31
418	18536	4.61	1118	42173	4.41
438	18898	4.59	1138	43005	4.27
458	19260	4.77	1158	43837	4.36
477	19796	4.63	1178	44669	4.15
480	19881	4.54	1198	45558	4.42
498	20389	4.55	1218	46446	4.32
518	20954	4.65	1238	47335	4.39
538	21519	4.62	1258	48224	4.27
558	22083	4.64	1278	49113	4.19
578	22648	4.64	1298	50001	3.99
598	23213	4.53	1318	50890	4.04
618	23777	4.58	1338	51779	4.12
638	24342	4.58	1358	52668	4.05
658	24906	4.63	1377	53512	4.16
678	25471	4.76	1380	53645	4.15
698	26036	4.55	1398	54445	4.23
718	26600	4.76	1418	55334	4.14
738	27165	4.66	1438	56223	4.01
758	27730	4.37	1458	57111	4.08
776	28238	4.50	1478	58000	4.02

(continued on next page)

Table D.7 (continued)

depth (cm composite)	age cal (years BP)	*Uvigerina sp.* $\delta^{18}O$
1498	58550	4.22
1518	59100	4.31
1538	59650	4.06
1558	60200	4.17

Table D.8- ODP 1019 $\delta^{18}O$ record from *N. pachyderma* and *Uvigerina sp*.

depth (cm composite)	age cal (years BP)	*N. pachyderma* $\delta^{18}O$	*Uvigerina sp.* $\delta^{18}O$	difference
26	548	1.09	3.10	-2.01
50	1065	1.13	3.20	-2.07
100	2728	1.08	3.18	-2.10
150	4084	1.03	3.12	-2.09
176	4545	1.09	3.13	-2.04
225	5431	1.15	3.20	-2.05
250	5986	1.46	3.18	-1.72
296	7076	1.58	3.17	-1.59
303	7272	1.50	3.20	-1.70
323	7831	1.53	3.22	-1.69
326	7914	1.56	3.22	-1.66
343	8390	1.64	3.19	-1.55
350	8585	1.49	3.32	-1.83
363	8949	1.48	3.32	-1.84
375	9284	1.26	3.17	-1.91
383	9508	1.70	3.34	-1.64
400	9983	1.50	3.21	-1.71
403	10067	1.43	3.17	-1.74
403	10067	1.72	3.25	-1.53
413	10346	1.31	3.25	-1.94
413	10346	1.77	3.42	-1.65
414	10374	1.55	3.18	-1.63
422	10481	1.38	3.25	-1.87
423	10486	1.60	3.25	-1.65
433	10532	1.21	3.36	-2.15
433	10532	1.65	3.29	-1.64
443	10578	1.33	3.29	-1.96
446	10592	1.30	3.29	-1.99
453	10625	1.34	3.47	-2.13
453	10625	1.53	3.30	-1.77
463	10671	1.38	3.30	-1.92
463	10671	1.29	3.22	-1.93
473	10717	1.25	3.38	-2.13
476	10731	1.20	3.36	-2.16
483	10764	1.23	3.44	-2.21

(continued on next page)

Table D.8 (continued)

depth (cm composite)	age cal (years BP)	*N. pachyderma* $\delta^{18}O$	*Uvigerina sp.* $\delta^{18}O$	difference
492	10805	1.17	3.50	-2.33
500	11392	1.28	3.32	-2.04
503	11612	1.33	3.39	-2.06
522	12588	1.82	3.51	-1.69
525	12599	1.67	3.61	-1.94
533	12628	1.90	3.37	-1.47
543	12665	1.59	3.54	-1.95
550	12690	1.67	3.54	-1.87
563	12738	1.82	3.67	-1.85
573	12774	1.89	3.88	-1.99
575	12782	1.77	3.69	-1.92
582	12812	1.83	3.69	-1.86
593	12903	1.55	3.62	-2.07
594	12911	1.71	3.68	-1.97
603	12986	1.49	3.66	-2.17
613	13068	1.40	3.67	-2.27
623	13174	1.71	3.73	-2.02
626	13234	1.45	3.67	-2.22
626	13234	1.55	3.65	-2.10
633	13372	1.63	3.65	-2.02
643	13570	1.62	3.78	-2.16
650	13709	1.50	3.63	-2.13
653	13768	1.65	3.63	-1.98
663	13966	1.74	3.82	-2.08
673	14164	1.75	3.68	-1.93
675	14204	1.49	3.82	-2.33
675	14204	1.62	3.70	-2.08
694	14580	1.64	3.81	-2.17
694	14580	1.58	3.69	-2.11
700	14699	1.82	3.74	-1.92
700	14699	1.51	3.83	-2.32
702	14738	1.73	3.76	-2.03
712	14940	2.09	3.74	-1.65
712	14940	1.71	3.82	-2.11
716	15032	1.86	3.96	-2.10
742	15632	2.05	3.76	-1.71
753	15886	2.18	3.71	-1.53
762	16094	2.14	3.71	-1.57
772	16325	2.21	3.63	-1.42
782	16556	2.39	3.78	-1.39
793	16810	2.40	4.22	-1.82
803	17041	2.27	4.10	-1.83
813	17272	2.06	4.14	-2.08
823	17474	2.54	4.00	-1.46
833	17562	2.27	4.17	-1.90
844	17659	2.18	4.05	-1.87

(continued on next page)

Table D.8 (continued)

depth (cm composite)	age cal (years BP)	*N. pachyderma* $\delta^{18}O$	*Uvigerina sp.* $\delta^{18}O$	difference
853	17738	2.12	4.07	-1.95
872	17904	1.92	4.18	-2.26
878	17957	2.44	4.16	-1.72
882	17992	2.28	4.41	-2.13
893	18089	2.30	4.18	-1.88
902	18168	2.25	4.23	-1.98
912	18255	2.23	4.16	-1.93
933	18440	2.27	4.18	-1.91
943	18527	2.24	4.22	-1.98
950	18589	2.02	4.23	-2.21
952	18606	1.96	4.24	-2.28
953	18615	2.22	4.30	-2.08
963	18854	2.04	4.47	-2.43
973	19109	2.02	4.17	-2.15
983	19364	2.17	4.53	-2.36
1002	19848	1.85	4.26	-2.41
1012	20103	1.90	4.48	-2.58
1023	20344	1.92	4.59	-2.67
1033	20564	2.00	4.43	-2.43
1036	20629	2.03	4.31	-2.28
1036	20629	2.00	4.45	-2.45
1043	20783	1.94	4.37	-2.43
1053	21002	1.89	4.46	-2.57
1062	21199	2.01	4.55	-2.54
1073	21440	1.97	4.52	-2.55
1082	21638	1.79	4.40	-2.61
1092	21857	2.08	4.82	-2.74
1102	22076	2.01	4.41	-2.40
1103	22098	1.90	4.52	-2.62
1112	22295	1.87	4.28	-2.41
1123	22536	1.90	4.45	-2.55
1133	22755	1.81	4.43	-2.62
1144	22997	1.91	4.49	-2.58
1152	23172	1.88	4.33	-2.45
1163	23413	1.92	4.35	-2.43
1178	23742	1.76	4.34	-2.58
1178	23742	2.16	4.48	-2.32
1193	24071	1.70	4.55	-2.85
1213	24509	1.77	4.51	-2.74
1252	24958	2.44	4.27	-1.83
1328	25790	2.26	4.31	-2.05
1402	26600	2.30	4.66	-2.36
1450	27126	2.29	4.30	-2.01
1477	27422	2.58	4.35	-1.77
1502	27695	2.35	4.30	-1.95
1552	28243	2.32	4.47	-2.15

(continued on next page)

Table D.8 (continued)

depth (cm composite)	age cal (years BP)	*N. pachyderma* $\delta^{18}O$	*Uvigerina sp.* $\delta^{18}O$	difference
1581	28561	2.37	4.34	-1.97
1602	28790	2.32	4.26	-1.94
1626	29053	2.37	4.38	-2.01
1653	29349	2.00	4.39	-2.39
1680	29645	2.17	4.27	-2.10
1697	29831	1.83	4.43	-2.60
1728	30170	2.06	4.43	-2.37
1732	30214	2.21	4.38	-2.17
1835	31342	2.37	4.26	-1.89
1909	32152	2.33	4.51	-2.18
1989	33028	2.42	4.37	-1.95
2059	33795	2.53	4.45	-1.92
2135	34627	2.45	4.45	-2.00
2209	35437	2.33	4.40	-2.07
2285	36270	2.12	4.53	-2.41
2409	37627	2.62	4.39	-1.77
2430	37857	1.85	4.34	-2.49
2456	38142	1.90	4.30	-2.40
2517	38810	1.98	4.59	-2.61
2545	39117	2.13	4.48	-2.35
2588	39588	2.29	4.32	-2.03
2597	39686	1.97	4.45	-2.48
2605	39774	2.01	4.45	-2.44
2617	39905	2.25	4.42	-2.17
2667	40453	2.56	4.35	-1.79
2695	40759	2.73	4.45	-1.72
2696	40770	2.68	4.45	-1.77
2728	41121	2.27	4.48	-2.21
2765	41526	2.01	4.45	-2.44
2832	42259	2.47	4.31	-1.84
3347	47899	2.49	4.51	-2.02
3421	48709	1.26	4.45	-3.19
3442	48939	1.51	4.40	-2.89
3472	49268	1.49	4.36	-2.87
3497	49541	0.93	4.51	-3.58
3521	49804	1.21	4.33	-3.12
3549	50111	1.09	4.30	-3.21
3571	50352	1.03	4.38	-3.35
3600	50669	1.08	4.43	-3.35
3621	50899	1.21	4.52	-3.31
3647	51184	1.24	4.33	-3.09
3671	51447	1.23	4.37	-3.14
3699	51753	1.28	4.30	-3.02
3721	51994	1.29	4.38	-3.09
3750	52312	1.79	4.50	-2.71
3768	52509	1.82	4.38	-2.56

(continued on next page)

Table D.8 (continued)

depth (cm composite)	age cal (years BP)	*N. pachyderma* $\delta^{18}O$	*Uvigerina sp.* $\delta^{18}O$	difference
3797	52826	2.01	4.38	-2.37
3871	53637	2.22	4.33	-2.11
3947	54469	2.37	4.41	-2.04
4087	56002	1.95	4.43	-2.48
4111	56265	1.96	4.39	-2.43
4340	58772	2.09	4.47	-2.38

APPENDIX E: Supplementary data for Chapter 5.

Table E.1 – Species relative percentages for method 1. For method 2, the "no-analog dataset" species names in gray boxes were removed and relative percentages recalculated for a closure of 100%.

Core ID (figure 5.1)	C1	C2	C3	C4	C5
Sample designation	W8809-11GC	W8909-24GC	TT39-15 REF	TT39-5AC REF	W8306-A1-RKC*
depth (cm)					
Freshwater	0.66	0.00	4.45	4.17	2.96
Benthics	0.00	0.00	1.11	0.00	0.00
Actinocyclus curvatulus	0.53	0.31	1.91	0.00	0.91
Actinocyclus normanii	1.32	0.31	1.59	1.19	1.37
Actinoptychus senarius	1.85	1.88	2.23	0.30	3.19
Stephanodiscus rotula (f. minutula)	0.00	0.00	0.00	0.00	0.46
Bacteriastrum spp.	0.00	0.00	0.00	0.30	0.00
Chaetoceros spores	60.16	36.42	27.34	15.50	24.57
Coscinodiscus decrescens	0.00	0.00	0.00	0.00	0.00
Coscinodiscus oculus iridis	0.00	0.00	0.00	0.00	0.00
Coscinodiscus marginatus	0.53	0.00	3.50	1.19	0.91
Coscinodiscus radiatus	0.53	5.97	7.00	4.17	5.46
Cyclotella litoralis	0.00	1.57	0.32	0.00	0.46
Cyclotella spp.	0.53	0.00	2.23	0.00	1.37
Cyclotella striata	0.53	0.00	0.32	0.30	0.46
Hemidiscus cuneiformis	1.06	1.57	0.32	0.00	0.00
Leptocylindrus spores	1.32	0.31	0.00	0.30	2.73
Melosira westi	0.00	0.00	1.27	0.00	0.00
Odontella aurita	0.00	0.31	0.00	0.00	2.28
Paralia sulcata	0.00	0.00	9.22	1.49	2.73
Rhizosolenia setigera	0.00	0.31	0.00	0.00	0.00
Rhizosolenia hebetata (f. hebetatata)	1.32	1.57	2.86	4.47	2.73
Rhizosolenia styliformis	0.00	0.31	0.32	0.00	0.00
Roperia tesselata	1.06	0.63	0.32	0.00	0.46
Stephanopyxis turris	0.00	0.00	0.00	0.00	0.00
Thalassiossira allenii	0.00	0.00	0.32	0.00	0.46
Thalassiossira anguste-lineata	0.79	2.51	0.32	0.89	0.46
Thalassiossira eccentrica	0.00	0.00	0.95	1.49	1.82
Thalassiossira leptotus	0.26	0.00	0.00	0.00	0.00
Thalassiossira lineata	0.00	0.00	0.00	0.00	2.28
Thalassiossira nanolineata	0.00	0.00	0.00	0.00	0.00
Thalassiossira oestrupii	0.79	0.94	2.86	4.17	1.37
Thalassiossira cf. *poroseriata*	0.00	0.00	0.64	0.00	0.00
Thalassiossira angulata and/or *pacifica*	0.53	0.94	0.95	1.49	0.00
Thalassiossira cf. *trifulta*	0.00	0.00	0.00	0.00	0.00
Thalassiossira sp.1	0.00	1.26	0.95	2.98	0.46
Thalassiossira sp.2	0.53	0.00	0.32	0.00	0.00
Thalassiossira sp.6	0.00	0.00	0.00	0.00	0.00
Thalassiossira spp.	0.00	0.31	0.00	0.00	0.00
Delphineis surilella	0.00	0.00	0.00	0.00	0.00
Delphineis karstenii	0.00	0.00	0.32	0.00	0.00
Fragilariopsis doliolus	4.22	7.69	2.23	4.92	3.75
Gomphonema constrictum	0.00	0.00	0.00	0.00	0.00
Lioloma elongatum	0.40	0.47	0.79	0.60	0.46
Lioloma pacificum	0.40	0.63	0.32	0.75	0.57
Lioloma spp.	0.00	0.00	0.00	0.89	0.68
Neodenticula seminae	0.79	1.57	5.72	29.06	22.18
Nitzschia gp *bicapitata*	0.00	0.00	0.32	0.30	0.23
Raphoneis amphiceros	0.26	1.41	0.00	0.00	0.00
Thalassionema bacillare	0.26	1.73	0.00	0.00	0.00
Thalassionema nitzschioides	19.13	26.22	14.63	16.39	12.51

(continued on next page)

Table E.1 (continued)

Core ID (figure 5.1)	C6	C7	C8	C9	C10
Sample designation	LG-85-NC 3GC	W8508-9GC	W7905-160G	W9205-1GC	7407Y-1 REF
depth (cm)					
Freshwater	0.99	2.76	0.62	1.36	0.33
Benthics	0.00	0.49	0.47	0.00	0.00
Actinocyclus curvatulus	0.66	0.00	0.31	0.00	0.00
Actinocyclus normanii	0.99	0.32	0.31	0.00	1.95
Actinoptychus senarius	0.00	2.59	1.56	1.36	0.33
Stephanodiscus rotula (f. minutula)	0.33	0.00	0.93	0.34	0.00
Bacteriastrum spp.	0.00	0.00	0.00	0.00	0.00
Chaetoceros spores	22.44	48.95	54.52	64.52	28.99
Coscinodiscus decrescens	0.00	0.00	0.00	0.00	0.00
Coscinodiscus oculus iridis	0.33	0.00	0.00	0.00	0.00
Coscinodiscus marginatus	0.33	0.00	0.62	0.68	0.00
Coscinodiscus radiatus	2.97	3.57	1.25	1.70	2.61
Cyclotella litoralis	0.00	0.00	0.00	0.00	0.00
Cyclotella spp.	0.99	0.65	0.31	0.68	0.33
Cyclotella striata	0.33	0.32	1.25	0.68	0.33
Hemidiscus cuneiformis	0.33	0.32	0.00	0.34	0.98
Leptocylindrus spores	1.32	0.32	1.56	1.02	0.00
Melosira westi	0.00	0.00	0.00	0.00	0.00
Odontella aurita	0.00	0.00	0.00	0.00	0.33
Paralia sulcata	0.66	0.97	2.18	1.36	0.33
Rhizosolenia setigera	0.00	0.00	0.00	0.00	0.00
Rhizosolenia hebetata (f. hebetatata)	2.97	0.00	0.31	1.70	0.33
Rhizosolenia styliformis	0.00	6.81	0.00	0.00	0.00
Roperia tesselata	1.32	0.00	0.00	1.02	2.28
Stephanopyxis turris	0.00	0.00	0.00	0.00	0.00
Thalassiossira allenii	0.33	0.00	0.00	0.00	0.00
Thalassiossira anguste-lineata	0.33	0.32	1.87	0.68	0.33
Thalassiossira eccentrica	2.31	0.65	0.00	0.34	1.63
Thalassiossira leptotus	0.00	0.00	0.00	0.00	0.00
Thalassiossira lineata	0.66	0.00	0.00	1.36	0.00
Thalassiossira nanolineata	0.00	0.00	0.31	0.00	0.00
Thalassiossira oestrupii	2.31	2.92	0.93	0.34	4.56
Thalassiossira cf. *poroseriata*	1.65	0.00	0.00	0.00	0.00
Thalassiossira angulata and/or *pacifica*	0.33	0.00	0.00	0.00	0.65
Thalassiossira cf. *trifulta*	0.00	0.00	0.00	0.00	0.00
Thalassiossira sp.1	0.33	0.00	0.31	0.34	0.00
Thalassiossira sp.2	0.00	0.00	0.00	0.00	0.00
Thalassiossira sp.6	0.00	0.00	0.00	0.00	0.00
Thalassiossira spp.	0.00	0.00	0.00	0.34	0.00
Delphineis surilella	0.33	0.81	0.62	0.68	0.65
Delphineis karstenii	0.33	0.00	0.78	0.00	0.16
Fragilariopsis doliolus	11.06	0.97	3.43	1.36	11.40
Gomphonema constrictum	0.00	0.00	0.00	0.00	0.00
Lioloma elongatum	0.50	0.97	0.31	0.17	0.49
Lioloma pacificum	1.32	1.78	0.31	0.17	0.65
Lioloma spp.	1.49	1.30	0.78	0.51	0.98
Neodenticula seminae	0.33	0.65	0.00	0.51	3.91
Nitzschia gp *bicapitata*	0.17	0.00	0.00	0.00	0.33
Raphoneis amphiceros	0.00	0.49	0.31	0.00	0.00
Thalassionema bacillare	0.33	0.00	0.31	0.00	0.65
Thalassionema nitzschioides	35.81	18.31	19.94	15.45	31.92

(continued on next page)

Table E.1 (continued)

Core ID (figure 5.1)	C11	C12	C13	C14
Sample designation	TT39-18 AC REF	TT29-22 AC REF	TT39-11 AC REF	TT31-011 GC REF
depth (cm)				
Freshwater	7.02	5.09	3.94	1.03
Benthics	0.34	0.38	0.47	0.00
Actinocyclus curvatulus	0.68	0.38	0.32	1.37
Actinocyclus normanii	1.03	0.38	1.26	0.00
Actinoptychus senarius	0.34	0.00	0.32	0.00
Stephanodiscus rotula (f. minutula)	0.00	0.75	0.00	0.34
Bacteriastrum spp.	0.00	0.00	0.00	0.00
Chaetoceros spores	32.53	25.66	41.32	1.03
Coscinodiscus decrescens	0.00	0.38	0.00	6.84
Coscinodiscus oculus iridis	1.03	0.00	0.00	0.00
Coscinodiscus marginatus	1.03	0.75	0.32	2.74
Coscinodiscus radiatus	3.08	3.02	3.15	6.15
Cyclotella litoralis	2.05	2.26	0.63	0.34
Cyclotella spp.	2.40	2.26	0.00	1.03
Cyclotella striata	0.00	0.38	2.52	0.00
Hemidiscus cuneiformis	0.34	0.00	0.32	1.03
Leptocylindrus spores	0.00	1.51	0.32	0.00
Melosira westi	0.00	0.00	0.63	0.00
Odontella aurita	0.00	0.00	0.00	0.00
Paralia sulcata	4.11	1.89	6.62	0.00
Rhizosolenia setigera	0.00	0.00	0.00	0.00
Rhizosolenia hebetata (f. hebetatata)	3.42	6.04	2.21	10.60
Rhizosolenia styliformis	0.00	0.00	0.00	0.00
Roperia tesselata	0.34	0.38	0.00	0.00
Stephanopyxis turris	0.00	0.00	0.00	0.34
Thalassiossira allenii	0.00	0.00	1.58	0.00
Thalassiossira anguste-lineata	0.00	0.00	0.32	0.00
Thalassiossira eccentrica	1.71	1.89	0.00	7.86
Thalassiossira leptotus	0.68	0.38	0.00	2.74
Thalassiossira lineata	0.00	0.00	0.00	0.00
Thalassiossira nanolineata	0.00	0.00	0.00	0.00
Thalassiossira oestrupii	4.45	3.02	1.26	15.73
Thalassiossira cf. *poroseriata*	0.00	0.00	0.00	0.00
Thalassiossira angulata and/or *pacifica*	0.00	0.00	1.58	0.00
Thalassiossira cf. *trifulta*	0.00	0.00	0.00	2.74
Thalassiossira sp.1	0.00	0.00	2.21	6.15
Thalassiossira sp.2	0.00	0.00	0.32	0.00
Thalassiossira sp.6	0.00	0.00	0.00	2.39
Thalassiossira spp.	0.00	1.13	0.00	3.42
Delphineis surilella	0.34	0.38	0.00	0.00
Delphineis karstenii	0.34	0.19	0.00	0.00
Fragilariopsis doliolus	2.23	0.94	1.26	4.27
Gomphonema constrictum	0.00	0.00	0.00	0.00
Lioloma elongatum	0.17	0.38	1.10	1.37
Lioloma pacificum	0.51	0.94	0.16	1.20
Lioloma spp.	1.03	2.83	0.00	3.76
Neodenticula seminae	4.45	7.92	3.15	7.35
Nitzschia gp *bicapitata*	0.51	1.51	0.79	0.00
Raphoneis amphiceros	0.00	0.00	0.00	0.00
Thalassionema bacillare	1.03	0.38	0.79	0.17
Thalassionema nitzschioides	20.03	19.06	17.35	6.67

(continued on next page)

Table E.1 (continued)

Core ID (figure 5.1)	C15	C16	C17	C18	C19
Sample designation	Y73-10-100 GC	W8209-19 GC	TT68-18 AC	TT39-19 REF	TT68-PC 27 REF
depth (cm)					
Freshwater	6.73	0.52	6.73	1.79	6.25
Benthics	0.00	0.35	1.87	0.00	0.45
Actinocyclus curvatulus	0.90	0.00	0.00	0.89	0.89
Actinocyclus normanii	0.00	0.00	0.75	0.89	0.00
Actinoptychus senarius	0.90	0.35	3.74	0.00	0.89
Stephanodiscus rotula (f. minutula)	0.00	1.05	1.87	1.79	1.79
Bacteriastrum spp.	0.90	0.00	0.37	0.00	0.00
Chaetoceros spores	41.26	38.39	29.16	21.43	41.96
Coscinodiscus decrescens	4.48	0.00	0.00	2.68	0.00
Coscinodiscus oculus iridis	0.00	0.00	0.00	0.00	0.00
Coscinodiscus marginatus	0.00	0.70	1.12	1.79	0.00
Coscinodiscus radiatus	3.59	2.79	3.36	0.00	2.68
Cyclotella litoralis	0.00	0.00	0.00	0.89	0.00
Cyclotella spp.	0.00	0.35	1.12	0.00	0.89
Cyclotella striata	0.00	0.70	1.50	0.00	0.89
Hemidiscus cuneiformis	0.00	0.00	0.37	0.89	0.00
Leptocylindrus spores	0.90	1.75	0.00	0.00	1.79
Melosira westi	0.00	0.00	0.00	0.00	0.00
Odontella aurita	0.00	0.00	0.37	0.89	0.89
Paralia sulcata	0.00	2.44	0.75	0.89	0.00
Rhizosolenia setigera	0.00	0.35	0.00	0.00	0.00
Rhizosolenia hebetata (f. hebetatata)	1.79	4.89	1.12	16.07	0.89
Rhizosolenia styliformis	0.00	0.00	0.00	0.00	0.00
Roperia tesselata	0.00	0.00	0.00	0.00	0.00
Stephanopyxis turris	0.00	0.00	0.00	0.00	0.89
Thalassiossira allenii	0.90	1.05	0.00	0.00	0.00
Thalassiossira anguste-lineata	0.00	0.00	0.00	0.00	0.00
Thalassiossira eccentrica	1.79	0.00	0.75	0.89	0.00
Thalassiossira leptotus	0.00	0.00	1.50	1.79	0.89
Thalassiossira lineata	0.00	0.00	0.00	0.00	0.00
Thalassiossira nanolineata	1.79	0.00	0.00	0.00	0.00
Thalassiossira oestrupii	0.00	0.00	0.00	0.89	2.68
Thalassiossira cf. *poroseriata*	0.00	0.00	0.00	0.00	0.00
Thalassiossira angulata and/or *pacifica*	0.00	0.00	0.37	0.00	0.00
Thalassiossira cf. *trifulta*	0.00	0.00	0.00	0.00	0.00
Thalassiossira sp.1	0.90	0.00	0.00	1.79	1.79
Thalassiossira sp.2	0.00	0.00	0.00	0.00	0.00
Thalassiossira sp.6	0.00	0.00	0.00	0.00	0.00
Thalassiossira spp.	0.00	1.75	1.87	7.14	0.89
Delphineis surilella	0.90	0.00	0.00	0.00	0.00
Delphineis karstenii	0.00	0.35	1.50	0.00	0.45
Fragilariopsis doliolus	0.90	2.44	2.24	1.34	3.13
Gomphonema constrictum	0.00	0.00	0.00	0.00	0.00
Lioloma elongatum	0.90	0.17	0.00	2.23	0.00
Lioloma pacificum	0.00	1.22	0.75	2.23	0.89
Lioloma spp.	2.69	0.70	0.00	2.68	1.34
Neodenticula seminae	2.24	0.87	0.93	8.48	1.79
Nitzschia gp *bicapitata*	0.00	0.17	6.54	0.45	2.23
Raphoneis amphiceros	0.45	0.87	1.12	0.00	0.89
Thalassionema bacillare	0.00	0.17	0.56	0.00	0.00
Thalassionema nitzschioides	25.11	34.21	24.11	17.41	20.09

(continued on next page)

Table E.1 (continued)

Core ID (figure 5.1)	C20	C21	C22	C23	C24
Sample designation	Y7409-15 24GC	W7905-163G	W7905-109G	W8809A-19GC	Y6908-5A
depth (cm)					
Freshwater	13.64	0.97	9.58	0.66	7.61
Benthics	6.06	0.00	0.15	0.00	0.46
Actinocyclus curvatulus	1.01	1.63	0.00	0.99	1.84
Actinocyclus normanii	4.04	0.00	0.00	0.00	0.00
Actinoptychus senarius	4.04	4.60	1.83	1.97	0.00
Stephanodiscus rotula (f. minutula)	4.04	0.00	0.61	0.00	0.46
Bacteriastrum spp.	5.05	0.98	0.30	0.00	0.92
Chaetoceros spores	9.09	50.49	55.10	39.14	12.44
Coscinodiscus decrescens	0.00	0.00	0.00	0.00	0.00
Coscinodiscus oculus iridis	0.00	0.00	0.00	0.00	0.00
Coscinodiscus marginatus	0.00	0.65	0.00	0.66	9.68
Coscinodiscus radiatus	1.01	2.28	1.22	4.28	0.92
Cyclotella litoralis	0.00	1.95	0.91	0.00	0.00
Cyclotella spp.	1.01	0.00	2.74	0.66	0.00
Cyclotella striata	1.01	0.98	0.30	0.00	0.00
Hemidiscus cuneiformis	0.00	0.65	0.30	0.00	0.00
Leptocylindrus spores	1.01	3.91	0.30	0.33	0.00
Melosira westi	0.00	0.00	0.00	0.00	0.00
Odontella aurita	1.01	2.93	0.30	0.99	0.00
Paralia sulcata	4.04	5.54	2.13	0.33	0.46
Rhizosolenia setigera	0.00	0.00	0.30	1.64	0.00
Rhizosolenia hebetata (f. hebetatata)	0.00	1.63	1.22	2.30	23.96
Rhizosolenia styliformis	1.01	0.00	0.00	0.00	0.00
Roperia tesselata	0.00	0.98	0.00	1.97	0.00
Stephanopyxis turris	0.00	1.30	0.00	0.33	0.00
Thalassiossira allenii	0.00	0.00	0.00	0.00	0.00
Thalassiossira anguste-lineata	0.00	0.32	0.00	0.00	0.00
Thalassiossira eccentrica	14.14	2.28	1.22	2.63	0.00
Thalassiossira leptotus	0.00	0.32	0.00	0.99	0.46
Thalassiossira lineata	0.00	0.32	0.00	0.00	0.00
Thalassiossira nanolineata	0.00	0.00	0.00	0.00	0.00
Thalassiossira oestrupii	0.00	0.65	0.30	0.99	3.23
Thalassiossira cf. *poroseriata*	0.00	0.00	0.00	0.00	0.00
Thalassiossira angulata and/or *pacifica*	0.00	0.00	0.00	0.00	0.00
Thalassiossira cf. *trifulta*	0.00	0.00	0.00	0.00	0.00
Thalassiossira sp.1	0.00	0.00	0.61	0.99	2.76
Thalassiossira sp.2	0.00	0.00	0.00	0.00	9.22
Thalassiossira sp.6	0.00	0.00	0.00	0.00	0.00
Thalassiossira spp.	0.00	0.32	0.30	0.00	0.92
Delphineis surilella	1.94	0.00	0.00	0.00	0.00
Delphineis karstenii	0.97	0.00	0.76	0.33	0.00
Fragilariopsis doliolus	0.00	1.47	0.61	5.59	0.23
Gomphonema constrictum	3.03	0.00	0.00	0.00	0.00
Lioloma elongatum	0.00	0.16	0.30	0.49	2.07
Lioloma pacificum	0.00	0.49	0.00	0.82	1.15
Lioloma spp.	0.00	0.65	0.76	0.82	6.45
Neodenticula seminae	0.00	0.00	0.91	1.81	3.69
Nitzschia gp *bicapitata*	0.00	0.00	1.52	0.16	0.46
Raphoneis amphiceros	1.52	0.65	2.13	0.33	0.00
Thalassionema bacillare	0.00	0.00	0.00	0.00	0.00
Thalassionema nitzschioides	12.63	8.96	14.31	28.13	9.68

(continued on next page)

Table E.1 (continued)

Core ID (figure 5.1)	C25	C26	C27	C28	C29
Sample designation	W8909-31	AT8408-17	W7610B1-7MGREF	W89097GC	TT39-AC12REF
depth (cm)					
Freshwater	2.80	1.42	3.46	1.12	4.50
Benthics	0.00	0.89	0.16	0.00	0.32
Actinocyclus curvatulus	0.00	0.35	1.32	1.50	1.58
Actinocyclus normanii	0.00	0.00	0.00	0.00	1.27
Actinoptychus senarius	2.24	1.06	1.32	1.85	0.82
Stephanodiscus rotula (f. minutula)	0.00	0.35	0.00	0.00	0.00
Bacteriastrum spp.	0.37	0.00	0.00	0.75	1.27
Chaetoceros spores	36.26	43.26	58.88	43.44	33.54
Coscinodiscus decrescens	0.00	0.00	0.00	0.00	0.00
Coscinodiscus oculus iridis	0.00	0.00	0.00	0.00	0.00
Coscinodiscus marginatus	1.12	0.00	0.00	1.17	0.99
Coscinodiscus radiatus	4.86	1.77	1.32	4.87	1.90
Cyclotella litoralis	1.50	0.71	1.32	0.00	0.63
Cyclotella spp.	1.50	0.00	0.99	0.75	1.58
Cyclotella striata	0.00	0.35	0.66	2.62	0.00
Hemidiscus cuneiformis	0.37	0.00	0.00	0.75	0.00
Leptocylindrus spores	0.00	1.77	3.29	2.62	3.16
Melosira westi	0.00	0.00	0.00	0.00	0.00
Odontella aurita	0.00	0.35	0.33	0.37	0.00
Paralia sulcata	1.87	0.71	2.63	0.75	3.80
Rhizosolenia setigera	0.00	0.00	0.00	0.00	0.00
Rhizosolenia hebetata (f. hebetatata)	8.22	0.71	2.96	2.25	2.21
Rhizosolenia styliformis	0.00	0.00	0.00	0.00	0.00
Roperia tesselata	0.37	0.00	0.00	1.50	0.00
Stephanopyxis turris	0.37	0.00	0.00	0.00	0.00
Thalassiossira allenii	0.00	0.00	0.00	0.00	0.00
Thalassiossira anguste-lineata	0.00	0.00	0.00	0.37	0.00
Thalassiossira eccentrica	1.50	3.90	1.64	2.25	4.43
Thalassiossira leptotus	1.87	1.06	0.33	1.87	0.00
Thalassiossira lineata	0.00	0.00	0.00	0.00	0.00
Thalassiossira nanolineata	0.00	0.00	0.00	0.00	0.00
Thalassiossira oestrupii	2.24	3.19	0.00	1.50	1.90
Thalassiossira cf. *poroseriata*	0.00	0.00	0.00	0.00	0.00
Thalassiossira angulata and/or *pacifica*	0.00	0.00	0.00	0.00	0.00
Thalassiossira cf. *trifulta*	0.00	0.00	0.00	0.00	0.00
Thalassiossira sp.1	0.00	0.35	0.00	0.00	1.27
Thalassiossira sp.2	1.50	1.42	0.00	0.00	0.00
Thalassiossira sp.6	0.00	0.00	0.00	0.00	0.00
Thalassiossira spp.	0.37	0.71	0.00	1.87	2.53
Delphineis surilella	0.00	0.00	0.00	0.00	0.00
Delphineis karstenii	0.00	0.50	0.82	0.00	0.42
Fragilariopsis doliolus	1.87	2.48	0.33	5.61	2.37
Gomphonema constrictum	0.00	0.00	0.00	0.00	0.00
Lioloma elongatum	0.00	0.18	0.16	0.00	0.32
Lioloma pacificum	1.87	0.35	0.49	0.37	0.32
Lioloma spp.	2.24	0.35	1.51	0.37	0.63
Neodenticula seminae	0.37	5.68	0.82	1.12	6.01
Nitzschia gp *bicapitata*	0.00	0.35	0.33	0.37	0.47
Raphoneis amphiceros	1.12	0.00	1.51	0.37	0.32
Thalassionema bacillare	0.00	0.00	0.00	0.00	0.32
Thalassionema nitzschioides	23.93	23.58	14.47	15.74	18.67

(continued on next page)

Table E.1 (continued)

	C30					
Sample designation	ODP1019D	ODP1019D	ODP1019D	ODP1019D	ODP1019D	ODP1019D
depth (cm)	2	12	22	32	42	62
Freshwater	0.00	0.00	0.16	0.44	0.78	0.00
Benthics	1.24	0.00	0.00	0.00	0.31	0.00
Actinocyclus curvatulus	0.93	1.00	0.32	1.17	0.63	0.96
Actinocyclus normanii	0.93	0.00	0.00	0.29	0.00	0.00
Actinoptychus senarius	1.24	3.48	3.20	0.00	1.88	0.64
Stephanodiscus rotula (f. minutula)	0.62	0.00	0.64	0.59	0.00	0.00
Bacteriastrum spp.	0.00	0.00	0.00	0.00	0.00	0.00
Chaetoceros spores	43.30	43.78	40.64	49.56	47.02	60.77
Coscinodiscus decrescens	0.00	0.00	0.00	0.00	0.00	0.00
Coscinodiscus oculus iridis	0.31	0.00	0.00	0.00	0.00	0.00
Coscinodiscus marginatus	1.87	0.00	2.24	1.47	0.94	0.32
Coscinodiscus radiatus	2.18	4.48	1.92	0.29	0.31	0.96
Cyclotella litoralis	3.43	3.98	1.60	0.29	0.00	1.29
Cyclotella spp.	0.00	0.00	0.00	0.00	0.00	0.00
Cyclotella striata	0.00	0.00	0.00	0.00	1.25	0.00
Hemidiscus cuneiformis	1.25	1.00	1.28	0.29	1.25	0.32
Leptocylindrus spores	3.12	3.98	5.12	4.99	4.39	0.96
Melosira westi	0.00	0.00	0.00	0.00	0.00	0.00
Odontella aurita	0.93	1.49	0.32	0.88	0.00	0.64
Paralia sulcata	2.49	1.49	1.60	1.17	1.88	1.93
Rhizosolenia setigera	0.00	0.00	0.00	0.00	0.00	0.00
Rhizosolenia hebetata (f. hebetatata)	0.00	1.99	0.96	0.00	0.00	0.00
Rhizosolenia styliformis	0.00	0.50	0.00	0.29	0.63	0.00
Roperia tesselata	2.49	1.49	2.56	0.59	1.57	0.00
Stephanopyxis turris	0.00	0.50	0.00	0.29	0.00	0.32
Thalassiossira allenii	0.00	0.00	0.00	0.00	0.00	0.00
Thalassiossira anguste-lineata	0.31	1.49	0.00	0.59	0.00	0.32
Thalassiossira eccentrica	1.56	1.00	1.92	0.59	2.19	1.61
Thalassiossira leptotus	0.62	0.50	0.00	0.29	1.25	0.32
Thalassiossira lineata	0.31	0.00	0.00	0.00	0.00	0.00
Thalassiossira nanolineata	0.00	0.00	0.00	0.00	0.00	0.00
Thalassiossira oestrupii	0.93	1.49	0.64	0.59	0.63	1.29
Thalassiossira cf. *poroseriata*	0.00	0.00	0.00	0.00	0.00	0.00
Thalassiossira angulata and/or *pacifica*	0.00	0.00	0.00	0.00	0.00	0.00
Thalassiossira cf. *trifulta*	0.00	0.00	0.00	0.00	0.00	0.00
Thalassiossira sp.1	0.00	0.00	0.00	0.00	0.00	0.00
Thalassiossira sp.2	0.00	0.00	0.00	0.00	0.00	0.00
Thalassiossira sp.6	0.00	0.00	0.00	0.00	0.00	0.00
Thalassiossira spp.	0.00	0.00	0.00	0.00	0.00	0.00
Delphineis surilella	0.00	0.00	0.32	0.00	0.47	0.00
Delphineis karstenii	0.31	0.00	0.00	0.00	0.00	0.00
Fragilariopsis doliolus	2.49	2.99	4.48	6.30	3.92	4.18
Gomphonema constrictum	0.00	0.00	0.00	0.00	0.00	0.00
Lioloma elongatum	0.93	0.25	0.64	0.29	0.16	0.16
Lioloma pacificum	1.25	0.50	0.48	0.44	0.31	0.00
Lioloma spp.	0.62	0.75	0.00	0.15	0.00	0.80
Neodenticula seminae	0.31	0.25	0.64	0.44	0.00	1.13
Nitzschia gp *bicapitata*	0.16	0.25	0.00	0.00	0.00	0.00
Raphoneis amphiceros	1.40	1.00	0.96	0.29	0.00	0.64
Thalassionema bacillare	0.00	0.25	0.00	0.00	0.00	0.00
Thalassionema nitzschioides	20.25	17.66	25.76	23.75	26.02	18.17

(continued on next page)

Table E.1 (continued)

Sample designation	ODP1019D	ODP1019D	ODP1019D	ODP1019D	ODP1019D	ODP1019D
depth (cm)	82	102	122	142	152	171
Freshwater	0.32	0.00	0.00	0.48	0.00	0.63
Benthics	0.00	0.00	0.00	0.24	0.48	1.11
Actinocyclus curvatulus	0.32	1.29	0.00	0.48	0.32	0.95
Actinocyclus normanii	0.00	0.00	0.00	0.00	0.00	0.00
Actinoptychus senarius	1.27	2.91	2.01	0.97	0.96	1.27
Stephanodiscus rotula (f. minutula)	0.00	0.00	0.00	0.00	0.00	0.00
Bacteriastrum spp.	0.00	0.00	0.00	0.00	0.32	0.00
Chaetoceros spores	62.74	56.54	56.62	52.78	69.33	61.90
Coscinodiscus decrescens	0.00	0.00	0.00	0.00	0.00	0.00
Coscinodiscus oculus iridis	0.00	0.00	0.00	0.00	0.00	0.00
Coscinodiscus marginatus	0.32	0.32	0.00	0.48	0.32	0.63
Coscinodiscus radiatus	0.32	1.29	0.34	1.45	0.00	1.59
Cyclotella litoralis	0.32	1.94	0.00	0.00	0.00	1.27
Cyclotella spp.	0.00	0.00	0.00	0.00	0.00	0.00
Cyclotella striata	0.00	0.00	0.00	1.45	0.00	0.00
Hemidiscus cuneiformis	0.32	0.32	0.34	0.00	0.00	0.00
Leptocylindrus spores	0.32	1.29	1.34	2.42	1.92	1.59
Melosira westi	0.00	0.00	0.00	0.00	0.00	0.00
Odontella aurita	0.64	1.29	1.01	0.00	0.00	0.32
Paralia sulcata	1.27	1.62	1.68	1.45	0.96	0.00
Rhizosolenia setigera	0.00	0.00	0.00	0.00	0.00	0.00
Rhizosolenia hebetata (f. hebetatata)	0.00	0.00	0.00	0.00	0.00	0.32
Rhizosolenia styliformis	0.64	0.32	2.01	0.48	0.00	0.00
Roperia tesselata	0.00	0.00	0.00	0.00	0.00	0.00
Stephanopyxis turris	0.96	0.00	0.34	0.48	0.32	0.32
Thalassiossira allenii	0.00	0.00	0.00	0.00	0.00	0.00
Thalassiossira anguste-lineata	0.00	0.32	0.34	0.00	0.00	0.00
Thalassiossira eccentrica	3.18	2.26	2.01	1.94	0.64	0.00
Thalassiossira leptotus	0.00	0.97	0.34	0.48	0.00	0.63
Thalassiossira lineata	0.00	0.00	0.00	0.97	0.00	0.00
Thalassiossira nanolineata	0.00	0.00	0.00	0.00	0.00	0.00
Thalassiossira oestrupii	1.27	0.97	0.67	1.45	0.32	1.27
Thalassiossira cf. *poroseriata*	0.00	0.00	0.00	0.00	0.00	0.00
Thalassiossira angulata and/or *pacifica*	0.00	0.00	0.00	0.00	0.00	0.00
Thalassiossira cf. *trifulta*	0.00	0.00	0.00	0.00	0.00	0.00
Thalassiossira sp.1	0.00	0.00	0.00	0.00	0.00	0.00
Thalassiossira sp.2	0.00	0.00	0.00	0.00	0.00	0.00
Thalassiossira sp.6	0.00	0.00	0.00	0.00	0.00	0.00
Thalassiossira spp.	0.00	0.00	0.00	0.00	0.00	0.00
Delphineis surilella	0.00	0.00	0.00	0.00	0.00	0.32
Delphineis karstenii	0.00	0.00	0.00	0.00	0.00	0.32
Fragilariopsis doliolus	5.10	1.45	3.52	2.42	1.28	0.79
Gomphonema constrictum	0.00	0.00	0.00	0.00	0.00	0.00
Lioloma elongatum	0.48	0.32	0.50	0.24	0.32	0.48
Lioloma pacificum	0.16	0.81	0.00	1.94	1.12	2.06
Lioloma spp.	0.16	0.16	0.17	0.48	0.00	0.00
Neodenticula seminae	0.96	0.65	0.00	1.94	0.64	0.32
Nitzschia gp *bicapitata*	0.00	0.00	0.00	0.00	0.00	0.32
Raphoneis amphiceros	0.00	0.32	0.17	0.97	0.32	0.00
Thalassionema bacillare	0.00	0.00	0.00	0.00	0.00	0.00
Thalassionema nitzschioides	15.13	19.55	25.13	20.58	19.81	20.95

(continued on next page)

Table E.1 (continued)

Sample designation	ODP1019D	ODP1019D	ODP1019D	ODP1019D	ODP1019D	ODP1019D
depth (cm)	191	211	231	251	271	291
Freshwater	0.00	0.00	0.63	0.49	0.95	3.62
Benthics	0.37	0.00	0.00	0.32	0.48	0.00
Actinocyclus curvatulus	0.37	0.31	0.32	1.62	0.00	0.00
Actinocyclus normanii	0.00	0.31	0.00	0.00	0.00	0.00
Actinoptychus senarius	0.74	0.31	0.00	0.00	0.00	0.00
Stephanodiscus rotula (f. minutula)	0.00	0.31	0.32	0.65	0.48	0.00
Bacteriastrum spp.	0.00	0.00	0.00	0.32	0.00	0.00
Chaetoceros spores	66.67	64.20	65.40	62.01	58.43	47.96
Coscinodiscus decrescens	0.00	0.00	0.00	0.00	0.00	0.00
Coscinodiscus oculus iridis	0.00	0.00	0.00	0.00	0.00	0.00
Coscinodiscus marginatus	0.00	0.00	0.32	0.00	1.43	0.00
Coscinodiscus radiatus	1.10	0.00	0.63	1.95	0.00	0.00
Cyclotella litoralis	1.47	0.31	0.95	0.65	0.95	0.90
Cyclotella spp.	0.00	0.00	0.00	0.00	0.00	0.00
Cyclotella striata	0.00	0.00	0.00	0.32	0.00	0.00
Hemidiscus cuneiformis	0.00	0.00	0.63	0.00	0.00	0.00
Leptocylindrus spores	1.10	3.09	1.27	2.27	4.75	0.90
Melosira westi	0.00	0.00	0.00	0.00	0.00	0.00
Odontella aurita	0.37	0.00	0.32	0.00	0.00	1.81
Paralia sulcata	1.10	0.62	0.32	1.30	0.48	0.00
Rhizosolenia setigera	0.00	0.00	0.00	0.00	0.00	0.00
Rhizosolenia hebetata (f. hebetatata)	0.00	0.62	0.63	0.00	1.43	0.90
Rhizosolenia styliformis	0.00	0.00	0.00	0.32	0.48	1.81
Roperia tesselata	0.00	0.00	0.00	0.00	0.00	0.00
Stephanopyxis turris	1.10	0.31	0.32	1.62	1.90	0.90
Thalassiossira allenii	0.00	0.00	0.00	0.00	0.00	0.00
Thalassiossira anguste-lineata	0.00	0.00	0.00	0.00	0.00	0.00
Thalassiossira eccentrica	0.37	1.85	0.00	0.97	0.00	0.00
Thalassiossira leptotus	0.00	0.93	0.63	0.00	0.48	0.00
Thalassiossira lineata	0.00	0.00	0.00	0.65	0.00	0.00
Thalassiossira nanolineata	0.00	0.00	0.32	0.32	0.00	1.81
Thalassiossira oestrupii	0.74	0.00	0.32	0.65	0.48	0.00
Thalassiossira cf. *poroseriata*	0.00	0.00	0.00	0.00	0.00	0.00
Thalassiossira angulata and/or *pacifica*	0.00	0.00	0.00	0.00	0.00	0.00
Thalassiossira cf. *trifulta*	0.00	0.00	0.00	0.00	0.00	0.00
Thalassiossira sp.1	0.00	0.00	0.00	0.00	0.00	0.00
Thalassiossira sp.2	0.00	0.00	0.00	0.00	0.00	0.00
Thalassiossira sp.6	0.00	0.00	0.00	0.00	0.00	0.00
Thalassiossira spp.	0.00	0.00	0.00	0.00	0.00	0.00
Delphineis surilella	0.00	0.00	0.00	0.00	0.00	0.00
Delphineis karstenii	0.18	0.00	0.32	0.00	0.48	0.90
Fragilariopsis doliolus	0.18	1.23	2.70	1.14	2.61	2.26
Gomphonema constrictum	0.00	0.00	0.00	0.00	0.00	0.00
Lioloma elongatum	0.74	0.15	0.48	0.49	0.95	0.90
Lioloma pacificum	1.10	0.62	0.63	0.49	0.48	1.81
Lioloma spp.	0.00	0.31	0.00	0.00	0.00	0.45
Neodenticula seminae	0.74	0.93	0.32	2.27	2.85	2.71
Nitzschia gp *bicapitata*	0.18	0.00	0.00	0.00	0.24	0.45
Raphoneis amphiceros	0.00	0.00	0.32	0.32	0.00	0.00
Thalassionema bacillare	0.00	0.00	0.00	0.00	0.00	0.00
Thalassionema nitzschioides	20.63	23.61	21.59	17.86	17.81	28.05

(continued on next page)

Table E.1 (continued)

Sample designation	ODP1019D	ODP1019D	MD	MD	MD	MD	MD	MD	MD	MD
depth (cm)	311	329	20	40	94	128	148	165	179.5	198
Freshwater	0.66	0.61	4.53	1.00	2.87	3.96	0.95	1.43	0.49	0.00
Benthics	0.66	0.00	0.00	0.00	0.00	0.50	0.00	0.00	0.00	0.00
Actinocyclus curvatulus	0.99	0.61	1.01	0.00	1.91	0.00	0.00	0.48	0.00	0.00
Actinocyclus normanii	0.00	0.00	1.01	1.00	0.00	0.00	0.48	0.95	0.49	0.98
Actinoptychus senarius	0.33	0.00	3.53	3.00	1.91	3.96	1.43	1.91	2.91	1.95
Stephanodiscus rotula (f. minutula)	0.00	0.30	0.50	1.00	0.00	0.00	0.95	0.00	0.00	1.95
Bacteriastrum spp.	0.00	0.00	0.00	0.00	0.00	0.00	0.00	0.00	0.49	0.98
Chaetoceros spores	58.98	65.05	38.29	31.00	22.97	36.63	27.08	46.30	43.69	53.66
Coscinodiscus decrescens	0.00	0.00	0.00	0.00	0.00	0.00	0.00	0.00	0.00	0.00
Coscinodiscus oculus iridis	0.00	0.00	0.00	0.00	0.00	3.96	0.00	1.91	0.00	0.00
Coscinodiscus marginatus	0.00	0.30	4.53	1.00	5.74	5.94	3.33	2.39	3.40	3.90
Coscinodiscus radiatus	0.66	0.91	3.53	11.00	6.70	0.99	0.95	0.48	1.94	1.95
Cyclotella litoralis	0.66	0.91	0.00	3.00	3.83	0.00	0.95	2.86	1.94	0.00
Cyclotella spp.	0.00	0.00	2.52	0.00	0.00	0.99	0.00	0.00	0.00	0.00
Cyclotella striata	0.00	0.00	0.00	0.00	0.00	0.00	0.00	0.95	0.00	0.00
Hemidiscus cuneiformis	0.33	0.00	0.00	0.00	0.00	0.00	0.00	0.00	0.49	0.00
Leptocylindrus spores	1.98	0.91	7.05	3.00	7.66	8.91	9.03	7.16	11.65	0.00
Melosira westi	0.00	0.00	0.00	0.00	0.00	0.00	0.00	0.00	0.00	0.00
Odontella aurita	0.33	0.30	0.00	0.00	0.96	0.00	0.48	0.00	0.00	0.00
Paralia sulcata	1.32	0.00	6.05	4.00	3.83	0.00	0.00	0.48	0.97	12.68
Rhizosolenia setigera	0.00	0.00	0.00	0.00	0.00	0.00	0.00	0.00	0.97	0.00
Rhizosolenia hebetata (f. hebetatata)	0.33	0.00	4.53	19.00	14.35	4.95	14.73	4.77	1.46	0.00
Rhizosolenia styliformis	0.66	0.00	0.00	0.00	0.00	0.00	0.48	0.00	0.00	0.00
Roperia tesselata	1.32	0.00	0.00	0.00	0.00	0.00	0.00	0.00	0.00	0.00
Stephanopyxis turris	0.00	0.00	1.01	3.00	0.00	0.99	3.33	0.48	0.00	3.90
Thalassiossira allenii	0.00	0.00	0.00	0.00	0.00	0.99	0.48	0.00	0.00	0.00
Thalassiossira anguste-lineata	0.00	0.00	0.00	0.00	0.00	0.00	0.00	0.00	0.00	0.00
Thalassiossira eccentrica	1.98	1.82	0.00	0.00	0.96	4.95	6.18	1.43	4.37	0.98
Thalassiossira leptotus	0.66	0.00	0.50	0.00	1.91	0.00	0.00	0.00	0.00	0.00
Thalassiossira lineata	0.00	0.00	0.50	3.00	3.83	2.97	0.48	0.48	3.88	0.98
Thalassiossira nanolineata	0.00	0.30	0.00	0.00	0.00	0.00	0.00	0.00	0.00	0.00
Thalassiossira oestrupii	0.33	0.61	1.01	2.00	0.00	0.00	0.48	3.34	3.40	0.98
Thalassiossira cf. *poroseriata*	0.00	0.00	0.00	0.00	0.00	0.00	0.00	0.00	0.00	0.00
Thalassiossira angulata and/or *pacifica*	0.00	0.61	0.00	0.00	0.00	0.00	0.00	0.00	0.97	0.00
Thalassiossira cf. *trifulta*	0.00	0.00	0.00	0.00	0.00	0.00	0.00	0.00	0.00	0.00
Thalassiossira sp.1	0.00	0.00	0.00	0.00	0.00	0.00	0.00	0.48	0.00	0.00
Thalassiossira sp.2	0.00	0.00	0.00	0.00	0.00	0.00	0.00	0.00	0.00	0.00
Thalassiossira sp.6	0.00	0.00	0.00	0.00	0.00	0.00	0.00	0.00	0.00	0.00
Thalassiossira spp.	0.00	0.00	2.52	0.00	0.96	0.00	0.00	0.00	0.00	0.00
Delphineis surilella	0.00	0.00	0.00	0.00	0.00	0.00	0.00	0.00	0.00	0.00
Delphineis karstenii	0.33	0.15	0.00	0.00	0.00	0.00	0.00	0.00	0.00	0.00
Fragilariopsis doliolus	7.41	4.84	0.50	0.00	6.22	0.00	0.00	0.48	0.00	0.00
Gomphonema constrictum	0.00	0.00	0.00	0.00	0.00	0.00	0.00	0.00	0.00	0.00
Lioloma elongatum	0.82	0.61	2.02	0.00	2.39	1.49	1.43	0.72	0.97	0.00
Lioloma pacificum	1.32	0.61	0.50	1.50	0.96	1.49	0.95	3.58	2.18	0.49
Lioloma spp.	0.16	0.15	1.76	0.00	0.48	0.00	1.43	1.19	0.49	0.49
Neodenticula seminae	1.81	1.82	1.76	0.00	0.00	0.00	0.00	0.95	0.49	2.44
Nitzschia gp *bicapitata*	0.00	0.00	0.50	0.00	0.00	0.50	0.48	0.00	0.00	0.00
Raphoneis amphiceros	0.00	0.00	0.00	0.00	1.44	0.00	0.00	0.00	2.43	0.00
Thalassionema bacillare	0.00	0.00	1.01	0.00	0.00	0.00	0.00	0.00	0.00	0.00
Thalassionema nitzschioides	15.32	17.40	10.33	11.50	8.13	12.38	16.86	12.89	8.01	10.73

(continued on next page)

Table E.1 (continued)

Sample designation	MD	MD	MD	MD	MD	MD	MD	MD	MD	MD	MD	MD
depth (cm)	218	238	258	278	298	378	418	438	458	477	498	518
Freshwater	3.97	1.22	1.29	1.43	1.28	22.50	22.67	15.84	9.02	15.92	15.92	8.82
Benthics	0.50	0.00	0.32	0.00	0.64	1.00	0.50	0.99	2.18	1.99	0.00	0.98
Actinocyclus curvatulus	0.00	0.00	0.00	0.00	0.00	1.00	0.00	0.50	1.56	3.98	0.00	0.00
Actinocyclus normanii	0.00	0.00	0.00	0.00	0.00	0.00	0.00	0.00	0.00	0.00	1.99	3.92
Actinoptychus senarius	1.49	0.00	1.94	0.29	0.96	4.00	4.03	6.44	8.09	12.94	29.85	7.84
Stephanodiscus rotula (f. minutula)	0.00	0.00	0.00	0.00	0.64	9.00	5.54	4.95	2.18	3.98	1.99	2.94
Bacteriastrum spp.	0.50	0.30	0.00	0.00	0.32	1.00	0.50	0.00	0.00	0.00	0.00	0.00
Chaetoceros spores	38.21	75.80	76.90	76.04	76.04	19.00	31.74	27.72	23.33	23.88	22.89	27.45
Coscinodiscus decrescens	0.50	0.00	0.00	0.00	0.00	0.00	0.00	0.00	0.00	0.00	0.00	0.00
Coscinodiscus oculus iridis	0.00	0.00	0.00	0.00	0.00	0.00	0.00	0.00	0.00	0.00	0.00	0.00
Coscinodiscus marginatus	3.97	1.22	1.94	1.15	1.28	3.00	1.51	1.49	2.80	4.98	3.98	5.88
Coscinodiscus radiatus	3.47	0.61	0.00	0.00	1.28	0.00	0.00	4.46	0.93	2.99	3.98	5.88
Cyclotella litoralis	0.99	1.22	0.65	0.00	1.28	0.00	0.00	0.00	0.00	0.00	0.00	0.00
Cyclotella spp.	0.00	0.00	0.00	0.00	0.00	0.00	0.00	0.00	0.00	0.00	0.00	0.00
Cyclotella striata	0.00	0.30	0.00	0.00	0.00	0.00	0.00	0.00	0.00	0.00	0.00	0.00
Hemidiscus cuneiformis	0.00	0.00	0.32	0.00	0.00	0.00	0.00	0.00	0.00	0.00	0.00	0.00
Leptocylindrus spores	1.99	0.30	1.29	1.43	1.60	0.00	0.00	0.50	0.93	0.00	0.00	0.98
Melosira westi	0.00	0.00	0.00	0.00	0.00	7.00	1.01	0.99	0.00	1.00	3.98	0.00
Odontella aurita	0.99	0.00	0.00	0.00	0.00	0.00	0.00	0.00	0.31	0.00	0.00	0.00
Paralia sulcata	14.89	0.30	0.00	0.00	0.32	0.00	1.01	0.00	0.31	0.00	0.00	1.96
Rhizosolenia setigera	0.50	0.00	0.00	0.00	0.00	0.00	0.00	0.00	0.00	0.00	0.00	0.00
Rhizosolenia hebetata (f. hebetatata)	2.48	0.00	0.00	0.29	0.00	0.00	0.00	0.00	0.00	0.00	0.00	0.00
Rhizosolenia styliformis	0.00	0.00	0.00	0.00	0.00	0.00	0.00	0.00	0.00	0.00	0.00	0.00
Roperia tesselata	0.00	0.00	0.00	0.00	0.00	0.00	0.00	0.00	0.00	0.00	0.00	0.00
Stephanopyxis turris	2.48	0.91	0.32	1.43	0.96	17.00	11.59	9.90	7.78	3.98	0.00	3.92
Thalassiossira allenii	0.50	0.00	0.00	0.29	0.00	0.00	0.00	0.00	0.00	0.00	0.00	0.00
Thalassiossira anguste-lineata	0.00	0.00	0.97	0.00	0.00	0.00	0.00	0.00	0.31	0.00	0.00	0.00
Thalassiossira eccentrica	1.49	2.44	0.32	2.58	0.32	0.00	2.02	0.00	3.11	1.00	0.00	1.96
Thalassiossira leptotus	0.00	0.91	0.32	0.00	0.64	0.00	2.52	0.00	0.62	1.00	2.99	0.98
Thalassiossira lineata	2.48	0.00	0.00	0.57	0.00	0.00	0.00	0.00	0.93	1.00	0.00	0.00
Thalassiossira nanolineata	0.00	0.00	0.00	0.00	0.00	0.00	0.00	0.00	0.00	0.00	0.00	0.00
Thalassiossira oestrupii	0.99	0.30	0.65	0.00	0.00	1.00	0.00	0.50	0.31	0.00	0.00	0.00
Thalassiossira cf. *poroseriata*	0.00	0.00	0.00	0.00	0.00	0.00	0.00	0.00	0.00	0.00	0.00	0.00
Thalassiossira angulata and/or *pacifica*	0.00	0.30	0.97	0.86	0.32	0.00	0.00	0.00	0.93	0.00	0.00	0.00
Thalassiossira cf. *trifulta*	0.00	0.00	0.00	0.00	0.00	0.00	0.00	0.00	0.00	0.00	0.00	0.00
Thalassiossira sp.1	0.00	0.00	0.00	0.00	0.00	0.00	0.00	0.00	0.00	0.00	0.00	0.00
Thalassiossira sp.2	0.00	0.00	0.00	0.00	0.00	0.00	0.00	0.00	0.00	0.00	0.00	0.00
Thalassiossira sp.6	0.00	0.00	0.00	0.00	0.00	0.00	0.00	0.00	0.00	0.00	0.00	0.00
Thalassiossira spp.	0.00	0.00	0.00	0.00	0.00	0.00	0.00	0.00	0.00	0.00	0.00	0.00
Delphineis surilella	0.99	0.00	0.00	0.00	0.64	0.00	3.53	11.88	21.46	5.97	3.48	17.65
Delphineis karstenii	0.50	0.46	1.62	1.15	0.32	0.00	0.50	0.00	0.31	1.00	0.00	0.49
Fragilariopsis doliolus	0.00	0.30	0.00	0.00	0.16	0.00	0.00	0.00	0.00	0.00	0.00	0.00
Gomphonema constrictum	0.00	0.00	0.00	0.00	0.00	0.00	0.00	0.00	0.00	0.00	0.00	0.00
Lioloma elongatum	0.50	0.30	0.81	0.43	0.48	0.00	0.00	0.25	0.16	0.00	0.00	0.00
Lioloma pacificum	1.99	0.91	0.48	0.43	0.48	0.00	0.25	0.00	0.00	0.00	0.00	0.00
Lioloma spp.	0.74	0.15	0.16	0.57	0.96	0.00	0.00	0.00	0.00	0.00	0.50	0.00
Neodenticula seminae	0.50	0.15	0.16	0.29	0.00	1.50	2.27	1.49	0.93	1.00	0.50	0.98
Nitzschia gp *bicapitata*	0.00	0.00	0.00	0.43	0.16	0.00	0.00	0.50	0.00	0.00	0.00	0.00
Raphoneis amphiceros	0.99	0.30	0.32	1.29	0.96	0.00	0.00	1.24	2.18	3.98	2.49	0.98
Thalassionema bacillare	0.00	0.00	0.00	0.43	0.00	0.00	0.00	0.00	0.00	0.00	0.00	0.00
Thalassionema nitzschioides	8.93	9.89	7.59	6.89	7.19	0.00	5.29	3.47	7.47	2.49	2.49	4.41

(continued on next page)

Table E.1 (continued)

Sample designation	MD	MD	MD	MD	MD	MD	MD	MD	MD	MD	MD	MD
depth (cm)	538	558	578	598	618	638	658	678	718	738	776	798
Freshwater	9.18	5.91	9.85	35.82	12.75	9.00	6.67	9.00	15.84	14.00	14.04	9.35
Benthics	0.00	0.00	0.00	0.00	0.00	5.00	1.90	0.00	0.45	1.00	0.00	0.00
Actinocyclus curvatulus	0.48	0.49	0.00	0.00	10.78	7.00	12.38	7.00	8.14	16.00	6.14	0.93
Actinocyclus normanii	2.90	0.49	0.99	0.00	0.00	0.00	0.00	0.00	0.00	0.00	0.00	0.00
Actinoptychus senarius	11.11	6.90	18.72	7.96	14.71	10.00	14.29	20.00	4.52	4.00	2.63	5.61
Stephanodiscus rotula (f. minutula)	4.35	1.97	1.97	4.98	0.98	6.00	0.95	2.00	4.52	2.00	0.00	3.74
Bacteriastrum spp.	0.00	0.00	0.00	0.00	0.98	0.00	0.00	0.00	0.00	0.00	0.88	0.00
Chaetoceros spores	28.02	54.68	33.50	15.92	19.61	21.00	20.00	9.00	10.86	16.00	36.84	11.21
Coscinodiscus decrescens	0.00	0.00	0.00	0.00	0.00	0.00	0.00	0.00	0.00	0.00	0.00	0.00
Coscinodiscus oculus iridis	0.00	0.00	0.00	0.00	0.00	0.00	0.00	0.00	0.00	0.00	0.00	0.00
Coscinodiscus marginatus	0.97	0.49	3.94	0.00	0.98	3.00	0.95	1.00	0.90	0.00	2.63	0.00
Coscinodiscus radiatus	3.86	2.96	3.94	1.99	0.00	0.00	2.86	7.00	12.67	2.00	0.00	1.87
Cyclotella litoralis	0.00	0.00	0.00	0.00	0.00	0.00	0.00	0.00	0.90	0.00	0.00	0.00
Cyclotella spp.	0.00	0.00	0.00	0.00	0.00	0.00	0.00	0.00	0.00	0.00	0.00	0.00
Cyclotella striata	0.00	0.00	0.00	0.00	0.00	0.00	0.00	0.00	0.00	0.00	0.00	0.00
Hemidiscus cuneiformis	0.00	0.00	0.00	0.00	0.00	0.00	0.00	0.00	0.00	0.00	0.00	0.00
Leptocylindrus spores	3.86	1.48	1.97	0.00	0.98	0.00	0.00	0.00	0.90	0.00	0.88	0.00
Melosira westi	0.00	0.00	1.97	6.97	0.00	0.00	0.00	0.00	0.00	0.00	0.00	0.00
Odontella aurita	0.00	0.00	0.00	0.00	0.98	0.00	0.00	0.00	1.81	1.00	0.00	0.00
Paralia sulcata	0.00	0.49	0.00	4.98	0.00	5.00	1.90	1.00	0.00	0.00	0.00	0.00
Rhizosolenia setigera	0.00	0.00	0.00	0.00	0.00	0.00	0.00	0.00	0.00	0.00	0.00	0.00
Rhizosolenia hebetata (f. hebetatata)	0.97	0.00	0.00	0.00	0.00	0.00	0.00	0.00	0.90	0.00	0.00	0.00
Rhizosolenia styliformis	0.00	0.00	0.00	0.00	0.00	0.00	0.00	0.00	0.00	1.00	0.00	0.00
Roperia tesselata	0.00	0.00	0.00	0.00	0.00	0.00	0.00	0.00	0.00	0.00	0.00	0.00
Stephanopyxis turris	3.86	6.40	0.99	0.00	7.84	9.00	10.48	32.00	23.53	15.00	7.89	42.99
Thalassiossira allenii	0.00	0.00	0.00	0.00	0.00	0.00	0.00	0.00	0.00	0.00	0.00	0.00
Thalassiossira anguste-lineata	0.00	0.00	0.00	0.00	0.00	0.00	0.00	0.00	0.00	0.00	0.00	0.00
Thalassiossira eccentrica	1.93	0.49	1.97	1.00	5.88	2.00	4.76	3.00	0.00	4.00	0.88	1.87
Thalassiossira leptotus	4.35	0.49	0.00	0.00	4.90	5.00	1.90	3.00	5.43	7.00	1.75	1.87
Thalassiossira lineata	0.00	0.00	0.00	0.00	0.00	0.00	0.00	0.00	0.00	0.00	0.00	0.00
Thalassiossira nanolineata	0.00	0.00	0.00	0.00	0.98	0.00	0.00	0.00	0.00	0.00	0.00	0.93
Thalassiossira oestrupii	0.00	0.00	0.00	0.00	0.00	0.00	0.00	0.00	0.00	0.00	1.75	0.93
Thalassiossira cf. *poroseriata*	0.00	0.00	0.00	0.00	0.00	0.00	0.00	0.00	0.00	0.00	0.00	0.00
Thalassiossira angulata and/or *pacifica*	0.97	0.00	0.00	0.00	0.00	0.00	0.00	0.00	0.00	0.00	0.00	0.00
Thalassiossira cf. *trifulta*	0.00	0.00	0.00	0.00	0.00	0.00	0.00	0.00	0.00	0.00	0.00	0.00
Thalassiossira sp.1	0.00	0.00	0.00	0.00	0.00	0.00	0.00	0.00	0.00	0.00	0.00	0.00
Thalassiossira sp.2	0.00	0.00	0.00	0.00	0.00	0.00	0.00	0.00	0.00	0.00	0.00	0.00
Thalassiossira sp.6	0.00	0.00	0.00	0.00	0.00	0.00	0.00	0.00	0.00	0.00	0.00	0.00
Thalassiossira spp.	0.00	0.00	0.00	0.00	0.00	0.00	0.00	0.00	0.00	0.00	0.00	0.00
Delphineis surilella	11.35	6.65	7.88	0.00	1.96	3.00	2.86	0.00	0.00	0.00	0.00	6.54
Delphineis karstenii	0.48	0.49	0.00	0.50	0.00	0.00	0.00	0.00	0.00	0.00	1.75	0.00
Fragilariopsis doliolus	0.00	0.00	0.00	0.50	0.00	0.00	0.00	0.00	0.00	0.00	0.00	0.00
Gomphonema constrictum	0.00	0.00	0.00	0.00	0.00	0.00	0.00	0.00	0.00	0.00	0.00	0.00
Lioloma elongatum	0.00	0.00	0.00	0.00	0.00	0.50	0.00	0.00	0.00	0.50	0.00	0.00
Lioloma pacificum	0.00	0.00	0.00	0.00	0.00	0.00	0.00	0.00	0.00	0.00	0.00	0.00
Lioloma spp.	0.24	0.00	0.00	0.00	0.00	0.00	0.00	0.00	0.00	0.00	0.00	0.00
Neodenticula seminae	0.48	0.00	0.00	1.49	3.43	1.50	5.24	0.00	1.81	3.00	0.88	0.93
Nitzschia gp *bicapitata*	0.00	0.25	0.49	0.50	0.00	0.50	0.00	0.00	0.00	0.00	0.00	0.00
Raphoneis amphiceros	2.66	0.99	2.96	0.00	1.96	2.00	1.90	0.00	0.00	0.00	5.70	1.87
Thalassionema bacillare	0.00	0.00	0.00	0.00	0.00	0.00	0.00	0.00	0.00	0.00	0.00	0.00
Thalassionema nitzschioides	5.07	4.93	5.91	4.48	6.37	6.50	10.00	1.00	3.62	5.50	12.72	6.54

(continued on next page)

Table E.1 (continued)

Sample designation	MD	MD	MD	MD	MD	MD	MD	MD	MD	MD	MD	MD
depth (cm)	818	838	858	878	898	918	938	958	978	998	1018	1038
Freshwater	3.59	16.51	9.66	8.00	6.67	2.82	1.43	0.63	3.40	3.23	2.49	3.92
Benthics	0.45	0.92	0.00	1.00	0.00	0.94	0.00	0.32	0.00	0.29	0.00	0.00
Actinocyclus curvatulus	6.28	0.00	1.93	0.00	3.81	1.88	1.43	0.32	2.91	2.06	3.98	0.00
Actinocyclus normanii	0.00	0.00	0.00	0.00	0.00	0.00	0.00	0.00	0.00	0.00	0.00	0.00
Actinoptychus senarius	5.38	0.00	0.00	0.00	6.67	0.94	1.14	2.53	1.94	3.52	2.49	1.96
Stephanodiscus rotula (f. minutula)	1.35	5.50	2.90	0.00	0.95	0.94	0.29	0.63	0.00	0.00	0.00	2.94
Bacteriastrum spp.	0.00	0.92	0.00	0.00	0.00	0.00	0.00	0.00	0.00	0.00	0.00	0.00
Chaetoceros spores	12.11	11.93	26.09	15.00	31.43	16.90	22.03	52.76	22.33	17.33	21.89	30.39
Coscinodiscus decrescens	0.00	0.00	0.00	0.00	0.00	0.00	0.00	0.00	0.49	0.00	0.00	0.00
Coscinodiscus oculus iridis	0.00	0.00	0.00	0.00	0.00	0.00	0.00	0.00	0.00	0.00	0.00	0.00
Coscinodiscus marginatus	0.45	0.00	0.97	0.00	0.00	0.94	1.14	0.32	0.00	0.00	1.49	0.00
Coscinodiscus radiatus	3.14	1.83	1.93	4.00	0.95	0.94	0.86	1.58	5.34	4.70	3.98	2.94
Cyclotella litoralis	0.00	0.00	0.00	0.00	0.00	0.00	0.00	0.00	0.00	0.00	0.00	0.00
Cyclotella spp.	0.00	0.00	0.00	0.00	0.00	0.00	0.00	0.00	0.00	0.00	0.00	0.00
Cyclotella striata	0.45	0.00	0.00	0.00	0.00	0.00	0.00	0.00	0.00	0.00	0.00	0.00
Hemidiscus cuneiformis	0.00	0.00	0.00	0.00	0.00	0.00	0.00	0.00	0.00	0.29	0.00	0.00
Leptocylindrus spores	0.00	0.92	0.00	0.00	3.81	0.00	0.57	0.63	0.97	0.59	0.50	0.00
Melosira westi	0.00	0.00	0.00	0.00	0.00	0.00	0.00	0.00	0.00	0.00	0.00	0.00
Odontella aurita	0.00	0.00	0.00	0.00	0.00	0.00	0.29	0.00	0.00	0.29	0.00	0.00
Paralia sulcata	9.42	2.75	0.00	2.00	1.90	0.00	2.00	0.32	3.40	1.76	0.00	0.98
Rhizosolenia setigera	0.00	0.00	0.00	0.00	0.00	0.00	0.00	0.00	0.00	0.00	0.00	0.00
Rhizosolenia hebetata (f. hebetatata)	0.00	0.00	0.00	0.00	0.00	0.00	0.00	0.00	0.00	0.00	0.00	0.00
Rhizosolenia styliformis	0.00	0.00	0.00	0.00	0.00	0.00	0.00	0.00	0.49	0.00	0.00	0.00
Roperia tesselata	0.00	0.00	0.00	0.00	0.00	0.00	0.00	0.00	0.00	0.00	0.00	0.00
Stephanopyxis turris	17.04	38.53	46.38	55.00	27.62	55.40	52.07	23.38	35.44	47.87	40.80	36.27
Thalassiossira allenii	0.00	0.00	0.00	0.00	0.00	0.00	0.00	0.00	0.00	0.00	0.00	0.00
Thalassiossira anguste-lineata	0.00	0.00	0.00	0.00	0.00	0.00	0.00	0.00	0.00	0.00	0.00	0.00
Thalassiossira eccentrica	5.83	1.83	0.97	0.00	2.86	4.69	2.58	2.53	5.83	2.35	4.98	1.96
Thalassiossira leptotus	0.45	3.67	1.93	3.00	2.86	3.76	0.86	2.21	2.43	2.35	1.99	0.00
Thalassiossira lineata	0.00	0.00	0.00	0.00	0.00	0.00	0.00	0.00	0.00	0.00	0.00	0.00
Thalassiossira nanolineata	0.00	0.92	0.00	1.00	0.00	0.94	1.14	0.32	0.97	0.88	0.50	0.00
Thalassiossira oestrupii	0.00	0.00	0.00	0.00	0.95	0.94	0.29	0.63	0.97	0.59	1.00	4.90
Thalassiossira cf. *poroseriata*	0.00	0.00	0.00	0.00	0.00	0.00	0.00	0.00	0.97	0.88	0.50	0.00
Thalassiossira angulata and/or *pacifica*	0.00	0.00	0.00	0.00	0.00	0.00	0.29	0.63	0.00	0.29	0.00	1.96
Thalassiossira cf. *trifulta*	0.00	0.00	0.00	0.00	0.00	0.00	0.00	0.00	0.00	0.00	0.00	0.00
Thalassiossira sp.1	0.00	0.00	0.00	0.00	0.00	0.00	0.00	0.00	0.00	0.00	0.00	0.00
Thalassiossira sp.2	0.00	0.00	0.00	0.00	0.00	0.00	0.00	0.00	0.00	0.00	0.00	0.00
Thalassiossira sp.6	0.00	0.00	0.00	0.00	0.00	0.00	0.00	0.00	0.00	0.00	0.00	0.00
Thalassiossira spp.	0.00	0.00	0.00	0.00	0.00	0.00	0.00	0.00	0.00	0.00	0.00	0.00
Delphineis surilella	3.36	0.00	0.00	0.00	0.95	1.88	2.58	0.00	2.18	3.38	0.00	0.00
Delphineis karstenii	0.45	0.92	0.00	0.00	0.00	0.00	0.57	0.00	0.49	1.62	0.50	0.00
Fragilariopsis doliolus	0.00	0.00	0.00	0.00	0.00	0.00	0.00	0.00	0.00	0.00	0.00	0.00
Gomphonema constrictum	0.00	0.00	0.00	0.00	0.00	0.00	0.00	0.00	0.00	0.00	0.00	0.00
Lioloma elongatum	0.90	0.00	0.00	0.50	0.00	0.00	0.14	0.47	0.24	0.00	0.00	0.00
Lioloma pacificum	0.45	0.00	0.00	0.00	0.00	0.00	0.00	0.00	0.00	0.00	0.25	0.00
Lioloma spp.	0.00	0.00	0.00	0.00	0.00	0.00	0.00	0.00	0.00	0.00	0.00	0.49
Neodenticula seminae	2.91	2.29	0.00	4.00	0.00	1.41	1.14	0.32	0.49	0.00	1.49	2.45
Nitzschia gp *bicapitata*	0.00	0.00	0.97	0.00	0.00	0.00	0.00	0.32	0.00	0.00	0.00	0.00
Raphoneis amphiceros	5.61	0.92	0.00	0.00	1.90	0.00	2.72	0.63	0.49	0.73	1.24	0.00
Thalassionema bacillare	0.00	0.00	0.00	0.00	0.00	0.00	0.00	0.00	0.00	0.00	0.00	0.00
Thalassionema nitzschioides	19.51	9.63	5.31	5.50	6.19	4.69	4.43	8.21	7.28	4.70	9.45	7.84

(continued on next page)

Table E.1 (continued)

Sample designation	MD	MD	MD	MD	MD	MD	MD	MD	MD	MD	MD	MD
depth (cm)	1058	1077	1098	1118	1138	1158	1178	1198	1238	1258	1278	1298
Freshwater	4.32	3.00	3.00	2.96	4.00	1.42	2.93	1.95	6.70	0.00	1.93	6.06
Benthics	0.33	1.00	0.00	0.00	0.00	0.00	0.00	0.49	0.96	0.00	0.97	0.00
Actinocyclus curvatulus	2.66	0.00	0.00	7.41	5.00	0.95	1.95	0.97	0.00	0.00	0.00	2.60
Actinocyclus normanii	0.00	0.00	0.00	0.00	0.00	0.00	0.00	0.00	0.00	0.00	0.00	0.00
Actinoptychus senarius	1.99	11.00	0.00	6.42	2.00	11.37	3.90	1.95	0.96	22.00	14.49	5.19
Stephanodiscus rotula (f. minutula)	0.66	1.00	1.00	0.49	0.00	2.37	0.00	0.00	1.91	0.00	0.00	1.73
Bacteriastrum spp.	0.00	0.00	0.00	0.49	0.00	0.00	0.00	0.00	0.00	0.00	0.00	0.00
Chaetoceros spores	47.84	17.00	21.00	28.64	17.00	24.17	27.32	42.34	19.14	5.00	4.83	19.91
Coscinodiscus decrescens	0.00	0.00	0.00	0.00	0.00	0.00	0.00	0.00	0.00	0.00	0.00	0.00
Coscinodiscus oculus iridis	0.00	0.00	0.00	0.00	0.00	0.00	0.00	0.00	0.00	0.00	0.00	0.00
Coscinodiscus marginatus	0.00	0.00	0.00	0.99	1.00	0.00	2.93	0.49	0.00	0.00	0.00	2.60
Coscinodiscus radiatus	1.33	8.00	3.00	4.44	2.00	3.79	0.98	1.46	8.61	2.00	6.76	7.79
Cyclotella litoralis	0.00	0.00	0.00	0.00	0.00	0.00	0.00	0.00	0.00	0.00	0.00	0.00
Cyclotella spp.	0.00	0.00	0.00	0.00	1.00	0.00	0.00	0.00	0.00	0.00	0.00	0.00
Cyclotella striata	0.00	0.00	0.00	0.00	0.00	0.00	0.00	0.00	0.00	0.00	0.00	0.00
Hemidiscus cuneiformis	0.00	0.00	0.00	0.00	0.00	0.00	0.00	0.00	0.00	0.00	0.00	0.00
Leptocylindrus spores	1.66	1.00	3.00	0.49	0.00	1.42	0.98	0.49	0.00	1.00	0.97	0.00
Melosira westi	0.00	0.00	0.00	0.00	0.00	0.00	0.00	0.00	0.00	0.00	0.00	0.00
Odontella aurita	0.00	0.00	1.00	0.00	1.00	0.47	0.00	0.00	0.00	0.00	0.00	0.00
Paralia sulcata	0.33	4.00	4.00	5.43	0.00	8.53	1.95	2.43	6.70	18.00	14.49	9.52
Rhizosolenia setigera	0.00	0.00	0.00	0.00	0.00	0.00	0.00	0.00	0.00	0.00	0.00	0.00
Rhizosolenia hebetata (f. hebetatata)	0.00	0.00	0.00	0.00	0.00	0.00	0.00	0.00	0.00	0.00	0.00	0.00
Rhizosolenia styliformis	0.00	0.00	0.00	0.00	0.00	0.00	0.00	0.00	0.00	0.00	0.00	0.00
Roperia tesselata	0.00	0.00	0.00	0.00	0.00	0.00	0.98	0.00	0.00	0.00	0.00	0.00
Stephanopyxis turris	24.58	40.00	37.00	20.25	53.00	25.59	20.49	14.60	39.23	41.00	48.31	19.05
Thalassiossira allenii	0.00	0.00	0.00	0.00	0.00	0.00	0.00	0.00	0.00	0.00	0.00	0.00
Thalassiossira anguste-lineata	0.00	0.00	0.00	0.00	0.00	0.00	0.00	0.00	0.00	0.00	0.00	0.00
Thalassiossira eccentrica	2.33	1.00	2.00	3.46	2.00	1.42	0.98	0.97	1.91	0.00	0.00	2.60
Thalassiossira leptotus	1.33	1.00	0.00	4.44	3.00	2.37	0.00	1.95	2.87	0.00	0.00	0.87
Thalassiossira lineata	0.00	0.00	0.00	0.00	0.00	0.00	0.98	0.00	0.00	0.00	0.00	0.00
Thalassiossira nanolineata	1.99	1.00	0.00	0.49	1.00	0.00	0.00	0.00	0.00	0.00	0.00	0.00
Thalassiossira oestrupii	0.33	1.00	0.00	0.00	0.00	0.00	0.00	0.00	0.00	0.00	0.00	0.00
Thalassiossira cf. *poroseriata*	0.00	1.00	0.00	0.00	0.00	0.00	0.00	0.00	0.00	0.00	0.00	0.00
Thalassiossira angulata and/or *pacifica*	0.33	0.00	0.00	1.48	0.00	0.47	2.93	3.89	0.00	0.00	0.00	0.00
Thalassiossira cf. *trifulta*	0.00	0.00	0.00	0.00	0.00	0.00	0.00	0.00	0.00	0.00	0.00	0.00
Thalassiossira sp.1	0.00	0.00	0.00	0.00	0.00	0.00	0.00	0.00	0.00	0.00	0.00	0.00
Thalassiossira sp.2	0.00	0.00	0.00	0.00	0.00	0.00	0.00	0.00	0.00	0.00	0.00	0.00
Thalassiossira sp.6	0.00	0.00	0.00	0.00	0.00	0.00	0.00	0.00	0.00	0.00	0.00	0.00
Thalassiossira spp.	0.00	0.00	0.00	0.00	0.00	0.00	0.00	0.00	0.00	0.00	0.00	0.00
Delphineis surilella	0.00	1.00	0.00	1.48	3.00	1.42	4.88	0.97	0.00	0.00	3.86	0.87
Delphineis karstenii	0.00	0.00	2.00	0.49	0.00	0.47	0.98	0.49	0.00	0.00	0.00	0.00
Fragilariopsis doliolus	0.00	0.00	0.00	0.00	0.00	0.00	0.49	0.24	0.00	0.00	0.00	0.00
Gomphonema constrictum	0.00	0.00	0.00	0.00	0.00	0.00	0.00	0.00	0.00	0.00	0.00	0.00
Lioloma elongatum	0.00	0.00	0.00	0.00	0.00	0.00	0.49	0.73	0.00	0.00	0.00	0.00
Lioloma pacificum	0.00	0.00	0.00	0.00	0.00	0.00	0.98	0.00	0.00	0.00	0.00	0.00
Lioloma spp.	0.00	0.50	0.50	0.00	0.00	0.00	0.00	0.00	0.00	0.00	0.00	1.30
Neodenticula seminae	0.83	1.00	1.50	0.49	1.50	1.66	0.98	1.46	4.78	3.00	0.00	0.00
Nitzschia gp *bicapitata*	0.17	0.00	0.00	0.00	0.00	0.00	0.00	0.00	0.00	0.00	0.00	0.00
Raphoneis amphiceros	1.33	0.00	2.00	0.25	0.00	1.66	0.98	2.43	0.48	0.50	0.00	0.87
Thalassionema bacillare	0.00	0.50	0.00	0.00	0.00	0.00	0.00	0.00	0.00	0.00	0.00	0.00
Thalassionema nitzschioides	5.65	3.00	18.00	9.38	4.00	9.24	20.00	19.71	3.83	6.50	2.42	17.32

(continued on next page)

Table E.1 (continued)

Sample designation	MD	MD	MD	MD	MD	MD	MD	MD	MD	MD	MD	MD
depth (cm)	1318	1338	1358	1377	1398	1418	1438	1458	1478	1498	1518	1538
Freshwater	0.94	2.87	3.43	2.97	3.97	2.82	10.33	1.44	1.00	8.41	10.38	10.84
Benthics	0.16	0.00	0.00	0.00	0.44	0.00	0.00	0.00	0.00	0.00	0.00	0.99
Actinocyclus curvatulus	0.94	1.91	1.25	0.99	4.86	5.18	0.00	8.13	1.66	0.00	0.00	0.00
Actinocyclus normanii	0.00	0.00	0.00	0.00	0.00	0.00	0.00	0.00	0.00	0.00	0.00	0.00
Actinoptychus senarius	2.83	1.91	3.12	0.99	1.77	3.76	0.94	2.39	1.66	2.80	0.94	1.97
Stephanodiscus rotula (f. minutula)	0.31	0.96	0.94	1.98	0.00	0.00	2.82	0.00	0.33	0.93	1.89	3.94
Bacteriastrum spp.	0.00	0.00	0.00	0.00	0.00	0.00	0.00	0.00	0.00	0.00	0.00	0.00
Chaetoceros spores	10.99	34.45	14.66	3.96	27.37	9.41	8.45	11.96	18.30	4.67	17.92	5.91
Coscinodiscus decrescens	0.00	0.00	0.00	0.00	0.00	0.00	0.00	0.00	0.00	0.00	0.00	0.00
Coscinodiscus oculus iridis	0.00	0.00	0.00	0.00	0.00	0.00	0.00	0.00	0.00	0.00	0.00	0.00
Coscinodiscus marginatus	0.31	0.96	0.31	0.00	0.00	0.00	0.00	0.00	0.00	0.00	0.00	0.00
Coscinodiscus radiatus	10.68	5.74	7.80	9.90	5.30	6.59	3.76	4.78	2.00	0.93	2.83	1.97
Cyclotella litoralis	0.00	0.00	0.00	0.00	0.00	0.00	0.00	0.00	0.00	0.00	0.00	0.00
Cyclotella spp.	0.00	0.00	0.00	0.00	0.00	0.00	0.00	0.00	0.00	0.00	0.00	0.00
Cyclotella striata	0.00	0.00	0.00	0.00	0.00	0.00	0.00	0.00	0.00	0.00	0.00	0.00
Hemidiscus cuneiformis	0.00	0.00	0.00	0.00	0.00	0.00	0.00	0.00	0.00	0.00	0.00	0.00
Leptocylindrus spores	0.00	0.00	0.00	0.00	0.00	0.00	0.00	0.00	0.00	0.00	0.00	0.00
Melosira westi	0.00	0.00	0.00	0.00	0.00	0.00	0.00	0.00	0.00	0.00	0.00	0.00
Odontella aurita	0.00	0.00	0.00	0.00	0.00	0.00	0.00	0.00	0.00	0.00	0.00	0.00
Paralia sulcata	2.20	2.87	2.18	0.99	1.77	3.29	6.57	4.31	2.33	1.87	0.94	1.97
Rhizosolenia setigera	0.00	0.00	0.00	0.00	0.00	0.00	0.00	0.00	0.00	0.00	0.00	0.00
Rhizosolenia hebetata (f. hebetatata)	0.00	0.00	0.00	0.00	0.00	0.00	0.00	0.00	0.33	0.00	0.00	0.00
Rhizosolenia styliformis	0.00	0.00	0.00	0.00	0.00	0.00	0.00	0.00	0.00	0.00	0.00	0.00
Roperia tesselata	0.00	0.00	0.00	0.00	0.00	0.00	0.00	0.00	0.00	0.00	0.00	0.00
Stephanopyxis turris	60.28	37.32	54.60	75.25	37.97	48.47	61.97	52.15	57.24	73.83	58.49	61.08
Thalassiossira allenii	0.00	0.00	0.00	0.00	0.00	0.00	0.00	0.00	0.00	0.00	0.00	0.00
Thalassiossira anguste-lineata	0.00	0.00	0.00	0.00	0.00	0.00	0.00	0.00	0.00	0.00	0.00	0.00
Thalassiossira eccentrica	0.00	0.96	0.62	0.99	0.88	0.47	0.94	0.96	0.00	0.00	0.00	0.00
Thalassiossira leptotus	0.00	0.96	0.31	0.00	1.32	1.41	0.00	1.44	2.33	0.00	0.00	0.00
Thalassiossira lineata	0.00	0.00	0.00	0.00	0.00	0.00	0.00	0.00	0.00	0.00	0.00	0.00
Thalassiossira nanolineata	0.00	0.00	0.00	0.00	0.00	0.00	0.00	0.00	0.00	0.00	0.00	0.00
Thalassiossira oestrupii	0.00	0.00	0.00	0.00	0.00	0.00	0.00	0.00	0.00	0.00	0.00	0.00
Thalassiossira cf. *poroseriata*	0.00	0.00	0.00	0.00	0.00	0.00	0.00	0.00	0.00	0.00	0.00	0.00
Thalassiossira angulata and/or *pacifica*	0.00	0.00	0.31	0.00	0.00	0.47	0.00	0.00	0.00	0.00	0.00	0.00
Thalassiossira cf. *trifulta*	0.00	0.00	0.00	0.00	0.00	0.00	0.00	0.00	0.00	0.00	0.00	0.00
Thalassiossira sp.1	0.00	0.00	0.00	0.00	0.00	0.00	0.00	0.00	0.00	0.00	0.00	0.00
Thalassiossira sp.2	0.00	0.00	0.00	0.00	0.00	0.00	0.00	0.00	0.00	0.00	0.00	0.00
Thalassiossira sp.6	0.00	0.00	0.00	0.00	0.00	0.00	0.00	0.00	0.00	0.00	0.00	0.00
Thalassiossira spp.	0.00	0.00	0.00	0.00	0.00	0.00	0.00	0.00	0.00	0.00	0.00	0.00
Delphineis surilella	0.31	0.00	0.31	0.00	0.44	2.59	0.94	1.20	3.83	0.93	0.00	0.99
Delphineis karstenii	0.31	0.00	0.31	0.00	0.00	1.41	0.00	0.00	0.33	0.00	0.00	0.00
Fragilariopsis doliolus	0.00	0.00	0.00	0.00	0.00	0.00	0.47	0.00	0.00	0.00	0.00	0.00
Gomphonema constrictum	0.00	0.00	0.00	0.00	0.00	0.00	0.00	0.00	0.00	0.00	0.00	0.00
Lioloma elongatum	0.00	0.00	0.62	0.00	0.44	0.24	0.00	0.00	0.00	0.00	0.00	0.00
Lioloma pacificum	0.00	0.48	0.31	0.00	0.00	0.00	0.00	0.00	0.00	0.00	0.00	0.00
Lioloma spp.	0.00	0.48	0.00	0.00	0.00	0.00	0.00	0.00	0.00	0.00	0.00	0.00
Neodenticula seminae	0.16	0.96	0.00	0.00	0.00	0.00	0.00	0.00	0.50	2.80	0.94	2.46
Nitzschia gp *bicapitata*	0.00	0.00	0.00	0.00	0.00	0.24	0.00	0.00	0.00	0.00	0.00	0.00
Raphoneis amphiceros	0.31	1.44	0.47	0.00	0.88	1.18	0.94	0.48	0.00	0.93	1.89	0.99
Thalassionema bacillare	0.00	0.00	0.00	0.00	0.00	0.00	0.00	0.00	0.00	0.00	0.00	0.00
Thalassionema nitzschioides	9.26	4.78	8.42	0.99	10.82	12.47	0.94	10.77	8.15	0.93	3.77	4.93

(continued on next page)

Table E.1 (continued)

Sample designation	MD
depth (cm)	1558
Freshwater	15.69
Benthics	0.98
Actinocyclus curvatulus	0.00
Actinocyclus normanii	0.00
Actinoptychus senarius	0.00
Stephanodiscus rotula (f. minutula)	4.90
Bacteriastrum spp.	0.00
Chaetoceros spores	12.75
Coscinodiscus decrescens	0.00
Coscinodiscus oculus iridis	0.00
Coscinodiscus marginatus	0.00
Coscinodiscus radiatus	0.00
Cyclotella litoralis	0.00
Cyclotella spp.	0.00
Cyclotella striata	0.00
Hemidiscus cuneiformis	0.00
Leptocylindrus spores	0.00
Melosira westi	0.00
Odontella aurita	0.00
Paralia sulcata	0.98
Rhizosolenia setigera	0.00
Rhizosolenia hebetata (f. hebetatata)	0.00
Rhizosolenia styliformis	0.00
Roperia tesselata	0.00
Stephanopyxis turris	50.98
Thalassiossira allenii	0.00
Thalassiossira anguste-lineata	0.00
Thalassiossira eccentrica	3.92
Thalassiossira leptotus	0.00
Thalassiossira lineata	0.00
Thalassiossira nanolineata	0.00
Thalassiossira oestrupii	0.00
Thalassiossira cf. *poroseriata*	0.00
Thalassiossira angulata and/or *pacifica*	0.00
Thalassiossira cf. *trifulta*	0.00
Thalassiossira sp.1	0.00
Thalassiossira sp.2	0.00
Thalassiossira sp.6	0.00
Thalassiossira spp.	0.00
Delphineis surilella	1.96
Delphineis karstenii	0.00
Fragilariopsis doliolus	0.00
Gomphonema constrictum	0.00
Lioloma elongatum	0.49
Lioloma pacificum	0.00
Lioloma spp.	0.00
Neodenticula seminae	0.98
Nitzschia gp *bicapitata*	0.00
Raphoneis amphiceros	0.00
Thalassionema bacillare	0.00
Thalassionema nitzschioides	3.43

APPENDIX F: Supplementary data for Chapter 6.

Table F.1 – Species numbers and correspondent names.

Species #	Species name
sp1	Actinocyclus spp
sp2	Actinoptychus spp
sp3	Azpeitia spp
sp4	Biddulphia spp
sp5	Cerataulus spp
sp6	Chaetoceros spores
sp7	Coscinodiscus spp
sp8	Hyalodiscus spp
sp9	Leptocylindrus spores
sp10	Melosira spp
sp11	Paralia sulcata
sp12	Psammodiscus nitidus
sp13	Thalassiosira spp
sp14	Triceratium spp
sp15	Cocconeis spp
sp16	Delphineis spp
sp17	Diploneis spp
sp18	Fragilaria spp
sp19	Grammatophora spp
sp20	Navicula spp
sp21	Navicula directa
sp22	Nitzschia spp
sp23	Nitzschia marina
sp24	Opephora spp
sp25	Plagiogramma spp
sp26	Thalassionema spp
sp27	Trachyneis aspera

Table F.2 – Diatom relative percentages for the core-top samples (sample ID referrers to table 6.2).

Sample ID	sp1	sp2	sp3	sp4	sp5	sp6	sp7	sp8	sp9	sp10	sp11	sp12	sp13	sp14
1	0.60	6.00	0.00	0.00	0.00	17.00	0.00	0.70	16.00	0.70	22.30	0.00	31.00	0.00
2	0.00	4.00	0.00	0.00	0.00	22.00	0.30	0.30	42.00	0.00	8.00	0.00	19.00	0.00
3	0.00	1.00	0.00	0.00	0.00	5.50	3.00	2.00	51.00	0.00	18.00	0.00	15.50	0.00
4	1.60	0.80	0.00	0.00	0.00	9.60	2.40	8.80	28.80	0.00	32.00	0.00	12.80	0.00
5	0.00	1.00	1.00	0.00	0.00	11.00	10.00	0.50	14.00	0.50	34.00	1.50	19.00	0.00
6	0.00	4.00	0.50	0.00	0.00	2.00	8.00	7.00	5.00	0.50	52.00	0.00	8.00	0.00
7	2.30	1.00	0.00	0.00	0.00	47.00	1.00	0.70	22.00	0.00	10.00	0.00	13.00	0.00
8	0.00	0.00	0.00	0.00	0.00	67.50	2.00	2.00	7.50	0.00	10.00	0.00	11.00	0.00
9	1.00	5.00	0.50	0.00	0.00	30.00	2.00	6.00	9.00	0.00	31.00	0.00	9.00	0.00
10	1.00	14.00	0.00	0.00	0.00	15.00	0.00	1.00	0.00	0.00	56.00	0.00	6.00	0.00
11	0.40	22.00	0.40	0.40	3.00	1.30	2.10	2.20	12.00	0.00	45.00	0.40	5.50	0.00
12	0.50	3.00	0.00	0.00	0.50	11.00	2.00	3.00	17.00	0.00	48.00	0.00	7.00	0.50
13	0.00	5.00	1.40	1.00	0.00	2.40	3.00	2.00	13.00	1.00	50.00	0.00	13.80	0.00
14	0.00	2.00	0.50	0.00	1.00	1.40	6.20	8.30	3.00	2.00	41.00	0.00	18.90	1.00
15	1.00	2.40	1.00	0.00	0.50	1.00	8.30	3.30	6.00	1.00	58.00	0.00	11.20	1.50
16	0.60	5.00	0.60	0.00	0.00	3.00	6.60	7.00	1.00	0.60	54.00	0.00	7.60	0.60
17	0.00	1.50	0.00	0.00	0.00	0.00	0.50	17.00	1.50	1.00	45.00	0.00	11.00	0.00
18	0.00	0.00	0.00	0.00	0.00	0.00	0.00	5.20	0.00	0.00	68.00	0.00	0.00	0.00
19	0.00	0.00	0.00	0.00	0.00	55.20	0.00	1.30	0.00	1.30	26.00	0.00	0.60	0.00
20	0.00	3.00	0.00	0.00	0.00	0.50	3.50	7.00	6.00	0.50	57.00	0.00	7.00	0.50
21	0.40	7.00	0.00	0.00	0.40	5.40	1.00	3.00	21.00	0.00	52.00	0.00	4.40	0.00
22	0.00	3.00	0.60	0.00	0.00	3.00	2.00	7.00	0.60	0.00	71.00	0.00	0.60	0.60
23	0.00	0.00	0.00	0.00	0.00	78.50	0.50	2.50	0.00	1.00	9.50	0.00	3.00	0.00
24	0.00	1.00	1.00	0.00	0.00	31.00	2.00	10.00	0.00	7.00	22.00	0.00	7.00	0.00
25	0.00	1.00	1.00	0.00	7.00	1.00	1.00	2.00	1.00	3.00	23.00	0.00	8.00	1.00
26	1.00	2.00	0.00	0.00	0.00	1.00	0.00	0.00	0.00	8.00	5.00	2.00	15.00	0.00
27	0.00	0.00	2.00	0.00	1.00	2.00	0.00	3.00	2.00	11.00	3.00	0.00	13.00	0.00
28	1.00	0.00	2.00	0.00	0.00	2.00	2.00	0.00	1.00	8.00	3.00	0.00	12.00	0.00
29	1.00	0.00	2.00	0.00	0.00	0.00	2.00	0.00	2.00	13.00	2.00	0.00	8.00	0.00
30	0.00	3.00	1.00	0.00	2.00	0.00	0.00	3.00	0.00	6.00	9.00	8.00	8.00	1.00
31	1.00	2.00	1.00	0.00	0.00	0.00	6.00	2.00	0.00	4.00	17.00	2.00	12.00	3.00
32	0.00	1.60	3.00	0.00	0.00	2.00	6.00	4.00	1.00	2.00	44.50	0.00	4.00	2.00
33	0.50	0.50	0.00	2.50	0.00	6.00	1.50	2.00	5.00	0.00	44.00	0.00	2.00	1.00
34	1.00	0.50	0.00	0.50	0.50	4.00	2.00	7.00	2.00	0.00	50.00	0.00	2.00	2.00
35	0.00	0.00	0.00	0.00	0.40	3.00	0.00	0.00	2.00	0.00	54.00	0.00	0.00	0.00
36	0.00	1.00	0.50	0.50	0.00	7.00	3.00	3.50	4.00	0.00	41.50	0.00	4.00	2.00
37	0.00	1.00	1.00	0.00	1.00	4.00	3.00	6.00	0.00	0.00	61.50	0.00	3.00	1.00
38	1.50	1.00	1.50	2.50	1.00	4.00	2.00	5.00	4.00	0.00	45.00	0.00	6.00	0.00

(continued on next page)

Table F.2 (continued)

Sample ID	sp15	sp16	sp17	sp18	sp19	sp20	sp21	sp22	sp23	sp24	sp25	sp26	sp27
1	1.00	0.00	0.00	2.00	0.00	0.00	0.10	0.30	0.00	0.00	0.00	0.10	0.30
2	0.60	0.70	0.00	1.50	0.00	0.00	0.00	0.10	0.00	0.00	0.00	1.00	0.00
3	0.00	0.00	0.70	0.00	1.00	0.00	0.00	1.00	0.00	0.00	0.00	0.00	0.00
4	0.00	0.00	1.20	0.00	1.20	0.00	0.00	0.80	0.00	0.00	0.00	0.00	0.00
5	0.00	0.00	1.00	0.10	0.50	1.00	0.00	1.00	0.00	0.00	0.00	0.00	0.00
6	0.10	0.10	1.30	0.00	0.70	0.00	0.00	2.00	0.00	1.00	0.00	0.00	0.50
7	0.50	0.00	0.30	0.50	0.00	0.00	0.10	0.70	0.00	0.10	0.00	0.00	0.00
8	0.00	0.00	0.00	0.00	0.00	0.00	0.10	0.00	0.00	0.00	0.00	0.00	0.00
9	0.40	0.00	1.70	0.00	0.00	0.80	0.00	0.80	0.00	0.00	0.00	0.00	0.40
10	0.00	0.00	0.00	0.00	0.00	0.00	0.00	0.00	0.00	0.00	0.00	0.00	1.00
11	1.40	0.00	0.80	0.00	0.00	0.10	0.00	0.00	0.00	0.10	0.80	0.10	0.40
12	0.00	1.00	1.50	0.00	0.00	0.00	0.00	0.50	0.00	0.10	1.00	1.00	1.00
13	0.10	0.00	1.90	0.00	0.10	1.00	0.50	1.00	0.00	0.00	0.00	0.00	1.00
14	1.00	0.00	4.00	0.00	2.40	0.00	1.00	3.90	0.10	0.50	0.00	0.10	1.00
15	0.00	0.00	2.00	0.10	0.50	0.00	0.50	0.50	1.50	0.00	0.00	0.00	0.00
16	0.10	0.60	3.60	0.00	0.60	0.00	3.00	2.00	0.00	0.00	0.00	0.00	0.00
17	2.00	0.50	12.00	0.00	2.00	1.50	0.00	0.50	0.00	0.00	0.50	0.00	1.50
18	0.60	0.00	0.60	5.20	0.00	1.30	0.00	0.60	0.00	0.00	0.60	0.00	0.00
19	12.30	0.00	0.60	0.00	1.90	0.00	0.00	0.00	0.00	0.00	0.00	0.00	0.00
20	2.50	0.00	3.00	0.00	2.50	0.00	0.00	2.00	0.00	0.50	2.00	0.00	0.00
21	0.80	0.00	0.10	0.00	0.40	0.00	0.40	1.00	0.10	0.00	0.00	0.00	1.00
22	0.60	0.00	3.30	0.10	0.60	0.60	0.00	2.00	0.00	0.60	0.00	0.00	2.40
23	0.00	0.00	1.00	0.00	1.00	0.00	0.00	2.00	0.00	0.00	0.00	0.00	0.00
24	2.00	0.00	2.00	0.00	7.00	0.00	0.00	2.00	0.00	0.00	0.00	0.00	1.00
25	3.00	0.00	19.00	1.00	1.00	1.00	14.00	1.00	0.10	0.00	0.00	3.00	2.00
26	0.00	0.00	4.00	0.00	0.00	0.00	0.00	1.00	2.00	0.00	0.00	47.00	0.00
27	0.00	0.00	2.00	0.00	0.00	0.00	0.00	1.00	1.00	0.00	0.00	50.00	0.00
28	0.00	0.00	0.00	0.00	0.00	0.00	0.00	0.00	0.00	0.00	0.00	52.00	0.00
29	0.00	0.00	0.00	0.00	0.00	0.00	0.00	0.00	0.00	0.00	0.00	64.00	0.00
30	2.00	0.00	18.00	0.00	0.10	2.00	3.00	2.00	0.00	0.00	0.00	20.00	3.00
31	0.00	0.00	14.00	0.00	1.00	1.00	14.00	2.00	0.00	0.00	1.00	3.00	2.00
32	0.00	0.00	11.60	0.00	0.60	0.00	12.00	1.00	0.00	0.00	0.00	0.60	3.00
33	2.00	7.00	10.00	0.00	0.10	3.50	4.00	0.00	0.50	0.00	2.00	1.50	0.50
34	2.00	2.00	9.50	0.00	0.00	10.00	0.00	1.00	0.00	0.00	0.00	0.50	1.00
35	4.00	5.00	10.00	0.00	0.00	3.00	3.00	1.60	1.00	0.40	0.50	0.80	2.20
36	0.00	2.50	10.50	0.00	0.10	1.00	8.00	3.00	0.10	0.00	1.00	1.00	2.50
37	0.00	3.00	4.00	0.00	0.10	0.10	7.50	2.00	0.10	0.00	0.00	1.00	1.00
38	1.00	0.50	8.00	0.00	0.50	1.00	8.00	3.00	0.50	0.00	0.00	0.50	1.00

(continued on next page)

Table F.2 (continued)

Sample ID	sp1	sp2	sp3	sp4	sp5	sp6	sp7	sp8	sp9	sp10	sp11	sp12	sp13	sp14
39	0.50	1.00	1.00	0.00	0.50	3.00	4.50	5.00	2.00	0.00	38.00	0.00	13.00	1.00
40	0.00	0.00	3.00	0.00	0.00	1.00	6.00	4.00	1.00	0.00	41.00	0.00	11.00	1.00
41	0.00	0.00	0.00	0.00	0.00	0.00	1.00	7.00	0.00	1.00	52.00	0.00	3.00	0.00
42	0.00	0.00	0.00	1.00	0.00	34.00	1.50	2.00	6.00	0.00	27.00	0.00	2.00	1.00
43	0.00	1.00	0.00	0.00	0.00	23.50	0.40	2.70	4.00	2.00	30.00	2.00	3.00	3.40
44	0.40	0.80	0.00	0.00	0.00	61.00	1.50	0.80	10.00	0.00	13.50	0.00	1.40	0.80
45	0.00	1.00	0.00	0.00	0.00	71.00	0.00	0.10	4.00	0.00	8.00	0.00	3.00	1.00
46	0.50	2.00	0.00	1.00	0.00	33.00	4.00	3.00	5.00	0.00	28.00	0.00	6.00	1.00
47	0.50	1.40	3.00	0.00	0.00	11.00	3.00	3.00	5.00	1.00	40.00	0.50	4.90	0.00
48	1.70	1.00	1.30	0.40	0.00	14.00	0.80	3.00	12.00	0.00	30.00	0.00	9.40	1.00
49	0.00	1.00	2.00	3.00	0.00	0.50	2.50	3.00	5.00	0.00	39.50	2.00	5.00	0.00
50	0.00	3.00	1.00	1.00	0.00	3.00	2.40	3.00	1.40	0.00	42.00	2.40	2.40	1.40
51	0.00	0.00	0.50	0.00	0.50	0.00	1.00	3.40	1.00	1.50	25.50	4.40	4.40	0.00
52	1.00	1.00	1.00	0.00	0.00	1.00	0.00	3.00	2.00	6.00	30.00	4.00	3.00	0.00
53	0.00	1.00	0.00	1.00	0.00	1.00	0.00	3.00	2.00	3.40	31.40	5.40	9.90	0.00
54	0.00	1.00	0.00	0.00	0.00	0.50	0.00	3.00	0.50	1.50	30.00	3.00	8.00	0.00
55	0.00	0.00	0.00	0.00	0.00	1.00	1.50	1.00	0.00	0.50	11.00	2.00	4.50	0.00
56	0.00	0.00	0.00	0.00	0.00	0.00	0.00	0.00	0.00	0.00	1.00	2.00	1.50	0.00
57	0.00	0.00	0.00	0.00	0.00	4.00	0.00	13.00	0.00	5.00	39.00	0.00	29.00	0.00
58	1.00	1.00	0.00	0.00	0.00	2.00	0.00	12.00	4.00	4.00	42.00	0.00	19.00	0.00
59	0.00	2.00	0.00	0.00	0.00	2.00	2.00	16.00	1.00	2.00	58.00	1.00	4.00	0.00
60	0.00	3.00	0.00	2.00	0.30	19.00	1.00	4.00	9.00	0.00	34.00	0.00	20.00	0.00
61	0.00	3.00	0.40	5.00	0.40	16.00	2.00	3.00	7.00	3.00	26.00	0.00	25.00	0.00
62	0.00	1.00	0.00	0.00	0.00	4.00	0.00	22.00	0.00	0.00	25.00	0.00	22.00	0.00
63	3.00	5.00	3.00	0.00	0.00	2.00	6.00	2.00	2.00	0.00	58.00	0.00	12.00	0.00
64	1.00	3.00	0.30	1.00	1.00	17.00	2.30	1.00	7.00	0.00	17.30	0.00	13.00	0.00
65	0.00	1.50	0.00	0.00	0.00	6.00	11.00	0.00	2.50	9.00	29.50	0.00	20.50	0.00
66	0.00	1.20	1.20	0.00	0.00	4.00	0.60	0.00	4.00	1.20	72.00	0.00	6.50	0.00
67	0.00	0.00	0.00	1.30	0.00	1.30	7.70	0.00	0.00	9.00	8.00	0.00	2.50	0.00
68	1.40	1.40	0.00	0.00	3.00	7.00	6.00	0.70	0.00	0.70	6.50	0.00	7.00	0.00

(continued on next page)

Table F.2 (continued)

Sample ID	sp15	sp16	sp17	sp18	sp19	sp20	sp21	sp22	sp23	sp24	sp25	sp26	sp27
39	0.00	2.00	10.50	0.00	0.00	0.50	6.00	0.10	1.00	0.00	0.50	1.00	3.00
40	0.00	1.00	11.00	0.00	0.00	2.00	8.00	4.00	3.00	0.00	0.10	2.00	1.00
41	0.00	0.00	21.00	0.00	0.00	0.00	1.00	0.00	0.00	0.00	0.00	1.00	13.00
42	1.00	2.00	6.00	0.00	2.50	2.00	4.00	0.10	0.00	0.00	2.00	0.00	0.40
43	1.00	6.70	7.50	0.00	0.40	1.40	1.00	0.80	1.00	0.00	2.40	2.00	0.40
44	0.00	3.50	2.40	0.00	0.40	0.40	1.20	0.10	0.10	0.00	0.10	0.10	0.40
45	0.00	1.00	4.60	0.00	2.00	0.60	0.30	0.00	0.30	0.30	0.00	1.60	0.00
46	0.50	1.00	4.00	0.00	0.10	0.50	1.00	3.00	1.00	0.00	1.00	0.10	0.50
47	0.00	1.00	7.00	0.00	1.00	0.00	5.00	1.50	2.00	0.50	1.40	0.50	2.00
48	0.00	2.00	7.80	0.00	0.80	0.00	2.00	0.10	5.00	0.00	1.30	1.30	2.00
49	0.50	2.50	16.00	0.00	4.00	2.00	6.00	1.00	0.00	0.50	0.00	0.00	1.00
50	0.40	1.80	17.40	0.00	3.80	2.80	2.00	1.00	0.40	0.00	0.00	0.10	1.40
51	7.10	0.50	26.00	1.70	0.00	4.50	0.00	5.10	0.00	0.00	2.00	0.00	0.50
52	6.00	1.00	15.00	0.00	1.00	2.00	0.10	5.00	0.00	1.00	0.00	2.00	0.00
53	3.00	1.50	16.70	0.00	6.00	2.50	0.00	2.00	0.00	0.50	2.00	0.00	0.50
54	3.00	0.00	19.40	0.00	2.50	4.00	0.00	9.40	0.00	0.00	2.00	0.00	0.50
55	42.00	1.00	11.00	0.00	1.50	0.50	0.10	1.50	0.00	15.50	2.00	0.00	0.50
56	28.00	1.00	26.50	0.50	0.00	7.00	0.00	0.00	0.00	4.50	1.00	0.00	0.00
57	0.10	0.00	1.00	0.00	0.00	0.00	0.00	1.00	1.00	0.00	0.00	0.00	0.00
58	0.00	0.00	0.00	0.00	0.00	0.00	0.00	3.00	0.00	0.00	0.00	1.00	0.00
59	2.50	0.00	3.00	0.00	4.40	0.00	0.00	2.00	0.10	0.00	0.00	0.00	0.00
60	0.00	0.00	0.30	0.30	0.00	0.00	0.00	0.70	0.10	0.30	0.00	0.70	0.30
61	0.40	0.40	0.40	0.40	0.00	0.00	0.00	0.40	0.00	0.00	0.00	2.00	2.00
62	1.00	0.00	3.00	0.00	1.00	1.00	1.00	2.00	0.00	0.00	0.00	0.00	3.00
63	2.00	0.00	1.00	1.00	0.00	0.00	0.00	1.00	0.00	0.00	0.00	0.00	1.00
64	6.00	0.00	10.00	3.00	0.70	1.00	0.00	3.00	0.00	0.70	0.30	1.00	0.30
65	1.00	1.00	2.30	0.00	1.00	0.00	0.00	1.50	1.00	0.00	1.00	6.80	1.00
66	0.60	0.60	2.60	0.00	2.20	0.00	1.20	0.00	0.30	0.00	0.00	2.20	0.00
67	2.60	0.00	4.50	0.00	0.00	0.00	0.00	0.00	0.00	0.00	0.00	53.00	0.00
68	0.00	0.00	1.40	0.70	0.70	0.00	0.00	3.10	0.40	0.00	0.00	36.00	0.70

Table F.3 - Diatom relative percentages for core KS11.

depth (cm)	Age	sp1	sp2	sp3	sp4	sp5	sp6	sp7	sp8	sp9	sp10	sp11	sp12	sp13	sp14
8	1031	0	0	1	0	0	25	0	0	4	11	30	0	3	0
18	2320	0	1	1	0	0	19	0	0	4	2	44	0	1	0
38	7174	0	0	0	0	0	41	1	0	3	1	36	0	0	0
48	12050	0	0	0	0	0	44	1	0	7	1	30	0	0	0
58	12732	0	2	0	0	0	74	1	0	0	0	25	0	1	0
68	13415	0	1	0	0	0	84	0	0	0	1	17	0	0	0
78	14097	0	0	0	0	0	62	0	0	1	3	31	0	2	0
98	14779	0	0	0	0	0	71	0	0	0	0	5	0	0	0
108	16144	0	0	0	0	0	101	0	0	0	0	3	0	1	0
118	16826	0	0	0	0	0	95	0	0	2	0	8	0	1	0
128	17509	0	0	0	0	0	68	1	0	3	1	24	0	6	0
138	17850	0	1	0	0	0	42	0	0	1	0	46	0	7	0
148	18104	0	1	0	0	0	77	1	0	0	0	26	0	4	0
158	18613	0	1	0	0	0	55	1	0	3	1	32	0	3	0
168	19122	0	2	0	0	0	40	1	1	2	1	31	0	0	0
178	19631	0	0	0	1	0	53	0	0	0	5	18	0	3	0
200	20140	1	0	1	1	0	39	0	1	2	0	6	0	1	0
218	20649	1	1	0	0	0	34	1	0	3	4	27	0	3	0
248	21769	0	1	0	0	0	43	0	0	2	4	17	0	0	0
278	22685	0	0	0	0	0	58	0	0	2	3	17	0	1	0
300	24110	0	0	1	0	0	45	0	0	0	0	7	0	5	0
422	24197	0	1	0	0	0	82	0	0	0	0	14	0	0	0
558	25420	1	0	0	0	0	50	0	0	0	0	13	0	1	0
748	25695	3	0	0	0	0	30	0	0	0	0	5	0	0	0

depth (cm)	Age	sp15	sp16	sp17	sp18	sp19	sp20	sp21	sp22	sp23	sp24	sp25	sp26	sp27
8	1031	0	1	3	1	2	1	0	2	0	0	0	10	0
18	2320	3	1	3	0	3	1	0	4	0	0	0	6	0
38	7174	0	0	1	0	4	0	0	5	0	0	0	5	0
48	12050	0	0	1	0	2	0	0	0	0	0	0	6	0
58	12732	1	0	0	0	1	0	0	1	0	0	0	2	0
68	13415	0	0	1	0	4	0	0	1	0	0	1	2	0
78	14097	0	0	1	0	1	1	0	1	0	1	0	3	0
98	14779	0	0	0	0	0	0	0	0	0	0	0	0	0
108	16144	0	0	0	0	0	0	0	0	0	0	0	0	0
118	16826	0	0	0	0	0	0	0	0	0	0	0	1	0
128	17509	1	1	1	0	0	0	0	1	0	0	1	1	0
138	17850	0	0	1	0	1	0	0	1	0	0	0	2	0
148	18104	0	0	1	0	1	0	0	1	0	0	0	1	0
158	18613	1	1	1	1	1	0	1	4	0	0	0	3	0
168	19122	2	0	3	0	0	0	0	1	0	0	1	3	0
178	19631	0	1	0	0	2	0	0	1	0	0	1	9	0
200	20140	0	0	0	3	0	0	0	0	0	0	0	4	0
218	20649	0	0	0	0	1	0	0	3	1	0	0	11	0
248	21769	0	0	1	1	1	0	0	0	1	0	0	19	0
278	22685	0	0	0	1	0	0	0	3	0	2	0	13	0
300	24110	0	1	0	1	0	0	1	0	0	0	4	13	0
422	24197	1	0	0	0	1	0	0	0	0	0	0	6	0
558	25420	0	0	1	0	1	0	0	1	0	0	1	0	0
748	25695	0	0	0	0	0	0	0	0	0	0	0	26	0

Table F.4 – Environmental information for the core-top samples (sample ID referrers to table 6.2).

Sample ID	Annual Chlorophyll (mg/m3)	Winter chlorophyll (mg/m3)	Summer chlorophyll (mg/m3)	Seasonal range chlorophyll (mg/m3)	Annual SST (°C)	Winter SST (°C)	Summer SST (°C)	Seasonal range SST (°C)
1	no info	no info	5.77	no info	no info	no info	14.82	no info
2	no info	no info	2.23	no info	no info	no info	16.34	no info
3	no info	no info	0.28	no info	no info	no info	17.51	no info
4	no info	no info	0.25	no info	no info	no info	17.60	no info
5	0.30	0.49	0.11	-0.38	15.82	13.79	17.85	4.07
6	0.32	0.37	0.26	-0.12	15.38	13.52	17.23	3.71
7	0.29	0.26	0.32	0.06	15.27	13.45	17.09	3.64
8	0.39	0.33	0.44	0.11	15.12	13.39	16.84	3.45
9	0.62	0.50	0.75	0.25	14.84	13.24	16.44	3.20
10	0.93	0.50	1.35	0.85	14.64	13.09	16.20	3.11
11	1.40	0.44	2.36	1.91	14.92	14.01	15.83	1.81
12	0.77	0.63	0.92	0.29	15.30	13.73	16.87	3.14
13	0.59	0.74	0.45	-0.29	15.45	13.56	17.33	3.77
14	0.42	0.61	0.23	-0.38	15.90	13.89	17.91	4.02
15	0.32	0.53	0.12	-0.40	16.19	14.14	18.25	4.10
16	0.34	0.57	0.10	-0.47	16.41	14.41	18.41	4.00
17	0.85	0.29	1.41	1.12	14.90	14.26	15.55	1.29
18	0.56	0.32	0.80	0.49	15.31	14.37	16.24	1.87
19	0.37	0.34	0.41	0.07	15.52	14.37	16.68	2.32
20	0.36	0.43	0.30	-0.13	15.67	14.21	17.13	2.92
21	0.34	0.43	0.24	-0.19	15.74	14.19	17.30	3.11
22	0.29	0.43	0.15	-0.29	15.89	14.17	17.61	3.44
23	0.18	0.28	0.08	-0.20	16.18	14.42	17.93	3.51
24	0.17	0.26	0.08	-0.19	16.65	14.65	18.64	4.00
25	0.30	0.41	0.19	-0.22	16.68	13.28	20.08	6.80
26	0.27	0.38	0.16	-0.22	16.92	13.67	20.17	6.50
27	0.25	0.35	0.15	-0.19	17.30	14.19	20.41	6.22
28	0.19	0.25	0.14	-0.10	17.63	14.77	20.49	5.72
29	0.17	0.21	0.12	-0.09	17.93	14.96	20.90	5.94
30	0.17	0.20	0.14	-0.06	17.25	14.74	19.75	5.01
31	0.21	0.24	0.18	-0.06	16.60	14.91	18.29	3.38
32	0.90	0.25	1.56	1.31	15.22	14.58	15.86	1.27
33	0.61	0.38	0.84	0.45	15.55	13.71	17.40	3.69
34	0.59	0.36	0.81	0.45	15.50	13.68	17.32	3.64
35	0.54	0.32	0.77	0.45	15.39	13.63	17.15	3.52
36	0.58	0.26	0.91	0.65	15.23	13.57	16.90	3.33
37	0.76	0.23	1.29	1.05	15.16	13.78	16.54	2.75

(continued on next page)

Table F.4 (continued)

Sample ID	Annual Chlorophyll (mg/m3)	Winter chlorophyll (mg/m3)	Summer chlorophyll (mg/m3)	Seasonal range chlorophyll (mg/m3)	Annual SST (^{o}C)	Winter SST (^{o}C)	Summer SST (^{o}C)	Seasonal range SST (^{o}C)
38	0.96	0.21	1.70	1.50	15.09	14.02	16.15	2.13
39	0.86	0.22	1.50	1.28	15.17	14.33	16.00	1.67
40	0.70	0.24	1.15	0.91	15.27	14.53	16.00	1.47
41	0.68	0.28	1.08	0.80	15.91	14.73	17.10	2.37
42	1.06	0.47	1.64	1.16	14.61	13.63	15.59	1.96
43	1.02	0.47	1.57	1.10	14.66	13.65	15.66	2.02
44	0.97	0.47	1.48	1.01	14.72	13.67	15.76	2.09
45	0.93	0.47	1.40	0.93	14.78	13.70	15.85	2.15
46	0.81	0.46	1.16	0.71	14.99	13.79	16.20	2.41
47	0.81	0.43	1.18	0.75	15.10	13.84	16.36	2.52
48	0.79	0.39	1.18	0.80	15.24	13.95	16.53	2.59
49	0.65	0.37	0.93	0.56	15.27	14.23	16.32	2.10
50	0.60	0.41	0.78	0.38	15.06	14.20	15.92	1.72
51	0.43	0.38	0.48	0.10	15.95	14.21	17.70	3.49
52	0.45	0.39	0.50	0.11	15.28	14.23	16.34	2.11
53	0.48	0.41	0.55	0.13	14.99	14.18	15.80	1.62
54	0.49	0.42	0.57	0.16	14.79	14.14	15.45	1.31
55	0.51	0.42	0.61	0.19	14.61	14.10	15.13	1.03
56	0.52	0.42	0.62	0.20	14.50	14.07	14.94	0.87
57	0.29	0.51	0.07	-0.44	16.61	14.35	18.88	4.53
58	0.14	0.21	0.07	-0.14	16.37	14.25	18.49	4.23
59	0.29	0.38	0.20	-0.18	15.88	13.75	18.01	4.26
60	0.36	0.40	0.33	-0.07	15.57	13.50	17.64	4.15
61	0.38	0.34	0.43	0.08	15.45	13.51	17.39	3.88
62	0.54	0.33	0.76	0.43	15.14	13.69	16.60	2.91
63	1.62	0.39	2.85	2.46	14.66	13.71	15.62	1.91
64	2.17	0.40	3.94	3.53	14.49	13.67	15.31	1.64
65	no info	no info	no info	no info	no info	no info	no info	no info
66	no info	no info	no info	no info	no info	no info	no info	no info
67	0.19	0.26	0.11	-0.15	17.46	15.86	19.05	3.19
68	0.18	0.23	0.13	-0.10	17.22	14.94	19.50	4.57